ALMA MATER STUDIORUM
UNIVERSITÀ DI BOLOGNA

DOTTORATO DI RICERCA IN

SCIENZE E TECNOLOGIE AGRARIE, AMBIENTALI E ALIMENTARI

Ciclo 38

Settore Concorsuale: 07/E1 - CHIMICA AGRARIA, GENETICA AGRARIA E PEDOLOGIA

Settore Scientifico Disciplinare: AGR/14 - PEDOLOGIA

DIGITAL SOIL MAPPING OF MOUNTAIN SOILS: FROM PEDODIVERSITY TO LAND VOCATION AND ECOSYSTEM SERVICES

Presentata da: William Trenti

Coordinatore Dottorato

Diana Di Gioia

Supervisore

Livia Vittori Antisari

Co-supervisore

Gloria Falsone

Esame finale anno 2026

CONTENTS

Digital Soil Mapping of Mountain Soils: From Pedodiversity to Land Vocation and Ecosystem Services

ABSTRACT

This doctoral research explored the application of Geographic Information System (GIS) and Digital Soil Mapping (DSM) techniques to improve soil mapping processes and support land management and biodiversity conservation, in alignment with the objectives of the National Biodiversity Future Center (NBFC). The study was conducted in two Regional Parks of the Northern Apennines, a region characterized by high environmental heterogeneity and a rich cartographic heritage. Traditional pedological knowledge and expert-driven selection of environmental covariates were first employed to delineate land units and produce a conventional soil map. Subsequently, DSM approaches using Random Forest models with recursive feature elimination were applied to generate an alternative soil map based on DEM derivatives and remotely sensed data, achieving high accuracy and interpretability. The analysis identified key drivers of soil differentiation, such as topography, insolation, vegetation indices, and proximity to water bodies, highlighting their potential for transferability to similar areas and for overcoming cartographic discontinuities. Complementary studies on the same area revealed that climate exerts a stronger influence than vegetation on soil evolution, and that considering soil diversity enhances understanding of organic matter dynamics.

The second component of this research addressed the reestablishment of chestnut cultivation in the Northern Apennines through a land suitability model that was tested on the municipality of Castel del Rio (BO). The resulting map identified both underutilized suitable lands and cultivated areas with significant limitations, findings that were corroborated by the severe landslides of May 2023. Moreover, the study suggested that land morphology and soil characteristics may influence the spread of ink disease, a major threat to chestnut groves.

Overall, this research demonstrates the value of integrating GIS-based modeling, soil science, and ecological understanding to generate spatial tools that inform sustainable land use, enhance soil and biodiversity conservation, and support the resilience of traditional agroecosystems.

1. GENERAL INTRODUCTION

Despite their central role in sustaining ecosystem services, soils remain underrepresented in decision-making processes related to land and biodiversity management. The lack of harmonized soil data and soil ecosystem service maps constrains the integration of pedodiversity into planning strategies, particularly in protected and fragile mountain areas. In this context, the National Biodiversity Future Center (NBFC), established under the Italian PNRR, aims to develop decision-support tools for park authorities to monitor, protect, and enhance biodiversity. The creation of soil maps represents a key objective, through the development of digital soil maps, GIS-based landscape units, and assessments of soil ecosystem services that are essential for guiding the sustainable management of protected areas. This effort is aligned with the EU Biodiversity Strategy for 2030, which calls for the restoration, valorization, and sustainable use of biodiversity to strengthen the resilience and multifunctionality of ecosystems.

Soil is regarded as one of the most complex ecosystems on Earth. It forms at the interface between the atmosphere, the lithosphere, and the hydrosphere, where its evolution is driven by the interaction between the five soil-forming factors: climate, parent material, relief, organisms, and time (Jenny, 1941). Soils represent complex and dynamic systems whose functions range from nutrient cycling, carbon sequestration, primary productivity, water regulation, and biodiversity support, making it the foundation of terrestrial ecosystems (FAO & ITPS, 2015). To highlight the importance of soil functions to human activities and needs, the concept of ecosystem services was remarked by the Millennium Ecosystem Assessment (MEA, 2005). Soil ecosystem services are benefits that are derived from soil functions, and include nutrient cycling, climate regulation, carbon sequestration, provision of habitats, food and materials, preservation of cultural heritage, and others. The ability of soil to provide ecosystem services depends on its characteristics and its health status. Soil characteristics vary across space and time according to the aforementioned soil forming factors, which, shaping soil genesis and evolution, produce a high degree of heterogeneity in soil types and properties. This concept is known as pedodiversity, and is increasingly recognized as the cornerstone of biodiversity because it governs vegetation patterns, microbial diversity, and ecosystem processes (Ibáñez et al., 1998), directly contributing to the provision of ecosystem services (Mikhailova et al., 2021; Adhikari & Hartemink, 2016). Soil health and functionality are linked to certain properties and processes which allow soil to continuously function as a vital living system (Doran et al., 1996). A central component of soil functionality and health is soil organic matter (SOM), which strongly influences physical, chemical, and biological properties (Hoffland et al., 2020). SOM regulates soil structure, nutrient cycling, and water retention, while also constituting a major reservoir of organic carbon. Changes in SOM quantity and quality, whether due to land use, climate change, or other disturbances, directly affect ecosystem functioning and services (Lorenz et al., 2019). Microorganisms play a fundamental role in SOM dynamics, as they drive the decomposition of organic matter and direct nutrient cycles (Piotrowska-Długosz et al., 2022). Soil microbial communities also produce extracellular enzymes that control the turnover of nutrients such as carbon, nitrogen, and phosphorus (Burns et al., 2013; Zuccarini et al., 2020). These enzyme activities respond rapidly to changes in soil moisture, SOM quality, and pedoclimatic stressors (Fanin et al., 2022), making them effective indicators of soil functionality and resilience (Bhaduri et al., 2022). Yet, while microbial ecology in the topsoil has been relatively well studied, subsoil microbiomes, which may constitute a major fraction of microbial biomass and influence long-term carbon stabilization, remain poorly understood (Jiao et al., 2018).

Mountain environments are particularly relevant for understanding pedodiversity and soil–ecosystem interactions. Covering approximately 30% of Europe's land surface, they are globally recognized as biodiversity hotspots and providers of essential ecosystem services such as water regulation, air purification, and climate mitigation (Perrigo et al., 2016; Locatelli et al., 2017). Yet, they are also among the most fragile ecosystems, highly sensitive to land use and climatic changes (Gutiérrez-Girón et al., 2015; Chakraborty, 2021): in fact, mountains are often designated as protected areas. Despite the role that soil plays both in the mitigation and adaptation to climate change, conservation planning frequently underestimates the role of soils. In Italy, the establishment of the National Biodiversity Future Centre (NBFC) marks a significant step toward integrating soil science into biodiversity strategies. In order to be effective, research must take into account the complexity of mountain ecosystems and the soil-landscape relationship, since soil forming factors are more diverse in mountain areas compared to plains (Romeo et al., 2015; Slaymaker et al., 2015). Elevation causes climatic shifts where, generally, temperature decreases and precipitation increases with altitude. This in turn influences the land cover and land uses, in a succession of phytoclimatic zones (De Philippis, 1937) and, often, increasing constraints for agriculture. The landform and characteristics such as slope and aspect, which are negligible in flat areas, exert a strong influence on the soil as well, since they directly determine the amount of solar radiation that an area receives, as well as the behavior of surface waters and, thus, the erosion and deposition processes (Masseroli et al., 2020; Egli & Poulenard, 2016). Orogenesis causes the different geologic substrates to deform and exposes them to the weathering action of the elements; compared to flatlands, mountain areas often see the compresence of substrates which are more diverse in age, origin, and composition (Gray, 2021). The intersection between landscape, soil processes, and ecological stress becomes particularly evident in the case of forest diseases, which are often mediated by soil conditions. In Italy, chestnut (*Castanea sativa* Mill.) forests represent a historical landscape that is now under threat from ink disease, caused primarily by *Phytophthora cambivora* and *P. cinnamomi*. The severity of this disease is modulated by soil moisture regimes, pH, organic matter content, and microbial community composition (Jung et al., 2018; Prospero et al., 2023). Climate change further exacerbates the problem by intensifying droughts, extreme rainfall, and milder winters, all of which interact with soil-forming factors to influence disease dynamics (Vettraino et al., 2005). In this context, soil and landscape characteristics of a territory, together with its socio-economic fabric, can be integrated into the concept of land vocation, which highlights the potential for the sustainable management of an area from an environmental, as well as economic and social point of view. The rediscovery and chestnut farming in the Apennines stands as an example of the role of pedological knowledge in promoting the conservation of rural landscapes while also sustaining communities.

Still, due to the inherent complexity and the difficulty in studying it, research on mountain soils is still scarce not only in Italy but worldwide (Rossiter, 2016; Hartemink et al., 2013).

Understanding these complex relationships requires not only site-specific soil analysis but also spatially explicit tools capable of capturing pedodiversity at landscape scales. Traditional soil surveys, while valuable, are often limited in mountainous terrains by accessibility, heterogeneity, and the fragmentation of existing cartographic resources. Digital Soil Mapping (DSM), supported by advances in GIS, remote sensing, and machine learning, provides a powerful means to overcome these challenges (Rossiter, 2016; Kidd et al., 2020). Random Forest algorithms, in particular, have proven highly effective in mapping soil classes and predicting soil properties in complex landscapes, identifying leading pedogenetic factors even in data-scarce environments (Belgiu & Drăguț, 2016; Wadoux et al., 2020). By integrating environmental covariates such as digital elevation models (DEMs) derivatives, vegetation indices, and lithological maps, DSM can reveal the soil–landscape relationships that drive pedodiversity even when the environmental mosaic is complex.

Given these considerations, the Northern Apennines, with their diverse topography and land use dynamics, provide an ideal case study for exploring the interplay between soil-forming factors, pedodiversity, organic matter dynamics, and ecological processes. Numerous projects were carried out in the Frignano and Corno alle Scale areas, the latest of which (Biodiversity Between the Roots, funded by the PNRR, in collaboration with Parchi Emilia Centrale) will result in a WebGIS platform for the dissemination of ecological and pedological knowledge.

1.1 OBJECTIVES

The research aims were to:

- develop and implement GIS- and DSM-based decision-support tools to map soil diversity, ecosystem services, and land vocation, providing spatially explicit knowledge for sustainable land management, biodiversity conservation, and climate adaptation strategies;
- evaluate the role of pedodiversity in regulating DNA-microbial community, nutrient cycling, enzyme activity, and ecological functionality across soil horizons;
- assess how geomorphological and pedoclimatic factors influence soil physicochemical properties, organic matter storage, and microbial community structure in mountain soils;
- investigate how soil–landscape relationships mediate forest resilience and susceptibility to stressors such as *Phytophthora* infections.

By integrating soil physicochemical analysis, microbial DNA metabarcoding, enzyme activity measurements, and geospatial modeling, this work aims to advance our understanding of mountain soil systems as multifunctional, biodiverse, and climate-sensitive environments.

REFERENCES

Adhikari, K., & Hartemink, A. E. (2016). Linking soils to ecosystem services—A global review. *Geoderma*, *262*, 101-111. https://doi.org/10.1016/j.geoderma.2015.08.009

Belgiu, M., & Drăguț, L. (2016). Random forest in remote sensing: A review of applications and future directions. *ISPRS journal of photogrammetry and remote sensing*, *114*, 24-31. https://doi.org/10.1016/j.isprsjprs.2016.01.011

Bhaduri, D., Sihi, D., Bhowmik, A., Verma, B. C., Munda, S., & Dari, B. (2022). A review on effective soil health bio-indicators for ecosystem restoration and sustainability. *Frontiers in Microbiology*, *13*, 938481. https://doi.org/10.3389/fmicb.2022.938481

Burns, R. G., DeForest, J. L., Marxsen, J., Sinsabaugh, R. L., Stromberger, M. E., Wallenstein, M. D., ... & Zoppini, A. (2013). Soil enzymes in a changing environment: current knowledge and future directions. *Soil Biology and Biochemistry*, *58*, 216-234. https://doi.org/10.1016/j.soilbio.2012.11.009

Chakraborty, A. (2021). Mountains as vulnerable places: a global synthesis of changing mountain systems in the Anthropocene. *GeoJournal*, *86*(2), 585-604. https://doi.org/10.1007/s10708-019-10079-1

De Philippis, A. (1937). Classificazioni ed indici del clima, in rapporto alla vegetazione forestale italiana. *Plant Biosystem*, *44*(1), 1-169. https://doi.org/10.1080/11263503709438750

Doran, J.W., Sarrantonio, M. and Liebig, M.A. (1996) Soil health and sustainability. Advances in Agronomy, 56, 1-54. http://dx.doi.org/10.1016/S0065-2113(08)60178-9

Egli, M., & Poulenard, J. (2016). Soils of mountainous landscapes. *International Encyclopedia of Geography: People, the Earth, Environment and Technology: People, the Earth, Environment and Technology*, 1-10. https://doi.org/10.1002/9781118786352.wbieg0197

Fanin, N., Mooshammer, M., Sauvadet, M., Meng, C., Alvarez, G., Bernard, L., ... & Nottingham, A. T. (2022). Soil enzymes in response to climate warming: Mechanisms and feedbacks. *Functional Ecology*, *36*(6), 1378-1395. https://doi.org/10.1111/1365-2435.14027

FAO and ITPS. (2015). Status of the World's Soil Resources (SWSR) – Main Report. Food and Agriculture Organization of the United Nations and Intergovernmental Technical Panel on Soils, Rome, Italy

Gray, M. (2021). Geodiversity: a significant, multi-faceted and evolving, geoscientific paradigm rather than a redundant term. *Proceedings of the Geologists' Association*, *132*(5), 605-619. https://doi.org/10.1016/j.pgeola.2021.09.001

Gutiérrez-Girón, A., Diaz-Pines, E., Rubio, A., & Gavilan, R. G. (2015). Both altitude and vegetation affect temperature sensitivity of soil organic matter decomposition in Mediterranean high mountain soils. *Geoderma*, *237*, 1-8. https://doi.org/10.1016/j.geoderma.2014.08.005

Hartemink, A. E., Krasilnikov, P., & Bockheim, J. G. (2013). Soil maps of the world. *Geoderma*, *207*, 256-267. https://doi.org/10.1016/j.geoderma.2013.05.003

Hoffland, E., Kuyper, T. W., Comans, R. N., & Creamer, R. E. (2020). Eco-functionality of organic matter in soils. *Plant and Soil*, *455*(1), 1-22. https://doi.org/10.1007/s11104-020-04651-9

Ibañez, J. J., De-Alba, S., Lobo, A., & Zucarello, V. (1998). Pedodiversity and global soil patterns at coarse scales (with discussion). *Geoderma*, *83*(3-4), 171-192. https://doi.org/10.1016/S0016-7061(97)00147-X

Jenny, H. (1941) Factors of Soil Formation: A System of Quantitative Pedology. Dover Publications, New York, 281 p.

Jiao, S., Chen, W., Wang, J., Du, N., Li, Q., & Wei, G. (2018). Soil microbiomes with distinct assemblies through vertical soil profiles drive the cycling of multiple nutrients in reforested ecosystems. *Microbiome*, *6*(1), 146. https://doi.org/10.1186/s40168-018-0526-0

Jung, T., Pérez-Sierra, A., Durán, A., Jung, M. H., Balci, Y., & Scanu, B. (2018). Canker and decline diseases caused by soil-and airborne Phytophthora species in forests and woodlands. *Persoonia-Molecular Phylogeny and Evolution of Fungi*, *40*(1), 182-220. 10.3767/persoonia.2018.40.08

Kidd, D., Searle, R., Grundy, M., McBratney, A., Robinson, N., O'Brien, L., ... & Triantafilis, J. (2020). Operationalising digital soil mapping–Lessons from Australia. *Geoderma Regional*, *23*, e00335. https://doi.org/10.1016/j.geodrs.2020.e00335

Locatelli, B., Lavorel, S., Sloan, S., Tappeiner, U., & Geneletti, D. (2017). Characteristic trajectories of ecosystem services in mountains. *Frontiers in Ecology and the Environment*, *15*(3), 150-159. https://doi.org/10.1002/fee.1470

Lorenz, K., Lal, R., & Ehlers, K. (2019). Soil organic carbon stock as an indicator for monitoring land and soil degradation in relation to U nited N ations' S ustainable D evelopment G oals. *Land Degradation & Development*, *30*(7), 824-838. https://doi.org/10.1002/ldr.3270

Masseroli, A., Bollati, I. M., Proverbio, S. S., Pelfini, M., & Trombino, L. (2020). Soils as a useful tool for reconstructing geomorphic dynamics in high mountain environments: The case of the Buscagna stream hydrographic basin (Lepontine Alps). *Geomorphology*, *371*, 107442. https://doi.org/10.1016/j.geomorph.2020.107442

McBratney, A. B., Santos, M. M., & Minasny, B. (2003). On digital soil mapping. *Geoderma*, *117*(1-2), 3-52. https://doi.org/10.1016/S0016-7061(03)00223-4

Mikhailova, E. A., Zurqani, H. A., Post, C. J., Schlautman, M. A., & Post, G. C. (2021). Soil diversity (pedodiversity) and ecosystem services. *Land*, *10*(3), 288. https://doi.org/10.3390/land10030288

Millennium Ecosystem Assessment. (2005). Ecosystems and human well-being: Synthesis. Island Press

Perrigo, A., Hoorn, C., & Antonelli, A. (2020). Why mountains matter for biodiversity. *Journal of Biogeography*, *47*(2), 315-325. https://doi.org/10.1111/jbi.13731

Piotrowska-Długosz, A., Długosz, J., Frąc, M., Gryta, A., & Breza-Boruta, B. (2022). Enzymatic activity and functional diversity of soil microorganisms along the soil profile–A matter of soil depth and soil-forming processes. *Geoderma*, *416*, 115779. 10.1016/j.geoderma.2022.115779

Prospero, S., Heinz, M., Augustiny, E., Chen, Y. Y., Engelbrecht, J., Fonti, M., ... & Fonti, P. (2023). Distribution, causal agents, and infection dynamic of emerging ink disease of sweet chestnut in Southern Switzerland. *Environmental Microbiology*, *25*(11), 2250-2265. https://doi.org/10.1111/1462-2920.16455

Romeo, R., Vita, A., Manuelli, S., Zanini, E., Freppaz, M., & Stanchi, S. (2015). Understanding Mountain Soils: A contribution from mountain areas to the International Year of Soils 2015.

Rossiter, D. G. (2016). Digital soil resource inventories: status and prospects in 2015. *Digital soil mapping across paradigms, scales and boundaries*, 275-286. https://doi.org/10.1007/978-981-10-0415-5_22

Slaymaker, O., Spencer, T., & Embleton-Hamann, C. (Eds.). (2015). *Geomorphology and global environmental change*. Cambridge University Press.

Vettraino, A. M., Morel, O., Perlerou, C., Robin, C., Diamandis, S., & Vannini, A. (2005). Occurrence and distribution of Phytophthora species in European chestnut stands, and their association with Ink Disease and crown decline. *European Journal of Plant Pathology*, *111*(2), 169-180. https://doi.org/10.1007/s10658-004-1882-0

Wadoux, A. M. C., Minasny, B., & McBratney, A. B. (2020). Machine learning for digital soil mapping: Applications, challenges and suggested solutions. *Earth-Science Reviews*, *210*, 103359. https://doi.org/10.1016/j.earscirev.2020.103359

Zuccarini, P., Asensio, D., Ogaya, R., Sardans, J., & Peñuelas, J. (2020). Effects of seasonal and decadal warming on soil enzymatic activity in a P-deficient Mediterranean shrubland. *Global Change Biology*, *26*(6), 3698-3714. 10.1111/gcb.15077

SYNOPTIC TABLE OF CONTENTS

This thesis is formed by six scientific articles: chapters 2 and 3 investigate soil mapping techniques and approaches in a complex mountainous environment; chapters 4 and 5 focus on pedodiversity and soil properties with an emphasis on soil forming factors, soil organic, and the microbial community; chapters 6 and 7 center on land vocation evaluation and soil-borne threats to chestnut cultivation.

Chapter Title	Objectives	Study areas	Methods	Results and deliverables	Key takeaway
2. Land Unit Delineation Based on Soil-Forming Factors: A Tool for Soil Survey in Mountainous Protected Areas	Assessing soil diversity in a protected mountain area	Frignano Regional Park, Corno alle Scale Regional Park	GIS-based, using DEMs and existing cartographic data coupled with legacy and ad-hoc profile data	Map of Land Units, soil map, transferable methodology.	Integrating multiple soil-forming factors can support spatial planning and ecological monitoring in areas where traditional sampling approaches are constrained
3. Mapping soils in temperate humid mountains: Random forests highlights optimal covariates in Northern Italy	Digitally mapping the distribution of soil classes in a complex area while retaining interpretability	Frignano Regional Park, Corno alle Scale Regional Park, and neighboring areas	Random forests with recursive feature elimination (RFE) using DEM derivatives, remotely sensed data and legacy soil data.	Detailed soil map, key soil forming factors in the area, transferable model.	Elevation, slope, insolation, NDVI during water stress, and distance from lakes as the main covariates affecting soil differentiation in the area.
4. Pedodiversity and Organic Matter Dynamics in the North Apennines (Italy): Relationships among Soil Types, Biodiversity, and Ecological Functionality	Exploring the effect of soil type on soil organic matter dynamics in the profile and the microbial community functionality in the first mineral horizon.	Beech forests of the Modena Apennine	Soil physico-chemical and biochemical analyses; DNA extraction of the soil microbial community with taxonomic and functional assignment; statistical methods.	SOC content and turnover rate were different according to soil type but rather similar in the A horizons, where microbial diversity and functionality were comparable.	Combining pedodiversity and microbial diversity generates a wider perspective on SOC dynamics.

Chapter Title	Objectives	Study areas	Methods	Results and deliverables	Key takeaway
5. Pedodiversity and Organic Matter Stock of Soils Developed on Sandstone Formations in the Northern Apennines (Italy)	Assessing pedodiversity according to soil forming factors and identifying the factors that most influence soil organic matter stock at 0-30 cm.	Mountains of Reggio Emilia, Modena, and Bologna.	Legacy soil profiles, soil physico-chemical analyses and ANOVA	Soil development was constrained by the soil forming factors. Both soil diversity and SOM stock changed mostly according to climate.	The observed spatial pedodiversity could be considered a critical basis for the protection of soil resources in mountain regions.
6. GIS-Based Geopedological Approach for Assessing Land Suitability for Chestnut (Castanea sativa Mill.) Groves for Fruit Production	Identifying the areas suitable to chestnut production and propose a remote-sensing-based methodology to identify the areas currently under chestnut cultivation.	Municipality of Castel Del Rio (BO)	GIS-based land evaluation, remotely-sensed data to identify chestnut trees based on phenology, and chestnut orchards based on plantation pattern.	Land suitability map and transferable method. The greatest constraint is slope. Some areas are cultivated despite the low suitability. The cultivated area is larger than that reported in official maps.	GIS-based approaches are effective in locating suitable areas for chestnut cultivation and in supporting decision-making in land management.
7. Hillslope morphological features modulate soil microbial communities and chestnut ink disease via clay and water redistribution	Evaluating whether the morphology of soil and related properties influence the development of ink disease throughout the entire soil profile.	Abandoned chestnut orchard in the Bologna Apennine	Elevation transect including two healthy trees and one ill tree; soil physico-chemical and biochemical analyses, DNA extraction and taxonomic assignment; statistical analyses.	Soil characteristics of the transect suggest that morphological features related to clay and water dynamics can favor the onset of ink disease. The soil microbial community near the ill tree had a different composition compared to the healthy trees.	Soil processes play a key role in shaping microbial communities and soil-borne pathogen dynamics through their influence on edaphic properties. Farmers should prevent waterlogging or avoid the cultivation of areas with poor drainage.

2. LAND UNIT DELINEATION BASED ON SOIL-FORMING FACTORS: A TOOL FOR SOIL SURVEY IN MOUNTAINOUS PROTECTED AREAS

Published in *Land* **2025**, *14*(8), 1683; https://doi.org/10.3390/land14081683

William Trenti [1], Mauro De Feudis [1*], Massimo Gherardi [2], Gilmo Vianello [3] and Livia Vittori Antisari [1]

[1] Department of Agricultural and Food Sciences, Alma Mater Studiorum-University of Bologna, Viale Fanin 40, Bologna, Italy
[2] Boreal Mapping, Via Casella, 23/a, 40030 Grizzana Morandi, Italy
[3] Accademia Nazionale di Agricoltura, Via Castiglione 11, 40124 Bologna, Italy
*correspondence: mauro.defeudis2@unibo.it

ABSTRACT

The present study applied a GIS-based methodology for assessing soil diversity in a protected mountain area of Italy. Using QGIS, morphological (i.e., altitude and slope), lithological, climatic, and land use layers were intersected to delineate 16 land units (LUs), each representing relatively homogeneous conditions for soil formation, according to Jenny's equation. To obtain the soil map units, a total of 112 soil profiles were analyzed, including 79 from previous studies and 33 that were newly excavated during 2023–2024 to fill gaps in underrepresented LU types. Most soils were classified as Inceptisols/Cambisols, occurring in both Dystric and Eutric variants, mainly in relation to lithology (i.e., arenaceous or pelitic facies). Alfisols, Umbrisols, and hydromorphic soils were also identified. The physicochemical properties showed marked variability among LUs, with sand content ranging from 39 to 798 g kg^{-1}, pH from 4.4 to 7.9, and organic carbon content from 1.6 to 6.1%. This LU-based framework allowed efficient field sampling, if compared to grid-based surveys, while retaining information on fine-scale pedodiversity. No quantitative accuracy assessment (e.g., boundary precision, internal homogeneity metrics) was conducted, even if the spatial coherence of the delineated

LUs was supported by the distribution of soil profiles, which provided empirical validation of the LU framework.

2.1 INTRODUCTION

Soils are complex and dynamic ecosystems whose ecological functionality emerges from the interplay among the five classic soil-forming factors—climate, parent material, topography, biota, and time—as conceptualized by Hans Jenny in 1941 (Salazar et al., 2023). The spatial variability in the intensity and interaction of these factors gives rise to a pronounced vertical and horizontal heterogeneity in soil properties, which is systematically described through hierarchical classification systems such as the USDA Soil Taxonomy and the World Reference Base for Soil Resources (Yaalon, 1995; Ibañez et al., 1998).

This heterogeneity—commonly referred to as soil diversity or pedodiversity—is a foundational concept in soil science (Ibañez et al., 1998), as it underpins a wide range of ecosystem functions and services, including nutrient cycling, carbon sequestration, primary productivity, and biodiversity support (Mikhailova et al., 2021; Adhikari & Hartemink, 2016). Despite its central role in regulating ecosystem dynamics, soil is often overlooked in biodiversity assessments and conservation strategies, which tend to focus on aboveground organisms—plants, animals, and microorganisms—while neglecting the integrating and regulating functions of soil systems.

Given the importance of soils and pedodiversity in shaping ecological processes, there is an increasing demand for high-resolution, spatially explicit, and up-to-date soil information to inform natural resource management, conservation strategies, and land use planning (Chen et al., 2022,7]. Soil maps are essential tools in this regard, as they link observable and measurable soil properties to their environmental context, thereby enabling the spatial assessment of soil functions and degradation risks. These maps are typically derived by integrating field observations, laboratory analyses, and geostatistical modeling of the relationships between soils and their forming factors (Stoorvogel et al., 2017; Sermin & Jeff, 2008; McBratney et al., 2000).

However, detailed and accurate soil maps are still lacking for many parts of the world—particularly in mountainous regions (Rossiter, 2016; Hartemink et al., 2013). In Italy, as in many other countries, the availability of high-resolution and up-to-date soil maps for mountain areas remains critically limited (e.g., Costantini & Lorenzetti, 2013; Arrouays et al., 2017; GSBI, 2020). Moreover, there is no standardized or widely accepted methodology for delineating land units or producing soil maps at regional and landscape scales in complex terrains.

In the context of land conservation and territorial planning, soil information must be integrated with other environmental and anthropogenic variables—such as climate, geology, geomorphology, vegetation, and land use history—to understand the drivers of ecosystem dynamics (McBratney et al., 2000; Smiraglia et al., 2013; Zonneveld, 1989). One promising approach is the subdivision of the landscape into land units (LUs), which are spatial domains characterized by sufficient environmental homogeneity (in terms of relief, climate, parent material, vegetation, etc.) to influence soil development and land use suitability (Fisher & Koven, 2020; Sonneveld, 2010; Kiryushin, 2020). Each LU can be regarded as a distinct ecological subsystem and provides a meaningful spatial framework for analyzing interactions among soils, land use, and biodiversity.

This spatial approach is especially relevant in mountain areas, which cover approximately 30% of Europe's land surface (Price, 2016) and are globally recognized as biodiversity hotspots (Perrigo et al., 2020). Mountain ecosystems deliver essential services such as water regulation, air purification, and climate moderation (Locatelli et al., 2017), but they are also particularly vulnerable to changing global pressures—including land use intensification, warming, and unsustainable development (Chakraborty, 2021; Macchi, 2010). As such, their conservation has become a strategic priority in environmental policy and biodiversity planning (D'Amico et al., 2020). While protected areas are key tools for safeguarding mountain ecosystems (Jenkins & Joppa, 2009; Chape et al., 2005), a critical mismatch persists between the ecological significance of these regions and the availability of adequate planning instruments—particularly in terms of soil-based data and decision-support tools.

In response to this gap, the National Biodiversity Future Centre (NBFC; www.nbfc.it) was established as Italy's first national research and innovation hub dedicated to biodiversity, funded by the Ministry of University and Research through the European Union's NextGenerationEU initiative. Within the NBFC's "Biodiversity 2030" framework, which aims to enhance biodiversity conservation in protected areas, we propose a soil knowledge tool tailored to mountainous landscapes.

This case study represents a novel application of GIS-based delineation of land units in mountain landscapes, demonstrating how integrating multiple soil-forming factors can support spatial planning and ecological monitoring in areas where traditional sampling approaches are limited.

Specifically, we present a GIS-based methodology that operationalizes Jenny's model of soil formation—expressed as soil = f(climate, organisms, relief, parent material, time)—to support soil surveys and the delineation of pedodiversity in mountain environments. The method relies on intersecting multiple thematic layers to define land units (LUs), which represent pedologically homogeneous areas. These LUs were used to guide targeted field surveys, allowing soil scientists to reasonably expect similar soil types within each unit, distinct from those in adjacent areas. Beyond guiding fieldwork, LUs also provide a reproducible spatial framework to support further pedological, ecological, and land use analyses.

2.1 MATERIALS AND METHODS

2.2.1. Conceptual Model for Land Unit and Soil Map Unit Delineation

Figure 1 illustrates the flowchart of the conceptual framework developed to delineate land units (LUs), which were then used to guide pedological surveys and construct the corresponding soil map units (SMUs).

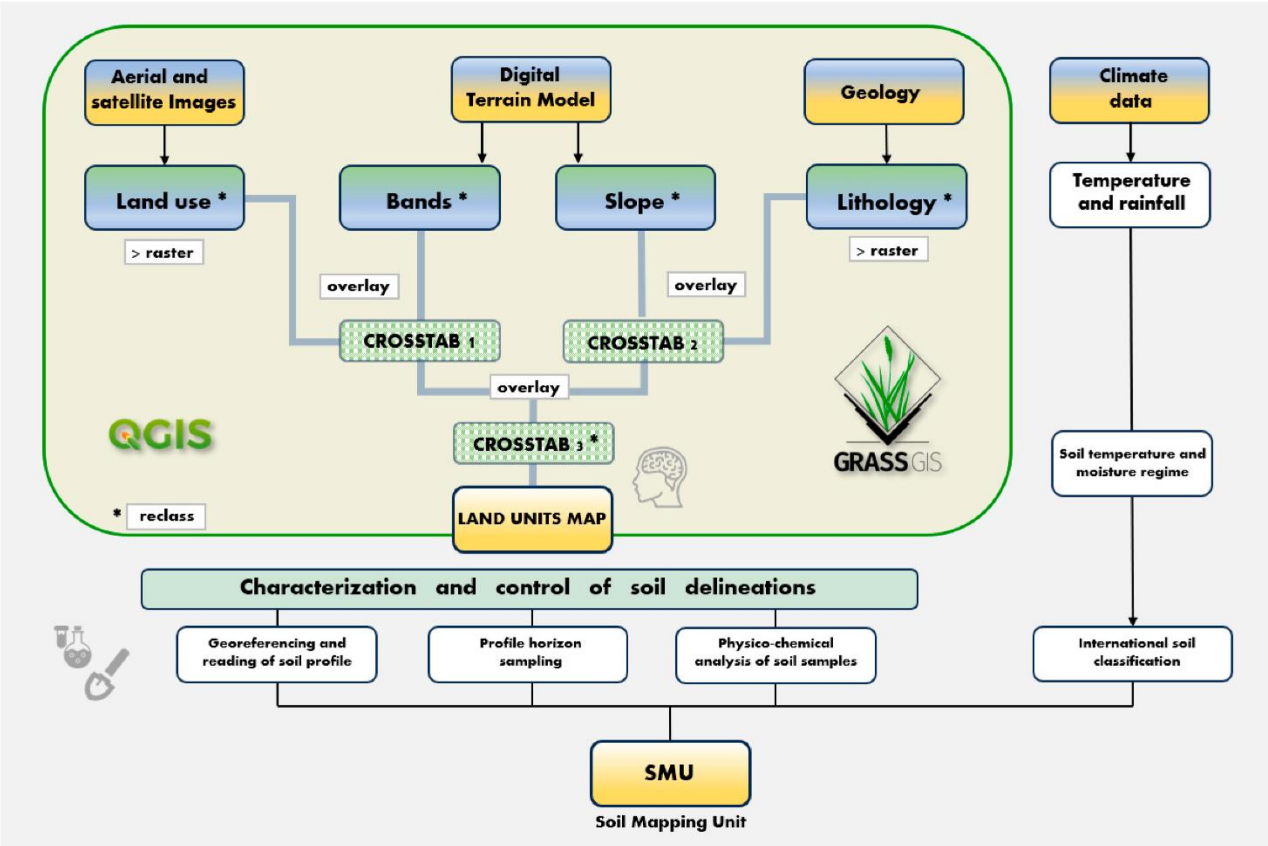

Figure 1. Methodological flowchart outlining the steps for identifying land units and soil map units.

The model is grounded in Jenny's soil formation equation, where soil is defined as a function of climate, organisms, relief, parent material, and time. To operationalize this concept, a set of spatial datasets—namely a lithological map, a land use map, and a digital elevation model (DEM)—were clipped to the boundaries of the study area and reclassified. These layers were overlaid to delineate environmentally homogeneous zones based on combinations of elevation class, dominant land use, lithology, and slope gradient.

Georeferenced soil profile data were assigned to the corresponding LUs and used to refine and validate their delineation. These units also served as a basis for targeted additional sampling. Soil temperature and moisture regimes were estimated from long-term climate data and integrated with field descriptions and laboratory analyses for soil classification. The resulting soil classes were used to characterize each LU, thereby defining soil map units (SMUs), i.e., spatial units representing assemblages of soil types with similar genesis and properties within discrete map polygons (Vincent et al., 2018; Odgers et al., 2014).

Geospatial analyses were carried out using QGIS 3.36 and GRASS GIS 8.2. Vector layers were managed in QGIS, while raster operations (e.g., overlays, reclassifications) were performed in GRASS GIS using modules such as r.cross and r.reclass.

2.2.2. Study Area Description

The study area encompasses the Frignano and Corno alle Scale Regional Parks, two contiguous protected areas located in the Northern Apennines of Emilia-Romagna (Italy), within the UNESCO-designated MAB Biosphere Reserve. Including the Fiumalbo valley, the area spans approximately 21,502 ha (Figure 2), and includes Mount Cimone (2165 m a.s.l.), the highest peak in the Northern Apennines.

Land Use. Land use data were derived from a high-resolution vector map (reference year 2017, published in 2020), scale 1:10,000, with a minimum mapping unit of 0.16 ha. Land cover classification was based on RGB and infrared orthophotos acquired through the TeA program (RER, 2020a) and conformed to the CORINE Land Cover nomenclature (Copernicus, 2021). The area is predominantly forested (~80%), with beech forests (~60%) between 900 and 1600 m a.s.l. dominating the landscape. Chestnut and oak woodlands (~9%) and conifer plantations (~5%) follow, while high-elevation shrublands and grasslands (~12%) and agricultural land (<1%) are also present. For modeling purposes, land use categories were reclassified into eight classes based on their pedogenetic influence.

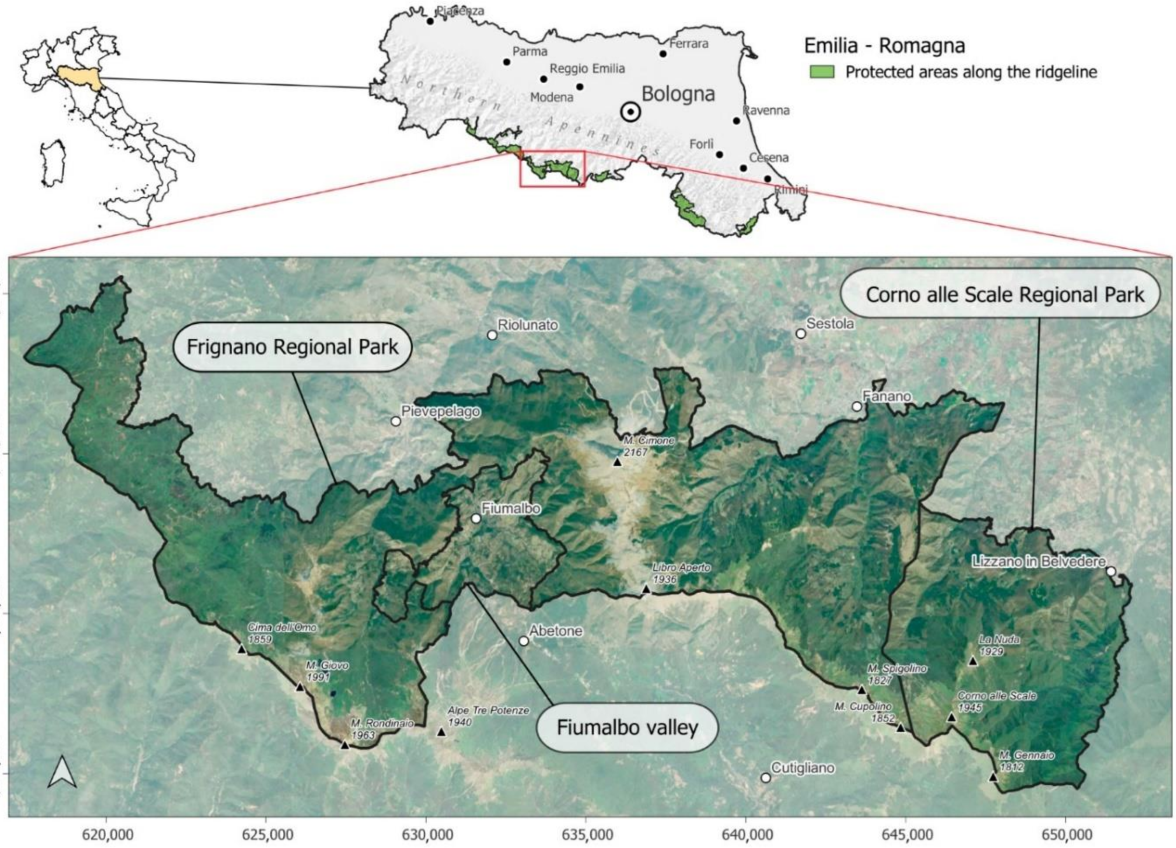

Figure 2. Study area including the Frignano and Corno alle Scale Regional Parks (Emilia-Romagna, Italy), WGS 84-UTM 32.

Lithology. The lithological map was obtained from a 1:10,000-scale geological database curated by the regional Geological Service (RER, 2020b). The substrate comprises sedimentary, metamorphic, and quaternary formations, grouped into eight lithological categories: (i) arenaceous formations (38%), (ii) arenaceous-pelitic (7%), (iii) pelitic-arenaceous (1%), (iv) marly-calcareous (3%), (v) clay-rich formations (6%), (vi) igneous/metamorphic rocks (<1%), (vii) quaternary deposits (43%), and (viii) alluvial terraces (2%).

Morphology. Topographic data were derived from a high-resolution (5 × 5 m) DEM based on 2009 LiDAR surveys (updated in 2014). Elevation ranges from 475 to 2165 m a.s.l. (mean: 1302 m). Steep slopes are predominantly associated with arenaceous formations, while gentler slopes occur on clay-rich substrates. Five elevation classes and three slope classes (<10%, 10–25%,

>25%) were defined, with thresholds consistent with FAO slope classes (FAO, 2018) and USDA Soil Taxonomy subgroups.

Climate. Climatic data for the period 1991–2020 (Figure A1) were provided by the ARPAE agency (ARPAE, 2024). The area shows a typical altitudinal gradient, with decreasing temperature and increasing precipitation with elevation. For example, Sestola (833 m a.s.l.) records an annual mean temperature of 10.6 °C and 1204 mm of precipitation, while Fiumalbo (1354 m a.s.l.) records 8.6 °C and 1872 mm. At Mount Cimone (2165 m a.s.l.), the average temperature drops to 2.2 °C and precipitation totals 733 mm annually (Vittori Antisari et al., 2018). Based on these data, soil temperature and moisture regimes were classified as follows: cryic/perudic (>2000 m a.s.l.), frigid/perudic (1600–2000 m), frigid/udic (1300–1600 m), and mesic/udic (<1300 m).

2.2.3. Soil Survey, Sampling, Laboratory Analyses, and Classification

A total of 112 soil profiles were used in this study (Table S1 of the Supplementary Materials). Of these, 79 were obtained from previous surveys conducted between 2010 and 2021 in the present study area (Vittori Antisari et al., 2018; Brombin et al., 2020; Dell'Abate et al, 2007; Falsone et al., 2015; Marinari et al., 2013; Vittori Antisari et al., 2008; Vittori Antisari et al., 2011; Vittori Antisari et al., 2015; Vittori Antisari et al.,, 2021; De Feudis et al., 2022). Although these earlier surveys were not originally designed according to the Land Unit (LU) framework, they were spatially referenced and described in sufficient detail to allow their integration into the present study. Meanwhile, 33 soil profiles were dug for the aim of this study during field campaigns in 2023 and 2024, as part of the NBFC project. Indeed, these new surveys aimed to fill gaps in spatial coverage and specifically targeted underrepresented combinations of soil-forming factors.

All profiles were excavated to the C or BC horizon and georeferenced. Each genetic horizon was described following the “Field Book for Describing and Sampling Soils” (Schoeneberger et al., 2012), recording properties such as structure, color, root presence, stoniness, horizon boundaries, depth, and thickness. Approximately 500 g per horizon was collected, air-dried, sieved (<2 mm), and analyzed.

Physicochemical analyses included:

- pH: measured potentiometrically in 1:2.5 soil–water suspension.
- Particle size: determined by pipette method after sodium hexametaphosphate dispersion (Gee & Bauder, 1986).
- Organic C and total N: determined via dry combustion (Flash 2000, Thermo Fisher Scientific, Waltham, MA, USA).
- Cation exchange capacity (CEC) and exchangeable bases (Ca, Mg, Na and K): extracted with 1 M NH4-acetate at pH 7 and analyzed by inductive coupled plasma optical emission spectrometry (ICP-OES, Arcos II, Kleve, Germany, Ameteck Spectro).
- Exchange acidity: determined by NaOH titration after KCl extraction.
- Base saturation: calculated as the percentage of Ca, Mg, K, and Na over total CEC (Winegardner, 1995).

Soils were classified according to the World Reference Base for Soil Resources (IUSS, 2022) and USDA Soil Taxonomy (USDA-NRCS, 2022).

2.3 RESULTS

2.3.1 Land Units

The integration of four thematic layers—reclassified elevation range, land use, slope classes, and lithological formations—allowed the delineation of 15 land units (LUs) with soil cover, plus one unit (lithoid outcrops and urban areas) considered not to be soil-bearing. Table 1 and Table 2 show the areas resulting from the intersection of reclassified elevation ranges (five classes) with land use types (eight classes), and of reclassified geological–lithological formations with slope gradient classes, respectively. As expected, most of the study area lies between 900 and 1600 m a.s.l., predominantly covered by beech forests (12,341 ha). Above 1600 m a.s.l., high-elevation heathland areas dominate, covering 2160 ha. Above 1600 m a.s.l., the high elevation heathland areas (2160 ha) dominate. It is worth noting that some beech forests (~500 ha) and conifer reforestations (~100 ha) were identified between 1600 and 1700 m a.s.l. However, these areas were excluded due to their limited extent and to maintain 1600 m a.s.l. as the upper threshold for forested areas. However, such forests were not considered because of their small area and to keep the 1600 m altitude as the cut-off for the forested area. Approximately 82% of the study area features slopes steeper than 25%, mainly occurring on arenaceous formations (7664 ha) and on chaotic, detrital formations and quaternary deposits (6580 ha).

Table 1. Areas obtained by crossing the considered elevation ranges and reclassified land uses.

Reclassified Land Uses	**Elevation Ranges (m Above Sea Level)**				
	<900	900–1300	1300–1600	1600–2000	>2000
	ha				
Urbanized areas	64.09	249.52	31.58	0.46	1.24
Agricultural and cultivated areas	36.99	190.62	40.52	0	0
Grassland, pastures and bushes	32.82	775.65	807.38	2159.63	39.72
Forest with prevalent beech	44.59	6112.05	6229.63	554.98	0
Forest of the sub-mountain plane, chestnuts	1514.12	847.52	369.28	19.69	0
Forest with prevalence conifers, reforestation	27.22	468.64	527.96	110.35	0
Lithoid outcrops	0.45	36.25	41.03	115.04	17.96
Water courses and bodies	10.66	9.79	13.02	1.51	0
Total area	1730.94	8690.04	8060.4	2961.66	58.92

Table 2. Areas obtained by crossing the reclassified lithology classes and slope gradient.

Reclassified Lithology	Slope Gradient (%)		
	0–10	10–25	>25
	ha		
Arenaceous formations	53.81	477.05	7664.51
Arenaceous-pelitic formations	5.19	48.55	1417.97
Pelitic-arenaceous formations	1.32	13.64	281.5
Marly-calcareous formations	7.95	72.68	648.49
Clay formations	25.92	254.68	1009.24
Igneous and metamorphic formations	0.03	0.25	5.81
Chaotic, detrital formations and quaternary deposits	351.12	2228.41	6580.69
Alluvial formations and river terraces	83.32	147.26	122.57
Total area	528.66	3242.52	17,730.78

The intersection of reclassified elevation ranges, land use, geological–lithological formations, and slope classes led to the identification of 15 land units (LUs) with soil presence (Table 3 and Figure 3), plus one additional unit expected to lack soil development (lithoid outcrops and urban areas).

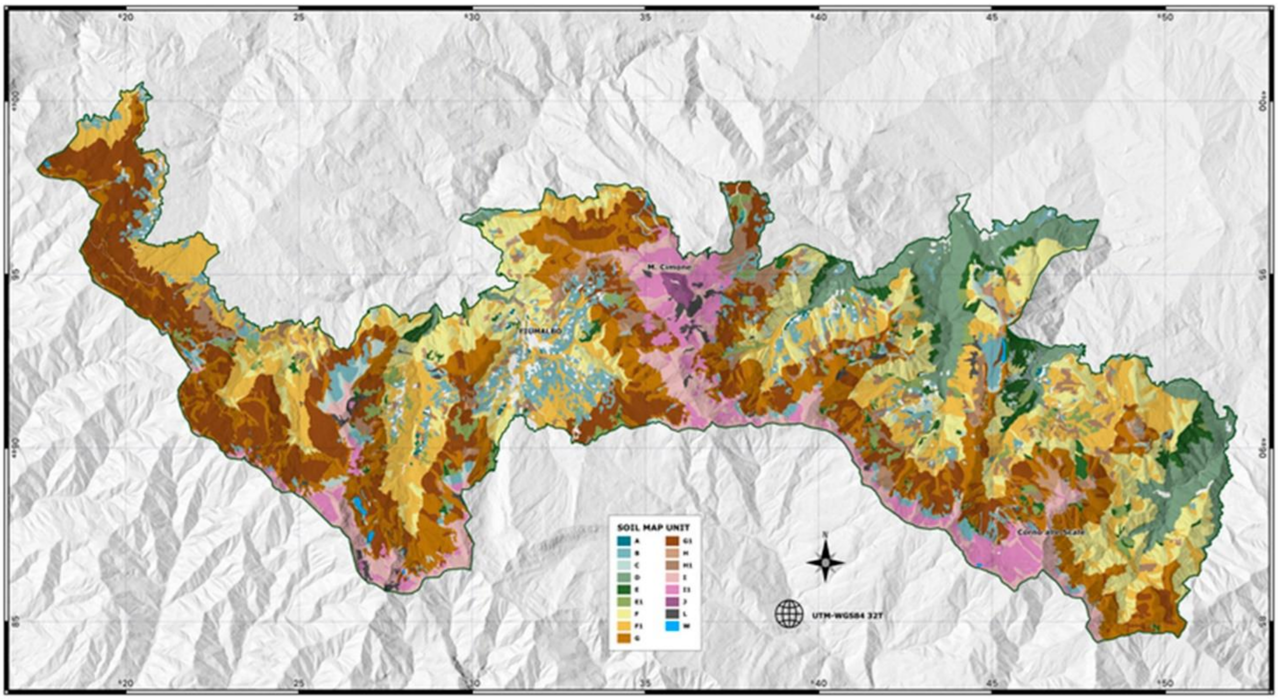

Figure 3. Soil map units in the Frignano Regional Park and Corno alle Scale Regional Park in Emilia-Romagna region (Italy).

Table 3. Land units obtained by the cross of land use, lithology, slope gradient and elevation ranges in the Frignano Regional park and Corno alle Scale regional park, Emilia-Romagna region, Italy.

Land Unit (Area)	**Description**
A (37.06 ha)	Arable land, tree crops, meadows on river terraces and alluvial deposits, mainly adjacent to watercourses, below 1000 m a.s.l., with slopes generally < 10%.
B (157.80 ha)	Land mainly cultivated for arable crops or used as pasture, mostly below 1300 m a.s.l., with slopes between 10 and 25%, on marly and clayey formations.
C (932.22 ha)	Areas used for arable crops or pasture, mostly below 1500 m a.s.l., with slopes between 10 and 25%, on arenaceous and arenaceous-pelitic formations, also in detrital facies.
D (1813.32 ha)	Transitional areas between submontane and montane zones (500–1200 m a.s.l.), with slopes between 10 and 25%, characterized by broadleaf tree and shrub cover, on marly, clayey, igneous-metamorphic formations and alluvial deposits.
E (1579.82 ha)	Areas between 500 and 1400 m a.s.l., mainly with slopes > 25%, in a mesic temperature regime, covered by basal and submontane forest, on arenaceous and arenaceous-pelitic formations.
E1 (969.08 ha)	Areas between 500 and 1400 m a.s.l., in a mesic temperature regime, with slopes between 15 and 30%, covered by basal and submontane forests, on quaternary deposits often in detrital or chaotic facies.
F (2865.55 ha)	Areas between 900 and 1300 m a.s.l., in a mesic temperature regime, covered by broadleaf forests dominated by beech, on arenaceous and arenaceous-pelitic formations.
F1 (2482.62 ha)	Areas between 900 and 1300 m a.s.l., in a mesic temperature regime, mainly with slopes >25%, covered by beech forests on quaternary deposits, often in detrital or chaotic facies.
G (3254.50 ha)	Areas between 1300 and 1600 m a.s.l., in transition from mesic to frigid temperature regimes, with slopes > 25%, covered by deciduous forests, mostly beech, on arenaceous and arenaceous-pelitic formations.
G1 (2735.38 ha)	Areas between 1300 and 1600 m a.s.l., in transition from mesic to frigid temperature regimes, with slopes > 25%, covered by deciduous forests, mostly beech, on quaternary deposits, often in glacial facies.
H (1135.22 ha)	Areas mostly between 900 and 1600 m a.s.l., covered by coniferous forests from artificial reforestation, mainly on arenaceous and arenaceous-pelitic formations, also in detrital facies.
I (2409.63 ha)	Areas between 1600 and 2000 m a.s.l., with slopes > 25%, characterized by polyphytic meadows and bilberry heaths, in a frigid temperature regime, mainly on arenaceous and glacial deposits.
I1 (504.82 ha)	Areas between 1600 and 2000 m a.s.l., with slopes between 20 and 30%, characterized by mountain grasslands, in a frigid temperature regime, mainly on pelitic and glacial deposits, and to a lesser extent on marly, clayey, and chaotic formations.
J (40.31 ha)	High-elevation grasslands above 2000 m a.s.l., in a cryic temperature regime, mainly on arenaceous and pelitic-arenaceous formations, also in detrital facies.
L (211.70 ha)	Lithoid outcrops on marly, clayey, arenaceous, and pelitic formations, also in detrital facies.

Land Unit (Area)	Description
W (22.56 ha)	Hydromorphic areas, submerged or intermittently emerged, associated with lake surfaces above 1200 m a.s.l., characterized by peat deposits.

The largest LUs were F/F1 (5348 ha), G/G1 (5989 ha), and I (2409 ha). LUs F/F1 and G/G1 correspond to elevations between 900 and 1300 m and 1300 and 1600 m a.s.l., respectively, and are both predominantly covered by beech forests. LUs G and G1 share similar soil-forming factors, differing mainly in lithology: G is underlain by arenaceous and arenaceous-pelitic formations, whereas G1 is predominantly composed of quaternary deposits, often in glacial detrital facies. LUs E and E1 are both located between 500 and 1400 m a.s.l., differing in lithology: LU E overlays arenaceous and arenaceous-pelitic formations, while LU E1 is developed on quaternary deposits, often in detrital and chaotic facies, and both are covered by basal and submontane forest. LU I is characterized by high-elevation (>1600 m a.s.l.) pasture habitats, mainly developed on arenaceous or glacial deposits. Natural and reforested coniferous forests (LU H) cover 1135 ha, mostly occurring between 900 and 1600 m a.s.l.

The defined LUs are also characterized by varying soil temperature regimes, ranging from mesic to cryic, while the soil moisture regime is generally udic or wetter.

2.3.2 Soil Map Units

According to the USDA-NRCS (USDA-NRCS, 2022) soil classification system, the investigated soils belong to the orders Entisols, Inceptisols, Alfisols, Mollisols, and Histosols, with Inceptisols being the most represented (e.g., Humudepts, Eutrudepts, Dystrudepts, Dystrocryepts, Humicryepts). According to the IUSS (IUSS, 2022) soil classification system, the soils fall within the Reference Soil Groups of Cambisols, Umbrisols, Regosols, Luvisols, Leptosols, Podzols, Stagnosols, and Histosols. Cambisols were the most widespread soil types. Most soils had continuous rock within 50 cm from the surface, corresponding to Lithic subgroups in the USDA-NRCS system and Leptic qualifiers in the IUSS classification. The delineated soil map units (SMUs) are shown in Figure 3 and described in Table 4. The main soil types associated with each SMU are illustrated in Figure 4. Each SMU was associated with one or more land units (LUs), based on observed pedogenetic processes and profile morphology. For instance, LUs F and F1, characterized by beech forests on arenaceous formations between 900 and 1300 m a.s.l., corresponded to SMUs with shallow Dystric Cambisols and Humudepts.

Figure 4. Representative pedological profiles of the different soil map units.

Table 4. Soil map units of the Frignano Regional park and Corno alle Scale regional park, Emilia-Romagna region, Italy. The soil types are classified according to IUSS (2022) and USDA-NRCS (2022) classification systems. In bold type are the most representative soil types within each soil map unit.

Soil Map Unit (Area)	Description	Soil Classification (IUSS 2022 / USDA-NRCS 2022)
A (37.06 ha)	Ap-B-C profiles, weakly developed, moderately deep, with anthropogenically influenced epipedon.	**Hortic or Irragric Fluvic Cambisols/Typic or Oxyaquic Udifluvents**
B (157.80 ha)	Shallow Ap-Bw-C profiles with vertic features and redoximorphic characteristics due to clay accumulation.	**Vertic Eutric Cambisols** (Oxyaquic), Leptic Eutric Cambisols/**Oxyaquic Eutrudepts**, Lithic Eutrudepts
C (932.22 ha)	Shallow to moderately deep Ap-AB-Bw-C profiles, weakly to moderately developed.	**Eutric Cambisols**, Dystric Cambisols/**Typic Eutrudepts**, Typic or Lithic Dystrudepts
D (1813.32 ha)	Shallow O-A-Bw-C profiles with thick organic horizons and weak cambic features.	**Leptic Eutric Cambisols** (Humic), Eutric Cambisols/**Typic Eutrudepts**, Typic Dystrudepts
E (1579.82 ha)	O-A-AB-C and O-A-C profiles, very shallow, weakly developed, stony.	**Leptic Skeletic Umbrisols**, Leptic Skeletic Regosols (Humic)/**Lithic Eutrudepts**, Typic Dystrudepts
E1 (969.08 ha)	Shallow O-A-AB-Bt-C profiles, developed with argic horizons. Some Bw-C profiles.	**Leptic Luvisols**, Epileptic Dystric Cambisols (Humic)/**Typic Hapludalfs**, Typic Dystrudepts, Typic Humudepts
F (2865.55 ha)	Shallow O-A-AB-Bw-C profiles with umbric features and moderate development.	**Leptic Skeletic Dystric Cambisols** (Humic)/**Lithic Humudepts**, Typic Dystrudepts, Lithic or Humic Dystrudepts,
F1 (2482.62 ha)	Moderately deep O-A-AB-Bw-C profiles with umbric epipedon and cambic horizon.	**Leptic Cambic Umbrisols**, Leptic Eutric Cambisols (Humic)/**Typic Humudepts**, Typic Hapludolls, Lithic or Typic Eutrudepts
G (3254.50 ha)	O-A-AB-Bw-C and O-A-AB-C profiles, shallow, stony, weak to moderate development.	**Leptic Skeletic Dystric Cambisols** (Loamic or Arenic), Dystric Leptosols (Humic)/**Typic Dystrudepts**, Lithic Udorthents
G1 (2735.38 ha)	O-A-AB-Bw-C and O-A-AB-C profiles, shallow, skeletal, moderately to poorly developed.	**Leptic Skeletic Dystric Cambisols** (Loamic, Humic), Umbric Cambic Dystric Leptosols/**Typic Dystrudepts**, Humic or Lithic Dystrudepts
H (1135.22 ha)	O-A-Bw-BC-C and O-AE-Bw-BC-C profiles, skeletal, with umbric/mollic epipedons and cambic horizon.	**Epileptic Cambic Skeletic Umbrisols**, Leptic Skeletic Dystric Cambisols (Loamic, Humic), Skeletic Dystric Cambisols (Protospodic)/**Typic or Lithic Humudept**, Humic Dystrudepts, Lithic Hapludolls, s
I (2409.63 ha)	O-AE-Bw-C profiles, shallow, moderately developed, often umbric.	**Leptic Dystric Cambisols** (Humic, Novic, Protospodic), Haplic Podzols (Humic)/**Lithic or Typic Dystrudepts**, Lithic Dystrudepts

Soil Map Unit (Area)	Description	Soil Classification (IUSS 2022 / USDA-NRCS 2022)
I1 (504.82 ha)	O-A-AE-Bw-CR and O-A-(Bw)-BC-Cr profiles, shallow and skeletal, limited development.	Leptic Skeletic Cambisols (Humic), Leptic Colluvic Skeletic Regosols/Lithic Hapludolls, Lithic Humudepts, Lithic or Typic Dystrudepts
J (40.31 ha)	A-(Bw)-C profiles, very shallow in cryic climate, minimal development.	**Epileptic Dystric Regosols** (Gelic), Dystric Leptosols (Gelic)/**Lithic Haplocryolls**, Lithic Dystrocryepts, Lithic Humicryepts,
L (211.70 ha)	Lithoid outcrops with minimal soils or initial pedogenesis (A-C).	**Leptic Regosols**, Lithic Skeletic Leptosols/**Lithic Entisols**
W (22.56 ha)	Hydromorphic profiles (OA-AC-BCg or Ag-ACg-Cg), with organic matter accumulation and water saturation.	**Gleyic (Dystric) Stagnosols** (arenic, colluvic, humic), Hemic or Fibric Leptic Histosols (Gleyic)/**Typic or Aeric Fluviwassents**, Hemic or Terric Haplofibrists, Oxyaquic Udifluvents

At elevations up to 1300 m a.s.l., the SMUs were mainly composed of Inceptisols, with Alfisols (E1) and Mollisols (F1 and H) occurring to a lesser extent, according to the USDA-NRCS (USDA-NRCS, 2022) classification. Under the IUSS (IUSS, 2022) classification, most SMUs were dominated by Cambisols, followed by Umbrisols (E, F1, and H), Regosols (E), and Luvisols (E1). In both classification systems, most SMUs exhibited dystric features, primarily due to the arenaceous nature of the parent material.

Above 1300 m a.s.l., SMUs were predominantly classified as Inceptisols, with Entisols (G and W), Mollisols (I1 and J), and Histosols and subaqueous soils, as Wassent (W) also represented, according to the USDA-NRCS (USDA-NRCS, 2022).

According to the IUSS (IUSS, 2022) classification, greater pedodiversity in terms of Soil Reference Groups was observed in SMUs above 1300 m a.s.l. compared to those at lower elevations. Overall, SMUs below 1300 m a.s.l. were dominated by moderately developed soils such as Cambisols and Inceptisols, while higher-elevation areas (>1300 m a.s.l.) exhibited greater pedodiversity, with increased occurrence of Leptosols, Podzols, and Histosols, reflecting harsher climatic conditions and lithological constraints.

2.3.3 Soil Physicochemical Properties Across Soil Map Units and Land Units

The physicochemical characterization of the soils sampled within the soil map units (SMUs) highlights the diversity of pedological conditions across the study area and provides support for the delineation of land units (LUs). The results are summarized in **Table 5**.

Table 5. Physicochemical properties of soils in the soil map units (SMUs) identified within the Frignano and Corno alle Scale Regional Parks. For each SMU, mean values and standard deviations (SD) are reported for particle-size distribution (sand, silt, and clay), soil pH, exchangeable calcium (Ca_{exch}), base saturation (BS), total nitrogen (Ntot), and organic carbon (OC). SMUs are spatially associated with land units (LUs) described in **Table 3**.

SMU	Sand	Silt	Clay	pH	Ca_{exch}	BS	Ntot	OC	
		g/kg			cmol(+)/kg		%		
B	75	625	300	7.3	9.6	71.0	0.3	2.9	mean
	29	74	87	0.7	2.9	11.6	0.3	3.1	SD
C	39	706	256	7.9	12.3	48.5	0.4	3.4	mean
	9	57	65	0.6	2.4	2.2	0.3	4.3	SD
D	170	505	325	5.1	2.3	56.7	0.2	2.0	mean
	199	159	111	0.2	0.7	20.3	0.1	2.2	SD
E	188	706	106	5.6	7.8	50.5	0.3	3.3	mean
	41	33	13	0.8	3.9	8.1	0.2	3.6	SD
E1	60	748	192	7.7	14.1	55.3	0.2	2.8	mean
	21	69	75	0.65	3.1	10.1	0.1	3.0	SD
F	304	573	123	4.9	9.2	20.7	0.3	4.1	mean
	47	51	24	0.1	1.1	8.3	0.1	2.4	SD
F1	544	398	58	5.3	4.5	40.2	0.4	4.5	mean
	11	8	13	0.4	1.0	3.4	0.5	5.7	SD
G	596	352	52	4.6	4.6	13.0	0.1	3.0	mean
	43	40	13	0.4	2.3	3.9	0.1	2.2	SD
G1	615	327	58	4.7	0.7	25.4	0.2	3.3	mean
	28	34	11	0.3	0.9	13.2	0.1	2.3	SD
H	572	299	129	4.4	0.2	13.6	0.2	2.4	mean

SMU	Sand	Silt	Clay	pH	Ca_{exch}	BS	Ntot	OC	
		g/kg			$cmol_{(+)}/kg$		%		
	51	59	16	0.3	0.0	3.5	0.1	1.3	SD
I	531	382	87	4.7	0.4	8.7	0.3	3.6	mean
	99	66	43	0.3	0.6	9.7	0.3	2.9	SD
I1	798	195	8	6.1	13.3	99.1	0.4	6.1	mean
	8	5	3	0.2	0.8	0.2	0.1	1.7	SD
J	670	284	45	6.1	12.3	93.2	0.3	3.4	mean
	10	12	3	0.1	1.1	0.6	0.0	0.4	SD
W	674	310	17	5.0	1.4	61.0	0.1	1.6	mean
	89	96	12	0.2	0.3	5.1	0.0	0.7	SD

Soil texture varied significantly among SMUs, reflecting differences in parent materials, slope gradients, and geomorphological settings within the corresponding LUs. For example, LU I1 and J, located at higher elevations (>1600 m a.s.l.), are characterized by soils with high sand content (798 and 670 g/kg, respectively) and minimal clay content, indicative of coarse material accumulation and limited pedogenesis. Conversely, LU D and B, situated in lower-elevation areas on finer substrates (e.g., marly or clayey formations), presented higher clay content (325 and 300 g/kg, respectively) consistent with higher weathering intensity or clay illuviation.

Soil reaction (pH) ranged from strongly acidic to slightly alkaline. Acidic conditions (pH < 5.5) dominated in SMUs corresponding to LUs G, H, and I, all located on steep slopes developed on arenaceous or glacial parent materials, often under beech, coniferous forests, and blueberry groves. In contrast, SMUs associated with LU B, C, and E1, developed on marly and clay-rich substrates or colluvial deposits, showed near-neutral to alkaline pH values (up to pH 7.9), suggesting limited leaching and a higher base status.

Exchangeable calcium (Ca_{exch}) followed a similar trend, with the highest concentrations recorded in LU C and E1 in addition to the presence of high-altitude Mollisols (J and I1), from 12.3 to 14.1 $cmol_{(+)}/kg$), while LU H had the lowest values (<1.5 $cmol_{(+)}/kg$), reflecting the combined influence of lithology and clime.

Base saturation (BS) further confirmed the contrast between eutric units (e.g., LU I1, J, E1), where BS exceeded 90%, and dystric units (e.g., LU G, H, I), with BS values below 15%. This pattern underscores the relevance of LU classification in predicting soil chemical fertility and ecological functioning.

The organic carbon (OC) and total nitrogen (Ntot) content were generally consistent with vegetation cover and climatic conditions. Generally, they decreased along the soil depth. Soils from LU I1 (Lithic Hapludoll) with limited anthropic disturbance and cooler microclimates showed the highest OC values (6.1%), confirming their role as organic matter reservoirs. In contrast, lower OC values were recorded in LU W and H, possibly due to hydromorphism and advanced leaching under coniferous cover.

These findings demonstrate that the land units (LUs), as delineated through the integration of soil-forming factors, also represent ecologically coherent areas in terms of soil physicochemical properties. The spatial correspondence between LUs and SMUs provides a robust framework for interpreting soil variability and pedodiversity and offers a valuable basis for monitoring, conservation planning, and ecosystem service assessment.

2.4 DISCUSSION

This study made efforts to propose a spatial classification of the Frignano and Corno alle Scale Regional Parks into land units (LUs), based on key soil-forming factors: land use, parent material, morphology, and climate. Soils, as living and non-renewable resources, play a crucial role in the provision of ecosystem services and are essential for biodiversity conservation, particularly in mountain landscapes (Costantini et al., 2022; Buol et al., 2011; CHauvier et al., 2021; Halleux, 2024).

Originally developed for land use planning (Vacca et al., 2014; Bastian, 2000; Di Lisio & Russo, 2010; Şahin & Bekişoğlu, 2009), the LU concept has also proven effective for field survey stratification and environmental evaluation (Bockheim et al., 2014; Adamchuk et al., 2011;

Bouma, 2020). Since each LU combines specific environmental and anthropogenic features, soils within a given LU are expected to share similar characteristics, thus reducing survey costs while improving representativeness.

In this study, 16 LUs were delineated. Despite attempts to cluster homogeneous zones, many soil map units (SMUs) included multiple soil types, consistent with the high pedodiversity commonly reported in mountain regions (Vittori Antisari et al., 2023; Vacek et al., 2020; Ibáñez & Feoli, 2013; Costantini & L'Abate, 2016). The fine-scale pedological heterogeneity observed in the study area is largely the result of a complex interplay between morphodynamic processes, microscale topographic variability, and the lasting effects of historical land use and glacial history. Specifically, in mountainous regions such as the northern Apennines, soil formation is heavily influenced by local slope instability, landslides, cryoturbation, and colluvial transport. These processes can lead to abrupt variations in soil depth, texture, and horizon development over very short distances (Irl et al., 2015; Garcia-Pausas et l., 2007). Moreover, microrelief features, including convex and concave landforms, depressions, and rocky outcrops, alter the redistribution of water, organic matter, and fine particles. This, in turn, fosters divergent soil development pathways even within the same LU (Shrestha et al., 2014; Alexander et al., 2016). The legacy of anthropogenic land use, such as historical coppicing, charcoal production, and intensive grazing, has also left lasting imprints on soil profiles, affecting their chemical and physical properties for decades or even centuries (Dufour et al., 2006; Ballabio, 2009). Additionally, glacial history plays a significant role: soils in previously glaciated areas are typically younger, less developed, and formed from heterogeneous parent materials such as glacial till and debris flows (Herbst et al., 2012; Geitner et al., 2011). Together, these interacting factors create a patchwork of soil types and developmental stages, even within areas that appear homogeneous at a broader scale. This intrinsic fine-scale heterogeneity underscores the limitations of coarse-resolution soil mapping and highlights the importance of adaptive survey frameworks, such as the LU-based approach used in this study, which can more effectively capture and interpret variability within land units.

Most soils in the study area were characterized by incipient development and belonged to the Inceptisols/Cambisols orders, with Dystrudepts/Dystric Cambisols being the most frequent. At higher elevations, soils with umbric epipedons were classified as Humudepts/Umbrisols, while Eutrudepts/Eutric Cambisols predominated in more base-rich substrates at lower elevations. The widespread presence of Cambisols across all lithologies suggests that pedogenesis may be constrained by steep slopes (>25% in 82% of the area) and by historical land use pressures, such as coppicing, grazing, and deforestation, which have promoted erosion and limited profile development (Fazlollahi Mohammadi et al., 2016; Badia et al., 2013; RER, 2012; RER, 2022; Agnoletti et l., 2022; Vacca et al., 2017; Quinton et al., 1997; Mohammad & Adam, 2010). Our findings align with the overarching patterns observed across Italian mountain regions, where Inceptisols/Cambisols dominate, especially over steep, sandy substrates (northern and central Apennines), with Leptosols and Podzols increasingly present at higher elevations (Vittori Antisari et al., 2023; De Feudis et al., 2025; Costantini et al., 2013). Globally, mountainous landscapes are known for high pedodiversity at fine spatial scales, driven by steep geomorphological gradients and microtopographic variability; such heterogeneity has been documented across the European biogeographical regions (Ibáñez et al., 2013). This underlines the relevance of our approach in capturing such diversity through a stratified analysis. In fact, in some low- to mid-elevation sites, more developed soils such as Hapludolls and Luvisols indicated possible pathways of pedogenic evolution under favorable morphological conditions. In contrast, cryic soils (e.g., Dystrocryepts, Haplocryolls) showed variable developmental stages despite uniform vegetation, likely influenced by microtopography or frost action. Hydromorphic areas (LU W), although limited in extent, revealed substantial pedodiversity, including Udifluvents, Histosols, and Fluviwassents, shaped by vegetation gradients and water saturation regimes.

In addition to taxonomic classification, the physicochemical properties of the soils (Table 5) provide valuable insights into pedogenetic processes across different LUs. Soils developed at lower elevations and on more stable surfaces—such as those in LUs B, C, and E1—showed neutral to slightly alkaline pH values (up to 7.9), high exchangeable calcium (up to 14.1 $cmol_{(+)}/kg$), and base saturation exceeding 50%. These conditions suggest low leaching intensity and a high weathering status of base-rich substrates, consistent with their classification as Eutrudepts or Luvisols (Tóth et al., 2013). By contrast, mid- and high-elevation soils (e.g., LUs F, G, H) were more acidic (pH 4.4–5.3), with lower Ca availability and base saturation, reflecting leaching-driven acidification and organic matter accumulation under forest cover—typical features of Dystrudepts and Umbrisols (Van Miegroet & Cole, 1985; Certini, 2005). In high-elevation units (e.g., I, J, W), coarse textures, shallow profiles, and low nutrient levels were prevalent, consistent with cryic or hydromorphic soils such as Cryepts, Histosols, and Fluviwassents (Bockheim, 2015; Schaetzl & Anderson, 2005; Egli et al., 2008). These patterns confirm the strong link between soil properties and the soil-forming factors used in LU delineation, supporting the LU approach as a cost-effective method to capture landscape-level soil variability (Arrouays et al., 2017; GSBI, 2020).

The combination of pre-existing soil data and newly collected data provided a solid foundation for validating the proposed LU-based soil map. While the earlier profiles ensured long-term coverage of the study area, the newly excavated soil profiles filled gaps in environmentally underrepresented contexts. This integrated dataset allowed for a realistic assessment of internal variability within the LUs and improved the overall reliability of the final classification. All 112 soil profiles were used to validate the LU-based soil map, ensuring that each LU was supported by field observations and that the map accurately reflected actual soil variability. This approach maximized the representativeness of the sampling network and enabled the assessment of pedodiversity across contrasting geomorphological and ecological settings.

However, it is important to mention that although this study did not include a quantitative assessment of the geometric accuracy of the LUs boundary or their internal homogeneity, their delineation was carried out at an operational scale of 1:25,000. This scale is appropriate for regional planning and the design of stratified soil surveys in mountainous contexts. The validity of the LU boundaries was supported by field verification using 112 georeferenced soil profiles. Field observations confirmed that most soils within a given LU shared similar morphological, physical, and chemical characteristics, consistent with the factors used in the delineation process. The consistency between expected and observed characteristics supports the reliability of our approach. The internal consistency of the LUs was also indirectly supported by the observed differentiation in key physico-chemical soil properties such as pH, base saturation and texture (Table 5) indicating that the classification effectively captured relevant pedogenetic variability. We acknowledge that a more formal accuracy assessment, combining targeted field validation with high-resolution techniques (e.g., remote sensing) and predictive statistical analyses (e.g., digital soil mapping), would strengthen the method and further enhance its cost-effectiveness and replicability in other protected and mountainous landscapes.

Overall, the identified land units and associated soil patterns offer a robust framework for environmental monitoring, conservation planning, and understanding of soil responses to climatic and anthropogenic drivers. The LU-based approach proves especially suitable for mountain landscapes, where traditional grid or random sampling methods are often impractical or inefficient.

2.5 CONCLUSIONS

GIS-based land units (LUs) model, defined by soil-forming factors, can improve stratified soil surveys and ecological monitoring in complex mountain landscapes.

In our case study, 16 LUs were identified, with LUs F/F1 (5348 ha), G/G1 (5989 ha), and I (2409 ha) as the largest ones. The soil analysis showed diverse conditions across LUs. For example, sandy soil particles dominated LUs I1 and J, with values ranging between 670 and 798 g/kg, while LUs D and B had more clay (from 300 to 325 g/kg) due to marly or clayey substrates. Soil pH varied widely, with acidic conditions in steep, forested areas (LUs G, H, I) and neutral to alkaline pH in LUs on clay-rich or colluvial soils (B, C, E1). Organic carbon content showed highest values in LU I1 (6.1%) due to the dense vegetation and minimal human impact.

Our approach can minimize soil sampling costs compared to grid sampling, considering that, to obtain the soil map, the soil profiles must be dug, and each genetic horizon described and sampled, then classified. In addition to guiding new field investigations, our framework can integrate existing soil data from literature and legacy surveys, thus maximizing the value of prior efforts. Furthermore, beyond its scientific applications, this approach could represent a valuable decision-support tool for park authorities, enabling more informed planning, conservation prioritization, and ecosystem service mapping in protected areas.

The lack of boundary accuracy in areas with complex microtopography, the limited validation in inaccessible zones, and some internal heterogeneity within LUs, indicating great pedodiversity, can be considered the major limitations. Future enhancements can incorporate satellite-derived indicators (e.g., NDVI) and machine learning approaches from digital soil mapping which could improve spatial detail, enhance boundary accuracy, and provide soil properties predictions and ecosystem services across the study area.

Mapping ecosystem services is recognized as vital for conservation planning, managing multifunctional landscapes and increasing protected areas according to Biodiversity 2030 European law. LUs model lays the foundation for the development of derived maps (i.e., carbon storage, water erosion, hydro-pedo-geological risks), providing a spatial structure that can support ecosystem service assessment—enabling efficient identification of hotspots, trade-offs, and conservation priorities.

We conclude that the LU-based method is a practical and replicable tool with strong potential for advancing soil-informed environmental management, biodiversity protection, and ecosystem service evaluation in mountain protected areas.

SUPPLEMENTARY MATERIALS

The following supporting information can be downloaded at: https://www.mdpi.com/article/10.3390/land14081683/s1, Table S1: Location of soil profiles.

AUTHOR CONTRIBUTIONS

Conceptualization, G.V. and L.V.A.; methodology, G.V. and L.V.A.; validation, L.V.A.; formal analysis, W.T. and M.G.; investigation, M.D.F. and W.T.; resources, L.V.A.; data curation, W.T., G.V. and L.V.A.; writing—original draft preparation, M.D.F.; writing—review and editing, M.D.F. and L.V.A.; visualization, W.T.; supervision, L.V.A.; funding acquisition, L.V.A. All authors have read and agreed to the published version of the manuscript.

FUNDING

This research was funded under the National Recovery and Resilience Plan (NRRP), Mission 4 Component 2 Investment 1.4—Call for tender No. 3138 of 16 December 2021, rectified by Decree n.3175 of 18 December 2021 of Italian Ministry of University and Research funded by the European Union—NextGenerationEU; Project code CN_00000033, Concession Decree No. 1034 of 17 June 2022 adopted by the Italian Ministry of University and Research, CUPJ33C22001190001, Project title "National Biodiversity Future Center—NBFC".

DATA AVAILABILITY STATEMENT

The raw data supporting the conclusions of this article will be made available by the authors on request.

ACKNOWLEDGMENTS

We would like to thank Hugo Ludlam for his thorough English editing of the entire manuscript.

CONFLICTS OF INTEREST

The authors declare no conflicts of interest.

APPENDIX A

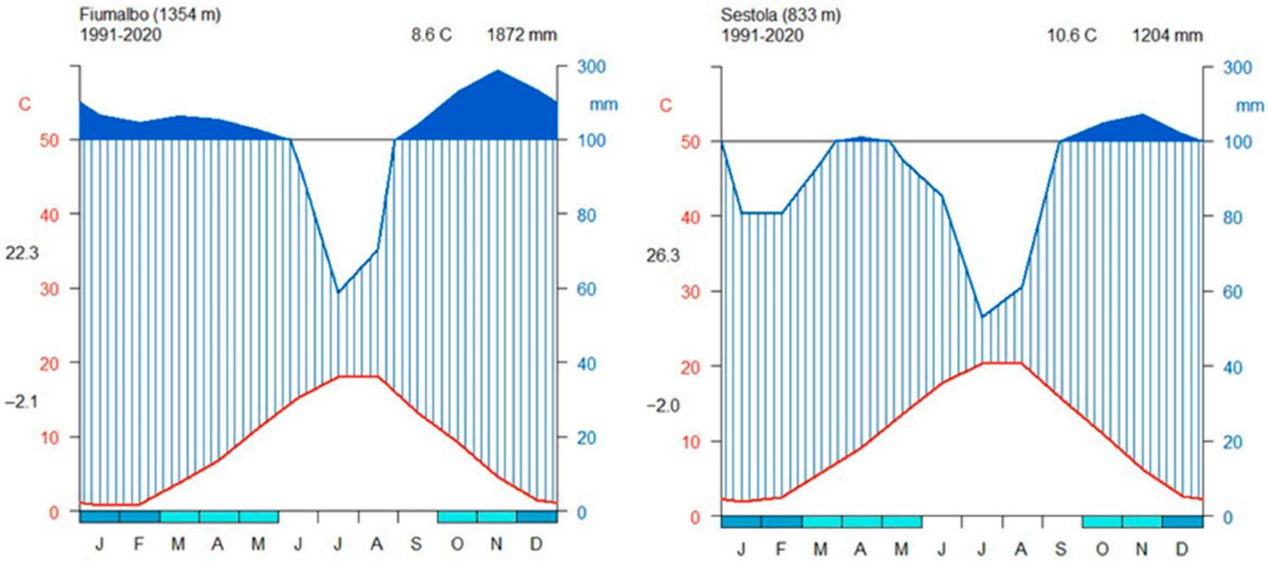

Figure A1. Bagnouls Gaussen climate diagrams referring to the thermopluviometric stations of Fiumalbo (1354 m a.s.l.) and Sestola (833 m a.s.l.).

REFERENCES

Adamchuk, V. I., Rossel, R. A. V., Marx, D. B., & Samal, A. K. (2011). Using targeted sampling to process multivariate soil sensing data. *Geoderma*, *163*(1-2), 63-73.

Adhikari, K., & Hartemink, A. E. (2016). Linking soils to ecosystem services—A global review. *Geoderma*, *262*, 101-111.

Agnoletti, M., Piras, F., Venturi, M., & Santoro, A. (2022). Cultural values and forest dynamics: The Italian forests in the last 150 years. *Forest Ecology and Management*, *503*, 119655.

Alexander, C., Deák, B., & Heilmeier, H. (2016). Micro-topography driven vegetation patterns in open mosaic landscapes. *Ecological indicators*, *60*, 906-920.

Anderson, S. (2005). *Soils: Genesis and geomorphology*. Cambridge University Press.

ARPAE. Tabelle Climatologiche. 2024. Available online: **https://www.arpae.it/it/temi-ambientali/clima/dati-e-indicatori/tabelle-climatiche** (accessed on 13 June 2025).

Arrouays, D., Leenaars, J. G., Richer-de-Forges, A. C., Adhikari, K., Ballabio, C., Greve, M., ... & Rodriguez, D. (2017). Soil legacy data rescue via GlobalSoilMap and other international and national initiatives. *GeoResJ*, *14*, 1-19.

Badía, D., Martí, C., Aznar, J. M., & León, J. (2013). Influence of slope and parent rock on soil genesis and classification in semiarid mountainous environments. *Geoderma*, *193*, 13-21.

Ballabio, C. (2009). Spatial prediction of soil properties in temperate mountain regions using support vector regression. *Geoderma*, *151*(3-4), 338-350.

Bastian, O. (2000). Landscape classification in Saxony (Germany)—a tool for holistic regional planning. *Landscape and urban planning*, *50*(1-3), 145-155.

Bockheim, J. G. (2014). Cryosols as a three-part system. In *Cryopedology* (pp. 7-21). Cham: Springer International Publishing.

Bockheim, J. G., Gennadiyev, A. N., Hartemink, A. E., & Brevik, E. C. (2014). Soil-forming factors and Soil Taxonomy. *Geoderma*, *226*, 231-237.

Bouma, J. (2020). Contributing pedological expertise towards achieving the United Nations sustainable development goals. *Geoderma*, *375*, 114508.

Brevik, E. C., Calzolari, C., Miller, B. A., Pereira, P., Kabala, C., Baumgarten, A., & Jordán, A. (2016). Soil mapping, classification, and pedologic modeling: History and future directions. *Geoderma*, *264*, 256-274.

Brombin, V., Mistri, E., De Feudis, M., Forti, C., Salani, G. M., Natali, C., ... & Bianchini, G. (2020). Soil carbon investigation in three pedoclimatic and agronomic settings of Northern Italy. *Sustainability*, *12*(24), 10539.

Buol, S. W., Southard, R. J., Graham, R. C., & McDaniel, P. A. (2011). *Soil genesis and classification*. John Wiley & Sons.

Certini, G. (2005). Effects of fire on properties of forest soils: a review. *Oecologia*, *143*(1), 1-10.

Chakraborty, A. (2021). Mountains as vulnerable places: a global synthesis of changing mountain systems in the Anthropocene. *GeoJournal*, *86*(2), 585-604.

Chape, S., Harrison, J., Spalding, M., & Lysenko, I. (2005). Measuring the extent and effectiveness of protected areas as an indicator for meeting global biodiversity targets. *Philosophical Transactions of the Royal Society B: Biological Sciences*, *360*(1454), 443-455.

Chauvier, Y., Thuiller, W., Brun, P., Lavergne, S., Descombes, P., Karger, D. N., ... & Zimmermann, N. E. (2021). Influence of climate, soil, and land cover on plant species distribution in the European Alps. *Ecological monographs*, *91*(2), e01433.

Chen, S., Arrouays, D., Mulder, V. L., Poggio, L., Minasny, B., Roudier, P., ... & Walter, C. (2022). Digital mapping of GlobalSoilMap soil properties at a broad scale: A review. *Geoderma*, *409*, 115567.

Copernicus. CORINE Land Cover (from 1990 to 2018). 2021. Available online: **https://land.copernicus.eu/user-corner/technical-library/corine-land-cover-nomenclature-guidelines/html/** (accessed on 13 June 2025)

Costantini, E. A., & L'Abate, G. (2016). Beyond the concept of dominant soil: Preserving pedodiversity in upscaling soil maps. *Geoderma*, *271*, 243-253.

Costantini, E. A., & Lorenzetti, R. (2013). Soil degradation processes in the Italian agricultural and forest ecosystems. *Italian Journal of Agronomy*, *8*(4), e28.

Costantini, E. A., & Mocali, S. (2022). Soil health, soil genetic horizons and biodiversity#. *Journal of Plant Nutrition and Soil Science*, *185*(1), 24-34.

Costantini, E. A., Barbetti, R., Fantappie, M., L'Abate, G., Lorenzetti, R., & Magini, S. (2013). Pedodiversity. In *The soils of Italy* (pp. 105-178). Dordrecht: Springer Netherlands.

D'Amico, M. E., Pintaldi, E., Sapino, E., Colombo, N., Quaglino, E., Stanchi, S., ... & Freppaz, M. (2020). Soil types of Aosta Valley (NW-Italy). *Journal of Maps*, *16*(2), 755-765.

De Feudis, M., Cardelli, V., Massaccesi, L., Bol, R., Willbold, S., Cocco, S., ... & Agnelli, A. (2016). Effect of beech (Fagus sylvatica L.) rhizosphere on phosphorous availability in soils at different altitudes (Central Italy). *Geoderma*, *276*, 53-63.

De Feudis, M., Falsone, G., Vianello, G., Agnelli, A., & Vittori Antisari, L. (2022). Soil organic carbon stock assessment in forest ecosystems through pedogenic horizons and fixed depth layers sampling: What's the best one?. *Land Degradation & Development*, *33*(9), 1446-1458.

De Feudis, M., Massaccesi, L., Poesio, C., Antisari, L. V., Bol, R., & Agnelli, A. (2025). Seasonal effects of altitude and vegetation on litter and organic carbon in deciduous and coniferous forest soils. *Geoderma*, *459*, 117382.

Dell'Abate, M. T., Giovannini, C., Pontalti, F., Vianello, G., & Vittori Antisari, L. (2007). Caratterizzazione quali-quantitativa della sostanza organica degli epipedon di suoli bruni acidi dell'appennino emiliano sotto bosco di latifoglie e di conifere. In *Atti Convegno Nazionale Società Italiana di Scienze del Suolo "Suolo Ambiente Paesaggio",* (Vol. 1, pp. 332-342). Società Italiana di Scienza del Suolo.

Di Lisio, A., & Russo, F. (2010). Thematic maps for land-use planning and policy decisions in the Calaggio stream catchment area. *Journal of Maps*, *6*(1), 68-83.

Dufour, A., Gadallah, F., Wagner, H. H., Guisan, A., & Buttler, A. (2006). Plant species richness and environmental heterogeneity in a mountain landscape: effects of variability and spatial configuration. *Ecography*, *29*(4), 573-584.

Egli, M., Mirabella, A., & Sartori, G. (2008). The role of climate and vegetation in weathering and clay mineral formation in late Quaternary soils of the Swiss and Italian Alps. *Geomorphology*, *102*(3-4), 307-324.

Falsone, G., Marinari, S., Vittori Antisari, L., & Vianello, G. (2015). Soil processes related to organic matter modifications following Douglas-fir mature reforestation. *Biology and Fertility of Soils*, *51*(3), 277-287.

Fao, F. A. O. S. T. A. T. (2018). Food and agriculture organization of the United Nations. *Rome, URL: http://faostat. fao. org*, *403*.

Fazlollahi Mohammadi, M., Jalali, S. G. H., Kooch, Y., & Said-Pullicino, D. (2016). Slope gradient and shape effects on soil profiles in the northern mountainous forests of Iran. *Eurasian soil science*, *49*(12), 1366-1374.

Fisher, R. A., & Koven, C. D. (2020). Perspectives on the future of land surface models and the challenges of representing complex terrestrial systems. *Journal of Advances in Modeling Earth Systems*, *12*(4), e2018MS001453.

Garcia-Pausas, J., Casals, P., Camarero, L., Huguet, C., Sebastia, M. T., Thompson, R., & Romanya, J. (2007). Soil organic carbon storage in mountain grasslands of the Pyrenees: effects of climate and topography. *Biogeochemistry*, *82*(3), 279-289.

Gee, G. W., & Bauder, J. W. (1986). Particle-size analysis. *Methods of soil analysis: Part 1 Physical and mineralogical methods*, *5*, 383-411.

Geitner, C., Tusch, M., Meißl, G., Kringer, K., & Wiegand, C. (2011). Effects of topography on the spatial distribution of soils: basic considerations on interdependencies and data sources with examples from the Eastern Alps. *Zeitschrift fur Geomorphologie Supplement*, *55*(3), 127-146.

GSBI, S. (2020). State of knowledge of soil biodiversity-Status, challenges and potentialities.

Halleux, V. (2024) *Soil Monitoring and Resilience (Soil Monitoring Directive)*; European Parliament: Strasbourg, France.

Hartemink, A. E., Krasilnikov, P., & Bockheim, J. G. (2013). Soil maps of the world. *Geoderma*, *207*, 256-267.

Herbst, P., Gross, J., Meer, U., & Mosimann, T. (2012). Geomorphographic terrain classification for predicting forest soil properties in Northwestern Switzerland.

Ibáñez, J. J., & Feoli, E. (2013). Global relationships of pedodiversity and biodiversity. *Vadose Zone Journal*, *12*(3), 1-5.

Ibañez, J. J., De-Alba, S., Lobo, A., & Zucarello, V. (1998). Pedodiversity and global soil patterns at coarse scales (with discussion). *Geoderma*, *83*(3-4), 171-192.

Ibáñez, J. J., Zinck, J. A., & Dazzi, C. (2013). Soil geography and diversity of the European biogeographical regions. *Geoderma*, *192*, 142-153.

Irl, S. D., Harter, D. E., Steinbauer, M. J., Gallego Puyol, D., Fernández-Palacios, J. M., Jentsch, A., & Beierkuhnlein, C. (2015). Climate vs. topography–spatial patterns of plant species diversity and endemism on a high-elevation island. *Journal of Ecology*, *103*(6), 1621-1633.

IUSS, W. (2022). World reference base for soil resources. International soil classification system for naming soils and creating legends for soil maps. *Vienna: International Union of Soil Sciences/IUSS*, 236-236.

Jenkins, C. N., & Joppa, L. (2009). Expansion of the global terrestrial protected area system. *Biological conservation*, *142*(10), 2166-2174.

Kiryushin, V. I. (2020). Methodology for integrated assessment of agricultural land. *Eurasian Soil Science*, *53*(7), 960-967.

Locatelli, B., Lavorel, S., Sloan, S., Tappeiner, U., & Geneletti, D. (2017). Characteristic trajectories of ecosystem services in mountains. *Frontiers in Ecology and the Environment*, *15*(3), 150-159.

Macchi, M. (2010). *Mountains of the World: ecosystem services in a time of global and climate change. Seizing opportunities: meeting challenges* (pp. vi+-21).

Marinari, S., Bonifacio, E., Moscatelli, M. C., Falsone, G., Antisari, L. V., & Vianello, G. (2013). Soil development and microbial functional diversity: Proposal for a methodological approach. *Geoderma*, *192*, 437-445.

McBratney, A. B., Odeh, I. O., Bishop, T. F., Dunbar, M. S., & Shatar, T. M. (2000). An overview of pedometric techniques for use in soil survey. *Geoderma*, *97*(3-4), 293-327.

Mikhailova, E. A., Zurqani, H. A., Post, C. J., Schlautman, M. A., & Post, G. C. (2021). Soil diversity (pedodiversity) and ecosystem services. *Land*, *10*(3), 288.

Mohammad, A. G., & Adam, M. A. (2010). The impact of vegetative cover type on runoff and soil erosion under different land uses. *Catena*, *81*(2), 97-103.

Odgers, N. P., Sun, W., McBratney, A. B., Minasny, B., & Clifford, D. (2014). Disaggregating and harmonising soil map units through resampled classification trees. *Geoderma*, *214*, 91-100.

Perrigo, A., Hoorn, C., & Antonelli, A. (2020). Why mountains matter for biodiversity. *Journal of Biogeography*, *47*(2), 315-325.

Price, M. F. (2016). Mountains move up the European agenda. *Mountain Research and Development*, *36*(3), 376-379.

Quinton, J. N., Edwards, G. M., & Morgan, R. P. C. (1997). The influence of vegetation species and plant properties on runoff and soil erosion: results from a rainfall simulation study in south east Spain. *Soil Use and Management*, *13*(3), 143-148.

RER. 2017—Coperture Vettoriali Uso del Suolo di Dettaglio—Edizione 2020. 2020a. Available online: **https://metasfera.regione.emilia-romagna.it/ricerca_metadato?uuid=r_emiro:2020-04-06T135318** (accessed on 13 June 2025)

RER. Banca Dati Geologica 1:10,000. 2020b. Available online: **https://metasfera.regione.emilia-romagna.it/ricerca_metadato?uuid=r_emiro:2017-06-12T113543** (accessed on 13 June 2025).

RER. Foto Aeree del Volo IGMI GAI 1954-1955. (2012) Available online: **https://geoportale.regione.emilia-romagna.it/applicazioni-gis/regione-emilia-romagna/cartografia-di-base/cartografia-storica/foto-aeree-del-volo-igmi-gai-1954-1955** (accessed on 13 June 2025).

RER. Ortofoto RER 1976-1978. (2022) Available online: **https://geoportale.regione.emilia-romagna.it/catalogo/dati-cartografici/cartografia-di-base/immagini/layer-8** (accessed on 13 June 2025).

Rossiter, D. G. (2016). Digital soil resource inventories: status and prospects in 2015. *Digital soil mapping across paradigms, scales and boundaries*, 275-286.

Şahin, Ş., & Bekişoğlu, Ü. (2009). Landscape planning and management strategies for the Zir Valley, near Ankara, Turkey. *Environmental geology*, *57*(2), 297-305.

Salazar, S., Ochoa, A., & McCarthy, P. J. (2023). How the visit of pedologist Hans Jenny to Colombia (1946–1947) contributed to the theory of soil-forming factors. *Geoderma*, *437*, 116575.

Schoeneberger, P.J.; Wysocki, D.A.; Benham, E.C. (2012) *Soil Survey Staff Field Book for Describing and Sampling Soils, Version 3.0*; Natural Resources Conservation Service, National Soil Survey Center: Lincoln, NE, USA

Shrestha, D. P., Suriyaprasit, M., & Prachansri, S. (2014). Assessing soil erosion in inaccessible mountainous areas in the tropics: The use of land cover and topographic parameters in a case study in Thailand. *Catena*, *121*, 40-52.

Smiraglia, D., Capotorti, G., Guida, D., Mollo, B., Siervo, V., & Blasi, C. (2013). Land units map of Italy. *Journal of Maps*, *9*(2), 239-244.

Sonneveld, M. P. W., Hack-ten Broeke, M. J. D., Van Diepen, C. A., & Boogaard, H. L. (2010). Thirty years of systematic land evaluation in the Netherlands. *Geoderma*, *156*(3-4), 84-92.

Stoorvogel, J. J., Bakkenes, M., Temme, A. J., Batjes, N. H., & ten Brink, B. J. (2017). S-world: A global soil map for environmental modelling. *Land Degradation & Development*, *28*(1), 22-33.

Tagil, S., & Jenness, J. (2008). GIS-based automated landform classification and topographic, landcover and geologic attributes of landforms around the Yazoren Polje, Turkey.

Tóth, G., Jones, A., Montanarella, L., Alewell, C., Ballabio, C., Carre, F., ... & YIGINI, Y. (2013). *LUCAS Topoil Survey-methodology, data and results*.

USDA-NRCS (2022). *Soil Survey Staff Keys to Soil Taxonomy*, 13th ed.; USDA-NRCS: Washington, DC, USA.

Vacca, A., Aru, F., & Ollesch, G. (2017). Short-term Impact of Coppice Management on Soil in a Quercus ilex l. Stand of Sardinia. *Land Degradation & Development*, *28*(2), 553-565.

Vacca, A., Loddo, S., Melis, M. T., Funedda, A., Puddu, R., Verona, M., ... & Schirru, P. (2014). A GIS based method for soil mapping in Sardinia, Italy: A geomatic approach. *Journal of environmental management*, *138*, 87-96.

Vacek, O., Vašát, R., & Borůvka, L. (2020). Quantifying the pedodiversity-elevation relations. *Geoderma*, *373*, 114441.

Van Miegroet, H., & Cole, D. W. (1985). Acidification Sources in Red Alder and Douglas Fir Soils-Importance of Nitrification. *Soil Science Society of America Journal*, *49*(5), 1274-1279.

Vincent, S., Lemercier, B., Berthier, L., & Walter, C. (2018). Spatial disaggregation of complex Soil Map Units at the regional scale based on soil-landscape relationships. *Geoderma*, *311*, 130-142.

Vittori Antisari, L., Agnelli, A., Corti, G., Falsone, G., Ferronato, C., Marinari, S., & Vianello, G. (2018). Modern and ancient pedogenesis as revealed by Holocene fire-Northern Apennines, Italy. *Quaternary International*, *467*, 264-276.

Vittori Antisari, L., Falsone, G., Carbone, S., Marinari, S., & Vianello, G. (2015). Douglas-fir reforestation in North Apennine (Italy): Performance on soil carbon sequestration, nutrients stock and microbial activity. *Applied Soil Ecology*, *86*, 82-90.

Vittori Antisari, L., Marinari, S., Dell'Abate, M. T., Baffi, C., & Vianello, G. (2011). Plant cover and epipedon SOM stability as factors affecting brown soil profile development and microbial activity. *Geoderma*, *161*(3-4), 212-224.

Vittori Antisari, L., Trenti, W., Buscaroli, A., Falsone, G., Vianello, G., & De Feudis, M. (2022). Pedodiversity and organic matter stock of soils developed on sandstone formations in the Northern Apennines (Italy). *Land*, *12*(1), 79.

Vittori Antisari, L., Trenti, W., De Feudis, M., Bianchini, G., & Falsone, G. (2021). Soil quality and organic matter pools in a temperate climate (Northern Italy) under different land uses. *Agronomy*, *11*(9), 1815.

Vittori Antisari, L.; Vianello, G.; Pontalti, F.; Lorito, S.; Gherardi, M. (2008) Land use effects on organic matter in brown soils of the emilian apennines. In *the Soils Tomorrow: Soils Changing in a Changing World, Proceedings of the 5th International Congress of the European Society for Soil Conservation "Soils Changing in a Changing World: The Soils of Tomorrow", Palermo, Italy, 25–30 June 2007*; Catena Verlag: Reiskirchen, Germany; pp. 311–328.

Winegardner, D. L. (1995). *An Introduction to Soils for Environmental Professionals*. Routledge.

Yaalon, D. H. (1995). The soils we classify Essay review of recent publications on soil taxonomy. *Catena*, *24*(4), 233-241.

Zonneveld, I. S. (1989). The land unit—a fundamental concept in landscape ecology, and its applications. *Landscape ecology*, *3*(2), 67-86.

3. MAPPING SOILS IN TEMPERATE HUMID MOUNTAINS: RANDOM FORESTS HIGHLIGHTS OPTIMAL COVARIATES IN NORTHERN ITALY.

Submitted to *Soil Science Society of America Journal* on October 13, 2025

William Trenti [1*], Mauro De Feudis [1], Livia Vittori Antisari [1], and Janis L. Boettinger [2]

[1] Department of Agricultural and Food Sciences, Alma Mater Studiorum-University of Bologna, Viale Fanin 40, 40127 Bologna, Italy
[2] Department of Plants, Soils, and Climate, Utah State University, 4820 Old Main Hill, Logan, Utah, USA
[*]correspondence: william.trenti2@unibo.it

ABSTRACT

As the protection and conservation of habitats gain importance in the environmental policies of many countries of the world, knowledge of the spatial distribution of soil types is increasingly needed for the management of natural and semi-natural lands. Mountainous areas harbor many such habitats thanks to their high environmental variability, but this complexity can make the study of such landscapes particularly challenging. Recently, digital soil mapping (DSM) has gained popularity with the increasing availability of informative layers that, together with soil observations and machine learning techniques such as random forests, allow the production of accurate soil maps. In this study we used random forests with recursive feature elimination to map the distribution of soil types in two protected natural parks in the mountains of Italy. We used 108 soil pedon observations and a subset of five covariates (elevation, diffuse insolation, NDVI, slope, and distance from lakes) selected by recursive elimination to carry out several predictions of soil functional group distribution. The final soil map was created using the modes of the predictions, obtaining a Kappa index of 0.82. The high user's accuracy allows this map to be confidently used by land managers, while the selected covariates identify climate/microclimate, vegetation, topography, and surface water as the leading pedogenetic factors in this landscape. Furthermore, running several predictions allows the mapping of soil

transition zones and complex areas which might require more careful management. Knowing which covariates are more influential in this landscape allows the optimization of soil survey efforts in similar areas.

3.1 INTRODUCTION

Soil is among the most fundamental compartments of the biosphere. Soil provides many ecosystem services, such as carbon sequestration, water regulation, food production, and harboring biodiversity, which depend on the soil and its health (FAO and ITPS, 2015). The challenges of climate change and the growing needs of implementing sustainable land management practices call for a thorough knowledge of the soil not only as a growing medium for crops, but as a fundamental part of terrestrial ecosystems. Pedology is the science that studies soil occurrence, genesis, evolution, and relationship with the landscape. Soil mapping is one of the possible products of pedological research and is a powerful tool both for the implementation of knowledge in land management and for the advancement of soil science itself (Ma et al., 2019). While soil mapping of agricultural areas has historically received more attention (Rossiter, 2016), mapping the diversity of soils in natural and semi-natural areas is necessary for sustainable land management and for understanding the role soils play in the mitigation and adaptation to climate change, sustenance of biodiversity, water regulation, and other ecosystem services (Brevik et al., 2016; Searle et al., 2021).

The National Biodiversity Future Centre (NBFC, www.nbfc.it) is the first National Research and Innovation Centre in Italy dedicated to biodiversity, funded by the Italian Ministry for University and Research through European Union resources under NextGenerationEU (next-generation-eu.europa.eu/index_en). A Hub & Spoke model has been established to tackle biodiversity loss and promote ecosystem resilience, aiming to increase protected areas as required by the European Union by 2030. In this context, a soil map is a key tool for conserving both pedodiversity and biodiversity and for the planning and management of protected areas, such as natural parks.

Many natural and semi-natural areas in the world, including most natural parks, are located in mountainous land. Soil mapping in mountains comes with specific constraints that make the task especially difficult. The complex landscape morphology, and, therefore, varying erosion/deposition rates, solar radiation received, and vegetational composition can produce a high diversity in soil characteristics at different scales, which needs to be addressed in all phases of the mapping process. As a consequence, surveying the soils of a mountainous landscape often requires more sampling effort than the survey of plains when other soil forming factors are similar. Furthermore, much of the area in mountains may not be accessible for soil sampling due to remoteness or safety concerns. After soil information is acquired, spatialization of the data must consider such variability and an appropriate soil-landscape model must be devised (Fridland, 1976).

Conventional soil mapping relies on available cartographic data and the pedologist's expertise to construct soil-landscape models. While this approach works well in areas where large amounts of cartographic information are available, its application becomes cumbersome in less known areas or where the existing cartographies suffer from administrative fragmentation. This can be the case with mountain areas, which often act as borders between countries or different administrative organizations within a country. Digital soil mapping (DSM) can overcome several of these limitations (Kidd et al., 2020; Zeraatpisheh et al., 2017). Machine learning algorithms have become the preferred tool for carrying out DSM (Wadoux et al., 2020). Among these tools, Random Forests has been successfully used to map soil classes in different settings (e.g., Heung et al., 2022; Mirakzehi et al., 2018; Barthold et al., 2013), and has been found to yield better results compared to other machine-learning methods (Brungard et al., 2015; Belgiu and Drăguț, 2016; Heung et al., 2017; Shukla et al., 2018; Assami and Hamdi-Aissa, 2019; Faouzi et al., 2023). By utilizing digital elevation models (DEMs) and remotely sensed data, the need for existing cartography and its consistency is largely reduced, thus making it possible to map previously unmapped areas and/or areas which cross administrative boundaries. The selection of the appropriate covariates among the numerous DEM derivatives and remotely sensed data should reflect the most relevant characteristics of the soil-landscape relationship (the *scorpan* model, as defined by McBratney et al., 2003), and several methods have been proposed to carry out this step (Wadoux et al., 2020; Kasraei et al., 2024). Among the remotely sensed covariates, indexes related to vegetation and the composition of the soil surface are the ones most often included (Wadoux et al., 2020). Reflectance from the soil surface can give important information such as soil texture, organic carbon content, mineral composition, and other information related to lithology, but the soil surface must be visible in order to collect this information. Therefore, remotely sensed data from the soil surface is often not available in temperate humid mountain areas, where the soil can be continuously covered by vegetation or forest litter.

In this framework, the goal of this study was to map the soil classes of two adjacent protected areas in the Italian mountains, and to identify the covariates which best describe the soil-landscape relationship. The Northern Apennine mountains' diverse topography, vegetation gradients, and land use dynamics make them into an ideal laboratory to investigate the relationship between soil and landscape in mountainous environments. In this paper, we demonstrate the development and use of a random forests model that identified an optimal set of environmental covariates, accurately mapped the distribution of soil functional groups, and ultimately produced a useful tool for gaining insights about soil differentiation and management.

3.2 MATERIALS AND METHODS

3.2.1 Study area

The study area included the Frignano and Corno alle Scale Regional Parks, two adjacent protected areas in the Northern Apennine mountains, Italy (Figure 1). These parks protect 20,023 ha of mountainous land, with an elevation range of 450 to 2,165 m above sea level (asl). The valley of Fiumalbo was also included in the study.

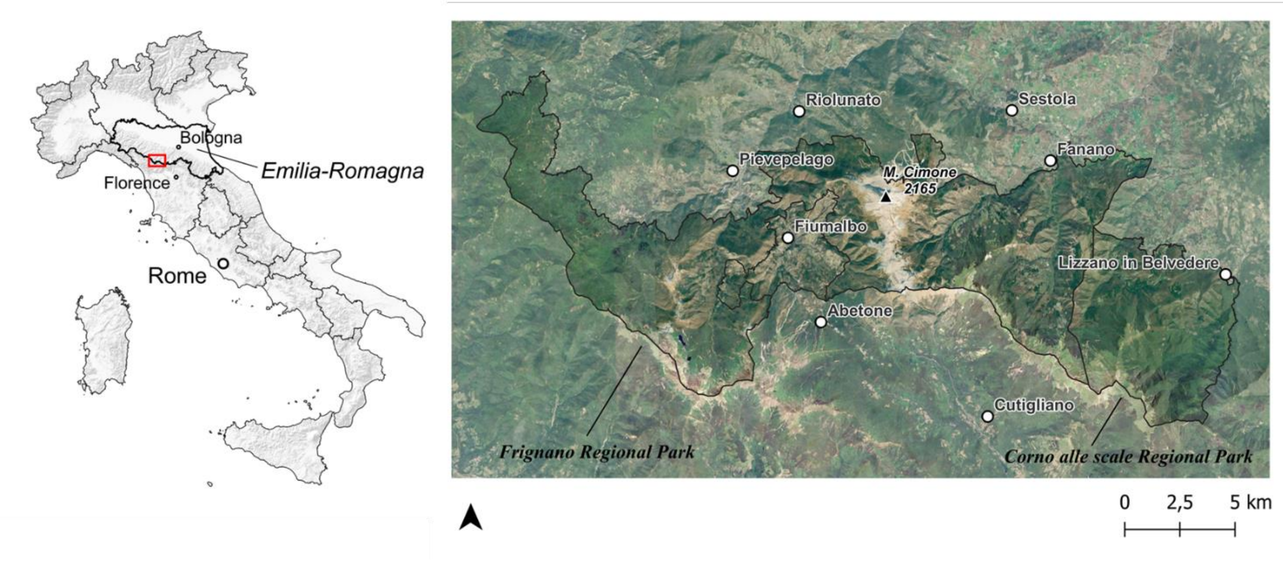

Figure 1. The study area in Emilia-Romagna (red rectangle on left) included the adjacent Frignano and Corno alle Scale Regional Parks and the valley of Fiumalbo in the Northern Apennine mountains in Italy.

The climate, which grows colder and more humid with elevation, ranges in mean annual temperature ranges from 12°C to 2°C, while mean annual precipitation ranges from 800 mm to over 2000 mm, with no arid period (ARPAE, 2024). Thus, the soil temperature regime in Soil Taxonomy can be expected to range from mesic to cryic, and the soil moisture regime can be expected to be udic or moister (Soil Survey Staff, 2022).

The soil parent material is mostly derived from sedimentary formations, with turbiditic sandstones underlying almost half of the area, and Quaternary deposits, mostly from landslides, underlying the other half. Less common parent materials include clays and marls (RER, 2020a). The influence of lithology is evident in the morphology of the area, with sandstones leading to higher peaks and steeper slopes compared to lower relief areas underlain by finer, less consolidated parent materials.

This area experienced human intervention since pre-Roman times, with intense manipulation of the native vegetation (Vittori Antisari et al., 2018). Areas below 800 m asl are characterized by oak forests (*Quercu cerris* L. and *Q. pubescens* Willd.) with presence of chestnut (*Castanea sativa* Mill.) and croplands, while the forests above 800 m asl are composed mainly of European beech (*Fagus sylvatica* L.), the dominant native tree species in this elevation range. The treeline sits at approximately 1600 m asl, and the peaks are vegetated by blueberry heaths and grasslands (RER, 2020b). Ever since the end of World War II this area, like most mountain areas in Italy, was largely abandoned after a period of over-exploitation. Many fields and pastures were colonized by the forest and conifer reforestations were planted in the elevation range of the beech (Agnoletti et al., 2022; Vittori Antisari et al., 2018). Today, beech forests make up most of the study area (Table 1) and, except for some rocky outcrops and towns, the whole area is covered by vegetation.

Table 1. Land uses in the study area.

Land use	Area (ha)	Area (%)
Croplands, vineyards, orchards	266.25	1.24
Meadows	561.54	2.61
Oak forests	1979.50	9.20
Beech forests	12932.20	60.12
Other broadleaf forests	52.23	0.24
Mixed forests	731.20	3.40
Coniferous forests	1134.72	5.28
Grasslands and shrublands	3258.47	15.15
Peat bogs	11.79	0.05
Water	14.89	0.07
Urban areas	354.91	1.65
Rocky outcrops	211.19	0.98

3.2.2 Soil sampling and classification

The soil pedons used for this study included legacy studies performed during the last 20 years (Brombin et al., 2020; Dell'Abate et al., 2007; Falsone et al., 2015; Marinari et al., 2013; Gherardi et al., 2008, 2011, 2015, 2018, 2021) (79 pedons) plus a new sampling campaign in 2023 and 2024 aimed at covering underrepresented areas and combinations of soil forming factors, especially land use and parent material (29 profiles, Trenti et al., 2025). The total amount of soil pedons was 108, and each was classified to subgroup according to Soil Taxonomy (Soil Survey Staff, 2022) (Table 2).

Table 2. Number of pedons found within each Soil Taxonomy subgroup and functional groups created for the scope of this study.

Soil Order	Soil Subgroup	No. of Pedons	Soil Functional Group
Histosols	Terric Haplofibrists	1	Hydromorphic Soils (Hys)
	Hemic Haplofibrists	1	Hydromorphic Soils (Hys)
Mollisols	Lithic Haplocryolls	1	Cryic Soils (CrS)
	Lithic Hapludolls	5	Hapludolls and Humudepts (Hum)
	Entic Hapludolls	1	Hapludolls and Humudepts (Hum)
	Typic Hapludolls	1	Hapludolls and Humudepts (Hum)
Alfisols	Typic Hapludalfs	2	Hapludalfs (Alfs)
Inceptisols	Lithic Humicryepts	1	Cryic Soils (CrS)
	Lithic Humudepts	7	Hapludolls and Humudepts (Hum)
	Psammentic Humudepts	1	Hapludolls and Humudepts (Hum)
	Typic Humudepts	8	Hapludolls and Humudepts (Hum)
	Lithic Dystrocryepts	1	Cryic Soils (CrS)
	Humic Lithic Dystrudepts	1	Humic Dystrudepts (HDys)
	Lithic Dystrudepts	14	Lithic Dystrudepts (LDys)
	Humic Dystrudepts	6	Humic Dystrudepts (HDys)
	Typic Dystrudepts	26	Typic Dystrudepts (TDys)
	Lithic Eutrudepts	5	Eutrudepts (Eut)
	Oxyaquic Eutrudepts	3	Hydromorphic Soils (Hys)
	Arenic Eutrudepts	1	Eutrudepts (Eut)
	Typic Eutrudepts	9	Eutrudepts (Eut)
Entisols	Oxyaquic Udifluvents	2	Hydromorphic Soils (Hys)
	Oxyaquic Udorthents	1	Hydromorphic Soils (Hys)
	Aeric Fluviwassents	1	Hydromorphic Soils (Hys)
	Typic Fluviwassents	5	Hydromorphic Soils (Hys)
	Lithic Udorthents	3	Entisols (Ent)
	Typic Udorthents	1	Entisols (Ent)

The problem of unbalanced distribution of soil classes has been addressed with statistical techniques by several studies (e.g., Sharififar and Sarmadian, 2023; Neyestani et al., 2021). For this study, we chose to merge some soil subgroups into functional groups, with the aim of highlighting major differences that could be important in a conservation and management framework (Table 2). The groups were as follows: Lithic Dystrudepts (*LDys*, n=14), Typic Dystrudepts (*TDys,* n=26), Humic Dystrudepts (Humic and Humic Lithic Dystrudepts, *HDys,* n=7), Hapludolls and Humudepts (*Hum,* n=23), Eutrudepts (except those in Oxyaquic subgroups, *Eutr,* n=15), Hydromorphic soils (Histosols, Fluviwassents and Oxyaquic subgroups, *HyS,* n=14), Cryic soils (soils with a cryic temperature regime, *CrS,* n=3), Hapludalfs (*Alfs,* n=2), and other Entisols (*Ents,* n=4).

3.2.3 Environmental covariates, random forests, mapping

Spatial analysis was performed in QGis 3.34.5 Prizren and RStudio 2023.06.0.

An iterative random forests approach with recursive feature elimination (RECFE) was chosen for the creation of the soil map based on the findings of Brungard et al. (2015).

3.2.3.1 Environmental covariates

A starting set of 21 covariates was derived from a 5x5 m DEM and from Sentinel-2 remote sensed data, plus a data layer representing distance from lakes (Table 3). The covariates were chosen based on expert knowledge of the area and were among the most utilized in digital soil mapping.

Table 3. Initial set of environmental covariates. The Retention score indicates how many times the covariate was retained during the recursive feature elimination (RECFE) process: the final set of covariates included those with a score higher than 50%, underscored in the table.

Covariate name	Description	Source	Retention score
<u>DEM</u>	Height above sea level	RER, 2019	100%
Profile curvature	Aspect change along a flow line	Calculated with RSAGA based on the DEM	0%
Plan curvature	Aspect change along a contour	Calculated with RSAGA based on the DEM	0%
Saga Wetness Index (SWI)	Modified Topographic Wetness Index	Calculated with RSAGA based on the DEM	3%
Inverse of the SWI		SWI^{-1}	7%
<u>Slope</u>	Rate of change of elevation along the steepest descent	Calculated with RSAGA based on the DEM	63%
Catchment area	Area that drains into a cell	Calculated with RSAGA based on the DEM	7%
Diffuse solar radiation of the summer solstice	Potential incoming solar radiation (diffuse)	Calculated with RSAGA based on the DEM	20%
<u>Diffuse solar radiation of the winter solstice</u>	Potential incoming solar radiation (diffuse)	Calculated with RSAGA based on the DEM	77%

Covariate name	Description	Source	Retention score
Diffuse solar radiation of the equinox	Potential incoming solar radiation (diffuse)	Calculated with RSAGA based on the DEM	20%
Direct solar radiation of the summer solstice	Potential incoming solar radiation (direct)	Calculated with RSAGA based on the DEM	7%
Direct solar radiation of the winter solstice	Potential incoming solar radiation (direct)	Calculated with RSAGA based on the DEM	3%
Direct solar radiation of the equinox	Potential incoming solar radiation (direct)	Calculated with RSAGA based on the DEM	7%
Distance from lakes	Distance from a lake or pond to a maximum of 250 m	*Proximity* command in QGis and RER, 2021	63%
NDVI of July 11, 2024 (normal year, full leaf cover)	Normalized Difference Vegetation Index	Copernicus Sentinel data (B08 – B04) / (B08 + B04)	10%
NDVI of March 24, 2022 (drought year, scarce leaf cover)	Normalized Difference Vegetation Index	Copernicus Sentinel data (B08 – B04) / (B08 + B04)	13%
NDVI of July 18, 2017 (drought year, full leaf cover)	Normalized Difference Vegetation Index	Copernicus Sentinel data (B08 – B04) / (B08 + B04)	77%
B12 of March 24, 2022 (drought year, scarce leaf cover)	Soil moisture	Copernicus Sentinel data	10%
B12 of July 18, 2017 (drought year, full leaf cover)	Nitrogen content	Copernicus Sentinel data	17%
B11/B08 of March 24, 2022 (drought year, scarce leaf cover)	Ferric oxides	Copernicus Sentinel data B11 / B08	10%
B11/B08 of July 18, 2017 (drought year, full leaf cover)	Moisture stress index	Copernicus Sentinel data B11 / B08	40%

The 5x5 DEM was downloaded from the Emilia-Romagna Region repository (RER, 2019) and the RSAGA package (Brenning, 2008) was used in RStudio to calculate several derivatives: slope, profile curvature, plan curvature, SAGA wetness index and its inverse, catchment area, and direct and diffuse solar radiation of the winter solstice, summer solstice, and the equinox.

Sentinel-2 L2 layers were downloaded from the Copernicus Hub and included bands from July 18, 2017 (full leaf cover) and March 24, 2022 (scarce snow cover and no leaf cover) (Copernicus

Sentinel data, 2017, 2022). These years were chosen because of their climatically dry conditions (ARPAE, 2023) which we hypothesized could show greater differences in the vegetation's reflectance compared to climatically normal years. The rasters included in the model were Band 12, the ratio between Band 08 and Band 11, and the Normalized Difference Vegetation Index (NDVI). An additional NDVI raster from July 11, 2024, was included, to account for normal precipitation conditions (Copernicus Sentinel data, 2024; ARPAE, 2023).

A layer representing the distance from bodies of water was calculated in QGis using the Proximity command (GDAL/OGR contributors, 2024) on a rasterized shapefile layer downloaded from the Emilia-Romagna Region repository (RER, 2021). The maximum distance to be calculated was set to 250 m.

All rasters were brought to a resolution of 5x5 m and clipped on a 1-km buffer around the study area. When necessary, rasters were log-transformed, and tails were cut at 1% and 99% of the distribution to remove outliers. All rasters were then rescaled to a range of 0 to 1.

3.2.3.2 Random Forests

Random forests (RF) was chosen to predict the distribution of soil classes because of its capacity to incorporate many covariates and the good results it yielded in similar studies (e.g., Brungard et al., 2015; Heung et al., 2017).

The prediction was performed in RStudio with the command "randomForest" from the package of the same name (Liaw and Wiener, 2002), by randomly dividing the dataset into training (70%) and validation (30%) subsets, with the number of trees set to 1000. Random forests was performed first using all covariates, then a subset was constructed via iteration and RECFE of the weakest covariate. The RECFE procedure was performed using the following steps:

1) A training dataset containing 70% and a validation dataset containing 30% of the original data was randomly created.
2) RF was performed using all the covariates.

3) RF was repeated excluding the covariate with the lowest mean decrease in accuracy (MDA), and the out-of-bag error (OOB) was plotted, along with the identifying number of the covariate that was excluded. This was repeated until only one covariate remained (Figure 2).

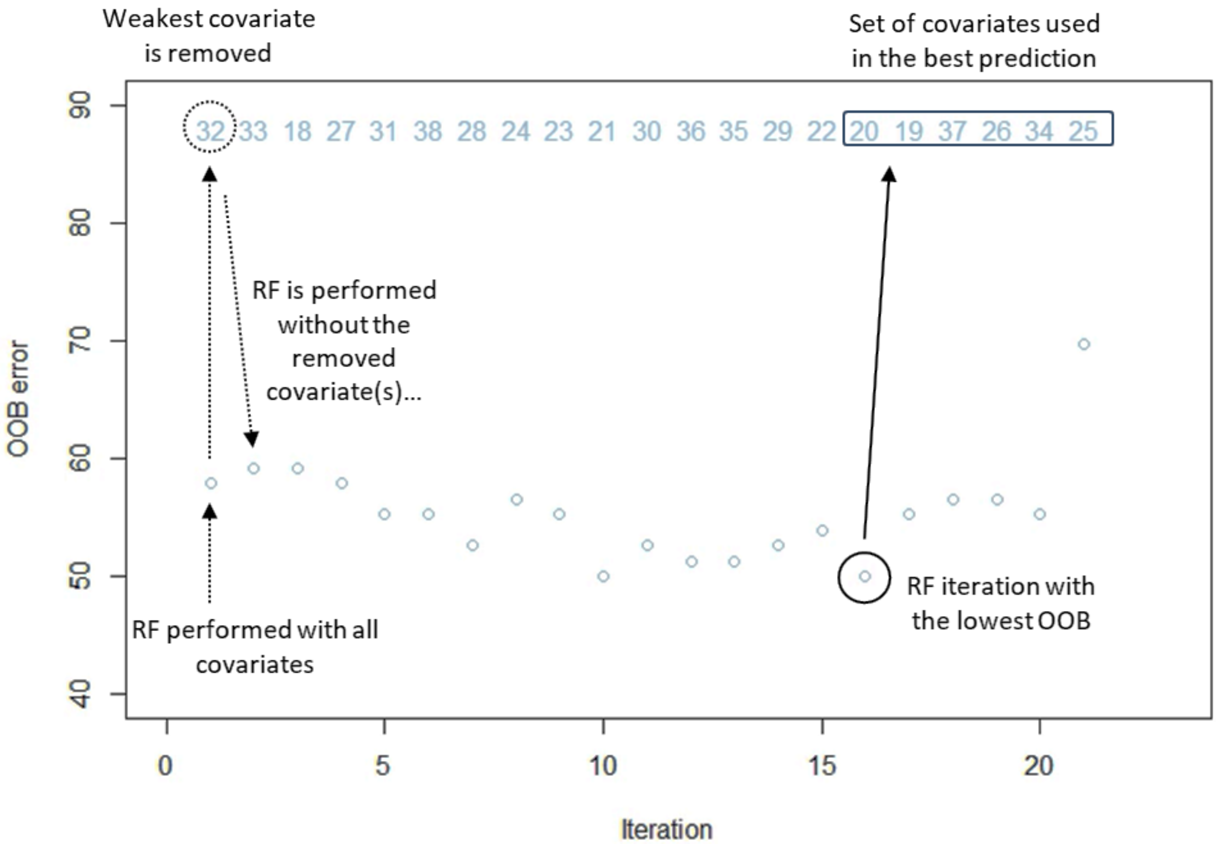

Figure 2. Illustration of the recursive feature elimination of the weakest variable. Random forests (RF) is iterated, each time removing the covariate with the lowest mean decrease in accuracy. The set of covariates that yielded the prediction with the lowest out-of-bag (OOB) error is highlighted.

4) Steps 2 and 3 above were repeated five times (Figure 3).

5) The resulting plot was visually inspected and the set of covariates that yielded the lowest OOB error and the least dispersion between iterations was annotated (Figure 3).

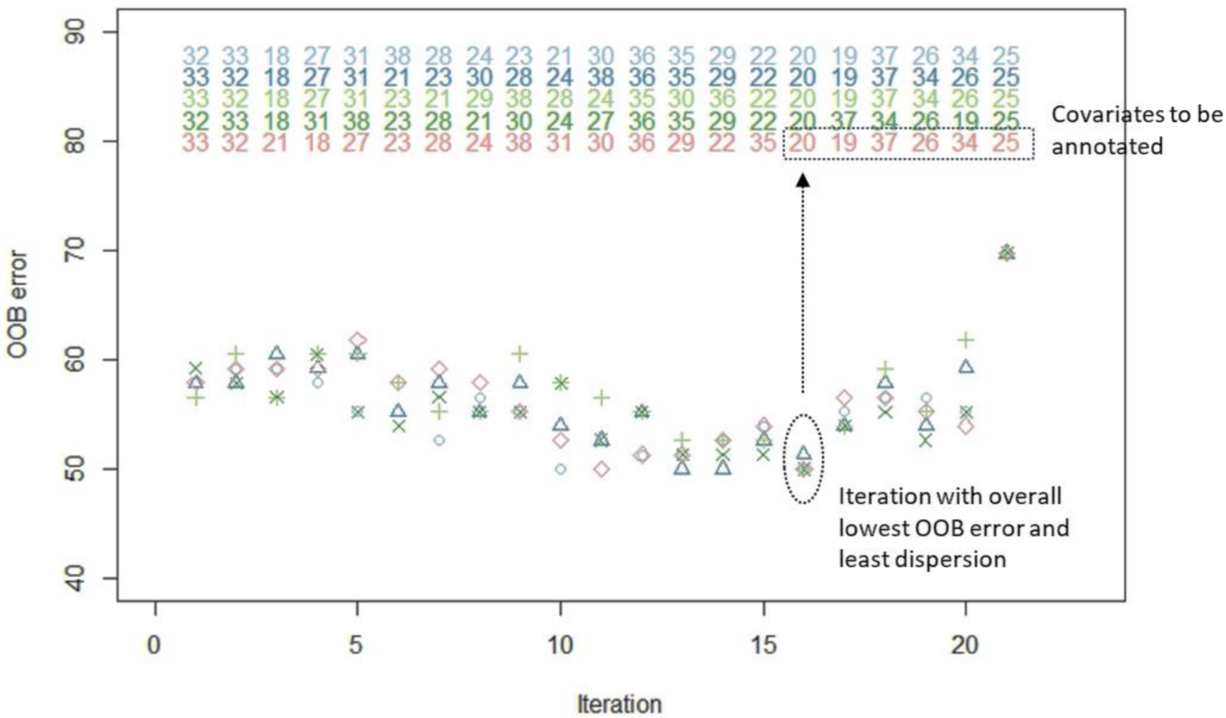

Figure 3. The set of covariates that yielded the predictions with the overall lowest OOB error and least dispersion between the OOB errors of the different predictions was annotated. After repeating this process 10 times on a different randomly created test subset, the covariates that were annotated at least five times were included in the final set.

6) Steps 1 through 5 were repeated 10 times.
7) Steps 1 through 6 were repeated three times. This allowed to calculate the Retention score, which is the average amount of times that each covariate was retained, in percent.
8) The covariates with a Retention score higher than 50% constituted the final set. Five RFs were computed with this final set of covariates, each with a different randomly generated training dataset.

3.2.3.3 Mapping

Each of the results from the five final RF computations was mapped using the "predict" command from the R package "raster" (Hijmans, 2023). Then, the maps were imported into QGis, and the r.series (GRASS development team, 2022) command was used to calculate the mode of each cell. The map depicting the mode was sieved with the GDAL command "Sieve" (GDAL/OGR contributors, 2024), to remove polygons smaller than 20 cells (500 m^2) and replace them with the value of the largest neighboring polygon. If a cell had two modes, then it was assigned to the soil class with the greatest overall area. A frequency map was also created, by assigning to each cell the amount of times that its class (i.e., the mode) was predicted in the five constituent maps and averaging the value with a 49-cell moving window (corresponding to 245 m) using the command r.neighbors (GRASS development team, 2022). The accuracy of prediction of the soil map was evaluated with a confusion matrix and the calculation of producer's accuracy, user's accuracy, overall accuracy, and Kappa index (Congalton, 1991):

$$Producer's\ accuracy = \frac{CCP_i}{OP_i}$$

$$User's\ accuracy = \frac{CCP_i}{PP_i}$$

$$Overall\ accuracy = \frac{CCP}{TP}$$

$$Expected\ accuracy = \frac{\sum \frac{CCP_i \times\ OP_i}{TP}}{TP}$$

$$Kappa = \frac{Overall\ accuracy - Expected\ accuracy}{1 - Expected\ accuracy}$$

Where: $CCP_{(i)}$ = correctly classified profiles (in class i); OP_i = observed profiles in class i; PP_i = predicted profiles in class i; TP = total number of profiles.

The map was then examined by pedologists with a thorough knowledge of the area, and correlation between the final set of covariates was evaluated in QGis with the r.covar command (GRASS Development Team, 2022). Correlations higher than 0.50 where furtherly evaluated with a moving-window correlation in R with the command "rasterCorrelation" from the package "spatialEco" (Evans and Murphy, 2023) with a scale window of 49 cells, corresponding to 245 m.

3.3 RESULTS

The RF performed using all the covariates yielded an OOB error of around 60%, and the map obtained from it did not make sense in pedological terms. Each iteration performed to obtain a subset of covariates also had an OOB error generally between 55% and 65% (Figures 2 and 3). While the RF performed with the final subset of five covariates also had an OOB error in that same range, the final map (Figure 4) looked consistent with the characteristics of the area and displayed high accuracy indexes. The final set of covariates comprised elevation above sea level (DEM), NDVI of a summer day from a drought year, diffuse solar radiation of the winter solstice, slope, and distance from lakes (Figure 5).

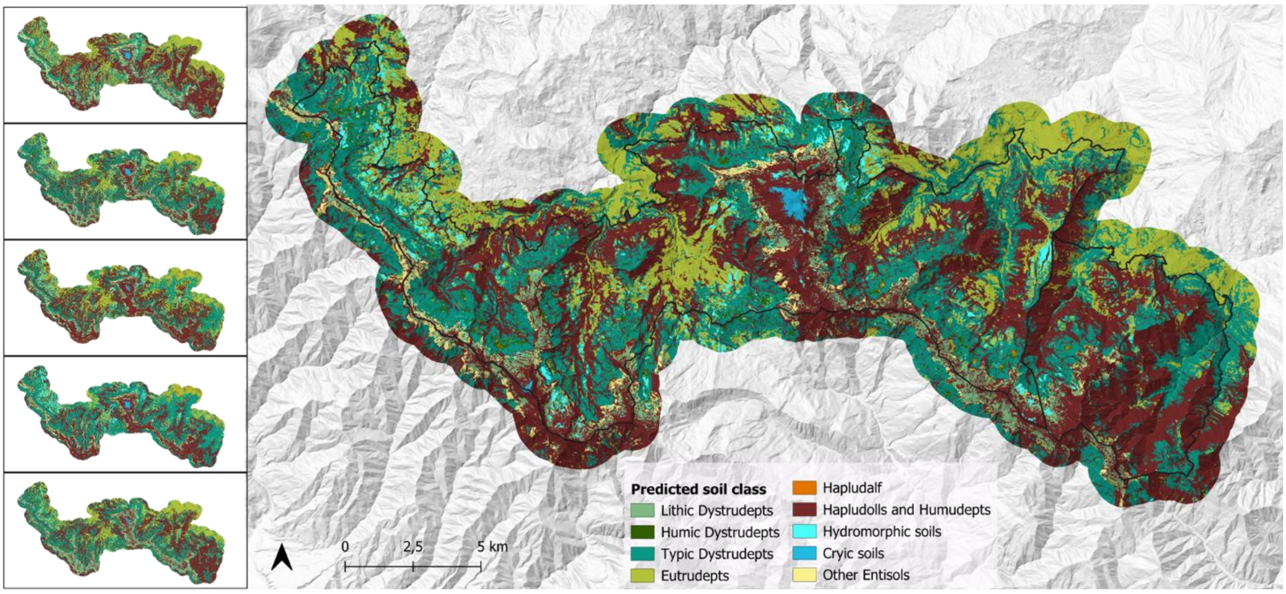

Figure 4. The five maps resulting from five random forests predictions using the final five covariates (left), and the mode of which yields the final soil map (right).

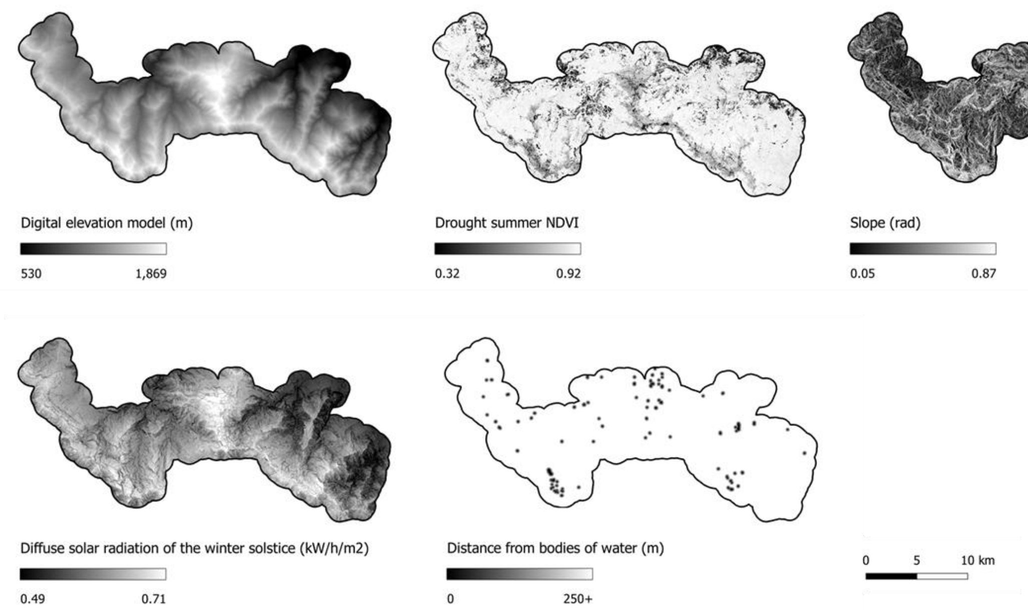

Figure 5. Final set of five covariates used to build the soil map. Tails were cut at 1% and 99% of the distribution to enhance visualization.

3.3.1 Map evaluation

The combination of five predictions made using elevation, slope, diffuse insolation of the winter solstice, the NDVI of a dry summer day, and distance from bodies of water as the main environmental covariates yielded a soil map characterized by high accuracy indices (Tables 3 and 4). All the calculated indexes reflect high accuracy, especially the user's accuracy, which suggests that the obtained map could be effectively used by land managers.

Table 3. Confusion matrix of the final soil map.

		observed									
		CrS	Ent	Eutr	Alfs	HDys	HyS	LDys	Hum	TDys	predicted total
predicted	CrS	**3**	0	0	0	0	0	0	0	0	**3**
	Ent	0	**3**	0	0	0	0	0	0	0	**3**
	Eutr	0	0	**12**	0	0	0	1	1	0	**14**
	Alfs	0	0	0	**2**	0	0	0	0	0	**2**
	HDys	0	0	0	0	**5**	0	0	0	0	**5**
	HyS	0	0	0	0	0	**13**	0	0	0	**13**
	LDys	0	1	0	0	0	0	**8**	0	1	**10**
	Hum	0	0	1	0	1	1	5	**21**	1	**30**
	TDys	0	0	2	0	1	0	0	1	**24**	**28**
	observed total	**3**	**4**	**15**	**2**	**7**	**14**	**14**	**23**	**26**	**108**

Table 4. Accuracy indexes calculated from the data in Table 3.

PRODUCER'S ACCURACY (%)		USER'S ACCURACY (%)	
CrS	100	CrS	100
Ent	75	Ent	100
Eutr	80	Eutr	86
Alfs	100	Alfs	100
HDys	71	HDys	100
HyS	93	HyS	100
LDys	57	LDys	80
Hum	91	Hum	70
TDys	92	TDys	86
EXPECTED ACCURACY = 14%			
OVERALL ACCURACY = 84%			
KAPPA = 82%			

Cryic soils (CrS) were predicted mostly above 1950 m asl (Figure 6a), which is consistent with the limit of the Cryic soil temperature regime identified by the literature for this area (Vittori Antisari et al., 2022), and is also where the highest diffuse solar radiation and lowest NDVI is found (Figure 6c, d). *Eutrudepts (Eutr)* were predicted mostly below 1500 m als and on gentle slopes (Figure 6a,b), which is where most agricultural areas (i.e., the best soils for agriculture) are or were historically located. *Typic Dystrudepts (TDys)*, the soils most frequently observed in the area, were predicted on slopes of medium steepness (Figure 6b) and either in areas with high diffuse insolation between 1200-1600 m asl or in areas with low diffuse insolation between 700-1000 m asl (Figure 4 and Fig 6a,c), which is consistent with the type of vegetation usually associated with these soils (*Fagus sylvatica* forests), which require cool temperatures and high humidity. *Lithic Dystrudepts (LDys)* were predicted mostly above the treeline and the model often flanked them with *Entisols (Ent)* (Figure 4): this is plausible given the steepness and rockiness of the slopes in these morphological situations. *Hapludalfs* (*Alfs)* were predicted mostly as small inclusions inside areas occupied by *TDys* or *Eutr* (Figure 4), where the slopes are gentle (Figure 6b) and the landscape morphology leads to water accumulation: it is credible that illuviation processes are promoted in these sectors. Most areas predicted as *Alfs* were surrounded by *Humic Dystrudepts (HDys)* (Figure 4), this is also plausible given the reduced erosion rates in these sectors that allow organic matter accumulation in the epipedon. The *Hum* class (Mollisols and Humudepts) was predicted more often than expected and mostly in two different situations: at medium elevations above *Eutr*, or at higher elevations between *LDys* and *CrS* (Figure 4), also on steep slopes (Figure 6b), and generally in areas with a lower insolation compared to other forest-related soil types (Figure 6c). While at higher elevations the prediction is plausible, since the soils are usually very shallow and thus the diagnostic epipedon can be very thin (Soil Survey Staff, 2022), the extension of this class on steep slopes at medium elevations (thus high erosion rates and relatively quick mineralization) should be verified. *Hydromorphic soils (HyS)* were predicted more often than expected as well, also in areas far away from mapped bodies of water (Figure 6e). The morphology where this class was predicted is consistent with water accumulation (Figure 6b); moreover, the westernmost sector of the study area, where the model predicted many *HyS*, is an area which is frequently affected by mudslides triggered by water saturation (RER, 2023). A rapid in-field assessment of hydromorphic conditions was carried out in the summer of 2025 in some unsurveyed areas classified as *Hys* that were far from mapped bodies of water and were not mapped as peat bogs. During these assessments, either extensive waterlogging was observed at the soil surface or redox depletions were observed within 50 cm of the soil surface. Only 9 cells (225 m^2) were assigned to a different class at each prediction, and therefore did not have a mode. In general, the predicted soil classes look plausible.

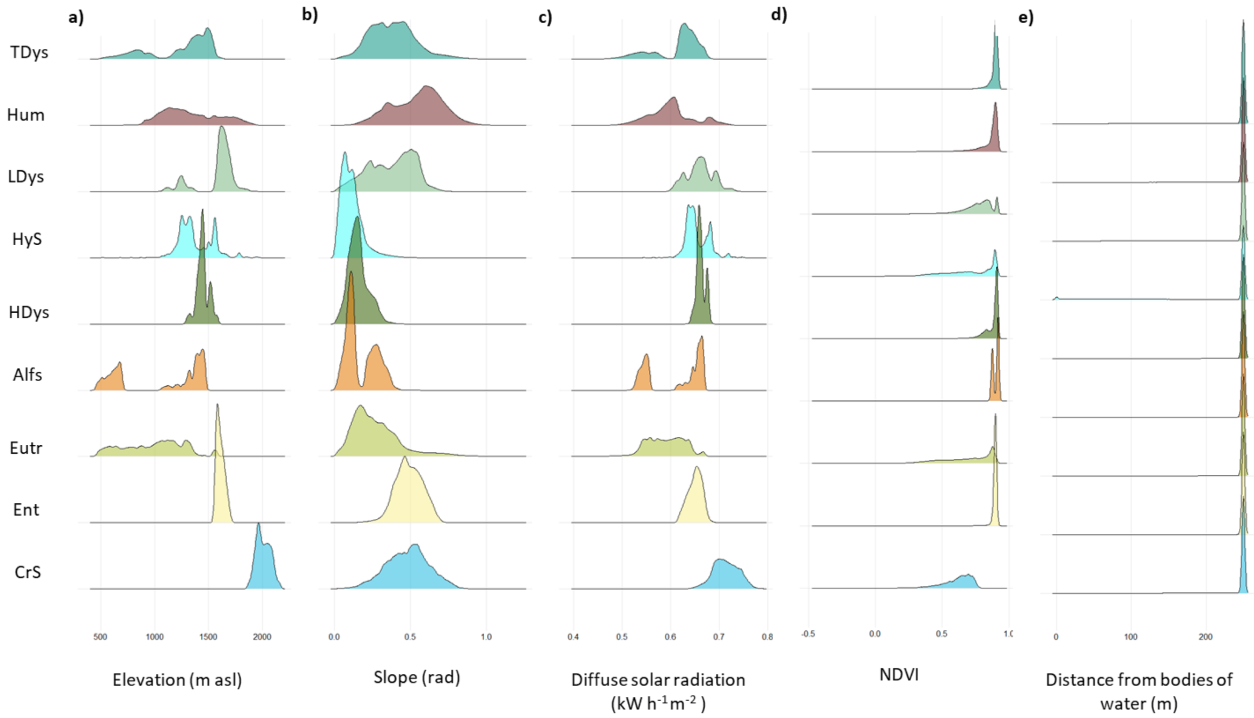

Figure 6. Ridgeline plots showing the distribution of the predicted soil functional group classes according to the final selected covariates.

A map showing the average frequency with which the assigned soil class was predicted in the five constituent maps is shown in Figure 7a, while the ridgeline plot in Figure 7b shows the density of the average frequency by assigned soil class. About 30% of the area, or roughly 10,000 ha, had an average frequency higher than 80%, meaning that, on average, the assigned soil class was predicted at least by four out of the five constituent maps. 68%, or 23,000 ha, had an average frequency between 60%-80%, while only 2% had a frequency below 60%. Figure 8a shows a detail of an area with relatively high uncertainty, where the second mode (where present) was mapped alongside the mode in the case of unimodal cells, or both modes were mapped in the case of bimodal cells. Given the distribution and relative position of the predicted classes, it can be hypothesized that they might indicate transitions between soil classes and/or complex areas where different types of soils might be intermingled in a small space, similar to the findings of Heung et al. (2017). As shown in Figure 8b, some soil classes (*CrS, Alfs, LDys, TDys*) are associated mostly with one other soil class, while others do not show clear tendencies towards specific classes. This could offer insights into the soil evolution pathways and the soil-landscape relationships in the area, and suggests that this DSM model not only incorporated pedological knowledge, but can also contribute to it (Ma et al., 2019)

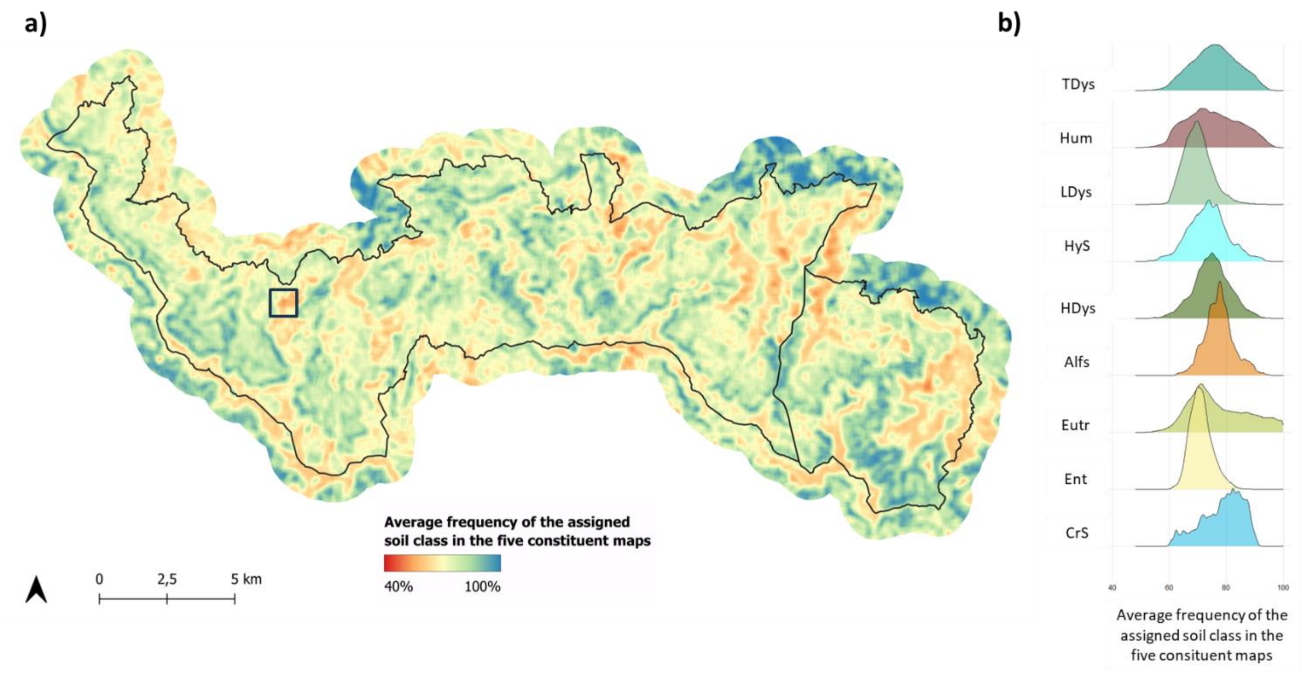

Figure 7. a) Map showing the average frequency of the assigned soil class in the five constituent maps, and b) the density of the same parameter grouped by assigned soil class.

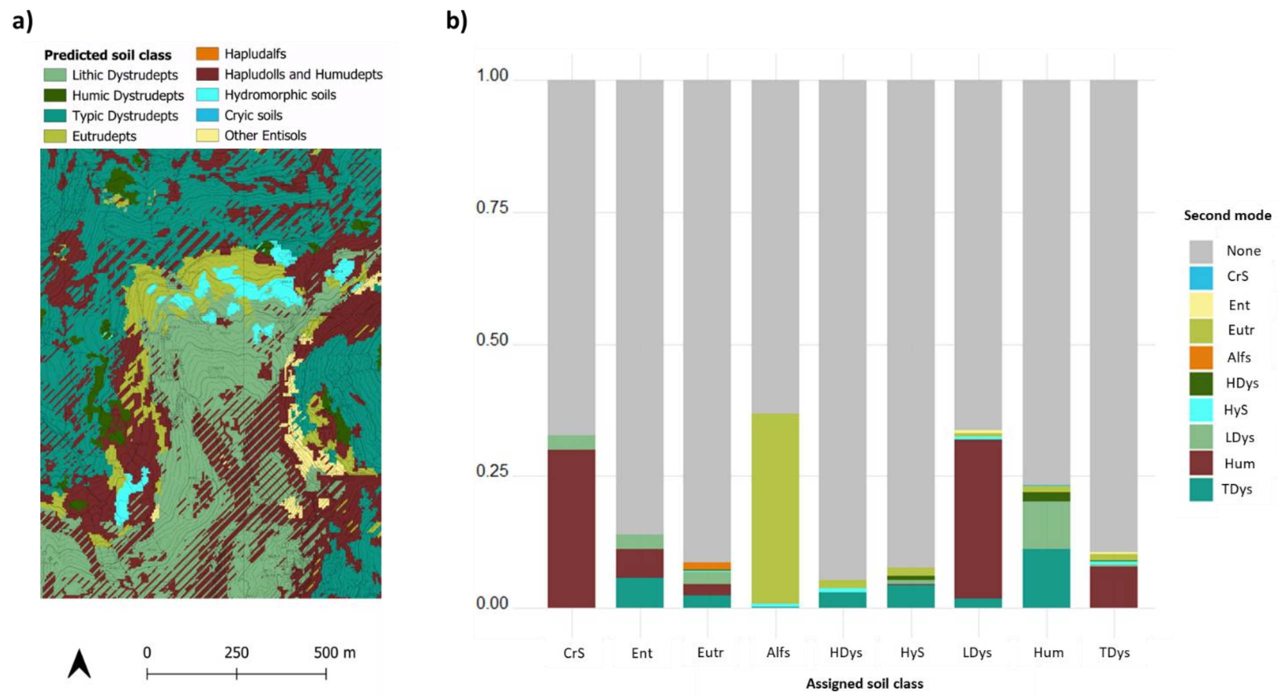

Figure 8. a) Detail of a section of the soil map (area in the square on Figure 7a) showing the mode (full color), the second mode (thin diagonal lines), and both modes (in the case of bimodal cells, thick diagonal lines); b) composition of the second mode for each assigned soil class.

3.3.2 Selected covariates and pedogenetic factors

The correlation matrix showed no correlation between the covariates, except for elevation and diffuse insolation which had a coefficient of 0.83 (Table 5).

Table 5. Pearson's correlation coefficient between the five final covariates. NDVI: NDVI of a dry summer day; DEM: elevation; Water: distance from bodies of water; Insolation: diffuse solar radiation of the winter solstice.

	NDVI	DEM	Water	Slope	Insolation
NDVI	1.00	0.06	0.07	0.19	-0.03
DEM	0.06	1.00	-0.07	0.06	0.83
Water	0.07	-0.07	1.00	0.09	-0.11
Slope	0.19	0.06	0.09	1.00	-0.49
Insolation	-0.03	0.83	-0.11	-0.49	1.00

A moving-window correlation was performed between the elevation and insolation data layers, which revealed that the correlation was spatially uneven with an average Pearson's coefficient of 0.21 and a standard deviation of 0.34. Therefore, the covariates selected in this process can be considered as not redundant.

3.4 DISCUSSION

This model used a small number of covariates compared to similar studies. For example, Heung et al. used a set of 18 (2017) and 35 (2022) covariates to map the distribution of soil types in British Columbia, while Barthold et al. (2013) used 16 covariates to map WRB Reference groups in inner Mongolia. Reducing the number of covariates has been shown to allow a better understanding of the relationship between soil and the environment while also conserving accuracy (Kasraei et al., 2024). Brungard et al. (2015) used RECFE to extract an optimal subset of 10, 6, and 7 covariates to map soil classes in semi-arid areas of New Mexico, Utah, and Wyoming, respectively, and found that potential soil moisture and vegetation were the best predictors for New Mexico, topographic indices performed best for Utah, and predictors related to soil moisture and parent material were more useful in modeling the soil distribution in

Wyoming. Similarly, Mirakzehi et al. (2018) found that the best predictors of soil subgroups in a river delta in eastern Iran were 8 covariates related to fluvial activity.

The five final covariates selected in this study point to a soil landscape shaped mainly by the interaction between climate/microclimate (elevation, diffuse insolation), vegetation (NDVI), morphology of the land (slope), and surface water (distance from lakes). Elevation was consistently the covariate with the greatest MDA, which made it the covariate with the highest retention score (Table 3). This was expected, as elevation change is a prominent characteristic in mountainous landscapes; the climate changes along this gradient, shaping the native vegetation and constraining the possible land uses. The diffuse solar radiation of the winter solstice is also related to the microclimate, and derives from the interaction with the morphology of the landscape, namely slope and aspect, but also accounts for the position of an area in relation to its surroundings. Solar radiation can be regarded as a more comprehensive covariate compared to the more commonly used eastness and northness in areas with high morphological complexity (Beaudette and O'Geene, 2009). Nevertheless, diffuse, rather than direct, solar radiation was retained by the elimination process. While direct solar radiation bears a more straight-forward relationship with aspect, diffuse solar radiation is more influenced by other morphological characteristics, which cause canyons to receive less light compared to wider valleys regardless of their orientation, for example, and is linked to potential soil moisture (Brungard et al., 2015). The NDVI is widely used in DSM for its capability of separating land cover types. Of the three NDVI layers, the one that showed the highest retention score was the NDVI of a summer day from a drought year, where the difference between vegetation types is more evident compared to the NDVI of a summer day of a year with average precipitation. Land cover is an important factor of soil formation, particularly in natural or semi-natural areas where the native vegetation has interacted with the soil for long periods of time. Slope is among the most straightforward morphological covariates in mountainous environments. It influences many aspects of soil formation primarily by driving the erosion and deposition processes, and acts as a limitation to some vegetation types and land uses. Closeness to a body of water causes the soil moisture regime to change within small distances. In this study area, saturated environments can develop into peat bogs, which are recognized as biodiversity hotspots and are featured in the EU 2030 Biodiversity strategy (European Commission, 2021). The fact that this environmental feature was identified among the main factors of soil differentiation remarks its importance in conservation frameworks.

Remarkably, the soil map was consistent with the lithologic composition of the region despite the lack of information regarding the parent material. In fact, while covariates related to soil mineralogy were present in the initial set, they were discarded during the RECFE process. Nevertheless, the classes *Eutr, HyS,* and *Alfs* (characterized by eutric conditions, hydromorphic features, and clay illuviation, respectively, which are all related to a fine soil texture), were the only classes the model often predicted on clayey and marly formations (Table 6) (RER, 2020a).

Table 6. Percentage of each soil class falling into arenaceous/arenaceous-pelitic formations or in clayey and marly formations. The areas outside of the boundary of the Emilia-Romagna region are not included in the count.

Lithology	CrS	Ent	Eutr	Alfs	HDys	HyS	LDys	Hum	TDys
Arenaceous and arenaceous-pelitic formations	96	95	47	54	70	49	79	83	73
Clayey and marly formations	4	5	53	46	30	51	21	17	27

This soil distribution might derive from the unique landscape morphology caused by different lithological formations (Heung et al.,2014; Bulmer et al., 2016), as well as from the typical land uses, meaning that other covariates compensated for the lack of remotely sensed data from the soil surface. While the presence of croplands in this region can be an indicator of fertile soils (e.g. Eutrudepts), the abandonment of agricultural practices in some areas after World War II may have caused the misclassification of the soils of these areas, which are now forests.

The soil map revealed how Hapludalfs are the rarest soil type in the study area, amounting to only 90 ha or 0.02% of the whole surface. The continuous area they cover is also the smallest compared to the other soil classes, averaging to only 1,554 m^2. They are also among the soil types in this region where soil evolution is more developed (Soil Survey Staff, 2022), making the zones where they occur of potential conservation interest.

3.4.1 Further applications

While soil mapping can give useful indications to land managers and stakeholders, this method could have further uses besides mapping the soil classes of an area after it has been surveyed. A product such as that of Figure 7a could be useful in identifying complex areas, which might need to be subjected to special management techniques, or areas which may require further sampling. The model used to map this specific area can be applied to regions with similar soil forming factors, and the "preliminary maps" obtained can be used to direct soil survey campaigns, as suggested by Scull et al. (2005). An example of this is shown in Figure 9, where the model was applied to the Casentino Forests National Park, 70 km to the southeast of the original study area. This national park has similar lithology and land uses but is slightly lower in elevation and has a slightly warmer and drier climate compared to the original study area. While the map in Figure 9a could give the surveyors an idea of what to expect and where, the map in Figure 9b could be used to identify the areas which might require denser sampling, with a potential overall optimization of the survey campaign. This is of particular interest since this park is split between the Emilia-Romagna and Tuscany regions, whose cartographies have different scales and were made using different techniques, thus conventional soil mapping in this park would require an extensive harmonization of the existing data (e.g., land cover maps, geologic maps) before being applied. In addition, knowing in advance which covariates might be more descriptive of an area also allows the application of Conditioned Latin hypercube sampling, a method which selects the sample locations to maximize the variability represented by the chosen covariates (Kienast-Brown et al., 2017).

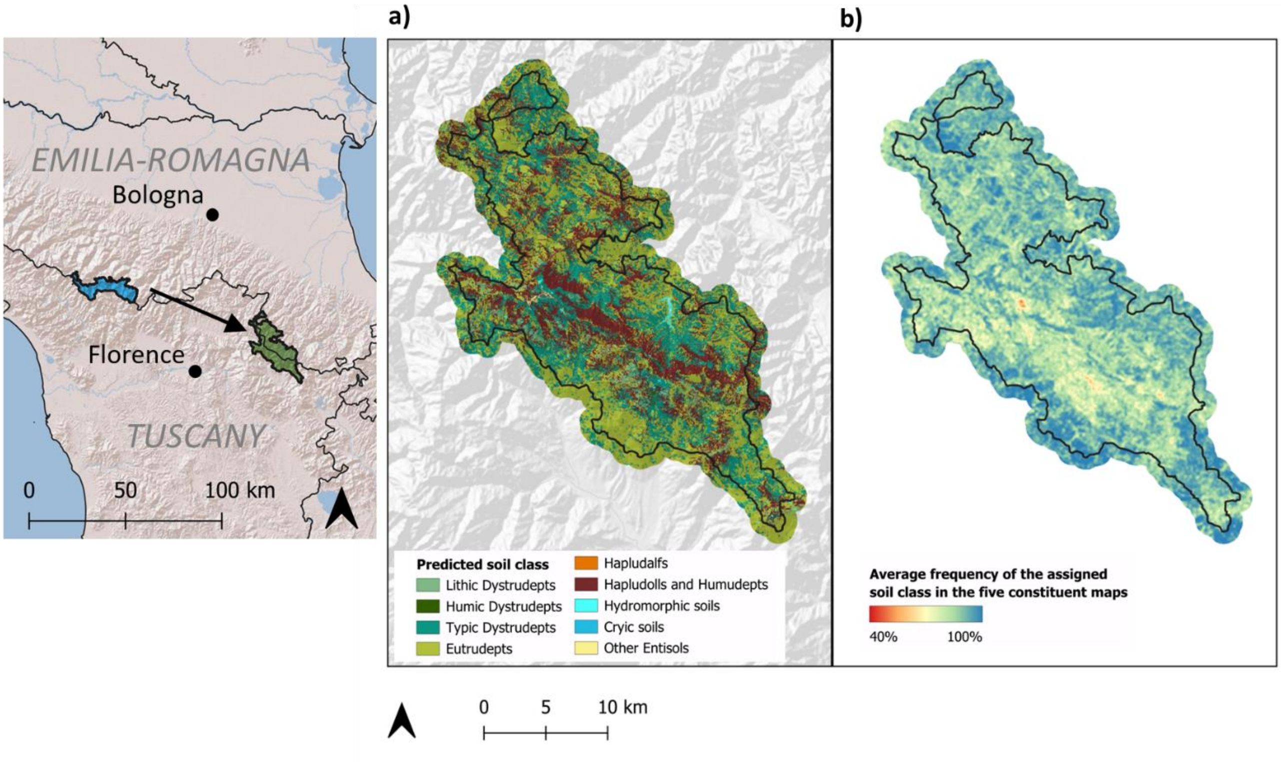

Figure 9. The model created in our study area (blue) was applied to the area of the Casentino Forests National Park (green) in a) a preliminary soil map, and b) the average frequency of the assigned soil class in the five constituent maps.

3.5 CONCLUSIONS

We used an iterative random forests approach with recursive feature elimination to identify an optimal subset of environmental covariates, which was then employed to run several predictions of soil type distribution in the Northern Apennines of Italy. The optimal subset included a total of five covariates: (1) elevation, which determined the climate at regional scale; (2) diffuse insolation, which was linked to climate at local scale; (3) the Normalized Difference Vegetation Index (NDVI), which represented the quality and health of the vegetation; (4) slope, one of the most determining topographic features in mountainous landscapes; and (5) distance from lakes, which represented abrupt changes in soil moisture regimes. The final soil map was intended to serve both researchers and land managers, in accordance with the goals of the NBFC to assess, conserve, and monitor terrestrial biodiversity. The high accuracy indices displayed by the final map showed that it can be effectively used as a tool to effectively manage these natural parks, but also as a mean to better understand the leading factors of soil differentiation in this and similar landscapes.

The model could also be applied to areas with similar soil-forming factors to produce preliminary soil maps that can be used to direct soil survey campaigns, thus optimizing the most expensive step of the soil mapping process. The model makes use of freely accessible data that is largely available worldwide. Its application is simple, and the resulting map, despite the complexity of the mountain landscape and the continuous vegetation cover that limits the use of remotely sensed data from the soil surface, presented high accuracy indices and was consistent with the characteristics of the area. Using a combination of predictions allows the exploration of the relationships between different soil types, the identification of areas with high uncertainty that might benefit from additional sampling, and the mapping of soil transition zones and complex areas that might require more careful management. Applying the model to other similar areas can aid the planning of new soil survey campaigns and increase their efficiency.

ACKNOWLEDGMENTS

Research funded under the National Recovery and Resilience Plan (NRRP), Mission 4 Component 2 Investment 1.4 - Call407for tender No. 3138 of 16 December 2021, rectified by Decree n.3175 of 18 December 2021 of Italian Ministry of University and Research funded by the European Union – NextGenerationEU; Project code CN_00000033, Concession409Decree No. 1034 of 17 June 2022 adopted by the Italian Ministry of University and Research, CUPJ33C22001190001,410Project title “National Biodiversity Future Center - NBFC”.

CONFLICT OF INTEREST

The authors declare no conflict of interest.

REFERENCES

Agnoletti, M., Piras, F., Venturi, M., & Santoro, A. (2022). Cultural values and forest dynamics: The Italian forests in the last 150 years. *Forest Ecology and Management*, *503*, 119655. https://doi.org/10.1016/j.foreco.2021.119655

ARPAE (2023). *Monitoraggio regionale siccità*. https://www.arpae.it/it/temi-ambientali/siccita/dati-e-indicatori/monitoraggio-siccita

ARPAE (2024). *Tabelle climatologiche*. https://www.arpae.it/it/temi-ambientali/clima/dati-e-indicatori/tabelle-climatiche

Assami, T., & Hamdi-Aïssa, B. (2019). Digital mapping of soil classes in Algeria–A comparison of methods. *Geoderma Regional*, *16*, e00215. https://doi.org/10.1016/j.geodrs.2019.e00215

Barthold, F. K., Wiesmeier, M., Breuer, L., Frede, H. G., Wu, J., & Blank, F. B. (2013). Land use and climate control the spatial distribution of soil types in the grasslands of Inner Mongolia. *Journal of Arid Environments*, *88*, 194-205. https://doi.org/10.1016/j.jaridenv.2012.08.004

Beaudette, D. E., & O'Geen, A. T. (2009). Quantifying the aspect effect: an application of solar radiation modeling for soil survey. *Soil Science Society of America Journal*, *73*(4), 1345-1352. https://doi.org/10.2136/sssaj2008.0229

Belgiu, M., & Drăguţ, L. (2016). Random forest in remote sensing: A review of applications and future directions. *ISPRS Journal of Photogrammetry and Remote Sensing*, *114*, 24-31. https://doi.org/10.1016/j.isprsjprs.2016.01.011

Brenning, A. (2008). Statistical geocomputing combining R and SAGA: The example of landslide susceptibility analysis with generalized additive models. *Hamburger Beiträge zur Physischen Geographie und Landschaftsökologie*, *19*(23-32), 410.

Brevik, E. C., Calzolari, C., Miller, B. A., Pereira, P., Kabala, C., Baumgarten, A., & Jordán, A. (2016). Soil mapping, classification, and pedologic modeling: History and future directions. *Geoderma*, *264*, 256-274. https://doi.org/10.1016/j.geoderma.2015.05.017

Brombin, V., Mistri, E., De Feudis, M., Forti, C., Salani, G. M., Natali, C., ... & Bianchini, G. (2020). Soil carbon investigation in three pedoclimatic and agronomic settings of Northern Italy. *Sustainability*, *12*(24), 10539. https://doi.org/10.3390/su122410539

Brungard, C. W., Boettinger, J. L., Duniway, M. C., Wills, S. A., & Edwards Jr, T. C. (2015). Machine learning for predicting soil classes in three semi-arid landscapes. *Geoderma*, *239*, 68-83. https://doi.org/10.1016/j.geoderma.2014.09.019

Bulmer, C., Schmidt, M. G., Heung, B., Scarpone, C., Zhang, J., Filatow, D., ... & Smith, S. (2016). Improved soil mapping in British Columbia, Canada, with legacy soil data and random forest. In *Digital soil mapping across paradigms, scales and boundaries* (pp. 291-303). Singapore: Springer Singapore. http://dx.doi.org/10.1007/978-981-10-0415-5_24

Congalton, R. G. (1991). A review of assessing the accuracy of classifications of remotely sensed data. *Remote Sensing of Environment*, *37*(1), 35-46. https://doi.org/10.1016/0034-4257(91)90048-B

Copernicus Sentinel data (2017). Copernicus browser. https://browser.dataspace.copernicus.eu/

Copernicus Sentinel data (2022). Copernicus browser. https://browser.dataspace.copernicus.eu/

Copernicus Sentinel data (2024). Copernicus browser. https://browser.dataspace.copernicus.eu/

Dell'Abate, M.T., Giovannini, C., Pontalti, F., Vianello, G., & Vittori Antisari, L. (2007). Caratterizzazione quali-quantitativa della sostanza organica degli epipedon di suoli bruni acidi dell'appennino emiliano sotto bosco di latifoglie e di conifere. In Gessa, C., Lorito, S., Vianello, G., & Vittori Antisari, L. (Eds.). (In Italian, with English abstract.) *Atti Convegno Nazionale Società Italiana di Scienze del Suolo "Suolo Ambiente Paesaggio"* (pp. 332 – 342). Società Italiana di Scienze del Suolo.

Evans JS, Murphy MA (2023). *spatialEco*. R package version 2.0-2, https://github.com/jeffreyevans/spatialEco

European Commission. (2021). EU biodiversity strategy for 2030. Publications Office of the EU.

Falsone, G., Marinari, S., Vittori Antisari, L., & Vianello, G. (2015). Soil processes related to organic matter modifications following Douglas-fir mature reforestation. *Biology and Fertility of Soils*, *51*(3), 277-287. https://doi.org/10.1007/s00374-014-0971-2

FAO and ITPS (2015). Status of the World's Soil Resources (SWSR) – Main Report. Food and Agriculture Organization of the United Nations and Intergovernmental Technical Panel on Soils, Rome, Italy

Faouzi, E., Arioua, A., Namous, M., Barakat, A., Mosaid, H., Ismaili, M., ... & Houmma, I. H. (2023). Spatial mapping of hydrologic soil groups using machine learning in the Mediterranean region. *Catena*, *232*, 107364. https://doi.org/10.1016/j.catena.2023.107364

Fridland, V.M. (1976). *Pattern of the soil cover.* Israel Program for Scientific Translations.

GDAL/OGR contributors (2024). GDAL/OGR Geospatial Data Abstraction software Library. Open Source Geospatial Foundation. https://gdal.org

Gherardi, M., Lorito, S., Pontalti, F., Vianello, G., & Vittori Antisari, L. (2007). Effect of different land use on soil organic matter in brown soils of the emilian Apennine. In *Abstracts*, *Changing Soils in a Changing World: the Soils of Tomorrow"* (Vol. 1, pp. 236-236). European Society for Soil conservation.

GRASS Development Team (2022). Geographic Resources Analysis Support System (GRASS) Software, Version 8.2. Open Source Geospatial Foundation. Electronic document: https://grass.osgeo.org, DOI: 10.5281/zenodo.5176030

Heung, B., Bulmer, C. E., & Schmidt, M. G. (2014). Predictive soil parent material mapping at a regional-scale: A Random Forest approach. *Geoderma*, *214*, 141-154. https://doi.org/10.1016/j.geoderma.2013.09.016

Heung, B., Bulmer, C. E., Schmidt, M. G., & Zhang, J. (2022). Provincial-scale digital soil mapping using a random forest approach for British Columbia. *Canadian Journal of Soil Science*, *102*(03), 597-620. https://doi.org/10.1139/cjss-2021-0090

Heung, B., Hodúl, M., & Schmidt, M. G. (2017). Comparing the use of training data derived from legacy soil pits and soil survey polygons for mapping soil classes. *Geoderma*, *290*, 51-68. https://doi.org/10.1016/j.geoderma.2016.12.001

Hijmans, R. (2023). *raster: Geographic Data Analysis and Modeling*. R package version 3.6-26, https://rspatial.org/raster.

Kasraei, B., Schmidt, M. G., Zhang, J., Bulmer, C. E., Filatow, D. S., Pennell, T., & Heung, B. (2024). A framework for optimizing environmental covariates to support model interpretability in digital soil mapping. *Geoderma*, *445*, 116873. https://doi.org/10.1016/j.geoderma.2024.116873

Kidd, D., Searle, R., Grundy, M., McBratney, A., Robinson, N., O'Brien, L., ... & Triantafilis, J. (2020). Operationalising digital soil mapping–Lessons from Australia. *Geoderma Regional*, *23*, e00335. https://doi.org/10.1016/j.geodrs.2020.e00335

Kienast-Brown, S., Libohova, Z., & Boettinger, J. (2017). Digital Soil Mapping. In Soil Survey Staff, Soil survey manual. (C. Ditzler, K. Scheffe, & H.C. Monger, Eds.). USDA Handbook 18. Washington, D.C.: Government Printing Office. Liaw A. & Wiener M. (2002). Classification and Regression by randomForest. *R News*, **2**(3), 18-22. https://CRAN.R-project.org/doc/Rnews/.

Ma, Y., Minasny, B., Malone, B. P., & Mcbratney, A. B. (2019). Pedology and digital soil mapping (DSM). *European Journal of Soil Science*, *70*(2), 216-235. **https://doi.org/10.1111/ejss.12790**

Marinari, S., Bonifacio, E., Moscatelli, M. C., Falsone, G., Antisari, L. V., & Vianello, G. (2013). Soil development and microbial functional diversity: Proposal for a methodological approach. *Geoderma*, *192*, 437-445. https://doi.org/10.1016/j.geoderma.2012.08.023

McBratney, A. B., Santos, M. M., & Minasny, B. (2003). On digital soil mapping. *Geoderma*, *117*(1-2), 3-52. https://doi.org/10.1016/S0016-7061(03)00223-4

Mirakzehi, K., Pahlavan-Rad, M. R., Shahriari, A., & Bameri, A. (2018). Digital soil mapping of deltaic soils: A case of study from Hirmand (Helmand) river delta. *Geoderma*, *313*, 233-240. https://doi.org/10.1016/j.geoderma.2017.10.048

Neyestani, M., Sarmadian, F., Jafari, A., Keshavarzi, A., & Sharififar, A. (2021). Digital mapping of soil classes using spatial extrapolation with imbalanced data. *Geoderma Regional*, *26*, e00422. https://doi.org/10.1016/j.geodrs.2021.e00422

RER (2019). *DTM 5x5*. Metasfera Regione Emilia-Romagna. https://metasfera.regione.emilia-romagna.it/ricerca_metadato?uuid=r_emiro:2016-08-08T155835

RER (2020a). *Banca dati geologica 1:10,000.* Metasfera Regione Emilia-Romagna. https://metasfera.regione.emilia-romagna.it/ricerca_metadato?uuid=r_emiro:2017-06-12T113543

RER (2020b). *Uso del suolo - 2020 - Coperture vettoriali di dettaglio - Edizione 2023.* Metasfera Regione Emilia-Romagna. https://metasfera.regione.emilia-romagna.it/ricerca_metadato?uuid=r_emiro:2023-04-27T171223

RER (2021). *DBTR - Specchio d'acqua - (SDA_GPG)*. Metasfera Regione Emilia-Romagna. https://geoportale.regione.emilia-romagna.it/catalogo/dati-cartografici/cartografia-di-base/database-topografico-regionale/idrografia/acque-interne-e-di-transizione/layer-4

RER (2023). *Banca dati geologica, 1:10.000 - Frane, depositi di versante e depositi alluvionali – 10k*. Metasfera Regione Emilia-Romagna. https://metasfera.regione.emilia-romagna.it/ricerca_metadato?uuid=r_emiro:2017-06-14T131444

Rossiter, D. G. (2016). Digital soil resource inventories: status and prospects in 2015. *Digital soil mapping across paradigms, scales and boundaries*, 275-286. https://doi.org/10.1007/978-981-10-0415-5_22

Scull, P., Franklin, J., & Chadwick, O. A. (2005). The application of classification tree analysis to soil type prediction in a desert landscape. *Ecological modelling*, *181*(1), 1-15. https://doi.org/10.1016/j.ecolmodel.2004.06.036

Searle, R., McBratney, A., Grundy, M., Kidd, D., Malone, B., Arrouays, D., ... & Andrews, K. (2021). Digital soil mapping and assessment for Australia and beyond: A propitious future. *Geoderma Regional*, *24*, e00359. https://doi.org/10.1016/j.geodrs.2021.e00359

Sharififar, A., & Sarmadian, F. (2023). Coping with imbalanced data problem in digital mapping of soil classes. *European Journal of Soil Science*, *74*(3), e13368. https://doi.org/10.1111/ejss.13368

Shukla, G., Garg, R. D., Srivastava, H. S., & Garg, P. K. (2018). An effective implementation and assessment of a random forest classifier as a soil spatial predictive model. *International Journal of Remote Sensing*, *39*(8), 2637-2669. https://doi.org/10.1080/01431161.2018.1430399

Trenti, W., De Feudis, M., Gherardi, M., Vianello, G., & Vittori Antisari, L. (2025). Land Unit Delineation Based on Soil-Forming Factors: A Tool for Soil Survey in Mountainous Protected Areas. *Land*, *14*(8), 1683. **https://doi.org/10.3390/land14081683**

Soil Survey Staff. (2022). *Keys to Soil Taxonomy (13th ed.)*. USDA Natural Resources Conservation Service.

Vittori Antisari, L., Agnelli, A., Corti, G., Falsone, G., Ferronato, C., Marinari, S., & Vianello, G. (2018). Modern and ancient pedogenesis as revealed by Holocene fire-Northern Apennines, Italy. *Quaternary International*, *467*, 264-276. https://doi.org/10.1016/j.quaint.2017.12.050

Vittori Antisari, L., Falsone, G., Carbone, S., Marinari, S., & Vianello, G. (2015). Douglas-fir reforestation in North Apennine (Italy): Performance on soil carbon sequestration, nutrients stock and microbial activity. *Applied Soil Ecology*, *86*, 82-90. https://doi.org/10.1016/j.apsoil.2014.09.009

Vittori Antisari, L., Marinari, S., Dell'Abate, M. T., Baffi, C., & Vianello, G. (2011). Plant cover and epipedon SOM stability as factors affecting brown soil profile development and microbial activity. *Geoderma*, *161*(3-4), 212-224. https://doi.org/10.1016/j.geoderma.2010.12.021

Vittori Antisari, L., Trenti, W., Buscaroli, A., Falsone, G., Vianello, G., & De Feudis, M. (2022). Pedodiversity and organic matter stock of soils developed on sandstone formations in the Northern Apennines (Italy). *Land*, *12*(1), 79. **https://doi.org/10.3390/land12010079**

Vittori Antisari, L., Trenti, W., De Feudis, M., Bianchini, G., & Falsone, G. (2021). Soil quality and organic matter pools in a temperate climate (Northern Italy) under different land uses. *Agronomy*, *11*(9), 1815. https://doi.org/10.3390/agronomy11091815

Wadoux, A. M. C., Minasny, B., & McBratney, A. B. (2020). Machine learning for digital soil mapping: Applications, challenges and suggested solutions. *Earth-Science Reviews*, *210*, 103359. https://doi.org/10.1016/j.earscirev.2020.103359

Zeraatpisheh, M., Ayoubi, S., Jafari, A., & Finke, P. (2017). Comparing the efficiency of digital and conventional soil mapping to predict soil types in a semi-arid region in Iran. *Geomorphology*, *285*, 186-204. https://doi.org/10.1016/j.geomorph.2017.02.015

4. PEDODIVERSITY AND ORGANIC MATTER DYNAMICS IN THE NORTH APENNINES (ITALY): RELATIONSHIPS AMONG SOIL TYPES, BIODIVERSITY, AND ECOLOGICAL FUNCTIONALITY

Published in *Forests* **2024, *15*(2), 353; https://doi.org/10.3390/f15020353**

Livia Vittori Antisari, Mauro De Feudis*, William Trenti, Gloria Falsone, Federico Puliga, Alessandra Zambonelli, Giulia Tabanelli & Fausto Gardini

Department of Agricultural and Food Sciences, Alma Mater Studiorum-University of Bologna, Viale Fanin 40, 40127 Bologna, Italy
*correspondence: mauro.defeudis2@unibo.it

ABSTRACT

Pedodiversity is generally neglected in studies concerning soil organic carbon (SOC). Therefore, this investigation aimed to explore the effect of soil types on the following: (1) soil processes related to organic matter (OM) dynamics along the profile; and (2) the microbial community and functionality within the uppermost horizon. Humic Dystrudepts (HD), Typic Dystrudepts (TD), and Humic Lithic Dystrudepts (HLD) were selected in beech forests of the Apennine ridge in the Emilia-Romagna Region (Italy). Soils were sampled by horizons until parent material, and physico-chemical and functional analyses were performed. The results showed that both HD and HLD soils had a higher SOC accumulation than TD, particularly within the deeper horizons. Such accumulation might be due to the lower turnover rate of soil OM forms, namely fulvic acid-like substances, humic acid-like substances, and non-extractable OM. Noteworthy, the A horizons showed slight differences in SOC among the soil types, suggesting similar SOC decomposition processes. This fact was confirmed by the lack of differences in microbial DNA-based diversity and functionality. This study highlighted the importance of combining pedodiversity and microbial diversity for a wider perspective on SOC dynamics.

4.1 INTRODUCTION

Soils are a part of the world's natural heritage, and they are ecosystems in which biological (biodiversity) and geological (geodiversity) resources coexist (Ibáñez et al., 2008). Soil represents a fundamental component of the natural environment and is responsible for many essential ecosystem services that contribute to water regulation and supply, climate regulation, biodiversity conservation, plant productivity, and carbon sequestration (FAO, 2015).

Pedodiversity, also known as soil diversity within an area, could further improve and enhance such ecosystem services due to its positive influence on biodiversity, food production, water conservation and transport, and many other ecological processes (Costantini & Mocali, 2022; Ibáñez & Feoli, 2013). Because of the diverse soil properties between different soil types and the consequent interrelationship with the soil ecological functions (Costantini & Mocali, 2022), the spatial variation of soil properties according to soil types was also described with the term "functional pedodiversity", which indicates the land's versatility to provide ecosystem functions (Fajardo et al., 2017). Unfortunately, pedodiversity is not a stable land characteristic since soil degradation processes due to accelerated erosion (Costantini & Lorenzetti, 2013; Lo Papa et al., 2011). This fact would highlight how much soils are complex and dynamic bodies whose properties are driven by the numerous processes that occur contemporary within them and by various biotic and abiotic factors and their interactions affecting the pedodiversity itself (Costantini & Mocali, 2022; Vittori Antisari et al., 2023; Abakumov, 2022; Vacek et al., 2020; D'Amico et al., 2020; Sorokin et al., 2021). Despite the importance of pedodiversity on soil functioning and ecosystem service provision (Krasilnikov et al., 2018), soil classification and, therefore, soil horizon sequence identification are still usually neglected in studies concerning nutrient cycling, organic matter dynamics, and more in general soil properties evaluation.

In the context of pedodiversity and its functions, previous studies reported the pivotal role of soil biodiversity on the performance of the soil ecosystem (Wagg et al., 2014; El Mutjar et al., 2019). In fact, the soil biota is involved in most of the key functions that the soil provides by driving the nutrient cycling processes, soil structural dynamics, degradation of pollutants, gas exchange, and regulation of plant communities (Breure, 2004). In this sense, earlier studies highlighted the positive relationship between soil functionality and soil quality (Bünemann et al., 2018; Drobnik et al., 2018). Soil organic matter (SOM) is widely recognized as the major soil component supporting the multiple soil ecosystem functions (Hoffland et al., 2020) and is used as the most important soil quality indicator (Lorenz et al., 2019; Bongiorno et al., 2019; Jensen et al., 2019). This is because several physical, chemical, and biological processes and properties are modulated by the SOM amount and its forms (Lavallee et al., 2020). SOM mainly derives from plant litter residue input and is degraded, transformed, and respirated by microbial communities (Islam etal., 2022). Consequently, the SOM degradation by-products are mainly composed of microbial-derived molecules (Kallenbach et al., 2016), which in the uppermost soil layer could be up to 62% of total SOM (Liang et al., 2019). Other than SOM, soil quality can be described by eco-physiological indices such as the metabolic quotient, the microbial quotient, and the Dilly index (Vittori Antisari et al., 2021; Mocali et al., 2008; Dilly et al., 2001; Dilly, 2005). However, the specific functioning of soil biodiversity within soil is still unclear (Wall et al., 2010), probably due to pedodiversity and its effect on the soil microbiome. In this sense, to fill this gap currently, there is much interest in linking microbiome composition and diversity to their functions within soil (Fierer, 2017; Antwis et al., 2017; Graham et al., 2016) and also through the investigation of the microbial functional gene composition (Fierer et al., 2021).

Hence, the main aims of the present investigation were as follows: (a) to evaluate the effect of soil types on soil processes related to nutrients and organic matter dynamics along the profile; and (b) to explore if soil type influences the microbial community and functionality within the uppermost horizon.

4.2 MATERIALS AND METHODS

4.2.1 Characterization of the Study Areas: Location, Climate, Land Use, and Vegetation

Three study areas (BAC, TAS, and PIA) were identified within the Frignano Regional Park, a protected area of 15,000 ha covering the Apennine ridge in the Emilia-Romagna Region (Italy), mainly covered by European beech (Fagus sylvatica L.) forests (Figure 1). The study areas were beech forests managed as high forests in TAS and PIA and as coppice in BAC.

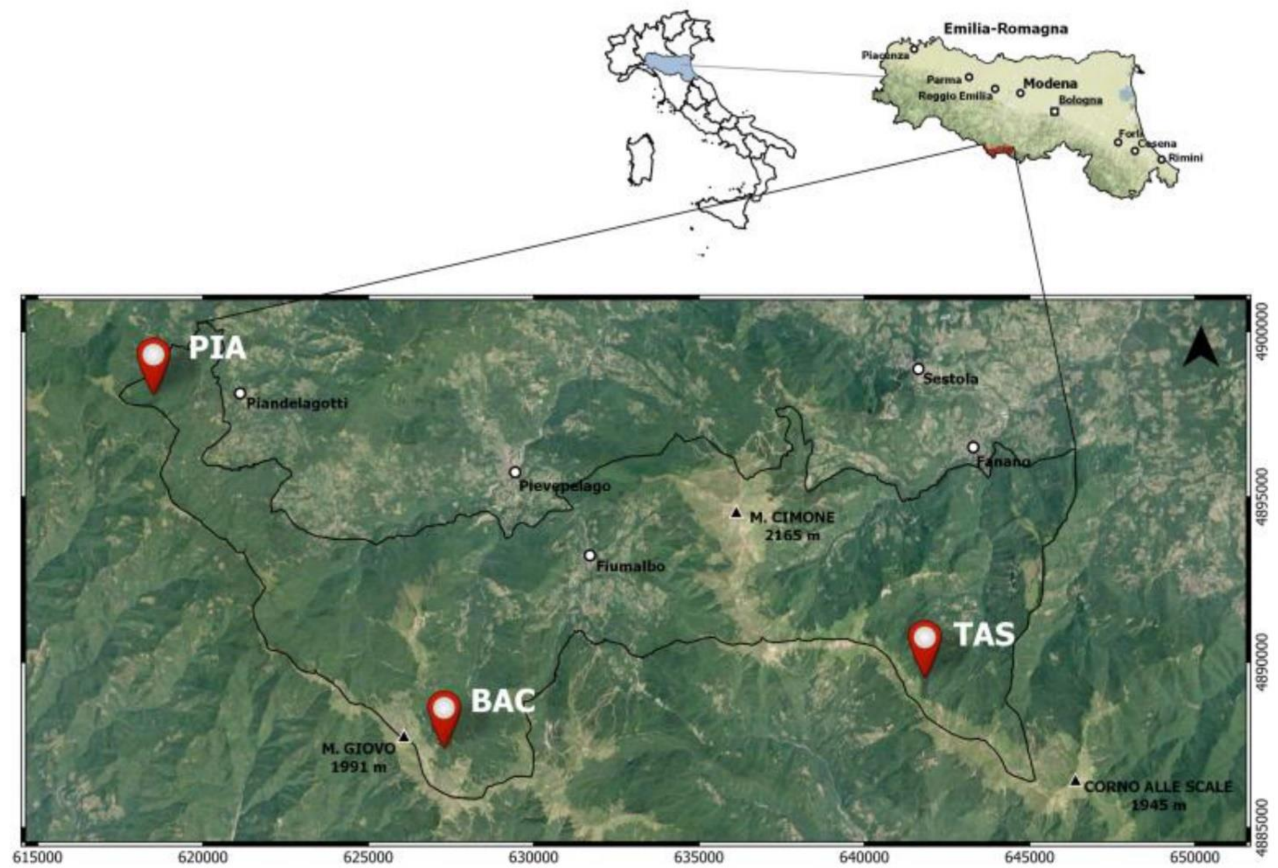

Figure 1. Localization of the study areas within the Frignano Regional Park (Northern Italy).

The study areas, at approximately 1500 m above sea level, are characterized by an average air temperature of 6.6 °C and mean annual precipitation of 1550 mm, mainly in autumn and spring.

The identification of the study areas was based in accordance with the "brown soils" characterization (Vittori Antisari et al., 2023) of high North Apennine. Soils develop on flysch of turbiditic origin, formed and developed on Modino, Cervarola (TAS and PIA), and Macigno (BAC) sandstone formations, as described by Vittori Antisari et al. (2022), which were the most frequent in the park (Antonioli & Cazzola, 1998). Humic Dystrudepts (HD), Typic Dystrudepts (TD), and Humic Lithic Dystrudepts (HLD) were selected in a soil survey opening profile as representative soils of the investigated sites (Table 1).

Table 1. Location, topographical features, and soil type of soil profiles. The X and Y coordinates (Xcoor and Ycoor, respectively) are based on the WGS84 UTM32 coordinate reference system. The soil type is based on the Soil Survey Staff (2014) classification system.

Profile	Xcoor	Ycoor	Elevation	Slope	Aspect	Soil Type
	mE	mN	m a.s.l.	°		
TAS 1	641,818	4,889,485	1517	25	E	Humic Dystrudept, coarse loamy over coarse loamy skeletal, frigid (HD)
TAS 2	641,876	4,889,540	1487	14	E	Humic Dystrudept, coarse loamy over coarse loamy skeletal, frigid (HD)
PIA 1	618,341	4,898,077	1501	2	NW	Typic Dystrudept, coarse loamy, skeletal, frigid (TD)
PIA 2	618,311	4,898,094	1484	31	NW	Typic Dystrudept, coarse loamy, skeletal, frigid (TD)
PIA 3	618,558	4,898,111	1457	9	N	Typic Dystrudept, coarse loamy, skeletal, frigid (TD)
PIA 4	618,491	4,898,090	1465	16	NE	Typic Dystrudept, coarse loamy, skeletal, frigid (TD)
BAC 1	627,259	4,887,352	1602	8	N	Humic Lithic Dystrudept, coarse loamy, skeletal (HLD)
BAC 2	627,165	4,887,374	1598	30	NW	Humic Lithic Dystrudept, sandy over coarse loamy, skeletal (HLD)
BAC 6	627,358	4,887,628	1601	5	W	Humic Dystrudept, coarse loamy, skeletal (HD)
BAC 7	627,298	4,887,626	1593	18	W	Humic Lithic Dystrudept, coarse loamy, skeletal (HLD)

4.2.2 Soil Survey

The survey took place at the end of September 2020 by digging soil profiles until at least the transitional pedogenetic horizon with the parent material (BC). The soil depth was less than 50 cm for those with lithic contact and between 65 and 75 cm for the other soil profiles. For each soil profile, the genetic horizons were described and sampled, as indicated by Schoeneberger et al. (Schoeneberger et al., 2012). For metabarcoding analyses performed on A horizons, three replicates for each site were taken using a sterilized soil core sampler that is 5 cm in diameter. The samples were transported in a sterile plastic bag, stored at 4 °C, and immediately processed upon return to the laboratory. The location of each soil profile is summarized in Table 1.

4.2.3 Soil Analysis

4.2.3.1 Physicochemical Soil Characteristics

The soil samples, including organic horizons, were air-dried and passed through a 2 mm sieve, determining the skeletal percentage for each horizon. An aliquot of sieved samples was finely ground using a steel ball mill. For the 2 mm sieved soil samples, the pH was determined potentiometrically in a 1:2.5 soil-to-deionized water ratio (pH-meter Crison, Barcelona, Spain), while the particle-size distribution was measured by the pipette method (Gee & Bauder, 1986).

4.2.3.2 Total Element Concentration

Briefly, 250 mg of soil samples were mineralized with aqua regia solution (2 mL 65% HNO_3 plus 6 mL 37% HCl, suprapur grade, Carlo Erba, Milano, Italy) using a microwave oven (Milestone 2100, Sorisone, Bergamo, Italy). After digestion, the soil sample solution was made up to 20 mL with Milli-Q ultrapure distilled water and filtered with Whatman 42 filter paper. The total amount of P, S, Ca, Mg, Fe, Al, and K was determined by inductively coupled plasma optical emission spectrometry (ICP-OES; Arcos II, Kleve, Germany, Ameteck Spectro). Each soil sample was analyzed three times, and the data were calibrated using International Reference Materials (BCR) and internal laboratory standards (Ferronato et al., 2021).

4.2.3.3 Organic C and Total N Determination and Stable Isotopes ($\delta^{13}C$ and $\delta^{15}N$)

The organic carbon (OC) and total nitrogen (N) contents of the finely ground samples were determined by a CHN elemental analyzer (Flash 2000, Thermo Fisher Scientific, Waltham, MA, USA) coupled with an isotope ratio mass spectrometer (IRMS Delta C or DELTA+XL, Thermo

Finnigan MAT, Bremen, Germany) for the stable carbon and nitrogen isotope (^{13}C and ^{15}N) determination, expressed as $\delta^{13}C$ (‰) and $\delta^{15}N$ (‰) with respect to the V-PDB universal reference standard for ^{13}C and air for nitrogen.

4.2.3.4 Total Element Concentrations

The soil organic matter of each horizon was chemically fractionated based on Agnelli et al. (Agnelli et al., 2014), with some adjustments. A sample of 10 g of soil was treated with 100 mL of deionized water and shaken on a horizontal shaker for 16 h at 25 °C, after which it was centrifuged, thus separating the supernatant from the precipitate. The first was sieved at 53 µm, and the particles retained by the sieve represented the POM (particulate organic matter). The precipitate was treated with 100 mL of NaOH 0.1 M, shaken for 24 h at 25 °C, and centrifuged again. The extract was filtered with a 0.45 µm polycarbonate filter, and the precipitate (the NEOM, non-extractable organic matter) was rinsed with deionized water to achieve a pH $\leq$ 7. The filtered extract was brought to a pH of about 1.5 with a solution of HCl 6M and left to settle overnight, after which it was centrifuged to separate the supernatant FS (fulvic acid-like substances) from the precipitated humic acid-like substances (HA). The first was neutralized with a solution of NaOH and placed in 1000 Da cutoff dialysis membranes (Spectra/Por® Dialysis membrane) against deionized water, while the latter was rinsed with deionized water. The obtained FS and HA were freeze-dried, while the POM and NEOM were dried at 40 °C. For each fraction, organic carbon, total nitrogen, and their isotopic ratios were determined using the CHN elemental analyzer coupled with an isotope ratio mass spectrometer.

4.2.3.5 Biochemical Soil Parameters

Basal respiration was determined by quantifying the CO_2-C released in the process of microbial respiration during 28 days of incubation at 25 °C, according to Vittori Antisari et al. (Vittori Antisari et al., 2015). Incubation was preceded by bringing the samples to 60% of their water-holding capacity and by a pre-incubation of 3 days. The amount of CO_2-C emitted after 1-3-7-10-14-21-28 days from the beginning of incubation was measured by alkali (Vittori Antisari et al., 2015). While the soil basal respiration (SBR) of each soil sample was computed as the average of the values measured during the incubation period, the cumulative amount of CO_2-C (RCUM) was expressed as the total amount of CO_2-C evolved during the 28 days of incubation.

Microbial biomass C and N (Cmic and Nmic) were estimated by the fumigation-extraction method using 0.5 M K_2SO_4 as the extracting solution (Brookes et al., 1985; Vance et al., 1987). Specifically, for each sample, 10 g of 2-millimeter air-dried soil was adjusted to 60% of the water holding capacity and pre-incubated for 5 days. The soil samples were fumigated with $CHCl_3$ for 24 h at 25 °C. Then, the fumigated and non-fumigated samples were shaken, filtered through a 0.45 μm membrane, and extracted with 40 mL of 0.5 M K_2SO_4 for 30 min. The C and N contents in the filtered solution were determined by a TOC-V CPN total organic carbon analyzer (Shimadzu, Kyoto, Japan). The microbial biomass C was calculated as EC/kEC, where EC = (organic C extracted from fumigated soils) − (organic C extracted from non-fumigated soils) and kEC = 0.45. Microbial biomass N was calculated as EN/kEN, where EN = (total N extracted from fumigated soils) − (total N extracted from non-fumigated soils) and kEN = 0.54.

According to Chantigny et al. (2007), C and N inside the filtered solution obtained from non-fumigated soil samples were considered water-extractable organic C (WEOC) and water-extractable N (WEN).

Then the mineralization quotient (qM; RCUM/OC), metabolic quotient (qCO_2; SBR/Cmic), and microbial quotient (qMIC; Cmic/OC) were also calculated, according to Anderson and Domsch (1989) and Mocali et al. (2008). Dilly's index was calculated as qCO_2/OC, according to Dilly (2005). The ratio indicated the efficiency of using the OC by soil microbial biomass (from 100 efficiency to >400 inefficiency).

4.2.3.6 DNA Extraction and Taxonomic Assignment

Total DNA extraction was performed on all organo-mineral horizons using DNeasy Power-Soil (Qiagen), following the manufacturer's instructions, and for each soil sample, three technical replicates were made.

For microbial and fungal communities, the 16S rDNA V3-V4 region using the locus-specific polymerase chain reaction (PCR) primers 16S 341F/805R (García-López et al., 2023) and the internal transcribed spacer (ITS) region using the primer pairs ITS1F/ITS4R (Gardes & Bruns, 1993; White et al., 1990) were amplified with the integration of relevant flow-cell binding domains and unique indices. The libraries obtained were sequenced on a MiSeq Illumina instrument using 300-bp paired-end mode, and the FASTQ sequences generated were analyzed using DADA2 version 1.12.1 (Callahan et al., 2016) in the R 3.5.1 environment. The reads were filtered and trimmed using the filterAndTrim function set to (270, 230).

The UNITE database was used to perform taxonomic assignments for fungi. For microbial communities, the taxonomic assignment was performed using SILVA nr database version 138, updated according to the reclassification of the genera *Bacillus* and *Lactobacillus,* and applying the assign Taxonomy and add Species functions.

4.2.4 Data Elaboration and Statistical Analysis

Statistical analyses were performed with RStudio 2023.03.0.

To compare soil horizons, cluster analysis using the Ward method (Packages: Factoextra e ggplot2) was performed on the dataset, grouping into three categories (O—organic horizons; A—organo-mineral horizons, which also included some statistical units like Oe and AB horizons; ENDO—mineral horizons). Furthermore, a principal component analysis (PCA) to evaluate the main parameters driving the variability among the statistical units was carried out (packages: FactoMineR). Because of the diverse horizon sequence among the investigated soil profiles and the clusters suggested by the cluster analysis, the data were grouped as organic (O; Oe and Oa horizons), organo-mineral (A; A horizons), and mineral (ENDO; AB, Bw, BC, C, and C_R horizons) layers. To evaluate differences among soil types and soil layers, a non-parametric ANOVA (Kruskal–Wallis test) was performed at $p < 0.05$ using the Agricolae package. Fisher's least significant difference post hoc test was used for comparing the means.

The relationship between the prevalent vertical decrease of OC and the increase of $\delta^{13}C$ in depth profiles was used as a natural indicator of SOC turnover (Acton et al., 2013). For each soil type and each SOM fraction, the slope (β) of the linear regression (y = a + βx) between the mean $\delta^{13}C$ values and their respective log-transformed C concentrations (g C kg^{-1}) was calculated and is referred to as the $\beta_{\delta 13C}$ value (Acton et al., 2013). In particular, "y" was the $\delta^{13}C$, "a" was the intercept of the liner regression, and "x" was the ln of SOC content. The distribution of ^{15}N along soil depth was compared among the investigated areas using the soil enrichment factor ($\varepsilon soil^{15}N$). It is defined as absolute enrichment between the litter (Oi horizon) and the other soil deeper horizons (e.g., organic other than Oi, A, and other mineral horizons here called ENDO) (Hobbie & Ouimette, 2009) and was calculated as follows:

$\varepsilon soil^{15}N$ (‰) = $\delta^{15}N$ (O, A, and ENDO horizons)–$\delta^{15}N$ Oi horizon (Lorenz et al., 2020).

The $\delta^{15}N$ of Oi was −5.2 ± 0.0, −5.3 ± 0.0, and −5.2 ± 0.0‰ for Humic, Humic Lithic, and Typic Dystrudepts, respectively.

Shannon and Simpson diversity indices were calculated to assess microbial and fungal biodiversity within the A horizon. Furthermore, fungal guilds were predicted using FungalTraits (Põlme et al., 2020).

4.3 RESULTS

4.3.1 Pedodiversity

The soil profiles were classified (**Table 1**), according to Soil Taxonomy classification (Soil Survey Staff, 2022), as Humic Dystrudepts (HD, which includes TAS1, TAS2, and BAC6), Humic Lithic Dystrudepts (HLD, which includes BAC1, BAC2, and BAC7), and Typic Dystrudepts (TD, which includes PIA1, PIA2, PIA3, and PIA4). A certain pedodiversity in the three sites was therefore already visible in subgroup soil classification based on soil color (upper 18 cm of soil depth darker in Humic subgroup) and depth of lithic contact (within 50 cm in Lithic subgroup).

4.3.2 Principal Component Analysis

The two main dimensions of PCA explained 71.1% of the variability of the statistical units (**Figure 2**). Such statistical units were distributed from left to right of the scatterplot, separating organic (Oe and Oa), organo-mineral (mostly A horizons and, to a lesser extent, AB horizons), and mineral (AB, Bw, BC, C, and C_R horizons) horizons, as aforesaid by cluster analysis.

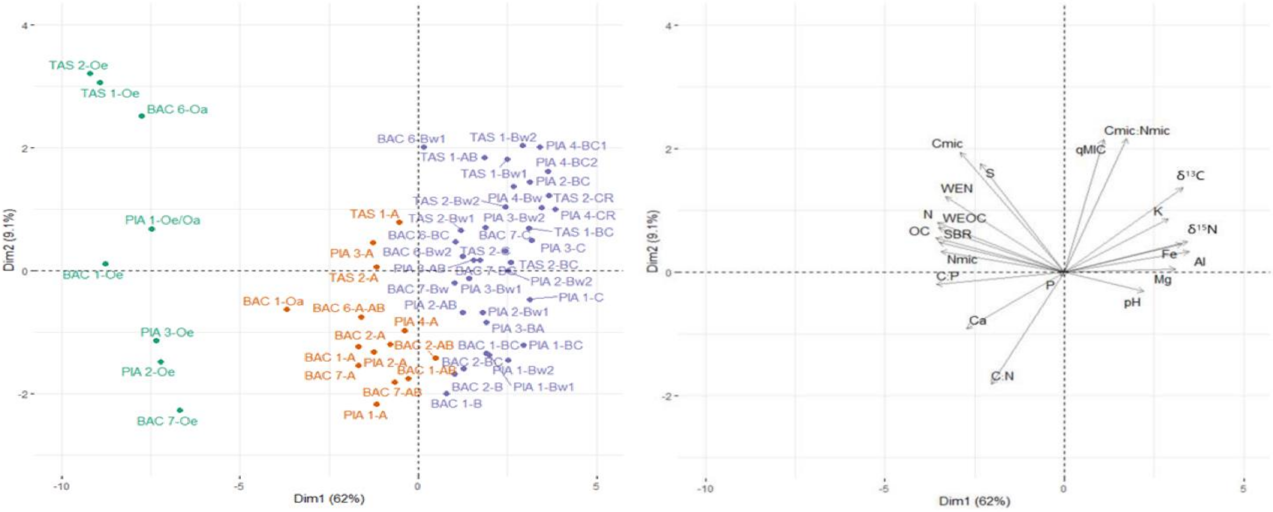

Figure 2. Principal component analysis: plot of statistical units grouped according to cluster analysis results (left); plot of variables (right).

As expected, the variables linked to biogeochemical cycles (OC, N, S, and P concentrations and C:P and C:N ratios), microbial biomass content (Cmic and Nmic), and its activity (SBR) characterized the organic horizons and, to a lesser extent, the organo-mineral horizons. $\delta^{13}C$ and $\delta^{15}N$ values as well as terrigenous element (Fe, Al, Mg, and K) contents were positively correlated to mineral horizons.

4.3.3 Soil Profiles, Features, and Organic Matter Characterization of Bulk Soil

Considering the different soil types (i.e., Humic Dystrudept—HD, Humic Lithic Dystrudept—HLD, and Typic Dystrudept—TD), the amount of both nutrients and total elements found in the O, A, and ENDO layers is shown in Table 2.

Table 2. Mean and standard deviation of the chemical properties of the organic (O; Oe and Oa horizons), organo-mineral (A; A horizons), and mineral (ENDO; AB, Bw, BC, C, and C_R horizons) layers of the investigated soils. Within each column, means shearing similar letters indicate non-significant differences according to the Kruskal–Wallis test.

	pH	N	OC	δ13C	δ15N	Al	Fe	Ca	Mg	P	S	OC:N	OC:P
		%	%	‰	‰	g kg^{-1}	g kg^{-1}	g kg^{-1}	g kg^{-1}	g kg^{-1}	g kg^{-1}		
Humic Dystrudepts													
O	4.0 c	1.8 a	37.9	−27.66 de	−2.82 c	7.5 c	6.0 d	3.9 ab	1.5 d	0.7 a	1.2 a	20.9 a	512 a
	(0.30)	(0.11)	(2.23) a	(0.60)	(1.30)	(1.22)	(0.97)	(0.12)	(0.09)	(0.10)	(1.21)	(0.44)	(103)
A	3.7 c	0.6 a	9.2	−26.79 cd	1.45 bc	27.2 bc	15.9 c	1.1 c	3.5 cd	0.7 ab	0.6 a	18.5 ac	185 ab
	(0.02)	(0.30)	(3.45) a	(0.29)	(1.73)	(9.83)	(0.83)	(0.44)	(0.23)	(0.43)	(0.56)	(6.07)	(96)
ENDO	4.5 b	0.2 b	3.3 b	−25.57 a	5.48 a	37.9 a	27.9 a	0.7 d	7.5 b	0.6 ab	0.2 bc	15.8 c	75 b
	(0.24)	(0.07)	(0.97)	(0.27)	(0.51)	(5.79)	(0.07)	(0.76)	(0.54)	(0.25)	(0.26)	(4.24)	(59)
p value	<0.05	<0.05	<0.05	<0.05	<0.05	<0.05	<0.05	<0.05	<0.05	ns	<0.05	<0.05	<0.05
Humic Lithic Dystrudepts													
O	4.3 bc	1.2 a	27.8 a	−28.13 e	−3.64 c	6.4 c	5.1 d	7.5 a	1.8 d	0.6 ab	0.8 a	22.6 a	475 a
	(0.35)	(0.32)	(8.79)	(0.46)	(1.15)	(5.4)	(4.23)	(3.64)	(0.02)	(0.10)	(0.14)	(1.17)	(111)
A	4.4 bc	0.5	9.4 a	−27.29 de	−1.56 c	23.3 bc	14.9 c	3.9 ab	4.4 cd	0.4 ab	0.4 ab	18.9 ac	228 ab
	(0.11)	(0.05) a	(0.79)	(0.07)	(0.07)	(0.03)	(0.09)	(0.04)	(0.04)	(0.04)	(0.07)	(0.34)	(6)
ENDO	4.6 ab	0.2 b	3.7 b	−26.55 c	3.60 b	32.4 b	23.6 b	2.7 b	7.1 b	0.3 b	0.2 cd	20.5 a	119 ab
	(0.27)	(0.08)	(1.33)	(0.49)	(2.00)	(5.9)	(5.61)	(0.52)	(0.24)	(0.07)	(0.03)	(2.38)	(40)
p value	<0.05	<0.05	<0.05	<0.05	<0.05	<0.05	<0.05	<0.05	<0.05	ns	<0.05	<0.05	<0.05
Typic Dystrudepts													
O	4.2 bc	1.5 a	36.2 a	−28.57 e	−3.89 c	9.9 c	8.0 d	3.6 ab	2.4 cd	0.6 ab	0.9 a	23.5 a	587 a
	(0.53)	(0.23)	(6.41)	(0.72)	(0.92)	(0.40)	(1.22)	(0.69)	(0.21)	(0.06)	(0.11)	(0.72)	(60)
A	3.9 c	0.4 a	8.7 a	−27.25 de	−0.11 c	28.2 bc	17.4 c	1.2 c	5.7 bc	0.5 ab	0.5 ab	20.4 ab	175 ab
	(0.11)	(0.18)	(2.76)	(0.42)	(0.72)	(1.45)	(0.73)	(0.57)	(0.32)	(0.36)	(0.16)	(5.07)	(99)
ENDO	4.7 a	0.1 c	2.1 c	−26.01 b	5.43 a	39.4 a	25.3 b	0.8 c	10.2 a	0.6 ab	0.2 d	16.6 bc	59 b
	(0.19)	(0.05)	(0.07)	(0.52)	(1.28)	(5.79)	(3.85)	(0.35)	(0.27)	(0.27)	(0.08)	(3.67)	(79)
p value	<0.05	<0.05	<0.05	<0.05	<0.05	<0.05	<0.05	<0.05	<0.05	ns	<0.05	<0.05	<0.05

N, OC, δ13C, δ15N, Al, Fe, Ca, Mg, P, and S are the concentrations of total nitrogen, organic carbon, 13C, 15N, total aluminum, total iron, total calcium, total magnesium, total phosphorus, and total sulfur, respectively; ns = non-significant.

The investigated soils showed acidic conditions without significant differences among the soil types, with the exception of the ENDO layer, which showed slightly higher pH values in TD than in HD. Along the soil depth, lower pH values in the O and A layers compared to ENDO were observed for both HD and TD (Table 2). Concerning the total amount of elements (i.e., N, P, S, OC, Al, Ca, Fe, and Mg), neither O nor A layers showed differences among the investigated soil types. The only difference occurred for Ca in the A layer, whose amount was more than three times higher in HLD than in HD and TD. Unlike the O and A, the ENDO layer showed some more differences among the soil types. In particular, the concentrations of N and OC had the lowest values in the TD (0.1 and 2.1%, respectively). The highest amounts of Fe and Mg were observed in HD and TD, respectively, while the lowest Al content was found in HLD. Finally, the Ca content decreased in the order HLD > HD > TD. Similar to the total amount of elements, the C:N and C:P ratios did not show differences among the soil types for the O and A layers. The ENDO layer showed the highest C:N ratio (20.5) within the HLD. As expected, the amount of nutrients related to the SOM cycle (i.e., N, OC, Ca, Mg, and S) decreased with depth; conversely, those related to the parent material (i.e., Al and Fe) increased. Noteworthy, the A layer generally had similar element contents to the O layer (i.e., OC, N, Al, Mg, and S). The C:N and C:P ratios showed some differences between the O and ENDO layers of HD and TD, with higher values in the most superficial layer than in the deepest layer. Regarding the $\delta^{13}C$ and $\delta^{15}N$, some differences among the soil types occurred only within the ENDO layer, where the lowest $\delta^{15}N$ value was observed within the HLD, while the $\delta^{13}C$ values decreased in the order HD > TD > HLD. Both $\delta^{13}C$ and $\delta^{15}N$ increased with depth, but with similar values between the O and A layers.

Concerning the stable isotope fractionation in biological processes (−0.97, −0.88, −0.83 with R2 0.86, 0.90, and 0.96 for HD, HLD, and TD, respectively) within the bulk soil, $\beta_{\delta 13C}$ values showed an increasing trend as follows: TD > HLD > HD, as well as high values, mainly in the A layer, of $\varepsilon soil^{15}N$ in HD (Figure 3).

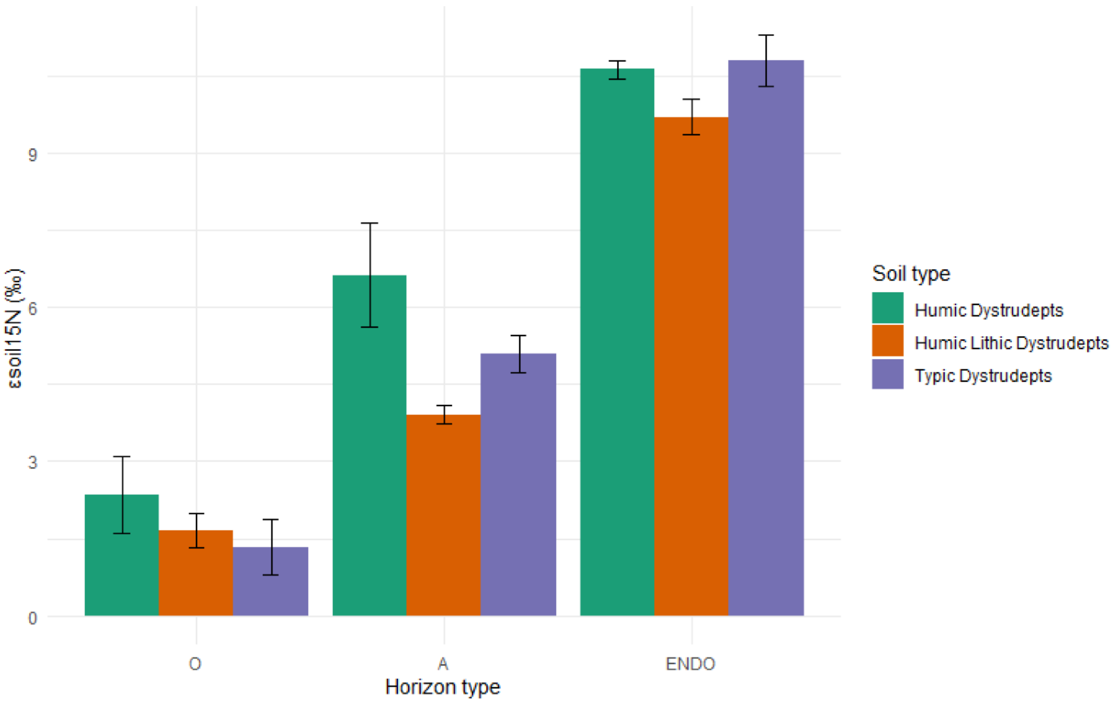

Figure 3. εsoil^{15}N values for organic (O; Oe and Oa horizons), organo-mineral (A; A horizons), and mineral (ENDO; AB, Bw, BC, C, and C_R horizons) layers. Error bars are the standard deviation.

4.3.4 Soil Organic Matter Fractions

The chemical characteristics of SOM fractions are shown in Table S1.

In all soil types, the $\beta_{\delta 13C}$ of the obtained SOM fractions (Table 3) showed higher values for the POM fraction, while the humic substances (FA and HA) showed the more negative ones.

Table 3. $\beta_{\delta 13C}$ and R2 values resulted from the linear regression between $\delta^{13}C$ and log C for the humic acid-like substances (HA), fulvic acid-like substances (FS), non-extractable organic matter (NEOM), and particulate organic matter (POM).

	HA		**FS**		**NEOM**		**POM**	
	$\beta\delta^{13}C$	**R^2**	**$\beta\delta^{13}C$**	**R^2**	**$\beta\delta^{13}C$**	**R^2**	**$\beta\delta^{13}C$**	**R^2**
Humic Dystrudepts	−1.11	1.00	ns	ns	−0.61	0.87	−0.17	0.98
Humic Lithic Dystrudepts	−1.04	0.88	−1.09	0.48	ns	ns	0.27	0.97
Typic Dystrudepts	−1.41	0.64	−1.38	0.98	−0.63	0.98	−0.09	0.80

ns = non-significant.

Through the comparison of soil types, the major differences occurred for POM and humic substances. Specifically, while the $\beta_{\delta 13C}$ values of POM followed the order HD < TD < HLD, for the humic substances, the $\beta_{\delta 13C}$ values showed TD < HD = HLD.

The pattern of $\delta^{15}N$ values in relation to the C:N ratio of each humic fraction along the profiles' horizons is shown in Figure 4. Generally, the $\delta^{15}N$ values of POM in the deep soil were more negative compared to other fractions, indicating a lower SOM transformation, with the exception of HLD, where a great transformation in the ENDO layer was found. In HLD, thinner soils occurred as lithic contact was within 50 cm of the soil surface. Therefore, the shallower depth of ENDO compared to other types of soil must be considered. The C:N ratio in deeper horizons increased, losing nitrogen between 40 and 60. In the ENDO layer, the $\delta^{15}N$ values were more positive, indicating a higher SOM transformation along the soil profile.

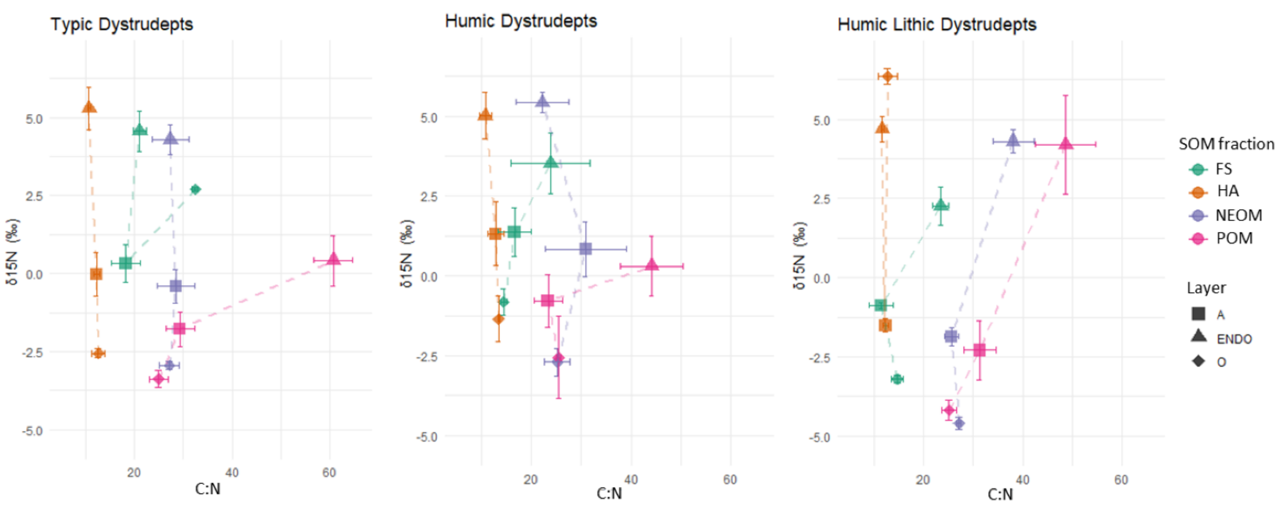

Figure 4. Plot between the $\delta^{15}N$ and C:N ratios of humic acid-like substances (HA), fulvic acid-like substances (FS), non-extractable organic matter (NEOM), and particulate organic matter (POM) for organic (O; Oe and Oa horizons), organo-mineral (A; A horizons), and mineral (ENDO; AB, Bw, BC, C, and C_R horizons) layers. The error bars are the standard deviations.

4.3.5 Biochemical Parameters

The water-soluble forms of organic C and N and the microbial biomass showed similar amounts among the soil types for both O and A layers. Some differences occurred for the ENDO layer, which showed the lowest contents of WEOC, WEN, Cmic, and Nmic within the TD. As expected, these C and N forms decreased with soil depth (Table 4).

Table 4. Mean and (standard deviation) of the biochemical properties of the organic (O; Oe and Oa horizons), organo-mineral (A; A horizons), and mineral (ENDO; Bw, BC, C, and C_R horizons) layers of the investigated soils. Within each column, means shearing similar letters indicate non-significant differences according to the Kruskal–Wallis test.

	WEOC	**WEN**	**Cmic**	**Nmic**	**Cmic:Nmic**	**qCO_2**	**qM**	**qMIC**	**Dilly's Index**
	mg kg^{-1}	**mg kg^{-1}**	**mg kg^{-1}**	**mg kg^{-1}**		**µgC-CO_2/µg Cmic**	**%**	**%**	
Humic Dystrudepts									
O	1967 a	337 a	1570 a	247 ab	6.2 ab	0.16 c	2.7 a	0.41 bc	41 c
	(362)	(110)	(243)	(87)	(1.62)	(0.30)	(0.01)	(0.03)	(2.1)
A	720 ab	69 ab	481 ab	70 bd	8.1 ab	1.1 a	2.3 ab	0.60 ab	117 bc
	(314)	(25)	(10)	(26)	(4.34)	(0.05)	(0.01)	(0.11)	(4.5)
ENDO	500 b	31 c	350 bc	37 d	12.5 a	0.47 b	1.6 c	0.98 a	159 bc
	(179)	(9)	(252)	(33)	(7.38)	(0.02)	(0.01)	(0.12)	(5.7)
p value	<0.05	<0.05	<0.05	<0.05	<0.05	<0.05	<0.05	<0.05	<0.05
Humic Lithic Dystrudepts									
O	1440 a	177 ab	843 ab	158 ab	5.4 ac	0.33 c	3.2 a	0.31 bc	113 bc
	(403)	(81)	(560)	(81)	(1.19)	(0.15)	(1.15)	(0.15)	(6.4)
A	657 ab	63 ab	300 bd	95 ac	3.2 bc	1.95 a	2.6 a	0.35 bc	213 ab
	(162)	(22)	(92)	(31)	(0.11)	(0.01)	(0.14)	(0.14)	(7.6)
ENDO	460 b	28 c	162 de	44 cd	6.9 bc	1.11 ab	1.6 bc	0.43 bc	303 ab
	(141)	(11)	(67)	(22)	(0.76)	(0.07)	(0.54)	(0.54)	(16.3)
p value	<0.05	<0.05	<0.05	<0.05	<0.05	<0.05	<0.05	<0.05	<0.05
Typic Dystrudepts									
O	1770 a	153 ab	523 ab	310 a	1.7 c	1.01 ab	2.9 a	0.16 c	167 ac
	(20)	(25)	(125)	(30)	(0.87)	(0.35)	(1.21)	(0.03)	(34.1)
A	696.3 ab	54 b	297 cd	83 bc	3.7 bc	3.05 a	2.6 a	0.35 bc	344 ab
	(211)	(13)	(87)	(46)	(2.11)	(0.21)	(0.67)	(0.04)	(67.2)
ENDO	336 c	18 d	118 e	12 e	14.4 a	0.57 b	1.8 bc	0.58 b	589 a
	(183)	(10)	(74)	(11)	(11.01)	(0.08)	(0.34)	(0.01)	(111,1)
p value	<0.05	<0.05	<0.05	<0.05	<0.05	<0.05	<0.05	<0.05	<0.05

WEOC, WEN, Cmic, and Nmic are the concentrations of the water-extractable organic carbon, water-extractable nitrogen, microbial biomass C, and microbial biomass N, respectively. qCO_2, qM, and qMIC are the metabolic, mineralization, and microbial quotients, respectively.

Regarding the indicators of soil microbial functionality, the qCO_2 showed differences among the soil types only for the O layer, with the highest values within the TD (1.0 μgC-CO_2/μgCmic). Instead, the qMIC showed some differences within the ENDO layer, with the highest value (9.8%) in HD. Considering the trend with depth, the qCO_2 showed a dissimilar trend among the considered soil types. Unlike qCO_2, the qM was similar between the O and A layers, which were higher compared to the ENDO layer. The qMIC, instead, showed some differences in HD and TD, with lower values in O than in the ENDO layer. The Dilly's index grew with increased depth, and HD showed along the soil profiles a great efficiency to use the OC by soil microbial biomass.

4.3.6 Functional and Genetic Biodiversity of Organo-Mineral Horizons

Figure 5 and Figure 6 show the phyla of bacterial and fungal populations, and no significant differences were found among the A horizons of soil types. This is congruent with the lack of significant differences in functional parameters of microbial biomass in the organic-mineral horizons. In fact, no differences in microbial parameters were found (Table 4) except for the amount of Cmic in HD, which was significantly higher than in HLD and TD.

In all soils, Firmicutes and Bacteroidota accounted for more than 75% of ATS, followed by Proteobacteria and Campylobacterota (Figure 5). Concerning fungal communities, Basidiomycota varied from 41% to 61%, followed by Ascomycota (from 14% to 22%) and Mortierellomycota (from 15% to 24%) (Figure 6).

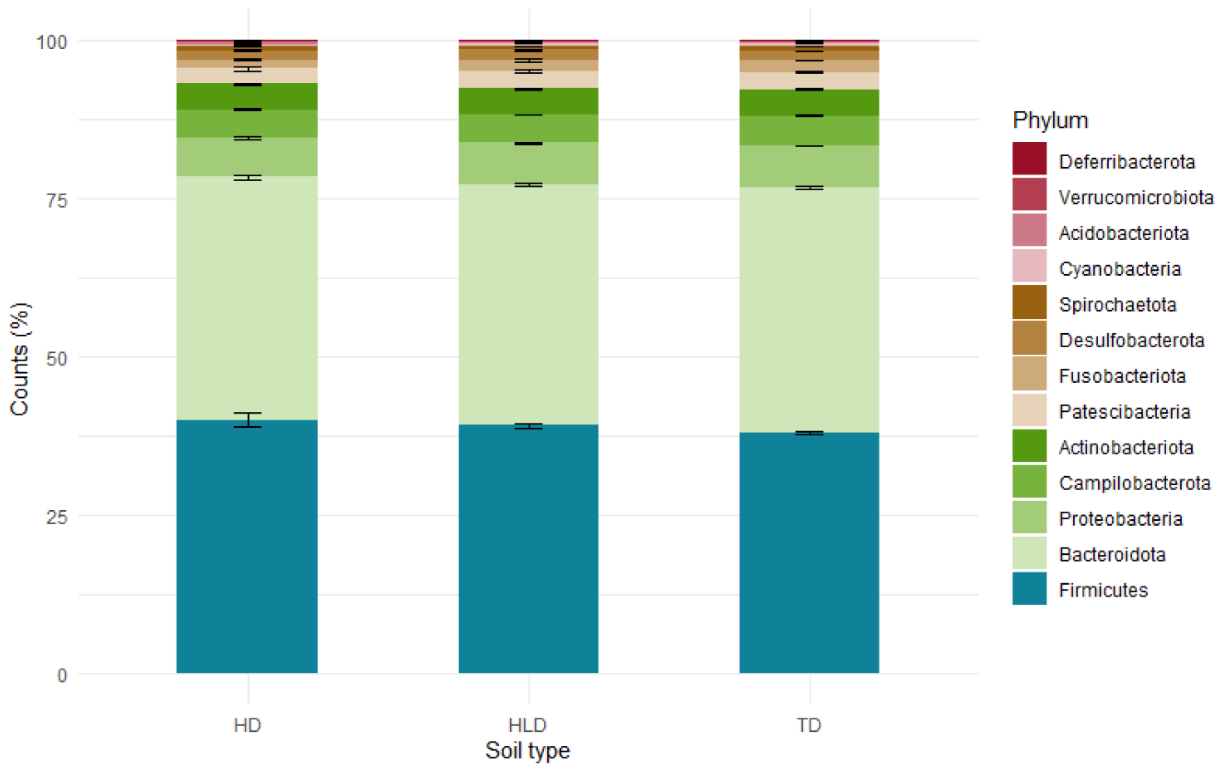

Figure 5. Phyla of bacterial populations characterizing A horizons in Humic, Humic Lithic, and Typic Dystrudepts. The error bars are the standard deviations.

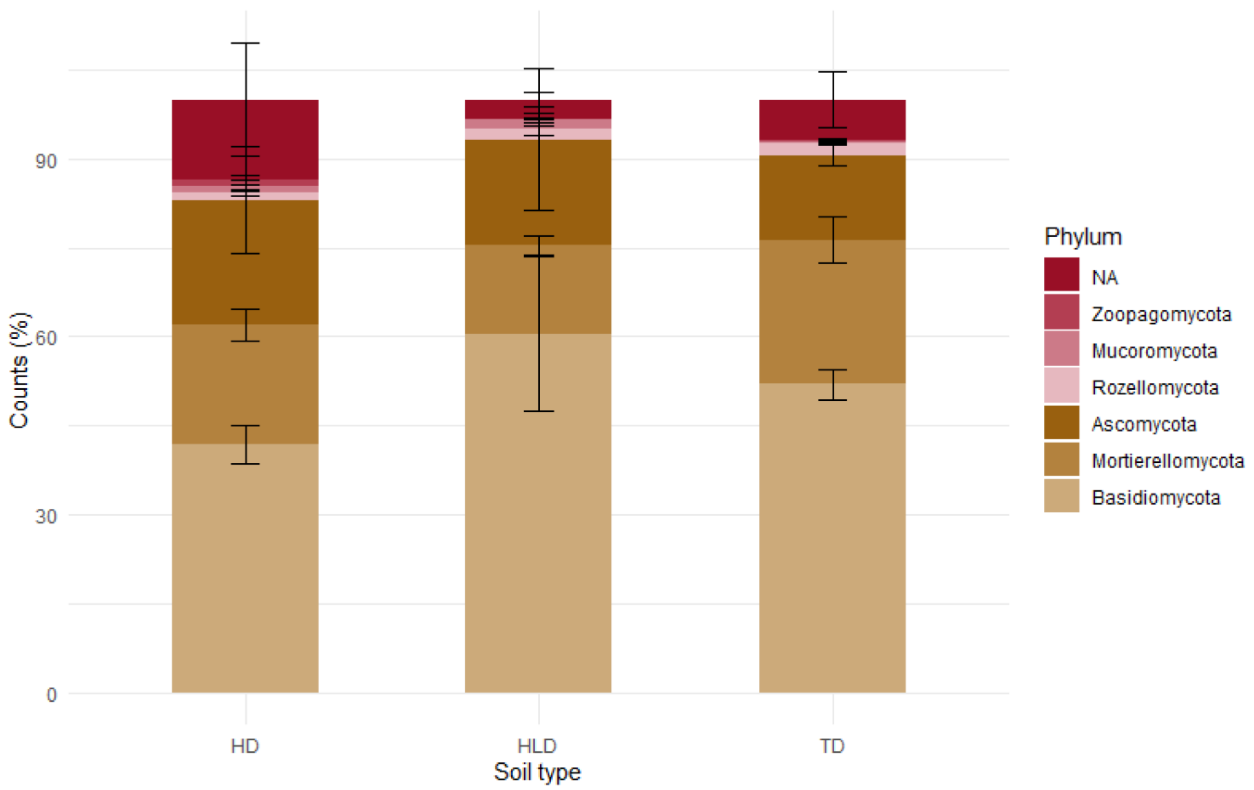

Figure 6. Phyla of fungi populations characterizing A horizons in Humic, Humic Lithic, and Typic Dystrudepts (HD, HLD, and TD, respectively). The error bars are the standard deviations.

Both Simpson's and Shannon's indexes highlighted a similarity between the bacterial populations in the three soil types at the phylum level (Simpson: 0.684, 0.692, and 0.696 in HD, HLD, and TD, respectively; Shannon: 1.47, 1.50, and 1.52 in HD, HLD, and TD, respectively). Similar values were found for fungal community at species level, for Simpson (0.8181, 0.8138, and 0.8564 in HD, HLD, and TD, respectively), and for Shannon index (2.667, 2.506, and 2.53 in HD, HLD, and TD, respectively).

Figure 7 shows the distribution of different fungi categories like ectomycorrhizal, litter-saprotroph, and soil-saprotroph fungi, highlighting a significantly higher prevalence of ectomycorrhizal fungi in all soil types. Litter saprotrophs are the least abundant group and appear to be absent in HLD. Despite that, no significant differences were found between soil types by considering fungal guilds.

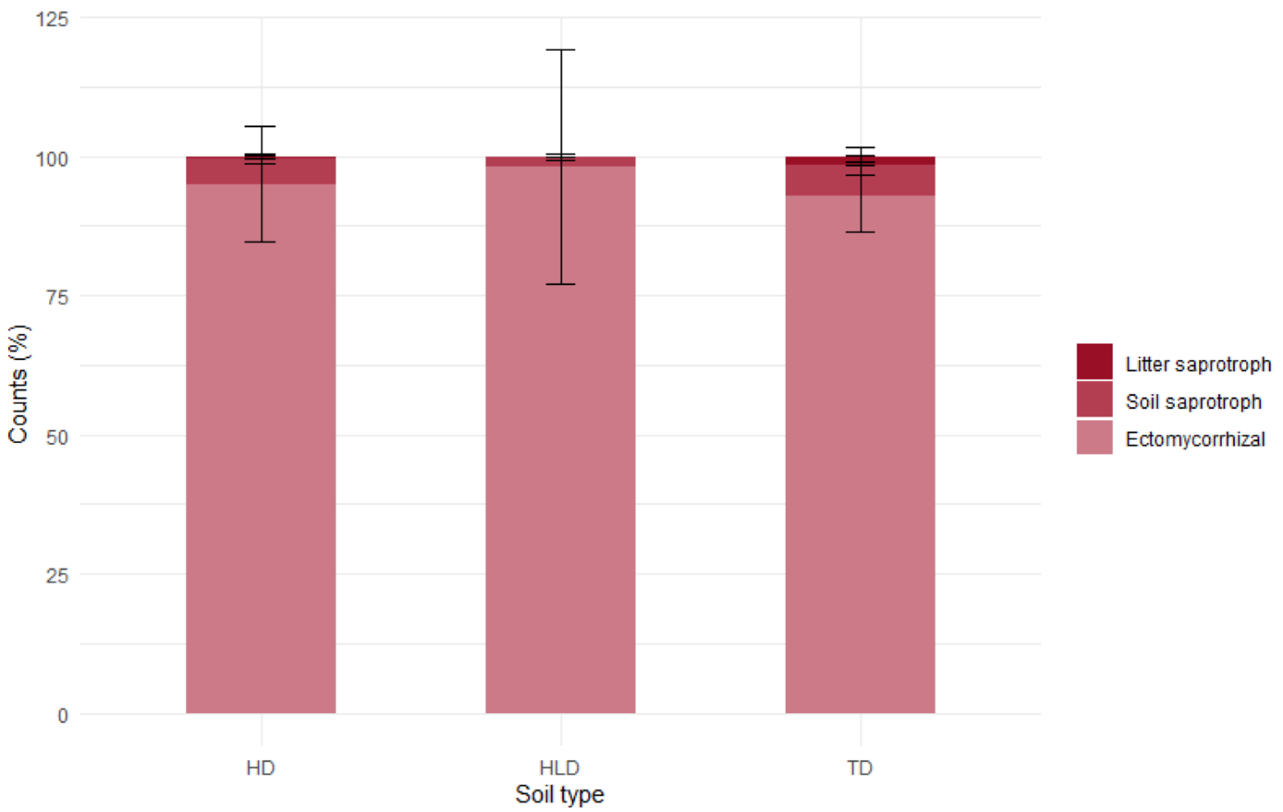

Figure 7. Distribution of ectomycorrhizal, litter saprotroph, and soil saprotroph within the A horizons in Humic, Humic Lithic, and Typic Dystrudepts (HD, HLD, and TD, respectively). The error bars are the standard deviations.

4.4 DISCUSSION

4.4.1 Chemical and Biochemical Features of the Investigated Soils

The investigated soil types (i.e., HLD, HD, and TD) are some of the most frequent in European beech forests in southern parts of Europe (Vittori Antisari et al., 2023; Merino et a., 2007; Conforti et al., 2020). In our study area, the lithic contact occurring within the 50 cm of soil depth for the HLD soil might be mainly due to the weaker alterability of the Macigno Massif sandstone formation, from where such soils developed (BAC), than the other sandstone formations (Vittori Antisari et al., 2023). However, at the BAC study site, the lack of lithic contact within the 50 cm of soil depth for the BAC6 soil profile could be attributed to its position. Specifically, the BAC6 soil profile was located on the ridge, which allowed the deepening of the soil (Conforti et al., 2020; Fazlollahi Mohammadi et al., 2016). Considering the soil profiles as a whole, a darker soil color observed within the upper 18 cm for the HLD and HD soils than TD (Soil Survey Staff, 2022) indicated an overall higher organic matter accumulation in HLD and HD compared to TD (Łachacz & Załuski, 2023; Ibáñez-Asensio et al., 2013). This fact might be attributed to the slightly lower plant biomass amount in the forests of TD than in those of HD and HLD due to the diverse beech forest management, which affects the organic matter input into the soils (Bruckman et al., 2011; Camponi et al., 2022).

The clustering of the soil horizons was similar for the investigated soil types, and it was driven by the chemical and biochemical features of soil horizons linked to organic C and N cycles. Specifically, the cluster grouping of the O horizons was positively related to the biochemical soil properties (i.e., Cmic, Nmic, SBR, and WEOC), suggesting the role of plant residue quality on both O horizon features and the degradation processes of organic matter (Córdova et al., 2018; Singh et al., 2022). Since the organic matter degradation byproducts get into the underlying A horizon (Bonifacio et al., 2013), this fact might explain the similar features observed among the A horizons. The clustering of O horizons positively driven by biochemical properties was in accordance with previous studies conducted in forest ecosystems (Stewart et al., 2011; Kohl et al., 2018). Also, it was interesting to observe that the distinction of the cluster containing the O horizons was strongly affected by Ca content, indicating the occurrence of an intense biocycling of such a nutrient (Berger et al., 2006). Calcium is a very scarce element in acidic soils, but beech trees can absorb it from the subsoil and transfer it to the soil surface via litterfall (Błońska et al., 2018; Ammer et al., 2006). In accordance with early studies (e.g., Agnelli et al., 2004), the Cmic content decreased with soil depth. However, it was interesting to observe that, considering each soil profile, the HD showed the highest soil microbial biomass and the Cmic represented between 4 and 10% of organic carbon (qMIC). All the investigated soil profiles showed a slight increase in the Cmic:Nmic ratio from the O to the ENDO layer, suggesting a shifting of the microbial community to a fungi-enriched community with depth (Wallenstein et al., 2006).

The qCO_2 values were higher in the A horizons than the ENDO ones in both HD and TD soils, indicating a higher energy demand by the microbial communities in topsoil than in ENDO (Mganga et al., 2016). However, using Dilly's index, it was interesting to observe higher values in TD than in HD and HLD, indicating a lower carbon use efficiency of the soil microbial community in the former than in the latter (Dilly, 2005), which further might have prevented the melanization process in the upper 18 cm of TD soil, as depicted by soil color.

4.4.2 Soil Organic Matter Turnover

The highly negative $\beta_{\delta 13C}$ values of bulk soil suggest a rapid turnover of the organic matter in all the investigated soil types (Acton et al., 2013), likely due to the coarse texture and the low interaction with the mineral phase (Hamzehpour et al., 2019). Although HD and HLD showed slightly more negative $\beta_{\delta 13C}$ values compared to TD, the higher organic matter accumulation defined by the darker soil color might be attributed to the long-lasting higher organic matter input due to the greater plant biomass amount (Ahirwal et al., 2014); Grüneberg et al., 2014). In accordance with early studies, the $\varepsilon soil^{15}N$ value increased with soil depth (Lorenz et al., 2020) due to the increase of degraded and ^{15}N-enriched organic matter (Hobbie & Ouimette, 2009; Lorenz et al., 2020).

Looking at the extracted organic carbon fractions, the organic carbon related to POM generally showed the highest ß$_{\delta 13C}$ values and therefore the lowest transformation rate. The POM fraction is recognized to be a labile organic matter fraction because of the absence of any physical protection, making it easily degradable by the microbial community (Zeller & Dambrine, 2011). Despite this, the highest ß$_{\delta 13C}$ values of POM might be attributed to the low degradation of such a fraction. In fact, the POM fraction showed the highest C:N ratio, which could indicate its low mineralization by the soil microbial community. Noteworthy, the similar POM C:N ratio between O and A layers would confirm the great influence of organic matter in O horizons on that of the underlying A horizon.

The highest δ^{13}C values of the humic substances (FS and HS) suggest how such compounds can be the results of microbial activity (Sen et al., 2020) and, therefore, they can be considered the most relevant by-product due to microbial SOM degradation and humification processes. In fact, early studies found that the humic substances could be easily degraded due to their low C:N ratio (Traversa et al., 2014; Traversa et al., 2011; Senesi et al., 1989) especially if not protected from the soil microbial community (Zavarzina et al., 2021). The relative low C:N ratio and high δ^{15}N value would confirm the transformation of humic substances by microbial biomass. The higher N content in HS than in FS is in accordance with early studies that demonstrated that FS are small N-enriched molecules (Ukalska-Jaruga et al., 2021) coming from the depolymerization and transformation of organic matter and therefore the most degraded organic molecules (Machado et al., 2020; Reemtsma et al., 2006).

Our findings generally showed that FS, HA, and NEOM had a lower turnover in HD and HLD compared to TD, which is in accordance with Ukalska-Jaruga et al.'s (Ukalska-Jaruga et al., 2021) finding that the type of soil can determine the direction of chemical organic matter's transformation. In particular, the NEOM fractions, which include highly aliphatic compounds (Hayes et al., 2017) such as cutin and suberin, which are abundant in beech plant residues (Berg

& McClaugherty, 2014; Hobbie et al., 2006), showed differences about $\beta_{\delta 13C}$ values among the soils.

4.4.3 Genetic and Ecophysiological Biodiversity of the A Horizons

The soil biochemical properties of organic-mineral horizons were greatly affected by the edaphic properties (Fierer et al., 2021; Ramírez et al., 2020). In this sense, because of both the lack of differences in the chemical properties of topsoil among the investigated soil types and the greater influence of organic matter quality compared to its quantity (Singh et al., 2022; Fanin et al., 2014), within the topsoil no differences in both biochemical properties and microbial community were observed. In fact, low variability in bacterial phyla among the investigated soils was found. Firmicutes and Bacteroidota, which accounted for approx. Moreover, 75% of the total ASV detected, are considered root-inhabiting communities and thus prevailing in the root endosphere (in this case up to 95% of ATS), and their prevalence is not affected by soil type. In addition, many of the genera belonging to these phyla are commonly part of the animal microbiota and, in particular, of the gut microbiome (Kuramae et al., 2011; Bulgarelli et al., 2013). Many of the remaining phyla (including Acidobacteriota) are signaled as members of the rhizosphere and excluded from the root endosphere niche. Within the soil microbiota, the *Bacteroidetes* tend to be a dominant phylum, just like in human and animal intestines, because of their ability to secrete diverse arrays of carbohydrate-active enzymes (CAZymes) that target the highly varied glycans in the soil (Larsbrink & McKee, 2020), which can be considered precursors of humic substances (Ziolkowska et al., 2020). Firmicutes have been found as dominant phyla in many forest soils around the world (Kuramae et al., 2012; Ahmad et al., 2009; Aislabie et al., 2009).

In our type of soils, much variability was detected in fungi communities, and Ascomycota, Basidiomycota, and Mortierellomycota can be considered the major microorganisms in forest soils, mostly involved in cellulose decomposition (Štursová et al., 2012). Ma et al. (2013) showed that Ascomycota were the dominant communities in the early and late stages of residue decomposition. Both litter and soil saprophyte communities were mainly detected in TD, suggesting a greater role for dead wood in SOM turnover and, therefore, for the fungal communities that degrade it. Indeed, saprophytic fungi degrade cellulose and lignin, suggesting different sources, in addition to litter, of SOM supply in TD compared to other soils.

4.5 CONCLUSIONS

In weakly developed Dystrudepts in mountain areas, soil organic matter quality seemed to be the main driving factor regulating soil biodiversity. Some differences in soil functionality, however, appeared related to pedodiversity, at least as detectable by the subgroup taxonomic level. In fact, lower melanization occurred in the upper part of the soil profile, where the plant density was lower and Typic Dystrudepts were present. Here, Dilly's index showed a lower efficiency of microbial biomass, and the highest presence of saprophytic fungi suggested the relevance of dead wood.

Because of the complex interlinks among pedodiversity, biodiversity, and soil functionality, our findings did not explain if the differences in biodiversity and soil functionality were the results of pedodiversity, or rather, if pedodiversity was their result. The proposed combined approach, considering soil diversity, however, appears to be very promising in investigations on soil C dynamics and in future research, and it could provide new insights into the complexity of the soil ecosystem.

SUPPLEMENTARY MATERIALS

The following supporting information can be downloaded at: https://www.mdpi.com/article/10.3390/f15020353/s1. Table S1: Concentrations of nitrogen (N), carbon (C), ^{13}C and ^{15}N, and C:N ratio in humic acid-like substances (HA), fulvic acid-like substances (FS), non-extractable organic matter (NEOM), and particulate organic matter (POM) for organic (O; Oe and Oa horizons), organo-mineral (A; A horizons), and mineral (ENDO; AB, Bw, BC, C, and C_R horizons) layers.

AUTHOR CONTRIBUTIONS

Conceptualization, L.V.A.; methodology, L.V.A.; validation, L.V.A., A.Z. and F.G.; formal analysis, W.T. and L.V.A.; investigation, M.D.F., W.T., G.F., F.P. and G.T.; resources, L.V.A.; data curation, W.T.; writing—original draft preparation, M.D.F. and F.P.; writing—review and editing, M.D.F., L.V.A., G.F., A.Z. and F.G.; visualization, M.D.F., W.T., L.V.A., F.P. and G.T.; supervision, L.V.A., A.Z. and F.G.; project administration, L.V.A.; funding acquisition, L.V.A. All authors have read and agreed to the published version of the manuscript.

FUNDING

Project funded by the European Union—NextGenerationEU, under the National Recovery and Resilience Plan (NRRP), project title "National Biodiversity Future Center—NBFC" (project code CN_00000033).

DATA AVAILABILITY STATEMENT

Data are contained within the article.

CONFLICTS OF INTEREST

The authors declare no conflicts of interest.

REFERENCES

Abakumov, E. (2022). Pedodiversity of Subboreal Ecosystems under Contrasting Geogenic Factors (Case Study of Samarskaya Luka, Middle Volga Region, Russia). *Geosciences*, *12*(12), 443.

Acton, P., Fox, J., Campbell, E., Rowe, H., & Wilkinson, M. (2013). Carbon isotopes for estimating soil decomposition and physical mixing in well-drained forest soils. *Journal of Geophysical Research: Biogeosciences*, *118*(4), 1532-1545.

Agnelli, A., Ascher, J., Corti, G., Ceccherini, M. T., Nannipieri, P., & Pietramellara, G. (2004). Distribution of microbial communities in a forest soil profile investigated by microbial biomass, soil respiration and DGGE of total and extracellular DNA. *Soil biology and Biochemistry*, *36*(5), 859-868.

Agnelli, A., Bol, R., Trumbore, S. E., Dixon, L., Cocco, S., & Corti, G. (2014). Carbon and nitrogen in soil and vine roots in harrowed and grass-covered vineyards. *Agriculture, ecosystems & environment*, *193*, 70-82.

Ahirwal, J., Nath, A., Brahma, B., Deb, S., Sahoo, U. K., & Nath, A. J. (2021). Patterns and driving factors of biomass carbon and soil organic carbon stock in the Indian Himalayan region. *Science of the Total Environment*, *770*, 145292.

Ahmad, N., Johri, S., Abdin, M. Z., & Qazi, G. N. (2009). Molecular characterization of bacterial population in the forest soil of Kashmir, India. *World Journal of Microbiology and Biotechnology*, *25*(1), 107-113.

Aislabie, J., Jordan, S., Ayton, J., Klassen, J. L., Barker, G. M., & Turner, S. (2009). Bacterial diversity associated with ornithogenic soil of the Ross Sea region, Antarctica. *Canadian journal of microbiology*, *55*(1), 21-36.

Ammer, S., Weber, K., Abs, C., Ammer, C., & Prietzel, J. (2006). Factors influencing the distribution and abundance of earthworm communities in pure and converted Scots pine stands. *Applied Soil Ecology*, *33*(1), 10-21.

Anderson, T. H., & Domsch, K. H. (1989). Ratios of microbial biomass carbon to total organic carbon in arable soils. *Soil biology and biochemistry*, *21*(4), 471-479.

Antonioli, N.; Cazzola, M. Geologia e geomorfologia (1998). In *Parco Regionale Alto Appennino Modenese*; Gruppo Editoriale Giunti: Firenze, Italy; pp. 41–49.

Antwis, R. E., Griffiths, S. M., Harrison, X. A., Aranega-Bou, P., Arce, A., Bettridge, A. S., ... & Sutherland, W. J. (2017). Fifty important research questions in microbial ecology. *FEMS Microbiology Ecology*, *93*(5), fix044.

Berg, B., & McClaugherty, C. (2008). *Plant litter: decomposition, humus formation, carbon sequestration*. Berlin, Heidelberg: Springer Berlin Heidelberg.

Berger, T. W., Swoboda, S., Prohaska, T., & Glatzel, G. (2006). The role of calcium uptake from deep soils for spruce (Picea abies) and beech (Fagus sylvatica). *Forest Ecology and Management*, *229*(1-3), 234-246.

Błońska, E., Klamerus-Iwan, A., Lasota, J., Gruba, P., Pach, M., & Pretzsch, H. (2018). What characteristics of soil fertility can improve in mixed stands of Scots pine and European beech compared with monospecific stands?. *Communications in Soil Science and Plant Analysis*, *49*(2), 237-247.

Bongiorno, G., Bünemann, E. K., Oguejiofor, C. U., Meier, J., Gort, G., Comans, R., ... & de Goede, R. (2019). Sensitivity of labile carbon fractions to tillage and organic matter management and their potential as comprehensive soil quality indicators across pedoclimatic conditions in Europe. *Ecological Indicators*, *99*, 38-50.

Bonifacio, E., Falsone, G., & Catoni, M. (2013). Influence of serpentine abundance on the vertical distribution of available elements in soils. *Plant and soil*, *368*(1), 493-506.

Breure, A. M. (2004, September). Soil biodiversity: measurements, indicators, threats and soil functions. In *International Conference Soil and Compost Eco-biology. Spain*.

Brookes, P. C., Landman, A., Pruden, G., & Jenkinson, D. S. (1985). Chloroform fumigation and the release of soil nitrogen: a rapid direct extraction method to measure microbial biomass nitrogen in soil. *Soil biology and biochemistry*, *17*(6), 837-842.

Bruckman, V. J., Yan, S., Hochbichler, E., & Glatzel, G. (2011). Carbon pools and temporal dynamics along a rotation period in Quercus dominated high forest and coppice with standards stands. *Forest Ecology and Management*, *262*(9), 1853-1862.

Bulgarelli, D., Schlaeppi, K., Spaepen, S., Van Themaat, E. V. L., & Schulze-Lefert, P. (2013). Structure and functions of the bacterial microbiota of plants. *Annual review of plant biology*, *64*(1), 807-838.

Bünemann, E. K., Bongiorno, G., Bai, Z., Creamer, R. E., De Deyn, G., De Goede, R., ... & Brussaard, L. (2018). Soil quality–A critical review. *Soil biology and biochemistry*, *120*, 105-125.

Callahan, B. J., McMurdie, P. J., Rosen, M. J., Han, A. W., Johnson, A. J. A., & Holmes, S. P. (2016). DADA2: High-resolution sample inference from Illumina amplicon data. *Nature methods*, *13*(7), 581-583.

Camponi, L., Cardelli, V., Cocco, S., Serrani, D., Salvucci, A., Cutini, A., ... & Corti, G. (2022). Effect of coppice conversion into high forest on soil organic C and nutrients stock in a Turkey oak (Quercus cerris L.) forest in Italy. *Journal of Environmental Management*, *312*, 114935.

Chantigny, M. H., Angers, D. A., Kaiser, K., & Kalbitz, K. (2007). Extraction and characterization of dissolved organic matter.

Conforti, M., Longobucco, T., Scarciglia, F., Niceforo, G., Matteucci, G., & Buttafuoco, G. (2020). Interplay between soil formation and geomorphic processes along a soil catena in a Mediterranean mountain landscape: an integrated pedological and geophysical approach. *Environmental Earth Sciences*, *79*(2), 59.

Córdova, S. C., Olk, D. C., Dietzel, R. N., Mueller, K. E., Archontouilis, S. V., & Castellano, M. J. (2018). Plant litter quality affects the accumulation rate, composition, and stability of mineral-associated soil organic matter. *Soil Biology and Biochemistry*, *125*, 115-124.

Costantini, E. A., & Lorenzetti, R. (2013). Soil degradation processes in the Italian agricultural and forest ecosystems. *Italian Journal of Agronomy*, *8*(4), e28.

Costantini, E. A., & Mocali, S. (2022). Soil health, soil genetic horizons and biodiversity. *Journal of Plant Nutrition and Soil Science*, *185*(1), 24-34.

D'Amico, M. E., Pintaldi, E., Sapino, E., Colombo, N., Quaglino, E., Stanchi, S., ... & Freppaz, M. (2020). Soil types of Aosta Valley (NW-Italy). *Journal of Maps*, *16*(2), 755-765.

Dilly, O. (2005). Microbial energetics in soils. In *Microorganisms in soils: roles in genesis and functions* (pp. 123-138). Berlin, Heidelberg: Springer Berlin Heidelberg.

Dilly, O., Bartsch, S., Rosenbrock, P., Buscot, F., & Munch, J. C. (2001). Shifts in physiological capabilities of the microbiota during the decomposition of leaf litter in a black alder (Alnus glutinosa (Gaertn.) L.) forest. *Soil Biology and Biochemistry*, *33*(7-8), 921-930.

Drobnik, T., Greiner, L., Keller, A., & Grêt-Regamey, A. (2018). Soil quality indicators–From soil functions to ecosystem services. *Ecological indicators*, *94*, 151-169.

El Mujtar, V., Muñoz, N., Mc Cormick, B. P., Pulleman, M., & Tittonell, P. (2019). Role and management of soil biodiversity for food security and nutrition; where do we stand?. *Global food security*, *20*, 132-144.

Fajardo, M. P., McBratney, A. B., & Minasny, B. (2017). Measuring functional pedodiversity using spectroscopic information. *Catena*, *152*, 103-114.

Fanin, N., Hättenschwiler, S., & Fromin, N. (2014). Litter fingerprint on microbial biomass, activity, and community structure in the underlying soil. *Plant and soil*, *379*(1), 79-91.

Fazlollahi Mohammadi, M., Jalali, S. G. H., Kooch, Y., & Said-Pullicino, D. (2016). Slope gradient and shape effects on soil profiles in the northern mountainous forests of Iran. *Eurasian soil science*, *49*(12), 1366-1374.

Ferronato, C., Vianello, G., Feudis, M. D., & Vittori Antisari, L. (2021). Technosols development in an abandoned mining area and environmental risk assessment. *Applied Sciences*, *11*(15), 6982.

Fierer, N. (2017). Embracing the unknown: disentangling the complexities of the soil microbiome. *Nature Reviews Microbiology*, *15*(10), 579-590.

Fierer, N., Wood, S. A., & de Mesquita, C. P. B. (2021). How microbes can, and cannot, be used to assess soil health. *Soil biology and biochemistry*, *153*, 108111.

Food and Agriculture Organization (FAO) (2015). *Status World's Soil Resouces: Main Report*; Intergovernmental Technical Panel on Soils (ITPS); Food and Agriculture Organization: Rome, Italy; 608p.

García-López, J. D., Barbieri, F., Banos, A., Madero, J. M. G., Gardini, F., Montanari, C., & Tabanelli, G. (2023). Use of two autochthonous bacteriocinogenic strains as starter cultures in the production of salchichónes, a type of Spanish fermented sausages. *Current Research in Food Science*, *7*, 100615.

Gardes, M., & Bruns, T. D. (1993). ITS primers with enhanced specificity for basidiomycetes-application to the identification of mycorrhizae and rusts. *Molecular ecology*, *2*(2), 113-118.

Gee, G. W., Bauder, J. W., & Klute, A. (1986). Methods of soil analysis, part 1, physical and mineralogical methods. *Soil Science Society of America, American Society of Agronomy*, *5*.

Graham, E. B., Knelman, J. E., Schindlbacher, A., Siciliano, S., Breulmann, M., Yannarell, A., ... & Nemergut, D. R. (2016). Microbes as engines of ecosystem function: when does community structure enhance predictions of ecosystem processes?. *Frontiers in microbiology*, *7*, 214.

Grüneberg, E., Ziche, D., & Wellbrock, N. (2014). Organic carbon stocks and sequestration rates of forest soils in G ermany. *Global change biology*, *20*(8), 2644-2662.

Haddix, M. L., Gregorich, E. G., Helgason, B. L., Janzen, H., Ellert, B. H., & Cotrufo, M. F. (2020). Climate, carbon content, and soil texture control the independent formation and persistence of particulate and mineral-associated organic matter in soil. *Geoderma*, *363*, 114160.

Hamzehpour, N., Shafizadeh-Moghadam, H., & Valavi, R. (2019). Exploring the driving forces and digital mapping of soil organic carbon using remote sensing and soil texture. *Catena*, *182*, 104141.

Hayes, M. H., Mylotte, R., & Swift, R. S. (2017). Humin: its composition and importance in soil organic matter. *Advances in agronomy*, *143*, 47-138.

Hobbie, E. A., & Ouimette, A. P. (2009). Controls of nitrogen isotope patterns in soil profiles. *Biogeochemistry*, *95*(2), 355-371.

Hobbie, S. E., Reich, P. B., Oleksyn, J., Ogdahl, M., Zytkowiak, R., Hale, C., & Karolewski, P. (2006). Tree species effects on decomposition and forest floor dynamics in a common garden. *Ecology*, *87*(9), 2288-2297.

Hoffland, E., Kuyper, T. W., Comans, R. N., & Creamer, R. E. (2020). Eco-functionality of organic matter in soils. *Plant and Soil*, *455*(1), 1-22.

Ibáñez, J. J., & Feoli, E. (2013). Global relationships of pedodiversity and biodiversity. *Vadose Zone Journal*, *12*(3), 1-5.

Ibáñez, J. J., Sánchez-Díaz, J., Rodríguez-Rodríguez, A., & Effland, W. R. (2008). Preservation of European soils: natural and cultural heritage. *Advances in Geoecology*, *39*, 37-59.

Ibáñez-Asensio, S., Marques-Mateu, A., Moreno-Ramón, H., & Balasch, S. (2013). Statistical relationships between soil colour and soil attributes in semiarid areas. *Biosystems Engineering*, *116*(2), 120-129.

Islam, M. R., Singh, B., & Dijkstra, F. A. (2022). Stabilisation of soil organic matter: interactions between clay and microbes. *Biogeochemistry*, *160*(2), 145-158.

Jensen, J. L., Schjønning, P., Watts, C. W., Christensen, B. T., Peltre, C., & Munkholm, L. J. (2019). Relating soil C and organic matter fractions to soil structural stability. *Geoderma*, *337*, 834-843.

Kallenbach, C. M., Frey, S. D., & Grandy, A. S. (2016). Direct evidence for microbial-derived soil organic matter formation and its ecophysiological controls. *Nature communications*, *7*(1), 13630.

Kohl, L., Philben, M., Edwards, K. A., Podrebarac, F. A., Warren, J., & Ziegler, S. E. (2018). The origin of soil organic matter controls its composition and bioreactivity across a mesic boreal forest latitudinal gradient. *Global Change Biology*, *24*(2), e458-e473.

Krasilnikov, P. V., Gerasimova, M. I., Golovanov, D. L., Konyushkova, M. V., Sidorova, V. A., & Sorokin, A. S. (2018). Pedodiversity and its significance in the context of modern soil geography. *Eurasian Soil Science*, *51*(1), 1-13.

Kuramae, E. E., Yergeau, E., Wong, L. C., Pijl, A. S., Van Veen, J. A., & Kowalchuk, G. A. (2012). Soil characteristics more strongly influence soil bacterial communities than land-use type. *FEMS microbiology ecology*, *79*(1), 12-24.

Kuramae, E., Gamper, H., van Veen, J., & Kowalchuk, G. (2011). Soil and plant factors driving the community of soil-borne microorganisms across chronosequences of secondary succession of chalk grasslands with a neutral pH. *FEMS microbiology ecology*, *77*(2), 285-294.

Łachacz, A., & Załuski, D. (2023). The usefulness of the Munsell colour indices for identification of drained soils with various content of organic matter. *Journal of Soils and Sediments*, *23*(11), 4017-4031.

Larsbrink, J., & McKee, L. S. (2020). Bacteroidetes bacteria in the soil: Glycan acquisition, enzyme secretion, and gliding motility. *Advances in applied microbiology*, *110*, 63-98.

Lavallee, J. M., Soong, J. L., & Cotrufo, M. F. (2020). Conceptualizing soil organic matter into particulate and mineral-associated forms to address global change in the 21st century. *Global change biology*, *26*(1), 261-273.

Liang, C., Amelung, W., Lehmann, J., & Kästner, M. (2019). Quantitative assessment of microbial necromass contribution to soil organic matter. *Global change biology*, *25*(11), 3578-3590.

Lo Papa, G., Palermo, V., & Dazzi, C. (2011). Is land-use change a cause of loss of pedodiversity? The case of the Mazzarrone study area, Sicily. *Geomorphology*, *135*(3-4), 332-342.

Lorenz, K., Lal, R., & Ehlers, K. (2019). Soil organic carbon stock as an indicator for monitoring land and soil degradation in relation to United Nations' Sustainable Development Goals. *Land Degradation & Development*, *30*(7), 824-838.

Lorenz, M., Derrien, D., Zeller, B., Udelhoven, T., Werner, W., & Thiele-Bruhn, S. (2020). The linkage of 13C and 15N soil depth gradients with C: N and O: C stoichiometry reveals tree species effects on organic matter turnover in soil. *Biogeochemistry*, *151*(2), 203-220.

Ma, A., Zhuang, X., Wu, J., Cui, M., Lv, D., Liu, C., & Zhuang, G. (2013). Ascomycota members dominate fungal communities during straw residue decomposition in arable soil. *PloS one*, *8*(6), e66146.

Machado, W., Franchini, J. C., de Fátima Guimarães, M., & Tavares Filho, J. (2020). Spectroscopic characterization of humic and fulvic acids in soil aggregates, Brazil. *Heliyon*, *6*(6).

Merino, A., Real, C., Álvarez-González, J. G., & Rodríguez-Guitián, M. A. (2007). Forest structure and C stocks in natural Fagus sylvatica forest in southern Europe: The effects of past management. *Forest Ecology and Management*, *250*(3), 206-214.

Mganga, K. Z., Razavi, B. S., & Kuzyakov, Y. (2016). Land use affects soil biochemical properties in Mt. Kilimanjaro region. *Catena*, *141*, 22-29.

Mocali, S., Paffetti, D., Emiliani, G., Benedetti, A., & Fani, R. (2008). Diversity of heterotrophic aerobic cultivable microbial communities of soils treated with fumigants and dynamics of metabolic, microbial, and mineralization quotients. *Biology and Fertility of Soils*, *44*(4), 557-569.

Põlme, S., Abarenkov, K., Henrik Nilsson, R., Lindahl, B. D., Clemmensen, K. E., Kauserud, H., ... & Tedersoo, L. (2020). FungalTraits: a user-friendly traits database of fungi and fungus-like stramenopiles. *Fungal diversity*, *105*(1), 1-16.

Ramírez, P. B., Fuentes-Alburquenque, S., Díez, B., Vargas, I., & Bonilla, C. A. (2020). Soil microbial community responses to labile organic carbon fractions in relation to soil type and land use along a climate gradient. *Soil Biology and Biochemistry*, *141*, 107692.

Reemtsma, T., These, A., Springer, A., & Linscheid, M. (2006). Fulvic acids as transition state of organic matter: indications from high resolution mass spectrometry. *Environmental science & technology*, *40*(19), 5839-5845.

Schoeneberger, P. J., Wysocki, D. A., & Benham, E. C. (Eds.). (2012). *Field book for describing and sampling soils*. Government Printing Office.

Sen, D. O. U., Jun, S. H. A. N., Xiangyun, S. O. N. G., Rui, C. A. O., Meng, W. U., Chenglin, L. I., & Song, G. U. A. N. (2020). Are humic substances soil microbial residues or unique synthesized compounds? A perspective on their distinctiveness. *Pedosphere*, *30*(2), 159-167.

Senesi, N., Miano, T. M., Provenzano, M. R., & Brunetti, G. (1989). Spectroscopic and compositional comparative characterization of IHSS reference and standard fulvic and humic acids of various origin. *Science of the total environment*, *81*, 143-156.

Singh, P., Ghosh, A. K., Kumar, S., Kumar, M., & Sinha, P. K. (2022). Influence of input litter quality and quantity on carbon storage in post-mining forest soil after 14 years of reclamation. *Ecological Engineering*, *178*, 106575.

Soil Survey Staff. (2022). Keys to Soil Taxonomy (13th ed.). USDA Natural Resources Conservation Service.

Sorokin, A., Owens, P., Láng, V., Jiang, Z. D., Michéli, E., & Krasilnikov, P. (2021). "Black soils" in the Russian Soil Classification system, the US Soil Taxonomy and the WRB: Quantitative correlation and implications for pedodiversity assessment. *Catena*, *196*, 104824.

Stewart, C. E., Neff, J. C., Amatangelo, K. L., & Vitousek, P. M. (2011). Vegetation effects on soil organic matter chemistry of aggregate fractions in a Hawaiian forest. *Ecosystems*, *14*(3), 382-397.

Štursová, M., Žifčáková, L., Leigh, M. B., Burgess, R., & Baldrian, P. (2012). Cellulose utilization in forest litter and soil: identification of bacterial and fungal decomposers. *FEMS microbiology ecology*, *80*(3), 735-746.

Traversa, A., D'Orazio, V., Mezzapesa, G. N., Bonifacio, E., Farrag, K., Senesi, N., & Brunetti, G. (2014). Chemical and spectroscopic characteristics of humic acids and dissolved organic matter along two Alfisol profiles. *Chemosphere*, *111*, 184-194.

Traversa, A., Said-Pullicino, D., D'Orazio, V., Gigliotti, G., & Senesi, N. (2011). Properties of humic acids in Mediterranean forest soils (Southern Italy): influence of different plant covering. *European Journal of Forest Research*, *130*(6), 1045-1054.

Ukalska-Jaruga, A., Bejger, R., Debaene, G., & Smreczak, B. (2021). Characterization of soil organic matter individual fractions (fulvic acids, humic acids, and humins) by spectroscopic and electrochemical techniques in agricultural soils. *Agronomy*, *11*(6), 1067.

Vacek, O., Vašát, R., & Borůvka, L. (2020). Quantifying the pedodiversity-elevation relations. *Geoderma*, *373*, 114441.

Vance, E. D., Brookes, P. C., & Jenkinson, D. S. (1987). An extraction method for measuring soil microbial biomass C. *Soil biology and Biochemistry*, *19*(6), 703-707.

Vittori Antisari, L., Falsone, G., Carbone, S., Marinari, S., & Vianello, G. (2015). Douglas-fir reforestation in North Apennine (Italy): Performance on soil carbon sequestration, nutrients stock and microbial activity. *Applied Soil Ecology*, *86*, 82-90.

Vittori Antisari, L., Trenti, W., Buscaroli, A., Falsone, G., Vianello, G., & De Feudis, M. (2022). Pedodiversity and organic matter stock of soils developed on sandstone formations in the Northern Apennines (Italy). *Land*, *12*(1), 79.

Vittori Antisari, L., Trenti, W., De Feudis, M., Bianchini, G., & Falsone, G. (2021). Soil quality and organic matter pools in a temperate climate (Northern Italy) under different land uses. *Agronomy*, *11*(9), 1815.

Wagg, C., Bender, S. F., Widmer, F., & Van Der Heijden, M. G. (2014). Soil biodiversity and soil community composition determine ecosystem multifunctionality. *Proceedings of the National Academy of Sciences*, *111*(14), 5266-5270.

Wall, D. H., Bardgett, R. D., & Kelly, E. (2010). Biodiversity in the dark. *Nature Geoscience*, *3*(5), 297-298.

Wallenstein, M. D., McNulty, S., Fernandez, I. J., Boggs, J., & Schlesinger, W. H. (2006). Nitrogen fertilization decreases forest soil fungal and bacterial biomass in three long-term experiments. *Forest Ecology and Management*, *222*(1-3), 459-468.

White, T. J., Bruns, T., Lee, S. J. W. T., & Taylor, J. (1990). Amplification and direct sequencing of fungal ribosomal RNA genes for phylogenetics. *PCR protocols: a guide to methods and applications*, *18*(1), 315-322.

Zavarzina, A. G., Danchenko, N. N., Demin, V. V., Artemyeva, Z. S., & Kogut, B. M. (2021). Humic substances: hypotheses and reality (a review). *Eurasian Soil Science*, *54*(12), 1826-1854.

Zeller, B., & Dambrine, E. (2011). Coarse particulate organic matter is the primary source of mineral N in the topsoil of three beech forests. *Soil Biology and Biochemistry*, *43*(3), 542-550.

Ziolkowska, A., Debska, B., & Banach-Szott, M. (2020). Transformations of phenolic compounds in meadow soils. *Scientific Reports*, *10*(1), 19330.

5. PEDODIVERSITY AND ORGANIC MATTER STOCK OF SOILS DEVELOPED ON SANDSTONE FORMATIONS IN THE NORTHERN APENNINES (ITALY)

Published in *Land* **2023, *12(1), 79;*** **https://doi.org/10.3390/land12010079**

Livia Vittori Antisari[1], William Trenti[1], Alessandro Buscaroli[3], Gloria Falsone[1], Gilmo Vianello[2] & Mauro De Feudis[1*]

[1] Department of Agricultural and Food Sciences, Alma Mater Studiorum-University of Bologna, Viale Fanin 40, Bologna, Italy
[2] Accademia Nazionale di Agricoltura, Via Castiglione 11, 40124 Bologna, Italy
[3] Department of Biological, Geological, and Environmental Sciences, Alma Mater Studiorum-University of Bologna, Via S. Alberto 163, 48100 Ravenna, Italy
[*]correspondence: mauro.defeudis2@unibo.it

ABSTRACT

Pedodiversity is considered the cornerstone of biodiversity. This work aimed to (1) assess pedodiversity according to vegetation, topographic factors, and lithology and to (2) identify the major soil-forming factors on soil organic matter (SOM) stock at a 0–30 cm depth. These goals were reached using data from 147 georeferenced soil profiles distributed along 400–1000 m (≤1000) and 1000–2134 m (>1000) altitudinal gradients in the northern part of the Apennine chain in Italy. Soils showed mainly weak or incipient development (i.e., Entisols and Inceptisols), which could be attributed to sand-based lithology, high slope gradients, and low SOM accumulation rates, which promote soil erosion processes. However, higher pedodiversity was observed at >1000 m than at ≤1000 m, likely due to the higher vegetation cover diversity and climate variability; Spodosols and Mollisols were also found. A greater SOM stock was found at >1000 than ≤1000 m, and vegetation seemed to not affect SOM amounts, suggesting a greater influence of climate on SOM content compared to vegetation. Considering ecosystem conservation, the observed spatial pedodiversity could be considered a critical basis for the protection of soil resources and pedodiversity itself in mountain regions.

5.1 INTRODUCTION

Biodiversity evaluation, also referred to as spatial diversity, is a major topic in ecosystem studies and is mostly applied to aboveground flora and fauna (Schneider et al., 2016; Hanz et al., 2022) but also recently to belowground biodiversity (Inkotte et al., 2022; Peng et al., 2022). Conversely, few investigations concerning pedodiversity were carried out (Costantini & Dazzi, 2013; Guo et al., 2003; Toomanian et al., 2006), although pedodiversity is considered the cornerstone of biodiversity given the strong relationship between soil and flora and fauna (Sokołowska et al., 2019; Casalini et al., 2019).

Pedodiversity is extremely complex and driven by factors involved in several soil formation processes (Jenny, 1941; Bockheim et al., 2014), making it difficult to quantify the influence of each factor on soil properties. Nowadays, because of the major role of soil in storing organic matter (Sorokin et al., 2021), several studies focused on identifying the factors that mostly significantly affect soil organic carbon (SOC) (Jiménez-González et al., 2020; Gray et al., 2015; Johnson et al., 2011). Indeed, the spatial changes in SOC amounts are dependent on biotic and abiotic factors such as climate, the amount and quality of plant debris, vegetation cover, and land use (Adiyah et al., 2022; Kögel-Knabner & Amelung, 2021; Weissert et al., 2016; Boudjabi et al., 2022). In addition, SOC stock is affected by soil development according to the different weight of each pedogenesis factor (Voltr et al., 2021; Gonçalves et al., 2017). In this regard, recent papers highlighted the importance of soil type knowledge in terms of lithology, the physicochemical characterization of organic debris, and pedogenetic horizons to determine soil forming processes, in order to understand the distribution and quality of SOC stock (Kögel-Knabner & Amelung, 2021; De Feudis et al., 2022a).

In recent decades, there has been growing interest in the knowledge of mountain soils because montane ecosystems are characterized both to have high pedodiversity (Philippis & Marion, 2004; Ibáñez & Feoli, 2013; Costantini & L'Abate, 2016) and to be sensitive to climate change (Gutiérrez-Girón et al., 2015; Djukic et al., 2010; Britton et al., 2011). The soil development in mountain environments is mainly influenced by geomorphological dynamics (Masseroli et al., 2020). The slope drives many processes, mainly associated with snow and water action. Erosion and soil accumulation processes shape the landscape and affect soil genesis, rejuvenating soils in erosion zones, making them thinner, or deepening soils in the accumulation areas (Egli & Poulenard, 2016). Furthermore, mountain areas are currently experiencing strong climatic changes that are altering temperatures, precipitation amounts and patterns, and duration of the seasons. For example, reduced snow cover periods were reported to coincide with increasing occurrences of summer droughts and winter freeze–thaw cycles in soils (Gobiet et al., 2014). Such climate changes modify the C amounts in mountain soils due to the modification of plant C inputs (Hagedorn et al., 2019), leading to the alteration of SOC immobilization–mineralization processes (Gutiérrez-Girón et al., 2015) and further interfering in soil formation processes. Mountain ecosystems are often characterized by poorly developed, shallow, and skeletal soils (Romeo et al., 2015). Organic C content is particularly important for soil fertility and the efficient functioning of such ecosystems (Prietzel & Christophel, 2014; Szewczyk et al., 2015). Although mountain soils store relevant amounts of organic C (De Feudis et al., 2022a; Gutiérrez-Girón et al., 2015; Garcia-Pausas et al., 2007), the effect of the simultaneous impact of environmental factors on the amount and spatial dynamics of SOC in mountain areas is still underestimated. This knowledge gap is mainly related to the complexity of mountain ecosystems due to the climate conditioning of geobotanic zonality (Gutman et al., 1984)and the vertical diversity of soil profiles and their biological activity (Ma et al., 2016; Ghosh et al., 2014; Jobbagy & Jackson, 2000; Józefowska & Miechówka, 2015). Further, mountain regions are characterized by greater geodiversity (Gray et al., 2021) than any other landscape (Slaymaker et al., 2015; Johnstone, 2021). All these factors make soils of mountain areas highly diverse (Romeo et al., 2015). While elevation and, therefore, temperature differences were identified as the dominant controls on mountain SOC at regional scales (Bargali & Bargali, 2020; Bangroo et al., 2020; Massaccesi et al., 2020), soil properties such as soil moisture, pH, and soil texture (Djukic et al., 2010; Bargali & Bargali, 2020; Leifeld et al., 2005) and vegetation/land use

(Canedoli et al., 2020; Yimer et al., 2006; Gebrehiwot et al., 2018) may introduce a large variability in mountain SOC at local scales.

As a whole, while several studies have reported the impact of lithology, vegetation type, and altitude on SOC stock, few studies have examined the effect of the aforementioned soil forming factors on soil N and other soil physical and chemical properties in mountain regions.

Given the little information about major factors affecting pedodiversity and soil properties (e.g., texture, pH, SOC, total N, exchangeable bases), changes in mountain ecosystems were determined using data from 147 soil profiles for georeferenced soils developed on sandstone formations and distributed in the northern part of the Apennine chain in Italy, at different altitudinal gradients from 400 to 2134 m above sea level (a.s.l.). The main aims of the present work were to: (1) assess the pedodiversity, meaning the classification of the soils themselves (Soil survey staff, 2014) and properties according to vegetation, morphological factors (i.e., altitude, slope, and exposure), and lithology and (2) identify the major soil forming factors on organic C and total N stocks at a 0–30 cm depth.

5.2 MATERIALS AND METHODS

This study used a dataset of 147 georeferenced soil profiles (Table S1 of the Supplementary Materials) located in the Northern Apennines in Italy. Such soil profiles are the result of projects financed by public institutions and self-financed projects conducted in the last 15–20 years by the authors of the present manuscript whose results were published in several papers (Brombin et al., 2020; Falsone et al, 2015; De Feudis et al., 2020a, 2020b,, 2022b; Dell'Abate et al., 2007; Vittori Antisari et al., 2008, 2010, 2011, 2013, 2015, 2018, 2021; Marinari et al., 2013; Marinari & Vittori Antisari, 2010). Specifically, the soil profiles were located at altitudes ranging from 200 to 2134 m a.s.l. and under different land uses, with 54 soil profiles under chestnut stands (CHE); 16 under conifer reforestation, mainly black pine (*Pinus nigra*), spruce (*Picea abies*), and Douglasia (*Pseudotsuga menziesii*) stands planted between World War II and the 1950s (CON);

30 under beech (*Fagus sylvatica*) forests (BEF); 18 under blueberry (*Vaccinium myrtillus* and *Vaccinium ulginosum*) habitats (BLB); 18 under mixed forests consisting mainly of abandoned chestnut stands invaded by other tree species (e.g., acacia, elm, oak, ash, and poplar) (MF); and 11 under grasslands (GS).

5.2.1 Parent material

The sites under investigation were characterized by diverse sandstone types as parent rock materials (Figure 1) whose chemical features (Dinelli et al., 1999; van de Kamp & Leake, 1995; Gazzi, 1963, 1966) are reported in Table A1 of Appendix A:

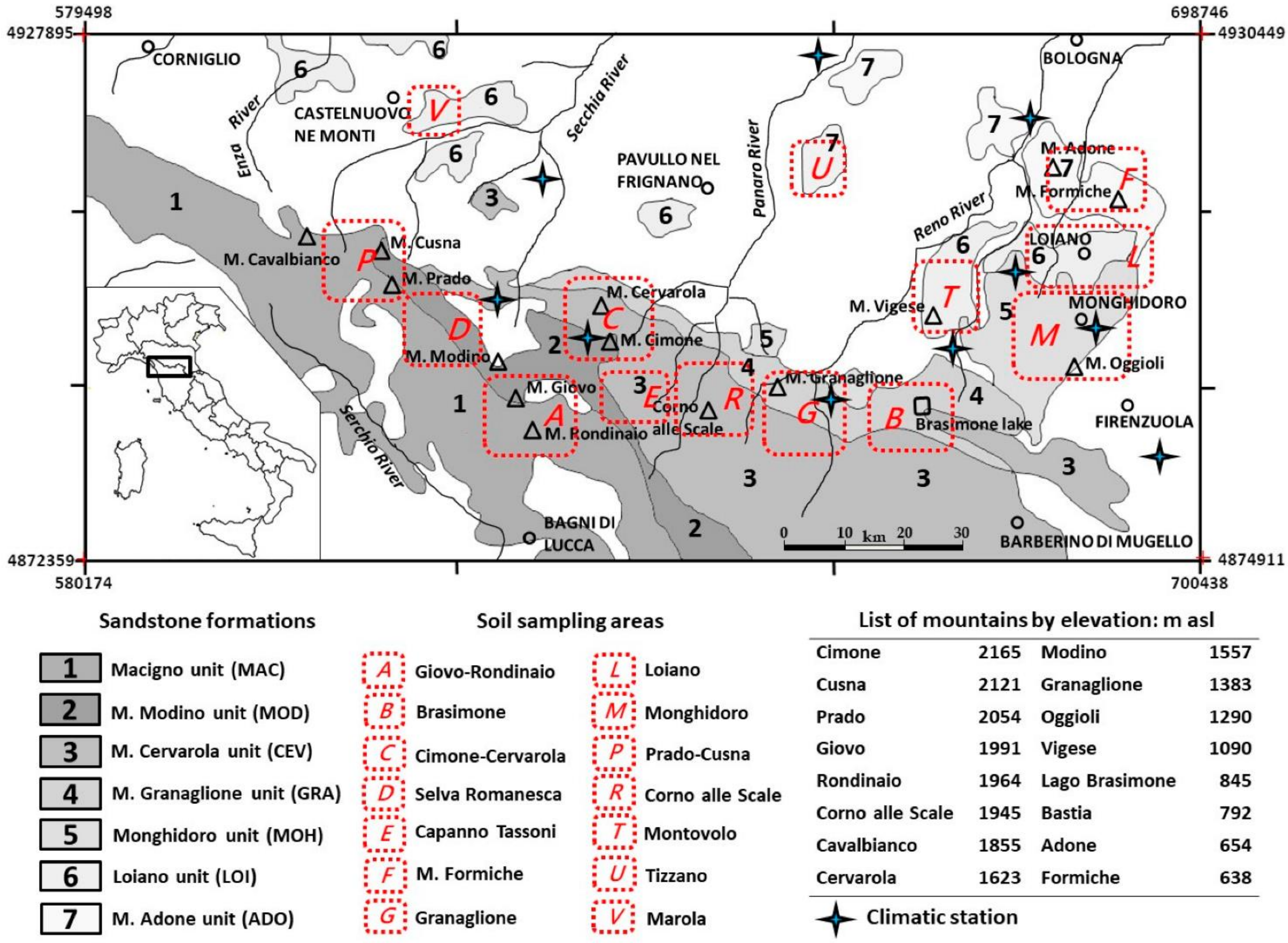

Figure 1. Location of the study sites comprising the database of the investigation.

- Monghidoro formation (MOH): Cretacic–Paleogene (External Ligurian Domain) thick-bedded turbidite sandstones, with microconglomerates at the base and alternating shales and siltstones;

- Loiano formation (LOI): Paleogene (Epiligurian succession) thick-bedded, weakly cemented sandstones;

- Castiglione dei Pepoli sandstones (GRA), dormant landslide deposits: Miocene (Cervarola–Falterona succession) turbiditic sandstones in shallow to medium-thick beds;

- Mount Cervarola sandstones, Dardagna member (CEV): Neogene (Cervarola–Falterona succession) alternating arenaceous and pelitic turbidite deposits, with intercalations of marly-calcareous turbidites, silty marls, calcarenites, and black clays. In the investigated area, there is a thick bed of black pelites and black and grey sandstones;

- Mount Modino sandstones (MOD): Paleogene–Neogene (Modino succession) arenaceous layers intercalated with thinly layered turbidites made of fine sandstones, siltstones, marls, or, rarely, shales;

- Macigno sandstones (MAC): late Oligocene (Tuscan succession) thick turbidite arenaceous sandstones and siltstones with rare thin carbonate beds and chaotic beds.

- Mount Adone formation (ADO): post-lower Pliocene (Pliocene and Pleistocene marine succession) prevailing sandstones, generally lightly cemented, with abundant silty-clay matrix and subordinate conglomerates, in medium layers to banks, alternating with pelitic sand with thin to thick stratifications.

5.2.2 Climate

The climate of the Northern Apennines is characterized by cold winters with frequent snowfalls and hot summers. The mean annual temperature of the study areas ranges from 14.6 °C at the lowest altitude to 3.3 °C at the highest (Table S2 of the Supplementary Materials). The lowest temperatures were recorded in January (1.18 °C on average) with the exception of the highest altitude, where the lowest temperatures were recorded in February (−3.3 °C), and the warmest ones were recorded in July and August. The mean annual cumulative precipitation was 1004 mm and ranged between 753 and 1703 mm (Table S1 of the Supplementary Materials) with an uneven distribution between the months. In addition, above 2000 m a.s.l., the snow covers the soils for about 6 months per year (from November to April), which also happens at Mount Cimone (Vittori Antisari et al., 2018). The mean air temperature and mean annual cumulative precipitation data were used to determine soil moisture and temperature regimes according to the Newhall Simulation Method (Van Wambeke et al., 1986). With the approximations allowed by the Soil Taxonomy (Soil survey staff, 2014), it was possible to identify a mesic temperature regime between 200 and 1300 m a.s.l. and a frigid temperature regime between 1300 to 2000 m. The soil moisture regime was found to be udic between 200 and 1800 m a.s.l. and perudic over 1800 m of altitude (Table 1).

Table 1. Altitudinal range, soil temperature regime, and soil moisture regime of the phytoclimatic zones and subzones of the northern Apennine chain, Italy, according to De Philippis (1951, 1937) and Soil Survey Staff (2014) and the location of soil profiles within the altitudinal ranges. The capital letters refer to soil sampling areas, as shown in Figure 1.

Phytoclimatic [a]		Altitude Range [a]	Soil Temperature Regime [b]	Soil Moisture Regime [b]	Soil Profile Number	Soil Profile Altitude range
Zone	Subzone	(m a.s.l.)				
Alpinetum		>2000	Cryic	Perudic	3	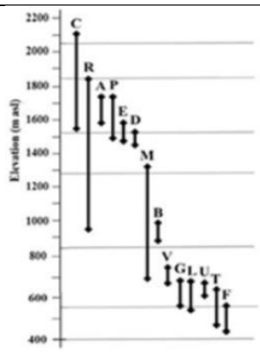
Picetum	cold	1800–2000	Frigid	Perudic	6	
	warm	1500–1800	Frigid	Udic	43	
Fagetum	cold	1300–1500	Frigid	Udic	16	
	warm	1000–1300	Mesic	Udic	11	
Castanetum	cold	600–1000	Mesic	Udic	13	
	warm	400–600	Mesic	Udic	57	

[a] De Philippis (1951, 1937); [b] Soil Survey Staff (2014).

5.2.3 Soil profiles

To evaluate the pedodiversity, soil profiles were dug until the parent materials were sampled and then analyzed via genetic horizons and classified according to Soil Survey Staff (2014). Due to the large spatial scale of the area considered in the present investigation, the soil profiles showed large morphological variability, with differences in the genetic horizon sequence, horizon thickness, and soil profile depth. To cope with these issues, in this study, the upper 30 cm of soil profiles was considered for evaluation of the soil physical–chemical properties, and the soil horizons included within this soil depth interval were grouped into three layers: layer A, which included the A horizons; layer B, which included the AB, BA, EA, EB, Bw, and BC horizons; and layer C, which included the CB and C horizons. As a whole, the minimum, maximum, and mean thickness was 1.0, 21.0, and 5.7 cm for layer A; 2.0, 23.0, and 10.1 cm for layer B; and 1.0, 27.0, and 14.1 cm for layer C, respectively.

5.2.4 Laboratory analyses

The pH was determined potentiometrically in deionized water with a 1:2.5 soil:water ratio using a pH-meter electrode (Crison, Germany). The particle size distribution was determined via the pipette method described by Gee and Bauder (1986), after the dispersion of soil samples with sodium hexametaphosphate solution. Organic C and total nitrogen (TOC and TN, respectively) contents were determined using a Thermo Scientific Lab EA-1110 dry combustion analyzer. Exchangeable Ca and other cations (Na, K, and Mg) and cation exchange capacity were determined through extraction with a 1 M NH_4-acetate solution at pH 7 (Soil survey laboratory staff, 2004). Cations were measured by inductively coupled plasma optical emission spectrometry (ICP-OES, Ametek, Arcos Spectro). Exchangeable Ca (Ca_{exch}) and the percentage of base saturation (BS) are reported in this study because of the well-known role of Ca exchange in promoting SOC storage (Rowley et al., 2018) and the importance of BS for soil taxonomic classification and soil fertility.

5.2.5 Soil Organic matter stock calculation

Organic C and TN stocks (SOC stock and TN stock, respectively) within a 0–30 cm soil depth were calculated by the sum of the SOC stock and TN stock of each horizon included within that interval depth using the equation in FAO (2019) and expressed as Mg ha^{-1}:

$$SOC\ stock\ and\ TN\ stock = TOC\ or\ TN\ \times BD\ \times thickness\ \times (1 - \frac{sk}{100})$$

where TOC or TN represents the contents of total organic carbon (%) and total nitrogen (%), BD is the bulk density (g cm^{-3}), and sk is the coarse fragment content (Ø > 2 mm; %) by volume.

BD was estimated according to the pedotransfer function proposed by Hollis et al. (2012) and broadly used for soils located within the Italian landscapes (Garlato et al., 2009; Conforti et al., 2016; Brenna et al., 2010; Ungaro et al., 2010; Faggian et al., 2012). The presence of coarse fragments was recorded during the field survey (FAO, 2006).

5.2.6 Statistical method

To better detect the influence of the soil formation factors related to altitude, the dataset was divided into two distinct ones: a dataset that grouped the soils located between 400 and 1000 m a.s.l. (hereafter ≤ 1000 m a.s.l.) and another including soils from 1000 to 2134 m a.s.l. (hereafter > 1000 m a.s.l.). Further, a clear vegetation type change was observed at 1000 m a.s.l. Indeed, below 1000 of altitude, CHE and MF generally shared the same altitudinal range. Similarly, the vegetation types found between 1000 and 2000 m of altitude (i.e., CON, BEF, BLB, and GS), in most of the cases, shared the same altitude.

Within each altitudinal range and without considering the soil types (pedodiversity), a Kruskal–Wallis one-way ANOVA (Hollander et al., 2013) was used to compare the effects of land-use and sandstone formation type on the investigated soil parameters. The Kruskal–Wallis test was also used to verify the effect of soil types (pedodiversity) on soil parameters without considering vegetation cover.

Hierarchical cluster analysis (CA) using Euclidean distance and Ward grouping methods (Murtagh & Legendre, 2014) was performed on the experimental data of the two altitudinal ranges (i.e., ≤1000 m a.s.l. and >1000 m a.s.l.) to cluster the collected soils in groups sharing similarities. The k-means method was then employed (Murtagh & Legendre, 2014), dividing the soil samples into a predetermined number of clusters, with the smallest difference observed between elements within each cluster and the largest one between the elements of different clusters. The groups obtained by CA were processed using the Kruskal–Wallis test to identify differences in the investigated soil parameters. To identify the main drivers affecting the groups obtained by CA, principal component analysis (PCA) was carried out.

A Kruskal–Wallis test was used to evaluate the statistical diversity of OC and TN stocks among the different uses of soil and between the two altitude ranges (i.e., ≤1000 m a.s.l. and >1000 m a.s.l.).

The statistical analysis was conducted using the R software (version 4.2.1) (Rstudio team, 2021).

5.3 RESULTS

5.3.1 Pedodiversity and Physicochemical Properties at Lower and Higher Altitude Range

Most of the investigated soils were classified as Inceptisols and Entisols (Table S1 of the Supplementary Materials) (Soil survey staff, 2014). Alfisols at low altitude (200 m a.s.l.), developed on the ADO sandstone type (Figure 1), were also found under CHE. However, because of the scarce number of replicates for soils from 200 to 400 m a.s.l., these samples were deleted from dataset and, therefore, their data were not further elaborated.

5.3.1.1 Lower altitudinal range

Within the ≤1000 m a.s.l. altitudinal range, soils were classified as Entisols (18%) and Inceptisols (82%). Most of the Entisols were Typic Udorthents (61%), which were mainly found within CHE, while Lithic Udorthents were less frequently found (39%) and were mainly observed under MF and within fields with slopes ≥ 30°. Most of the Inceptisols were classified as Typic Dystrudepts (74%) and mainly recorded under CHE. About 18% of Inceptisols were Lithic Dystrudepts, with most of them under CHE, and about 8% were Oxyaquic Dystrudepts, which were found under both CHE and MF. Eutrudepts were also found (18%), all of them under MF.

Taking into account the vegetation cover, CHE presented lower pH, BS values, and contents of Ca_{exch}, sand, and clay than MF (Table 2). No significant differences for the amounts of TOC and TN were observed (Table 2).

Table 2. Mean ± standard deviation of pH; base saturation (BS) and C:N ratio values; and concentrations of total organic carbon (TOC), total nitrogen (TN), exchangeable Ca (Ca_{exch}), sand, silt, and clay at a 0–30 cm soil depth, as well as identified soil types according to Soil Survey Staff (2014) of chestnut groves (CHE), mixed forests (MF), beech forests (BEF), blueberry (BLB), coniferous forests (CON), and grasslands (GS) located within 400–1000 m and 1000–2134 m altitudinal ranges of the northeastern Apennine chain (Italy). Within each altitudinal range, different letters indicate significant differences (Kruskal–Wallis test, $p < 0.05$) among the means.

	400–1000 m Altitudinal Range			**1000–2134 m Altitudinal Range**		
	CHE	**MF**	**BEF**	**BLB**	**CON**	**GS**
pH	5.1 ± 0.7 b	5.8 ± 1.2 a	4.6 ± 0.5 b	4.5 ± 0.3 b	4.8 ± 0.6 b	5.4 ± 0.8 a
TOC (g kg^{-1})	28.9 ± 28.1	30.7 ± 28.8	47.4 ± 30.0 a	52.1 ± 24.1 a	45.8 ± 24.4 a	45.8 ± 21.8 a
TN (g kg^{-1})	1.7 ± 1.5	1.8 ± 1.4	2.8 ± 1.7 b	3.5 ± 1.7 a	3.2 ± 1.3 a	3.9 ± 1.6 a
Caexch ($cmol_{(+)}$ kg^{-1})	5.1 ± 7.6 b	9.1 ± 6.0 a	5.7 ± 6.2 a	2.3 ± 2.7 b	7.8 ± 7.1 a	6.3 ± 5.2 a
BS (%)	31.3 ± 27.3 b	59.7 ± 29.4 a	37.3 ± 27.9 b	21.9 ± 16.2 c	46.4 ± 32.3 b	61.6 ± 33.5 a
C:N ratio	16.2 ± 6.3	17.1 ± 5.6	17.2 5.3 a	15.4 ± 4.8 b	14.1 ± 4.8 b	11.7 ± 1.8 c
Sand (%)	49.0 ± 15.0 b	57.0 ± 15.0 a	61.0 ± 13.8 ab	61.0 ± 15.0 ab	53.0 ± 20.8 b	63.0 ± 16.2 a
Silt (%)	40.0 ± 15.0 a	27.0 ± 12.0 b	30.0 ± 11.1 a	31.0 ± 11.9 a	36.0 ± 19.5 a	28.0 ± 12.4 a
Clay (%)	10.0 ± 4.9 b	16.0 ± 8.4 a	10.0 ± 6.9 ab	8.0 ± 5.4 b	11.0 ± 5.7 a	9.0 ± 6.8 ab
Orders	Subgroups		Subgroups			
Entisols	Lithic Udorthents	Lithic Udorthents	Lithic Udorthents	Typic Udorthents	Lithic Udorthents	Lithic Cryorthents
	Typic Udorthents	Typic Udorthents	Typic Udorthents		Typic Udorthents	Typic Udorthents
Mollisols						Lithic Hapludolls

Orders	Subgroups		Subgroups			
Inceptisols	Lithic Dystrudepts	Lithic Eutrudepts	Humic Lithic Dystrudepts	Lithic Dystrudepts	Lithic Dystrudepts	Lithic Dystrudepts
	Oxyaquic Dystrudepts	Typic Eutrudepts	Humic Lithic Eutrudepts	Humic Lithic Dystrudepts	Lithic Eutrudepts	
	Typic Dystrudepts	Lithic Dystrudepts	Humic Dystrudepts	Humic Dystrudepts	Humic Lithic Dystrudepts	
		Oxyaquic Dystrudepts	Oxyaquic Dystrudepts	Typic Dystrudepts	Humic Lithic Eutrudepts	
		Typic Dystrudepts	Typic Dystrudepts		Typic Dystrudepts	
			(Spodic) Lithic Dystrudepts		Typic Eutrudepts	
Spodosols			Lithic Haplohumods	Typic Haplorthods		Lithic Haplorthods

Comparing the soil subgroups, most of the investigated soils had a loam soil texture class (Table 3), with a trend toward a higher amount of sand observed among the Lithic Udorthents and Lithic Eutrudepts (sandy loam), with a higher amount of silt and lower amount of sand in Lithic Dystrudepts (silty loam) and a higher clay content and lower sand content in Typic Eutrudepts (sandy clay loam).

The soil subgroups identified at a ≤1000 m a.s.l. altitudinal range did not show differences in TOC and TN, although a higher C:N ratio was observed in Typic Dystrudepts compared to Lithic Dystrudepts and Lithic Udorthents. For the Ca_{exch}, BS, and pH, their values were generally lower in Oxyaquic and Typic Dystrudepts than in Eutrudepts and Entisols.

5.3.1.2 Higher altitude ranges

At >1000 m a.s.l., we observed higher pedodiversity compared to that of the lower altitudinal range dataset (≤1000 m a.s.l.) (Table 2). Soils were classified as Entisols, Inceptisols, and Spodosols (24, 53, and 8%, respectively). Mollisols were also found under mountain grassland (GS) and represented 4% of soils investigated within the >1000 m a.s.l. altitudinal range (Table 3). Specifically, Lithic Hapludolls were found under GS, showing only a mollic epipedon and no other diagnostic horizons due to the very shallow soil. Entisols were mainly represented by soils with udic and perudic moisture regimes and a temperature regime from frigid to cryic. Lithic Udorthents (27%) were found under CON and BEF, while Typic Udorthents (9%) were observed under all vegetation cover types (Table 2). A cryic soil temperature regime was observed under GS, where Lithic Cryorthents (4%) were identified.

Most of the Inceptisols had a dystric feature, namely, a base saturation of less than 60 percent at all subsurface horizons between 25 and 75 cm below the soil surface. Furthermore, about 25% of Inceptisols belonged to Typic Dystrudepts, and about 7% were Dystrudepts featuring a lithic contact within 50 cm of the soil surface and/or with an umbric or mollic epipedon less than 50 cm thick (Lithic Dystrudepts, Humic Dystrudepts and Humic Lithic Dystrudepts). Under BEF and CON, Eutrudepts (Humic Lithic Eutrudepts and Lithic Eutrudepts) were also found.

Taking into consideration the vegetation cover, the differences observed for both soil particle size distribution and TOC content were negligible. Notably, the lowest TN content and, as a consequence, the highest C:N ratio were found under BEF. BLB, instead, presented the lowest values of both Ca_{exch} content and BS. Finally, the highest pH values were observed under GS (Table 3).

Soils located at >1000 m a.s.l. belonged mostly to the sandy loam texture class (Table 4). Like at the ≤1000 m a.s.l. altitudinal range, no differences in TOC and TN were observed. The C:N ratio showed some differences, but no clear trend related to soil type was evident. However, as expected, Spodosols presented lower pH, Ca_{exch}, and BS than Mollisols.

Table 3. Mean ± standard deviation of sand, silt, clay, total organic carbon (TOC), total nitrogen (TN), and exchangeable Ca (Ca_{exch}) contents, base saturation (BS), and pH values, and texture class of soils identified at 400–1000 m above sea level and classified according to Soil Survey Staff (2014). Round brackets identify the number of soil profiles for each soil type. Within each column, different letters indicate significant differences among the values (Kruskal–Wallis test, $p < 0.05$).

Soil Order	Soil Subgroup	Sand	Silt	Clay	Texture	TOC	TN	C/N	Caexch	BS	pH
		%	%	%		g kg−1	g kg−1		cmol(+) kg−1	%	
Entisol	Lithic Udorthents (5)	65 ± 10 a	21 ± 8 c	14 ± 7 ab	SL	31.1 ± 27.7	2.0 ± 1.7	16.2 ± 6.0 bc	9.4 ± 9.4 ab	65.7 ± 22.8 a	5.7 ± 1.0 ab
	Typic Udorthents (8)	51 ± 16 cd	40 ± 17 b	10 ± 4 b	L	18.6 ± 18.5	1.2 ± 1.2	15.1 ± 6.3 ab	11.3 ± 10.4 ab	45.8 ± 27.8 b	5.7 ± 1.3 ab
Inceptisol	Lithic Dystrudepts (9)	36 ± 18 e	50 ± 19 a	14 ± 6 ab	SiL	27.6 ± 28.6	2.1 ± 1.9	12.4 ± 2.8 c	5.4 ± 3.8 bc	31.3 ± 17.6 bc	5.1 ± 0.4 bc
	Lithic Eutrudepts (5)	57 ± 14 bc	28 ± 10 c	15 ± 11 ab	SL	29.9 ± 26.9	1.9 ± 1.5	15.5 ± 4.2 ab	18.8 ± 12.4 a	77.4 ± 20.4 a	6.7 ± 1.2 a
	Oxyaquic Dystrudepts (4)	52 ± 13 cd	29 ± 10 c	19 ± 7 a	L	35.6 ± 40.1	2.1 ± 2.1	15.4 ± 3.8 ab	5.1 ± 6.6 bc	39.9 ± 28.9 bc	5.1 ± 0.6 c
	Typic Dystrudepts (39)	52 ± 13 cd	39 ± 11 b	9 ± 4 b	L	30.9 ± 28.4	1.6 ± 1.4	18.1 ± 7.0 a	3.3 ± 4.4 c	26.6 ± 21.5 c	4.9 ± 0.5 c
	Typic Eutrudepts (2)	52 ± 7 ce	27 ± 4 c	21 ± 6 a	SCL	29.9 ± 30.9	1.7 ± 1.6	15.8 ± 3.6 ab	9.2 ± 6.1 ab	72.1 ± 21.4 ab	6.3 ± 1.2 ab

SL is sandy loam; L is loam; SiL is silty loam; SCL is sandy clay loam.

Table 4. Mean ± standard deviation of sand, silt, clay, total organic carbon (TOC), total nitrogen (TN), and exchangeable Ca (Ca_{exch}) contents, base saturation (BS), and pH values, and texture class soils identified within the 1000–2134 m above sea level altitudinal range and classified according to Soil Survey Staff (2014). Round brackets indicate the number of soil profiles identified for each soil type. Within each column, different letters indicate significant differences among the values (Kruskal–Wallis test, $p < 0.05$).

Soil Order	Soil Subgroup	Sand	Silt	Clay	Texture	TOC	TN	C/N	Caexch	BS	pH
		%	%	%		g kg−1	g kg−1		cmol(+) kg−1	%	
Entisol	Lithic Cryorthent (3)	54 ± 18 d	32 ± 11 ad	14 ± 9 ab	SL	41.5 ± 14.0	3.6 ± 1.1	11.5 ± 2.1 d	8.2 ± 6.0 ab	71.5 ± 23.2 a	5.6 ± 1.0 ab
	Lithic Udorthent (6)	58 ± 13 d	27 ± 11 bc	14 ± 7 a	SL	40.9 ± 27.1	2.6 ± 1.6	16.8 ± 7.1 ab	6.4 ± 5.6 bc	51.7 ± 20.1 bc	4.7 ± 0.4 cd
	Typic Udorthent (7)	56 ± 23 d	36 ± 21 ab	8 ± 4 bd	SL	54.2 ± 21.2	3.9 ± 1.5	14.1 ± 4.1 bd	5.2 ± 6.2 cd	46.5 ± 31.4 bc	5.0 ± 0.5 bc
Inceptisol	(Spodic) Lithic Dystrudepts (2)	77 ± 6 a	19 ± 4 d	4 ± 3 d	LS	59.3 ± 31.7	3.6 ± 2.5	16.9 ± 3.9 ab	2.6 ± 2.3 d	37.6 ± 18.8 ce	4.9 ± 0.3 bc
	Humic Dystrudepts (4)	52 ± 13 d	38 ± 11 a	10 ± 5 ab	L	42.3 ± 27.0	2.5 ± 1.3	16.7 ± 7.0 ab	1.5 ± 0.8 d	17.2 ± 6.2 fg	4.6 ± 0.3 cd
	Humic Lithic Dystrudepts (9)	60 ± 15 d	31 ± 11 ac	9 ± 7 bd	SL	47.5 ± 22.1	3.3 ± 1.4	14.3 ± 2.1 ac	2.0 ± 2.7 d	25.8 ± 18.8 eg	4.6 ± 0.3 cd
	Humic Lithic Eutrudepts (4)	70 ± 13 ac	23 ± 10 cd	7 ± 4 cd	SL	34.3 ± 22.5	2.5 ± 1.3	13.2 ± 4.7 cd	10.3 ± 8.9 ab	69.1 ± 30.6 ab	5.4 ± 0.7 ab
	Lithic Dystrudepts (5)	73 ± 8 ab	20 ± 8 d	6 ± 4 d	SL	39.5 ± 20.5	3.2 ± 1.8	12.7 ± 2.1 cd	3.5 ± 4.7 d	39.5 ± 35.3 df	5.0 ± 0.5 b
	Lithic Eutrudepts (3)	42 ± 24 d	45 ± 26 ac	14 ± 6 a	L	47.9 ± 23.2	3.4 ± 1.4	14.7 ± 7.2 bd	12.6 ± 5.2 a	73.9 ± 16.9 a	5.3 ± 0.7 ab
	Typic Dystrudepts (19)	59 ± 13 d	32 ± 10 ab	8 ± 5 bd	SL	52.1 ± 29.3	3.1 ± 1.8	16.8 ± 4.1 ab	6.3 ± 6.4 bc	24.3 ± 20.8 eg	4.4 ± 0.3 e
Spodosol	Typic Haplorthod (4)	62 ± 11 cd	28 ± 9 ac	10 ± 4 ac	SL	57.1 ± 36.5	3.8 ± 2.5	15.4 ± 5.2 ac	2.4 ± 1.7 d	19.1 ± 16.1 g	4.5 ± 0.4 de
	Lithic Haplohumod (2)	58 ± 15 d	37 ± 10 ab	4 ± 3 d	SL	64.1 ± 31.2	3.5 ± 1.8	17.7 ± 5.7 a	3.6 ± 3.0 cd	39.9 ± 20.6 ce	4.4 ± 0.3 de
Mollisol	Lithic Hapludoll (3)	57 ± 25 bd	36 ± 20 ac	6 ± 6 d	SL	46.4 ± 22.3	3.8 ± 1.2	11.6 ± 2.3 cd	9.0 ± 4.9 ab	93.5 ± 6.3 a	6.2 ± 0.2 a

5.3.2 Cluster analysis (CA) and Principal Component Analysis (PCA)

5.3.2.1 Lower altitudinal ranges

CA was used to cluster the soil samples collected from each horizon of the study sites located at ≤1000 m a.s.l. into three clusters (Figure S1 of the Supplementary Materials). One cluster (hereafter called Cluster 1) included 45 statistical units mostly belonging to layer A. The largest cluster (hereafter called Cluster 2) had 145 statistical units including soil samples from layer B and layer C. The smallest cluster (hereafter called Cluster 3) mainly included soil samples collected under CHE, although the A horizons of CHE were also found. The Kruskal–Wallis test carried-out on the identified clusters showed the highest values of pH (5.9), TOC content (58.3 g kg^{-1}), TN content (3.7 g kg^{-1}), Ca_{exch} content (13.6 cmol $_{(+)}$ kg^{-1}), BS content (66.4%), and clay content (15%) for the soil samples of Cluster 1. Between Cluster 2 and 3, some further differences were observed: TOC and TN contents were higher in Cluster 3 than in Cluster 2, while Cluster 2 had higher contents of sand and silt than Cluster 3 (Table 5).

Table 5. Mean of sand, silt, clay, total organic carbon (TOC), total nitrogen (TN), and exchangeable Ca (Ca_{exch}) contents, and BS, TOC–to–TN ratio (C:N), and pH values of the clusters obtained via cluster analysis on the set of data below 1000 m above sea level. Within each column, values sharing similar letters do not indicate significant differences (Kruskal–Wallis test, $p < 0.05$).

Cluster	Sand	Silt	Clay	TOC	TN	Caexch	BS	C:N	pH
	%	%	%	g kg^{-1}		cmol $_{(+)}$ kg^{-1}	%		
1 (45)	54 a	31 b	15 a	58.3 a	3.7 a	13.6 a	66.4 a	16.3	5.9 a
2 (145)	55 a	35 a	10 b	19.1 c	1.2 c	3.4 b	29.8 b	15.5	5.0 b
3 (23)	25 b	65 c	10 b	38.9 b	1.3 b	8.4 b	31.5 b	21.7	5.3 b

The first two principal components of PCA, performed on the dataset at below 1000 m a.s.l. explained 51.0% of the total variance (Figure 2). PCA allowed us to identity pH, OC, TN, sand, silt, Ca_{exch}, and BS as the main soil parameters in the separation of the clusters (Figure 2).

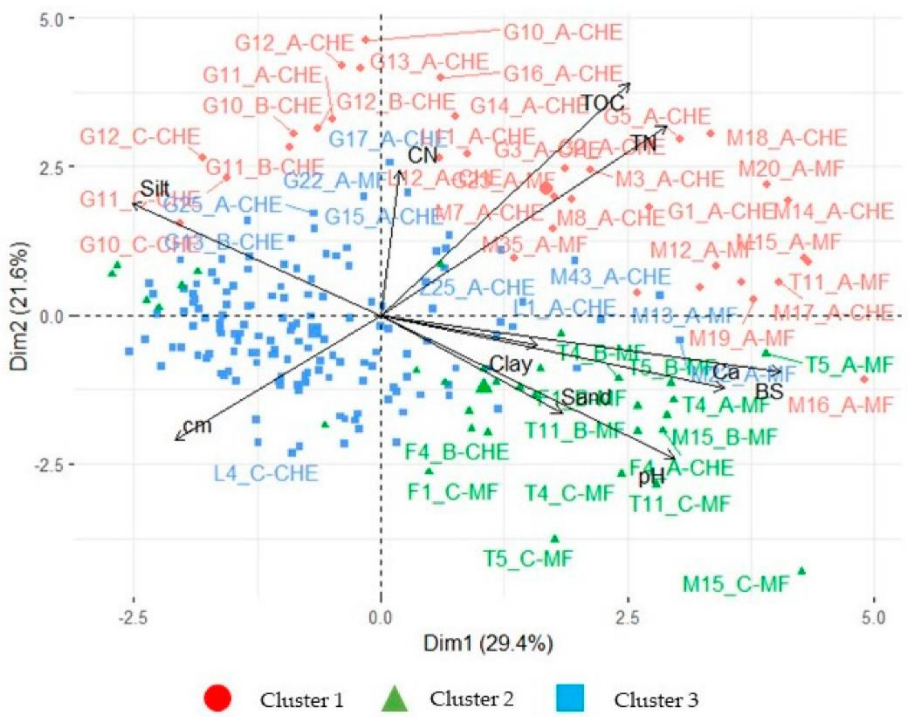

Figure 2. Principal component analysis (PCA) obtained from the dataset at a 400–1000 m altitudinal range. The distinct colors indicate the three clusters distributed along the principal component (Dim) 1 and 2. The sample codes included the sampling area, profile number, layers, and vegetation cover. The variables are in black. BS = base saturation; Ca = exchangeable Ca; TN = total N; OC = soil organic C; CN = OC–to–N ratio; cm = microbial biomass C.

5.3.2.2 Higher altitude range

The CA performed on soil horizons of the study sites located at >1000 m a.s.l. produced three clusters (Figure S2 of the Supplementary Materials). The smallest cluster (hereafter called Cluster I) had 35 statistical units and included mainly horizon A of the soils characterized by MOD and CERV sandstone types. The largest cluster (hereafter called Cluster II) had 130 statistical units and included deeper horizons. The third cluster (hereafter called Cluster III) had 54 statistical units and included the A horizons of soils developed on the other sandstone types. The highest pH value was observed in Cluster I (5.7) and the lowest one in Cluster III (4.3) (Table 6). Both TOC and TN showed the highest contents in Cluster III (81.4 and 5.4 g kg^{-1}, respectively) and the lowest in Cluster II. Ca_{exch} and BS showed the highest values in Cluster I (13.2 $cmol_{(+)}$ kg^{-1} and 88.3%, respectively) and the lowest ones in Cluster II (3.0

cmol $_{(+)}$ kg^{-1} and 26.6%, respectively). For the particle size distribution, Cluster II showed the lowest sand content and the highest clay content (57 and 11%, respectively).

Table 6. Mean of sand, silt, clay, total organic carbon (TOC), total nitrogen (TN), and exchangeable Ca (Ca_{exch}) contents, and BS, TOC–to–TN ratio (C:N), and pH values of the clusters obtained via cluster analysis on the set of data for the 1000 m above sea level altitudinal range. Within each column, values sharing similar letters do not indicate significant differences (Kruskal–Wallis test, $p < 0.05$).

Cluster	Sand	Silt	Clay	TOC	TN	Caexch	BS	C:N	pH
	%	%	%	g kg^{-1}		cmol$_{(+)}$ kg^{-1}	%		
I (33)	60 a	34 a	6 b	44.2 b	3.4 b	13.2 a	88.3 a	12.7	5.7 a
II (130)	57 b	32 ab	11 a	35.6 c	2.3 c	3.0 c	26.6 c	16.0	4.7 b
III (54)	65 a	28 b	7 b	81.4 a	5.4 a	6.1 b	37.0 b	15.4	4.3 c

For the above 1000 m a.s.l. altitudinal range, the first two principal components of the PCA explained 47.1% of the total variance (Table 3). PCA showed the great influence of pH, TN, TOC, sand, silt, $Ca_{exch,}$ and BS on the distinctions among the clusters identified by CA (Figure 3).

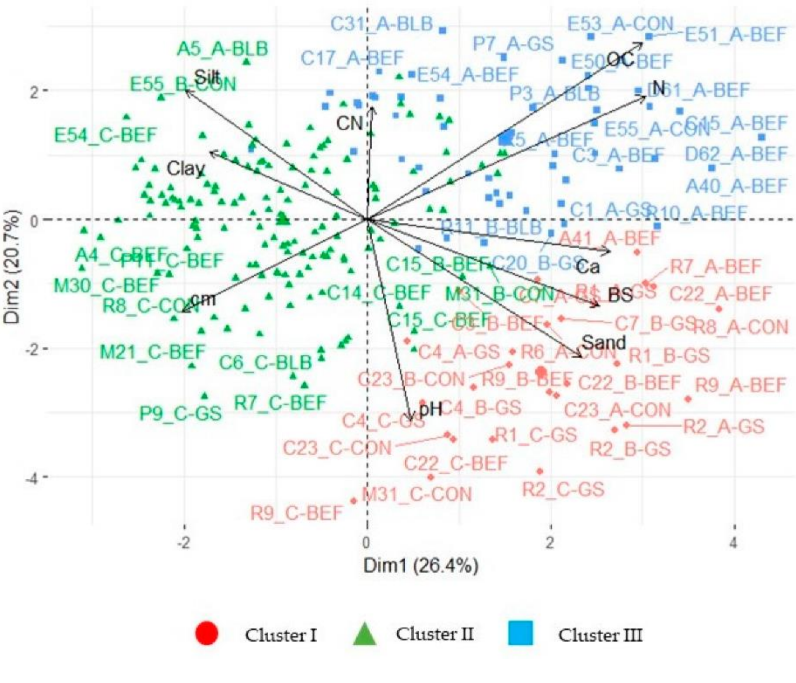

Figure 3. Principal component analysis (PCA) obtained from the dataset at a 1000–2134 m altitudinal range. The distinct colors identified the three clusters distributed along principal components (Dim) 1 and 2. The sample codes included the sampling area, profile number, layer, and vegetation cover. The variables are in black. BS = base saturation; Ca = exchangeable Ca; N = total N; OC = soil organic C; CN = OC–to–N ratio; cm = microbial biomass C.

5.3.3 Organic C and Total N stocks

SOC and TN stocks differed within altitude classes and vegetation covers (Table 7). Both SOC and TN stocks showed the lowest values at the ≤1000 m a.s.l. altitudinal range. These differences were confirmed by the vegetation covers of CHE and MF. The main covers at ≤1000 m a.s.l. showed lower stocks of SOC and TN compared to the vegetation types located at a higher altitudinal range (73.3 and 4.6, and 70.8 and 4.7 Mg ha^{-1} for CHE and MF, respectively). Within the higher altitudinal interval, the SOC stock did not differ, while a lower TN stock (7.2 Mg ha^{-1}) was found under BEF than under BLB, GS, and CON.

Table 7. Mean ± standard error of soil organic carbon stock (SOC stock) and total nitrogen stock (TN stock) in chestnut groves (CHE), coniferous forests (CON), beech forests (BEF), blueberry habitat (BLB), mixed forests (MF), and grasslands (GS) and at 400–1000 and 1000–2134 m above sea level (a.s.l.). For the vegetation types and altitudinal ranges, different letters within each column indicated significant differences (Kruskal–Wallis test, $p < 0.05$).

		SOC Stock	**TN Stock**
		Mg ha^{-1}	
Vegetation type	BEF	118.4 ± 30.0 a	7.2 ± 2.5 b
	BLB	141.1 ± 42.2 a	9.6 ± 2.2 a
	CHE	73.3 ± 36.1 b	4.6 ± 1.7 c
	CON	117.9 ± 24.7 a	9.3 ± 2.5 a
	GS	128.7 ± 46.5 a	11.4 ± 3.9 a
	MF	70.8 ± 25.9 b	4.7 ± 1.9 c
Altitudinal range (m a.s.l.)	≤1000	72.7 ± 33.9 b	4.6 ± 1.7 b
	>1000	125.3 ± 38.5 a	8.8 ± 3.0 a

5.4 DISCUSSION

5.4.1 Factors affecting pedodiversity

The investigated soils are located in a large altitudinal range, and, as a consequence, different hydrological and temperature regimes are present (from udic to perudic and from mesic to cryic, respectively), defining the different climates and phytoclimatic zones (Figure 1 and Table 1).

In the investigated sites, the soils were mainly characterized by weak or incipient development, mainly including Entisols and Inceptisols (Table 2), which could be attributed to the sand-based lithology, high slope gradients, and low organic matter accumulation rates promoting soil erosion processes and, therefore, weak soil development. Specifically, sandstone weathering processes generate soils with low clay and base contents and a weak soil structure (Vittori Antisari et al., 2011; Marinari & Vittori Antisari, 2010; Evans et al., 2021), making them vulnerable to erosion. With organic matter serving as the major actor for the formation and stabilization of soil aggregates (Sithole et al., 2019; Sarker et al., 2018), such vulnerability was further boosted by low clay content, which likely limited organic carbon retention within the mineral horizons (De Feudis et al., 2022a; Islam et al., 2022; Schweizer et al., 2019) and led to thin A horizons (5.5 cm, on average). However, the incorporation of organic matter within the mineral horizons was likely further prevented by acidic conditions resulting in the accumulation of organic matter on the soil surface as organic horizons (Zanella et al., 2018). The weak soil development could be also attributed to the steepness of the study sites since most of the investigated soils had a slope gradient greater than 11°, which is considered the threshold for the occurrence of intense soil erosion (García-Ruiz et al., 2015). Therefore, the sandstone lithology, weak soil organic matter accumulation, and high slope gradients of these mountain areas of the Apennines promoted the formation of young and poorly developed soils (i.e., Entisols and Inceptisols). Conversely, where erosion is limited, and favorable development conditions occur, such as the study sites at the highest elevations with north–northeast exposure, more intense pedogenesis occurs and is mainly driven by podzolization processes (i.e., Spodosols).

Taking into consideration the altitudinal ranges, higher pedodiversity was observed at both the order and subgroup levels in a range of >1000 m a.s.l. compared to that found in the range of ≤1000 m a.s.l. (Table 2). Because of the role of vegetation type on soil properties and development (D’Amico et al., 2014; Maxbauer et al., 2017; Cerqueira et al., 2012), the highest pedodiversity found at >1000 m a.s.l. might be attributable to the higher vegetation cover diversity compared to that at ≤1000 m a.s.l., as discussed in the following paragraphs.

However, the highest vegetation cover diversity observed at >1000 m a.s.l. could be, in turn, due to the higher climate variability in terms of the mean air temperature, which is in accordance with several previous studies (Bruun et al., 2006; Gastauer et al., 2020), demonstrating the great influence of climate changes related to altitude on vegetation placement within the different phytoclimatic zones. Indeed, while from about 400 to 1000 m a.s.l., the mean air temperature decreased by about 2 °C, within the >1000 m a.s.l. altitudinal range, the temperature change was about 6 °C (Table S2 of the Supplementary Materials). Additionally, the different mean air temperatures recorded along the elevation gradient affected soil processes with the resulting development of different soil types (Pintaldi et al., 2019; Egli et la., 2004; De Feudis et al., 2016).

5.4.2 Properties of soils at 400-1000 m a.s.l.

The investigated area ranging between 400 and 1000 m a.s.l. belongs to the Castanetum phytoclimatic zone (Table 1), which has been populated since ancient times by chestnut stands (Pezzi et al., 2011). Here, suitable soils for chestnut stands are present and are formed on sedimentary or siliceous soils (Pereira et al., 2011) where acidic conditions predominate (Arrobas et al., 2018). Acidic soils are, in fact, favorable for the growth of such plant species (De Feudis et al., 2022a; De Feudis et al., 2021; Melicharová & Vizoso-Arribe, 2012), with chestnut being susceptible to the presence of the carbonates that typically come from limestone and marl (Papaioannou et al., 2022). The investigated CHE soils were sampled from a mountain farm and had suitable physicochemical characteristics to produce chestnut plants with a good vegetative and adaptive state (Mellano et al., 2012). Indeed, marked dystric characteristics (Lithic, Oxyaquic, and Typic Dystrudepts) characterized by low values of pH, Ca_{exch} content, BS, and amount of the finest soil particles were monitored under chestnut stands (Table 2). Further, CHE was mainly found on soils developed from parent materials, which were mainly poor in Ca and clay particles (i.e., GRA and MOH). Thus, under CHE, very weak soil variability was observed, mainly because of the ancient human-based selection of soils for plant chestnut stands. Unlike CHE, natural or semi-natural MFs were more evenly distributed among the different investigated sandstone formations. Thus, even if sandstone lithology limited diversity at the level of soil order, the presence of marly pelitic intercalations within the sandstone formation could generate differences at the soil subgroup level. Besides dystric features, under MF, eutric features were found (Lithic and Typic Eutrudepts) in soil developed on marl-enriched sandstones. The presence of such $CaCO_3$-rich intercalation promoted the development of soils with high pH values, Ca_{exch} content, and BS percentages (Table 3).

Independently from sandstone formations, nonparametric statistical investigations (i.e., CA and PCA) highlighted that the highest values of BS, TOC, TN, and Ca_{exch} were observed in the A horizon, (Table 5 and Figure 2). This would suggest intense processes within this horizon related to the organic C cycle. Specifically, despite the parent material, the higher values of Ca_{exch} content and BS found in the A horizon could be attributed to the degradation of plant residues (Wang et al., 2021), as supported by the higher TOC content (Gruba & Mulder, 2015; Ramos et al., 2018). Thus, organic C cycle occurring in the A horizon allowed us to enhance nutrient (i.e., Ca) concentrations at the soil surface in soils that developed from nutrient-poor parent materials. The A horizons, however, were quite thin, with their mean values of thickness being 5.5 cm (from 1 to 12 cm). The key role of the A horizons in improving soil properties coupled with their thin thickness highlighted the vulnerability of these soils to degradation in areas such as mountainous regions, where soil erosion processes can be intense.

5.4.3 Properties of Soils at the 1000–2134 m a.s.l. Altitudinal Range

The altitudinal range from 1000 to 2134 m a.s.l. included Fagetum, Picetum, and Alpinetum phytoclimatic zones. Different moisture and temperature regimes were recorded from udic to perudic and from mesic to frigid and cryic, respectively (Table 1). The large variability in phytoclimatic zones, soil moisture, and temperature regimes further promoted pedodiversity within the >1000 m a.s.l. altitudinal range. In the northern Apennines, above the timberline and close to the top of the mountains, the primary grasslands occurred as the end of the elevation sequence of both primary heaths and secondary grasslands (Pignatti, 1994). The highest land here includes ridges and steep slopes lashed by winds with high speed that carry away the snowpack accumulating in other areas, increasing the risk of frozen of soils with a consequent effect on the vegetation (Tomaselli et al., 2019). Three soil profiles were studied in the Alpinetum phytoclimatic zone of Mount Cimone under Nardetum GS (Benatti et al., 2019). These profiles were classified as Lithic Cryorthents, characterized by BS > 70% due to the presence of Ca_{exch} on the soil exchange complex. Under Nardetum GS located at the lower altitudes of Corno alle Scale, Lithic Mollisols were found. In Mollisols, it was possible to highlight a greater thickness of the A horizon compared to that in Entisols, but the physicochemical features of these soils were very similar (Table 4). Above the tree line, shrub communities with a predominance of Ericaceae dominated the mountain heathland (BLB, *Vaccinium myrtillus* and *Vaccinium gaultherioides* Bijelow) (Tomaselli et al., 1996; Alessandrini et al., 2003). BLB soils showed marked dystric characteristics that were affected by strong leaching (low Ca_{exch} and BS), which, in some cases, resulted in spodic characteristics (Spodic Lithic Dystrudepts) at Corno alle Scale, while Spodosols (Typic Haplorthod) were found at Mount Prado and Mount Cusna. At Mount Cimone, Vittori Antisari et al. (2018) investigated paleosols containing, at varying depths (but never exceeding 30 cm), a carbon-enriched horizon (Aub) that separated the top of the soil profile, called modern, from the buried soil, called ancient, showing well-expressed spodic properties. Therefore, in the present study, only modern-developed soils were taken into consideration, thereby providing a rather simple sequence of horizons (A-Bw-C).

It was unexpected to observe the highest C:N ratio of soils under BEF (Table 2). Indeed, the relatively low C:N ratio of beech residues is commonly recognized (Lorenz et al., 2020; Spohn & Chodak, 2015). The high C:N ratio due to the lowest TN content found in the soils under BEF might be attributable to the fast degradation rate of such residues (Osei et al., 2021; Mora et al., 2021). Specifically, the high rates of degradation mobilize a large amount of N, which, if not promptly uptaken by plants, can be lost through leaching.

Similar to the comparison between vegetation types, the soil subgroups identified at >1000 m a.s.l. did not show differences in soil texture (Table 4) likely due to the even distribution of such soil types on the different lithologies. Taking into consideration the investigated soil chemical properties (i.e., TOC, TN, C:N, pH, BS, and Ca_{exch}), although some differences could be observed among the soil subgroups, a clear trend was not identified (Table 4) due to the wide distribution of these subgroups within the study area in terms of vegetation, topography, and climate.

As observed for soils at the ≤1000 m a.s.l. altitudinal range, the CA performed for the soils at higher altitudes showed differentiation between the A horizons and the subsurface ones (Table 6). As already observed for the lower altitude, in A horizons at higher altitudes (Cluster I and III), the C cycling facilitated improvement of soil nutrient content, increasing Ca and BS values compared to deeper horizons (Cluster II). However, unlike the comparison between the soil subgroup vegetation types, the CA highlighted the influence of lithology on the A horizon's development. Indeed, the A horizons of soils developed on MOD and CERV showed the highest values of Ca_{exch} content, BS, and pH in accordance with the chemical composition of MOD and CERV (Table A1) compared to that of the other lithologies found at >1000 m a.s.l.

5.4.4 Organic C and Total N Stocks within 0–30 cm Soil Depth

According to previous studies (De Feudis et al., 2022a; Tashi et al., 2016), within the study area, greater SOC and TN stocks were found at >1000 m a.s.l. compared to ≤1000 (Table 7). Such results were confirmed by vegetation type; indeed, the lowest SOC and TN stocks were observed under CHE and MF, both located at ≤1000 m a.s.l. These findings indicate the greater influence of climate on SOC and TN contents compared to vegetation, as observed by previous studies (Massaccesi et al., 2020; Oueslati et al., 2013). Indeed, although the vegetation affected the organic matter quality (Díaz-Pinés et al., 2011; Kumar et al., 2017) until now, the lower mean air temperatures occurring at higher elevations strongly reduced organic matter mineralization by the microbial community (Tewksbury & Van Miegroet, 2007; Wiesmeier et al., 2019). Overall, despite the higher SOC and TN stocks at >1000 m a.s.l. compared to those at ≤1000 m, it is important to highlight that our study sites featured soils highly vulnerable to organic C loss due to the aforementioned topographic and edaphic factors, namely, the low amount of clay particles and the generally high slope gradient (Clark et al., 2022; Angst et al., 2021; La Manna et al., 2021; Heger et al., 2021).

5.5 CONCLUSIONS

The present study highlighted relatively young soils (mainly Entisols and Inceptisols) in the study area. The wide distribution of Entisols and Inceptisols could be attributable to the area's sand-based lithology, high slope gradients, and low organic matter accumulation rates, which make soils vulnerable to erosion processes and, therefore, do not promote soil development. Taking into consideration the subgroup level of the Soil Taxonomy classification, higher pedodiversity was found at altitudes >1000 m a.s.l. compared to those at ≤1000 m, likely due to the higher vegetation diversity and larger mean air temperature ranges at the former altitude compared to the latter.

Within the ≤1000 m a.s.l. altitudinal range, chestnut stands were present in the Castanetum phytoclimatic zone and were characterized by soils with dystric features (Lithic, Oxyaquic, and Typic Dystrudepts) and low values of pH, Ca_{exch} content, BS, and the finest soil particles. Unlike chestnut, the mixed forests contained soils with both dystric and eutric features because such soils also developed on marl-enriched sandstone.

The lower mean air temperatures recorded at >1000 m a.s.l. compared to the lower altitudinal range promoted the accumulation of soil organic matter, which likely reduced the erosion processes and, therefore, promoted soil development. Indeed, at >1000 m, Mollisols and Spodosols were found in addition to Entisols and Inceptisols.

Taking into consideration the SOM stock, the present study demonstrated the greater role of climate (i.e., temperature) on soil organic matter compared to vegetation. Indeed, a clear difference was observed between the investigated altitudinal ranges, while the SOM stock did not show differences between the vegetation types included within each altitudinal range. However, we are aware that the results of the present study need to be interpreted with caution, as we did not compare similar vegetation at different altitudes since vegetation is affected by climate change with respect to altitude.

The spatial pedodiversity observed in the northern part of the Apennine chain in Italy could be considered a critical basis for the protection of soil resources and pedodiversity itself in mountain regions, which are characterized by high complexity related to topography, lithology, and vegetation.

SUPPLEMENTARY MATERIALS

The following supporting information can be downloaded at: **https://www.mdpi.com/article/10.3390/land12010079/s1**, Figure S1: Dendrogram obtained via hierarchical cluster analysis performed on soil samples from 400–1000 m above sea level; Figure S2: Dendrogram obtained via hierarchical cluster analysis performed on soil samples at 1000–2134 m above sea level; Table S1: Soil type, coordinates, aspect, slope gradient, vegetation type, and altitude of plots under investigation; Table S2: Monthly and yearly mean air temperatures and cumulative precipitation.

AUTHOR CONTRIBUTIONS

Conceptualization, L.V.A. and G.V.; methodology, L.V.A. and G.V.; validation, L.V.A., G.F. and M.D.F.; formal analysis, L.V.A. and W.T.; investigation, L.V.A., G.V., G.F. and A.B.; resources, L.V.A.; data curation, W.T.; writing—original draft preparation, M.D.F.; writing—review and editing, L.V.A., G.F. and M.D.F.; visualization, L.V.A. and M.D.F.; supervision, L.V.A. and M.D.F.; funding acquisition, L.V.A. All authors have read and agreed to the published version of the manuscript.

FUNDING

This research was funded by “Apennine Project, grant number RFOVittori”, “CASTANI-CO, Emilia Romagna Regional rural development program 2014–2020–number 5015571”, “Boschiamo Emilia Romagna Regional rural development program 2014–2020–number 5112703”, “Biodiversamente Castagno, Emilia Romagna Regional rural development program 2014–2020–number 5015570”, and “Castagni parlanti, Emilia Romagna Regional rural development program 2014–2020–number 5111733”.

CONFLICTS OF INTEREST

The authors declare no conflicts of interest.

APPENDIX A

Table A1. Mean chemical composition of the sandstone formations according to Dinelli et al. (1999), van de Kamp and Leake (1995), and Gazzi .

	MAC	MOD	CEV	GRA	MOH	LOI	ADO
SiO_2 (%)	67.1	62.27	60.57	63.46	70.33	72.43	58.46
TiO_2 (%)	0.49	0.5	0.5	0.71	0.3	0.23	0.69
Al_2O_3 (%)	12.94	11.25	12.50	16.57	13.79	14.01	13.11
Fe_2O_3 (%)	4.2	4.11	3.91	4.87	2.02	1.43	5.27
MnO (%)	0.07	0.07	0.1	0.13	0.05	0.02	0.13
MgO (%)	3.46	3.43	3.08	4.63	1.09	1.07	2.12
CaO (%)	2.33	5.08	7.09	0.35	0.73	0.21	7.78
Na_2O (%)	2.76	2.68	2.7	2.38	2.27	3.02	2.59
K_2O (%)	2.19	2.29	2.07	2.48	3.6	4.31	2.64
P_2O_5 (%)	0.13	0.14	0.13	0.22	0.09	0.05	0.15

MAC: Macigno sandstones; MOD: Mount Modino sandstones; CEV: Mount Cervarola sandstones; GRA: Castiglione dei Pepoli sandstones; MOH: Monghidoro formation; LOI: Loiano formation; ADO: Mount Adone formation.

REFERENCES

Adiyah, F., Michéli, E., Csorba, A., Weldmichael, T. G., Gyuricza, C., Ocansey, C. M., ... & Fuchs, M. (2022). Effects of landuse change and topography on the quantity and distribution of soil organic carbon stocks on Acrisol catenas in tropical small-scale shade cocoa systems of the Ashanti region of Ghana. *Catena*, *216*, 106366.

Alessandrini, A., Foggi, B., Rossi, G., & Tomaselli, M. (2003). La flora di altitudine dell'Appennino tosco-emiliano. In *La flora di altitudine dell'Appennino tosco-emiliano*. (pp. 3-328). Tipografia Moderna.

Angst, G., Pokorný, J., Mueller, C. W., Prater, I., Preusser, S., Kandeler, E., ... & Angst, Š. (2021). Soil texture affects the coupling of litter decomposition and soil organic matter formation. *Soil Biology and Biochemistry*, *159*, 108302.

Arrobas, M., Afonso, S., & Rodrigues, M. Â. (2018). Diagnosing the nutritional condition of chestnut groves by soil and leaf analyses. *Scientia Horticulturae*, *228*, 113-121.

Bangroo, S. A., Najar, G. R., Achin, E., & Truong, P. N. (2020). Application of predictor variables in spatial quantification of soil organic carbon and total nitrogen using regression kriging in the North Kashmir forest Himalayas. *Catena*, *193*, 104632.

Bargali, K., & Bargali, S. S. (2020). Effect of size and altitude on soil organic carbon stock in homegarden agroforestry system in Central Himalaya, India. *Acta Ecologica Sinica*, *40*(6), 483-491.

Benatti, A., Bal, M., Allée, P., Bosi, G., & Mercuri, A. M. (2019). Plant landscape reconstruction above the current timberline at the Monte Cimone and Corno alle Scale mountain areas (Northern Apennines, Italy) during the Late Holocene: The evidence from soil charcoal. *The Holocene*, *29*(11), 1767-1781.

Bockheim, J. G., Gennadiyev, A. N., Hartemink, A. E., & Brevik, E. C. (2014). Soil-forming factors and Soil Taxonomy. *Geoderma*, *226*, 231-237.

Boudjabi, S., & Chenchouni, H. (2022). Soil fertility indicators and soil stoichiometry in semi-arid steppe rangelands. *Catena*, *210*, 105910.

Brenna, S., Stolbovoy, V., Rocca, R., & Sciaccaluga, M. (2010, August). Potential carbon sequestration of Lombardy soils (Italy). In *Proceedings of the 19th World Congress of Soil Science, Soil Solutions for a Changing World, Brisbane, Australia* (pp. 1-6).

Britton, A. J., Helliwell, R. C., Lilly, A., Dawson, L., Fisher, J. M., Coull, M., & Ross, J. (2011). An integrated assessment of ecosystem carbon pools and fluxes across an oceanic alpine toposequence. *Plant and Soil*, *345*(1), 287-302.

Brombin, V., Mistri, E., De Feudis, M., Forti, C., Salani, G. M., Natali, C., ... & Bianchini, G. (2020). Soil carbon investigation in three pedoclimatic and agronomic settings of Northern Italy. *Sustainability*, *12*(24), 10539.

Bruun, H. H., Moen, J., Virtanen, R., Grytnes, J. A., Oksanen, L., & Angerbjörn, A. (2006). Effects of altitude and topography on species richness of vascular plants, bryophytes and lichens in alpine communities. *Journal of Vegetation Science*, *17*(1), 37-46.

Canedoli, C., Ferrè, C., El Khair, D. A., Comolli, R., Liga, C., Mazzucchelli, F., ... & Padoa-Schioppa, E. (2020). Evaluation of ecosystem services in a protected mountain area: Soil organic carbon stock and biodiversity in alpine forests and grasslands. *Ecosystem services*, *44*, 101135.

Casalini, A. I., Bouza, P. J., & Bisigato, A. J. (2019). Geomorphology, soil and vegetation patterns in an arid ecotone. *Catena*, *174*, 353-361.

Cerqueira, B., Vega, F. A., Silva, L. F., & Andrade, L. (2012). Effects of vegetation on chemical and mineralogical characteristics of soils developed on a decantation bank from a copper mine. *Science of the Total Environment*, *421*, 220-229.

Clark, K. E., Stallard, R. F., Murphy, S. F., Scholl, M. A., González, G., Plante, A. F., & McDowell, W. H. (2022). Extreme rainstorms drive exceptional organic carbon export from forested humid-tropical rivers in Puerto Rico. *Nature communications*, *13*(1), 2058.

Conforti, M., Matteucci, G., & Buttafuoco, G. (2017). Organic carbon and total nitrogen topsoil stocks, biogenetic natural reserve 'Marchesale'(Calabria region, southern Italy). *Journal of Maps*, *13*(2), 91-99.

Costantini, E. A., & Dazzi, C. (Eds.). (2013). *The soils of Italy* (pp. 19-38). Dordrecht, Netherlands: Springer.

Costantini, E. A., & L'Abate, G. (2016). Beyond the concept of dominant soil: Preserving pedodiversity in upscaling soil maps. *Geoderma*, *271*, 243-253. Gutiérrez-Girón, A., Diaz-Pines, E., Rubio, A., & Gavilan, R. G. (2015). Both altitude and vegetation affect temperature sensitivity of soil organic matter decomposition in Mediterranean high mountain soils. *Geoderma*, *237*, 1-8.

D'Amico, M. E., Freppaz, M., Filippa, G., & Zanini, E. (2014). Vegetation influence on soil formation rate in a proglacial chronosequence (Lys Glacier, NW Italian Alps). *Catena*, *113*, 122-137.

De Feudis, M., Cardelli, V., Massaccesi, L., Bol, R., Willbold, S., Cocco, S., ... & Agnelli, A. (2016). Effect of beech (Fagus sylvatica L.) rhizosphere on phosphorous availability in soils at different altitudes (Central Italy). *Geoderma*, *276*, 53-63.

De Feudis, M., Falsone, G., & Antisari, L. V. (2021). Mid-term (30 years) changes of soil properties under chestnut stands due to organic residues management: An integrated study. *Catena*, *198*, 105021.

De Feudis, M., Falsone, G., Vianello, G., & Antisari, L. V. (2020a). Stable organic carbon pool rises in soil under chestnut (Castanea sativa Mill.) forest for timber production after 15 years since grafting onto satin-cut stumps. *EQA-International Journal of Environmental Quality*, *40*, 1-10.

De Feudis, M., Falsone, G., Vianello, G., & Vittori Antisari, L. (2020b). The conversion of abandoned chestnut forests to managed ones does not affect the soil chemical properties and improves the soil microbial biomass activity. *Forests*, *11*(8), 786.

De Feudis, M., Falsone, G., Vianello, G., Agnelli, A., & Vittori Antisari, L. (2022a). Soil organic carbon stock assessment in forest ecosystems through pedogenic horizons and fixed depth layers sampling: What's the best one?. *Land Degradation & Development*, *33*(9), 1446-1458.

De Feudis, M., Selmi, C., Falsone, G., Missere, D., Di Bonito, M., & Antisari, L. V. (2022b). The importance of incorporating soil in the life cycle assessment procedure to improve the sustainability of agricultural management. *Catena*, *218*, 106563.

De Philippis, A. (1937). Classificazioni ed indici del clima, in rapporto alla vegetazione forestale italiana. *Plant Biosystem*, *44*(1), 1-169.

De Philippis, A. D. (1951). Forest ecology and phytoclimatology. *Unasylva*, *5*, 1.

Dell'Abate, M. T., Giovannini, C., Pontalti, F., Vianello, G., & Vittori Antisari, L. (2007). Caratterizzazione quali-quantitativa della sostanza organica degli epipedon di suoli bruni acidi dell'Appennino emiliano sotto bosco di latifoglie e di conifere. In *Atti Convegno Nazionale Società Italiana di Scienze del Suolo "Suolo Ambiente Paesaggio",* (Vol. 1, pp. 332-342). Società Italiana di Scienza del Suolo.

Díaz-Pinés, E., Rubio, A., Van Miegroet, H., Montes, F., & Benito, M. (2011). Does tree species composition control soil organic carbon pools in Mediterranean mountain forests?. *Forest Ecology and Management*, *262*(10), 1895-1904.

Dinelli, E., Lucchini, F., Mordenti, A., & Paganelli, L. (1999). Geochemistry of Oligocene–Miocene sandstones of the northern Apennines (Italy) and evolution of chemical features in relation to provenance changes. *Sedimentary Geology*, *127*(3-4), 193-207.

Djukic, I., Zehetner, F., Tatzber, M., & Gerzabek, M. H. (2010). Soil organic-matter stocks and characteristics along an Alpine elevation gradient. *Journal of Plant Nutrition and Soil Science*, *173*(1), 30-38.

Egli, M., & Poulenard, J. (2016). Soils of mountainous landscapes. *International Encyclopedia of Geography: People, the Earth, Environment and Technology: People, the Earth, Environment and Technology*, 1-10.

Egli, M., Mirabella, A., Mancabelli, A., & Sartori, G. (2004). Weathering of soils in alpine areas as influenced by climate and parent material. *Clays and clay minerals*, *52*(3), 287-303.

Evans, D. L., Quinton, J. N., Tye, A. M., Rodés, Á., Rushton, J. C., Davies, J. A. C., & Mudd, S. M. (2021). How the composition of sandstone matrices affects rates of soil formation. *Geoderma*, *401*, 115337.

Faggian, V., Bini, C., & Zilioli, D. M. (2012). Carbon stock evaluation from topsoil of forest stands in NE Italy. *International journal of phytoremediation*, *14*(4), 415-428.

Falsone, G., Marinari, S., Vittori Antisari, L., & Vianello, G. (2015). Soil processes related to organic matter modifications following Douglas-fir mature reforestation. *Biology and Fertility of Soils*, *51*(3), 277-287.

FAO (2006). Agriculture Organization of the United Nations (2006) Guidelines for Soil Description, 4th ed. *Information Division FAO: Rome*.

FAO (2019). Measuring and modelling soil carbon stocks and stock changes in livestock production systems: guidelines for assessment; Version 1. In *Livestock Environmental Assessment and Performance (LEAP) Partnership*; FAO: Rome, Italy; 170p

Garcia-Pausas, J., Casals, P., Camarero, L., Huguet, C., Sebastia, M. T., Thompson, R., & Romanya, J. (2007). Soil organic carbon storage in mountain grasslands of the Pyrenees: effects of climate and topography. *Biogeochemistry*, *82*(3), 279-289.

García-Ruiz, J. M., Beguería, S., Nadal-Romero, E., González-Hidalgo, J. C., Lana-Renault, N., & Sanjuán, Y. (2015). A meta-analysis of soil erosion rates across the world. *Geomorphology*, *239*, 160-173.

Garlato, A., Obber, S., Vinci, I., Sartori, G., & Manni, G. (2009). Stock attuale di carbonio organico nei suoli di montagna del Veneto. *Studi Trentini di Scienze Naturali. Suoli degli ambienti alpini*, *85*, 69-82.

Gastauer, M., Thiele, J., Porembski, S., & Neri, A. V. (2020). How do altitude and soil properties influence the taxonomic and phylogenetic structure and diversity of Brazilian páramo vegetation?. *Journal of Mountain Science*, *17*(5), 1045-1057.

Gazzi, P. (1963). Ordine di apparizione dei minerali pesanti nella formazione di Monghidoro e nella serie di Loiano (Appennino Bolognese). *Mineral. Petrogr. Acta*, *9*, 79–95..

Gazzi, P. (1966). Le arenarie del flysch sopracretaceo dell'Appennio modenese: correlazioni con il flysch di Monghidero. *Mineralogica et Petrographica Acta*, *12*, 69-97.

Gebrehiwot, K., Desalegn, T., Woldu, Z., Demissew, S., & Teferi, E. (2018). Soil organic carbon stock in Abune Yosef afroalpine and sub-afroalpine vegetation, northern Ethiopia. *Ecological processes*, *7*(1), 1-9.

Gee, G. W., Bauder, J. W., & Klute, A. (1986). Methods of soil analysis, part 1, physical and mineralogical methods. *Soil Science Society of America, American Society of Agronomy*, *5*.

Ghosh, B. N., Sharma, N. K., Alam, N. M., Singh, R. J., & Juyal, G. P. (2014). Elevation, slope aspect and integrated nutrient management effects on crop productivity and soil quality in North-west Himalayas, India. *Journal of Mountain Science*, *11*(5), 1208-1217.

Gobiet, A., Kotlarski, S., Beniston, M., Heinrich, G., Rajczak, J., & Stoffel, M. (2014). 21st century climate change in the European Alps—A review. *Science of the total environment*, *493*, 1138-1151.

Gonçalves, D. R. P., de Moraes Sá, J. C., Mishra, U., Cerri, C. E. P., Ferreira, L. A., & Furlan, F. J. F. (2017). Soil type and texture impacts on soil organic carbon storage in a sub-tropical agro-ecosystem. *Geoderma*, *286*, 88-97.

Gray, J. M., Bishop, T. F., & Wilson, B. R. (2015). Factors controlling soil organic carbon stocks with depth in eastern Australia. *Soil Science Society of America Journal*, *79*(6), 1741-1751.

Gray, M. (2021). Geodiversity: a significant, multi-faceted and evolving, geoscientific paradigm rather than a redundant term. *Proceedings of the Geologists' Association*, *132*(5), 605-619.

Gruba, P., & Mulder, J. (2015). Tree species affect cation exchange capacity (CEC) and cation binding properties of organic matter in acid forest soils. *Science of the Total Environment*, *511*, 655-662.

Guo, Y., Gong, P., & Amundson, R. (2003). Pedodiversity in the United States of America. *Geoderma*, *117*(1-2), 99-115.

Gutiérrez-Girón, A., Diaz-Pines, E., Rubio, A., & Gavilan, R. G. (2015). Both altitude and vegetation affect temperature sensitivity of soil organic matter decomposition in Mediterranean high mountain soils. *Geoderma*, *237*, 1-8.

Gutman, G., Ohring, G., & Joseph, J. H. (1984). Interaction between the geobotanic state and climate: A suggested approach and a test with a zonal model. *Journal of Atmospheric Sciences*, *41*(18), 2663-2678.

Hagedorn, F., Gavazov, K., & Alexander, J. M. (2019). Above-and belowground linkages shape responses of mountain vegetation to climate change. *Science*, *365*(6458), 1119-1123.

Hanz, D. M., Cutts, V., Barajas-Barbosa, M. P., Algar, A. C., Beierkuhnlein, C., Fernández-Palacios, J. M., ... & Irl, S. D. (2022). Climatic and biogeographical drivers of functional diversity in the flora of the Canary Islands. *Global Ecology and Biogeography*, *31*(7), 1313-1331.

Heger, A., Becker, J. N., Navas, L. K. V., & Eschenbach, A. (2021). Factors controlling soil organic carbon stocks in hardwood floodplain forests of the lower middle Elbe River. *Geoderma*, *404*, 115389.

Hollander, M., Wolfe, D. A., & Chicken, E. (2013). *Nonparametric statistical methods*. John Wiley & Sons. New York, NY, USA.

Hollis, J. M., Hannam, J., & Bellamy, P. H. (2012). Empirically-derived pedotransfer functions for predicting bulk density in European soils. *European Journal of Soil Science*, *63*(1), 96-109.

Ibáñez, J. J., & Feoli, E. (2013). Global relationships of pedodiversity and biodiversity. *Vadose Zone Journal*, *12*(3), 1-5.

Inkotte, J., Bomfim, B., da Silva, S. C., Valadão, M. B. X., da Rosa, M. G., Viana, R. B., ... & Pereira, R. S. (2022). Linking soil biodiversity and ecosystem function in a Neotropical savanna. *Applied Soil Ecology*, *169*, 104209.

Islam, M. R., Singh, B., & Dijkstra, F. A. (2022). Stabilisation of soil organic matter: interactions between clay and microbes. *Biogeochemistry*, *160*(2), 145-158.

Jenny, H. (1941). *Factors of soil formation: a system of quantitative pedology*. McGraw-Hill: New York, NY, USA.

Jiménez-González, M. A., Álvarez, A. M., Carral, P., & Almendros, G. (2020). Influence of soil forming factors on the molecular structure of soil organic matter and carbon levels. *Catena*, *189*, 104501.

Jobbágy, E. G., & Jackson, R. B. (2000). The vertical distribution of soil organic carbon and its relation to climate and vegetation. *Ecological applications*, *10*(2), 423-436.

Johnson, K. D., Harden, J., McGuire, A. D., Bliss, N. B., Bockheim, J. G., Clark, M., ... & Valentine, D. W. (2011). Soil carbon distribution in Alaska in relation to soil-forming factors. *Geoderma*, *167*, 71-84.

Johnstone, J. (2021). Alpine plant life: Functional plant ecology of high mountain ecosystems. By Christian Körner. *Mt. Res. Dev.* **2021**, *41*, M1–M2.

Józefowska, A., & Miechówka, A. (2015). Enzymatic activity and enchytraeids abundance in agricultural mountain soils. *Soil Sci. Annu*, *66*(3), 133-138.

Kögel-Knabner, I., & Amelung, W. (2021). Soil organic matter in major pedogenic soil groups. *Geoderma*, *384*, 114785.

Kumar, A., Sharma, M. P., & Taxak, A. K. (2017). Effect of vegetation communities and altitudes on the soil organic carbon stock in kotli bhel-1A Catchment, India. *CLEAN–Soil, Air, Water*, *45*(8), 1600650.

La Manna, L., Tarabini, M., Gomez, F., & Rostagno, C. M. (2021). Changes in soil organic matter associated with afforestation affect erosion processes: The case of erodible volcanic soils from Patagonia. *Geoderma*, *403*, 115265.

Leifeld, J., Bassin, S., & Fuhrer, J. (2005). Carbon stocks in Swiss agricultural soils predicted by land-use, soil characteristics, and altitude. *Agriculture, Ecosystems & Environment*, *105*(1-2), 255-266.

Lorenz, M., Derrien, D., Zeller, B., Udelhoven, T., Werner, W., & Thiele-Bruhn, S. (2020). The linkage of 13C and 15N soil depth gradients with C: N and O: C stoichiometry reveals tree species effects on organic matter turnover in soil. *Biogeochemistry*, *151*(2), 203-220.

Ma, H. P., Yang, X. L., Guo, Q. Q., Zhang, X. J., & Zhou, C. N. (2016). Soil organic carbon pool along different altitudinal level in the Sygera Mountains, Tibetan Plateau. *Journal of Mountain Science*, *13*(3), 476-483.

Marinari, S., & Antisari, L. V. (2010). Effect of lithological substrate on microbial biomass and enzyme activity in brown soil profiles in the northern Apennines (Italy). *Pedobiologia*, *53*(5), 313-320.

Massaccesi, L., De Feudis, M., Leccese, A., & Agnelli, A. (2020). Altitude and vegetation affect soil organic carbon, basal respiration and microbial biomass in Apennine forest soils. *Forests*, *11*(6), 710.

Masseroli, A., Bollati, I. M., Proverbio, S. S., Pelfini, M., & Trombino, L. (2020). Soils as a useful tool for reconstructing geomorphic dynamics in high mountain environments: The case of the Buscagna stream hydrographic basin (Lepontine Alps). *Geomorphology*, *371*, 107442.

Maxbauer, D. P., Feinberg, J. M., Fox, D. L., & Nater, E. A. (2017). Response of pedogenic magnetite to changing vegetation in soils developed under uniform climate, topography, and parent material. *Scientific reports*, *7*(1), 17575.

Melicharová, L., & Vizoso-Arribe, O. (2012). Situation of sweet chestnut (Castanea sativa Mill.) in Spain, Galicia: a review. *Sci. Agric. Bohem*, *2012*, 78–84

Mellano, M. G., Beccaro, G. L., Donno, D., Marinoni, D. T., Boccacci, P., Canterino, S., ... & Bounous, G. (2012). Castanea spp. biodiversity conservation: collection and characterization of the genetic diversity of an endangered species. *Genetic Resources and Crop Evolution*, *59*(8), 1727-1741.

Mora, J. L., Molina–Clerencia, M., Girona–García, A., Martí–Dalmau, C., & Badía–Villas, D. (2021). Factors controlling the buildup of humus and particulate organic matter in European beech and Scots pine stands at their southernmost distribution limits (Moncayo Massif, Spain). *Geoderma*, *401*, 115211.

Murtagh, F., & Legendre, P. (2014). Ward's hierarchical agglomerative clustering method: which algorithms implement Ward's criterion?. *Journal of classification*, *31*(3), 274-295.

Osei, R., Titeux, H., Bielak, K., Bravo, F., Collet, C., Cools, C., ... & Ponette, Q. (2021). Tree species identity drives soil organic carbon storage more than species mixing in major two-species mixtures (pine, oak, beech) in Europe. *Forest Ecology and Management*, *481*, 118752.

Oueslati, I., Allamano, P., Bonifacio, E., & Claps, P. (2013). Vegetation and topographic control on spatial variability of soil organic carbon. *Pedosphere*, *23*(1), 48-58.

Papaioannou, E., Kostopoulou, S., & Stefanou, S. (2022). The effect of the conversion of chestnut (Castanea sativa Mill.) forests to orchards on soil fertility and nutrient content in leaves. *Catena*, *211*, 105948.

Peng, Y., Holmstrup, M., Schmidt, I. K., De Schrijver, A., Schelfhout, S., Heděnec, P., ... & Vesterdal, L. (2022). Litter quality, mycorrhizal association, and soil properties regulate effects of tree species on the soil fauna community. *Geoderma*, *407*, 115570.

Pereira, M. G., Caramelo, L., Gouveia, C., Gomes-Laranjo, J., & Magalhães, M. (2011). Assessment of weather-related risk on chestnut productivity. *Natural Hazards and Earth System Sciences*, *11*(10), 2729-2739.

Pezzi, G., Maresi, G., Conedera, M., & Ferrari, C. (2011). Woody species composition of chestnut stands in the Northern Apennines: the result of 200 years of changes in land use. *Landscape ecology*, *26*(10), 1463-1476.

Phillips, J. D., & Marion, D. A. (2005). Biomechanical effects, lithological variations, and local pedodiversity in some forest soils of Arkansas. *Geoderma*, *124*(1-2), 73-89.

Pignatti, S. (1994). The climax vegetation above timberline in the northern and central Apennines. *Fitosociologia*, *26*, 5-17.

Pintaldi, E., Viglietti, D., D'Amico, M. E., Magnani, A., & Freppaz, M. (2019). Abiotic parameters and pedogenesis as controlling factors for soil C and N cycling along an elevational gradient in a subalpine Larch forest (NW Italy). *Forests*, *10*(8), 614.

Prietzel, J., & Christophel, D. (2014). Organic carbon stocks in forest soils of the German Alps. *Geoderma*, *221*, 28-39.

Ramos, F. T., Dores, E. F. D. C., Weber, O. L. D. S., Beber, D. C., Campelo Jr, J. H., & Maia, J. C. D. S. (2018). Soil organic matter doubles the cation exchange capacity of tropical soil under no-till farming in Brazil. *Journal of the Science of Food and Agriculture*, *98*(9), 3595-3602.

Romeo, R., Vita, A., Manuelli, S., Zanini, E., Freppaz, M., & Stanchi, S. (2015). Understanding Mountain Soils: A contribution from mountain areas to the International Year of Soils 2015. The Food and Agriculture Organization (FAO): Rome, Italy, 2015; pp. 1–169. ISBN 978-92-5-108804-3

Rowley, M. C., Grand, S., & Verrecchia, É. P. (2018). Calcium-mediated stabilisation of soil organic carbon. *Biogeochemistry*, *137*(1), 27-49.

Rstudio Team Rstudio (2022). Integrated Development Environment for R 2021. Available online: https://www.rstudio.com/products/rstudio/ (accessed on 18 October 2022).

Sarker, T. C., Incerti, G., Spaccini, R., Piccolo, A., Mazzoleni, S., & Bonanomi, G. (2018). Linking organic matter chemistry with soil aggregate stability: Insight from 13C NMR spectroscopy. *Soil Biology and Biochemistry*, *117*, 175-184.

Schneider, F. D., Brose, U., Rall, B. C., & Guill, C. (2016). Animal diversity and ecosystem functioning in dynamic food webs. *Nature Communications*, *7*(1), 12718.

Schweizer, S. A., Bucka, F. B., Graf-Rosenfellner, M., & Kögel-Knabner, I. (2019). Soil microaggregate size composition and organic matter distribution as affected by clay content. *Geoderma*, *355*, 113901.

Sithole, N. J., Magwaza, L. S., & Thibaud, G. R. (2019). Long-term impact of no-till conservation agriculture and N-fertilizer on soil aggregate stability, infiltration and distribution of C in different size fractions. *Soil and Tillage Research*, *190*, 147-156.

Slaymaker, O., Spencer, T., & Embleton-Hamann, C. (Eds.). (2009). *Geomorphology and global environmental change*. Cambridge University Press.

Soil Survey Laboratory Staff (2004). Soil survey laboratory methods manual. In *Soil Survey Investigations Report*; USDA-SCS: Washington, DC, USA; Volume 42, p. 700.

Soil Survey Staff (2014). Keys to soil taxonomy, 12th ed. *United States Department of Agriculture: Washington, DC, USA*.

Sokołowska, J., Józefowska, A., Woźnica, K., & Zaleski, T. (2019). Interrelationship between soil depth and soil properties of Pieniny National Park forest (Poland). *Journal of Mountain Science*, *16*(7), 1534-1545.

Sorokin, A., Owens, P., Láng, V., Jiang, Z. D., Michéli, E., & Krasilnikov, P. (2021). "Black soils" in the Russian Soil Classification system, the US Soil Taxonomy and the WRB: Quantitative correlation and implications for pedodiversity assessment. *Catena*, *196*, 104824.

Spohn, M., & Chodak, M. (2015). Microbial respiration per unit biomass increases with carbon-to-nutrient ratios in forest soils. *Soil Biology and Biochemistry*, *81*, 128-133.

Szewczyk, A., Kaniuczak, J., Hajduk, E., & Knap, R. (2015). Physical and chemical properties of selected soils from the surroundings of the Magura National Park (southern Poland). *Soil Science Annual*, *66*(1), 36-44.

Tashi, S., Singh, B., Keitel, C., & Adams, M. (2016). Soil carbon and nitrogen stocks in forests along an altitudinal gradient in the eastern Himalayas and a meta-analysis of global data. *Global change biology*, *22*(6), 2255-2268.

Tewksbury, C. E., & Van Miegroet, H. (2007). Soil organic carbon dynamics along a climatic gradient in a southern Appalachian spruce–fir forest. *Canadian journal of forest research*, *37*(7), 1161-1172.

Tomaselli, M., Carbognani, M., Foggi, B., Petraglia, A., Rossi, G., Lombardi, L., & Gennai, M. (2019). The primary grasslands of the northern Apennine summits (N-Italy): a phytosociological and ecological survey. *Tuexenia*, *39*.

Tomaselli, M., Del Prete, C., & Manzini, M. L. (1996). Parco regionale dell'Alto Appennino modenese: L'ambiente vegetale. Regione Emilia-Romagna: Bologna, Italy.

Toomanian, N., Jalalian, A., Khademi, H., Eghbal, M. K., & Papritz, A. (2006). Pedodiversity and pedogenesis in Zayandeh-rud Valley, central Iran. *Geomorphology*, *81*(3-4), 376-393.

Ungaro, F., Staffilani, F., & Tarocco, P. (2010). Assessing and mapping topsoil organic carbon stock at regional scale: a scorpan kriging approach conditional on soil map delineations and land use. *Land Degradation & Development*, *21*(6), 565-581.

van de Kamp, P. C., & Leake, B. E. (1995). Petrology and geochemistry of siliciclastic rocks of mixed feldspathic and ophiolitic provenance in the Northern Apennines, Italy. *Chemical Geology*, *122*(1-4), 1-20.

Van Wambeke, A., Hastings, P., & Tolomeo, M. (1986). Newhall Simulation Model: A BASIC Program for the IBM PC. *Dept. of Agronomy, Cornell University, Ithaca, NY.*

Vittori Antisari, L., Agnelli, A., Corti, G., Falsone, G., Ferronato, C., Marinari, S., & Vianello, G. (2018). Modern and ancient pedogenesis as revealed by Holocene fire-Northern Apennines, Italy. *Quaternary International*, *467*, 264-276.

Vittori Antisari, L., Dell'Abate, M. T., Buscaroli, A., Gherardi, M., Nisini, L., & Vianello, G. (2010). Role of soil organic matter characteristics in a pedological survey:"Bosco Frattona" natural reserve (Site of Community Importance, Italy) case study. *Geoderma*, *156*(3-4), 302-315.

Vittori Antisari, L., Falsone, G., Carbone, S., & Vianello, G. (2013). Short-term effects of forest recovery on soil carbon and nutrient availability in an experimental chestnut stand. *Biology and Fertility of Soils*, *49*(2), 165-173.

Vittori Antisari, L., Falsone, G., Carbone, S., Marinari, S., & Vianello, G. (2015). Douglas-fir reforestation in North Apennine (Italy): Performance on soil carbon sequestration, nutrients stock and microbial activity. *Applied Soil Ecology*, *86*, 82-90.

Vittori Antisari, L., Marinari, S., Dell'Abate, M. T., Baffi, C., & Vianello, G. (2011). Plant cover and epipedon SOM stability as factors affecting brown soil profile development and microbial activity. *Geoderma*, *161*(3-4), 212-224.

Vittori Antisari, L., Trenti, W., De Feudis, M., Bianchini, G., & Falsone, G. (2021). Soil quality and organic matter pools in a temperate climate (Northern Italy) under different land uses. *Agronomy*, *11*(9), 1815.

Vittori Antisari, L., Vianello, G., Pontalti, F., Lorito, S., & Gherardi, M. (2008). Land use effects on organic matter in brown soils of the emilian apennines. In *The Soils of Tomorrow: Soils Changing in a Changing World*; CAB International: Wallingford, UK; pp. 311–328.

Voltr, V., Menšík, L., Hlisnikovský, L., Hruška, M., Pokorný, E., & Pospíšilová, L. (2021). The soil organic matter in connection with soil properties and soil inputs. *Agronomy*, *11*(4), 779.

Wang, L., Chen, Y., Zhou, Y., Zheng, H., Xu, Z., Tan, B., ... & Liu, Y. (2021). Litter chemical traits strongly drove the carbon fractions loss during decomposition across an alpine treeline ecotone. *Science of the Total Environment*, *753*, 142287.

Weissert, L. F., Salmond, J. A., & Schwendenmann, L. (2016). Variability of soil organic carbon stocks and soil CO2 efflux across urban land use and soil cover types. *Geoderma*, *271*, 80-90.

Wiesmeier, M., Urbanski, L., Hobley, E., Lang, B., von Lützow, M., Marin-Spiotta, E., ... & Kögel-Knabner, I. (2019). Soil organic carbon storage as a key function of soils-A review of drivers and indicators at various scales. *Geoderma*, *333*, 149-162.

Yimer, F., Ledin, S., & Abdelkadir, A. (2006). Soil organic carbon and total nitrogen stocks as affected by topographic aspect and vegetation in the Bale Mountains, Ethiopia. *Geoderma*, *135*, 335-344.

Zanella, A., Ponge, J. F., Jabiol, B., Sartori, G., Kolb, E., Gobat, J. M., ... & Viola, F. (2018). Humusica 1, article 4: Terrestrial humus systems and forms—Specific terms and diagnostic horizons. *Applied Soil Ecology*, *122*, 56-74.

6. GIS-BASED GEOPEDOLOGICAL APPROACH FOR ASSESSING LAND SUITABILITY FOR CHESTNUT (CASTANEA SATIVA MILL.) GROVES FOR FRUIT PRODUCTION

Published in *Forests* **2023**, *14*(2), 224; **https://doi.org/10.3390/f14020224**

Marco Rossi [1], Mauro De Feudis [1*], William Trenti [1], Massimo Gherardi [2], Gilmo Vianello [3] and Livia Vittori Antisari [1]

[1] Department of Agricultural and Food Sciences, Alma Mater Studiorum-University of Bologna, Viale Fanin 40, Bologna, Italy
[2] Boreal Mapping, Via Casella, 23/a, 40030 Grizzana Morandi, Italy
[3] Accademia Nazionale di Agricoltura, Via Castiglione 11, 40124 Bologna, Italy
[*]correspondence: mauro.defeudis2@unibo.it

ABSTRACT

The identification of mountainous areas suitable for chestnut stands for fruit production (CSFP) is raising increasing interest among researchers. This work aimed to (*i*) identify the areas suitable for CSFP shown in a land suitability map easy to read by land planners, and (*ii*) propose a remote-sensing-based methodology able to identify the lands currently under cultivation for CSFP. This study was conducted using the QGIS software for the Municipality of Castel del Rio, Emilia-Romagna Region, Italy. To obtain the land suitability map, topographic, lithological, and pedological data were acquired, and the areas located between 200 and 1000 m of altitude, with north exposition, a slope < 20°, sandstone-based lithology, and soils with dystric features were selected. The currently cultivated areas for CSFP were identified through remote-sensing images of the early spring period, which were delineated and georeferenced. The findings showed that only 10% of the whole study site area can be considered suitable for CSFP. Further, most of the currently cultivated CSFP (59%) are in non-suitable areas characterised by high slope gradients. The methodology applied in this study can easily provide detailed information about the suitable areas for CSFP and the areas currently cultivated with chestnut, thus allowing accurate land-use planning and land conservation.

6.1 INTRODUCTION

Sweet chestnut (Castanea sativa Mill.) is one of the most widespread deciduous tree species in Europe (Conedera et al., 2016). Such large distribution was attributed to the multipurpose of chestnut stands because they can be used for firewood, timber, and food production for both human and animal feeding (Conedera & Krebs, 2007; Conedera et al., 2004b). In Italy, chestnut stands cover about 800,000 ha (Tamantini et al., 2022), 34,273 ha of which is designated for fruit production (ISTAT, 2020). Sweet chestnut has significantly influenced the development of Italian mountainous areas, establishing the so-called “civilisation of the chestnut tree” (Conedera et al., 2004a). However, after World War II, rural depopulation due to changing social needs (Zlatanov et al., 2013), the spread of the chestnut blight (Chryphonectria parasitica (Murr.) Barr) and ink (Phytophthora cambivora (Petri) Buism.) diseases (Pezzi et al., 2011) and the introduction of the Asian Chestnut Gall Wasp (Dryocosmus kuriphilus Yasumatsu) promoted chestnut stand abandonment (Conedera et al., 2021).

Due to the increased worldwide demand for chestnut nuts in the last decade (FAOSTAT, 2022), linked to their nutritional characteristics (Massantini et al., 2021) and the increasing interest in chestnut wood (Nocetti et al., 2016), both the planting of new chestnut stands and the recovery of suitable abandoned chestnut areas is advisable. In this context, land evaluation for identifying the areas suitable for chestnut stands is essential to prevent the loss of ecosystem services and to ensure high chestnut yield. Therefore, land evaluations that include knowledge of soils, lithology, and morphological features have been recognised as an important requirement in the agricultural planning process (Siqueira et al., 2010; Vasu et al., 2018; Ray et al., 2021) because they ensure both long-term primary production and the optimum and sustainable utilisation of the available land resources (AbdelRahman et al., 2016; Özşahin & Ozdes, 2022).

The development of a land evaluation model is prioritised for those plant species growing in mountainous areas, such as chestnut, mainly due to the high degradation vulnerability of these areas (Alewell et al., 2008). In fact, mountain soils are generally defined as poorly developed, skeletal, shallow, acidic, and relatively infertile (FAO, 2015). Hence, knowing the potential of a mountainous area to sustain plant growth and productivity through the evaluation of their pedoclimatic and morphological characteristics could be considered of pivotal importance for the recovery of mountain agricultural activities (Bruzzese et al., 2020).

Going back for generations, the evaluation of the inherent characteristics of the land has always involved farmers in developing land-use systems that would be well adapted to the potentials and constraints of their land. Land planning needs tools able to elaborate the information gathered from remote-sensing data with enhanced spatial and temporal resolutions, using instruments capable of processing multiple pieces of information, to avoid subjective errors. Progress in geographical information system (GIS) technologies allows for the processing of a large number of spatial data and the provision of more accurate and accessible information about the land (Arnous & Hassan, 2006). GIS can perform numerous tasks using both spatial and attribute data. One of the most useful features of GIS is the ability to overlay different layers or maps that are relevant to the same spatial area (De Feudis et al., 2021). In addition, the use of GIS allows for the development of models from which a new thematic map (e.g., land suitability map) can be formed from a set of thematic maps (De Feudis et al., 2021). Therefore, GIS is a powerful tool in spatial decision-making processes for sustainable development in rural areas (Kurowska et al., 2020). In addition, GIS is an effective software for census land uses in both field-scale and remote-sensing approaches (Mikoláš et al., 2019; Atay Kaya, 2020), which could help to reduce the poor accuracy and limited updating of cadastral data concerning land use (Cienciała et al., 2021).

Besides powerful tools such as GIS, land evaluation processes require scientific procedures for an objective assessment of the potential and constraints of a given land for agricultural purposes (Lauteri et al., 2009). A scientific system able to provide information about the appropriateness of land to sustain plant growth was developed by the Food and Agriculture Organization (FAO)

(Brinkman & Young, 1976). Specifically, the FAO developed the term "land suitability", which estimates the fitness of soil and its landscape for the production of a specific agricultural crop (Brinkman & Young, 1976). Land suitability assessment and classification are based on the required inputs, such as labour, fertilisers, or irrigation, necessary for specified cultures.

Over time, land evaluation methods have become more sophisticated (Sonneveld et al., 2010), and with the enhanced availability of large georeferenced datasets and GIS technologies, evaluations have become more accurate and oriented toward specific vegetation types (Triantafilis et al., 2001; Joss et al., 2008; Elsheikh et al., 2013).

To further support land evaluation processes, remote sensing was largely used by several researchers (Aymen et al., 2021; Yalew et a., 2016; Saleh et al., 2015; Tercan & Dereli, 2020). These authors used the remote-sensing methodology to acquire information about the topography, land use, and the presence of waterbodies and buildings. In terms of land use, several investigations used GlobCover2009 (Yalew et a., 2016), Landsat (Tercan & Dereli, 2020), and Corine Land Cover (Tercan & Dereli, 2020), but evaluations of their images did not include the classification of chestnuts.

In the context of the restoration of CSFP in the Apennine Mountain Range in Italy and using advanced GIS-based tools and processes, the main aims of the present work were to develop a method able to a) identify the areas, from a geomorphological and pedological point of view, that can potentially allow for CSFP cultivation; b) provide maps that can be updated with further details and are easy to read by land planners, showing the areas suitable for CSFP; and c) propose a remote-sensing-based methodology able to identify the lands currently under cultivation for CSFP.

6.2 MATERIALS AND METHODS

6.2.1 Study area framing

The study area chosen matches the Municipality of Castel del Rio (Barycentric coordinates 44°12′50″ N 11°30′15″ E), located in the Emilia-Romagna Region, in the hilly mountainous areas of the northern part of the Apennine Mountain Range in Italy (**Figure 1**).

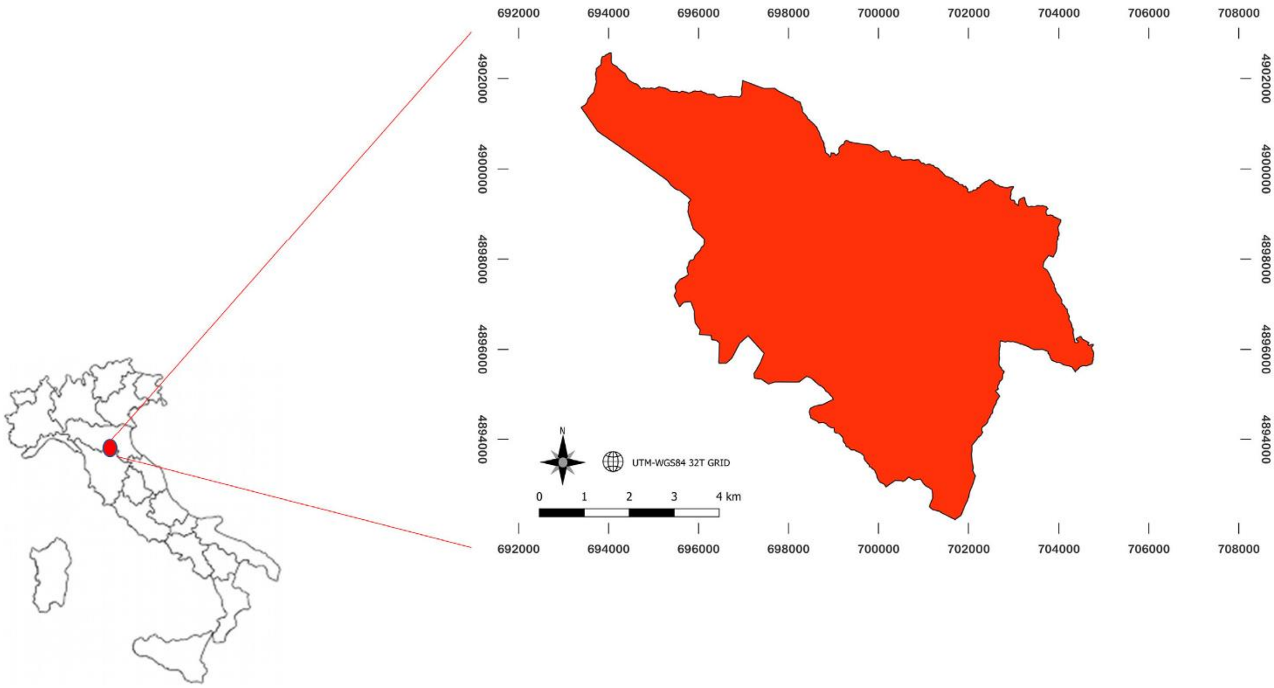

Figure 1. Study area: the Municipality of Castel del Rio, located in the Emilia-Romagna Region, Italy.

Fruit chestnut groves have been historically present in Castel del Rio as in almost all the mountainous areas of the Apennines. The Municipality of Castel del Rio did not undergo a serious abandonment of chestnut groves after World War II because of the creation of a protected geographical designation entitled "Marrone di Castel del Rio", which helps farmers to market their products better.

The study site is about 52.5 km^2 wide and has an average altitude of 476 m above sea level, ranging between 151 and 959 m above sea level (asl), and it is characterised by a warm temperate climate, with an average annual rainfall of about 1060 mm and an average temperature of about 13.7 °C; the hottest month is July with an average temperature of about 24.4 °C (Antolini et al., 2015).

6.2.2 Indicators for the Assessment of Land Suitability for Chestnut Groves for Fruit Production

The land suitability of CSFP in the study area was investigated by considering altitude, exposure, slope gradient, lithology, and soil types. The data about altitude, exposure, and slope gradient were acquired from a digital terrain model (DTM), which is a topographic model of the bare Earth that can be manipulated with computer programs for further processing (i.e., altitude, exposure, and slope gradient). In the present study, the DTM was downloaded from the cartographic services of the Emilia-Romagna Region (Regione Emilia-Romagna, 2009), with a 5 × 5 m resolution. The geolithological map, with a scale of 1:10,000, was freely downloaded from the geological surveys of the Emilia-Romagna Region (Regione Emilia-Romagna, 2006). Given the geological complexity of the study area, geolithological formations were grouped according to their characteristics, in particular alluvial deposits, sandstones, marls, and clay formations (Figure 2a).

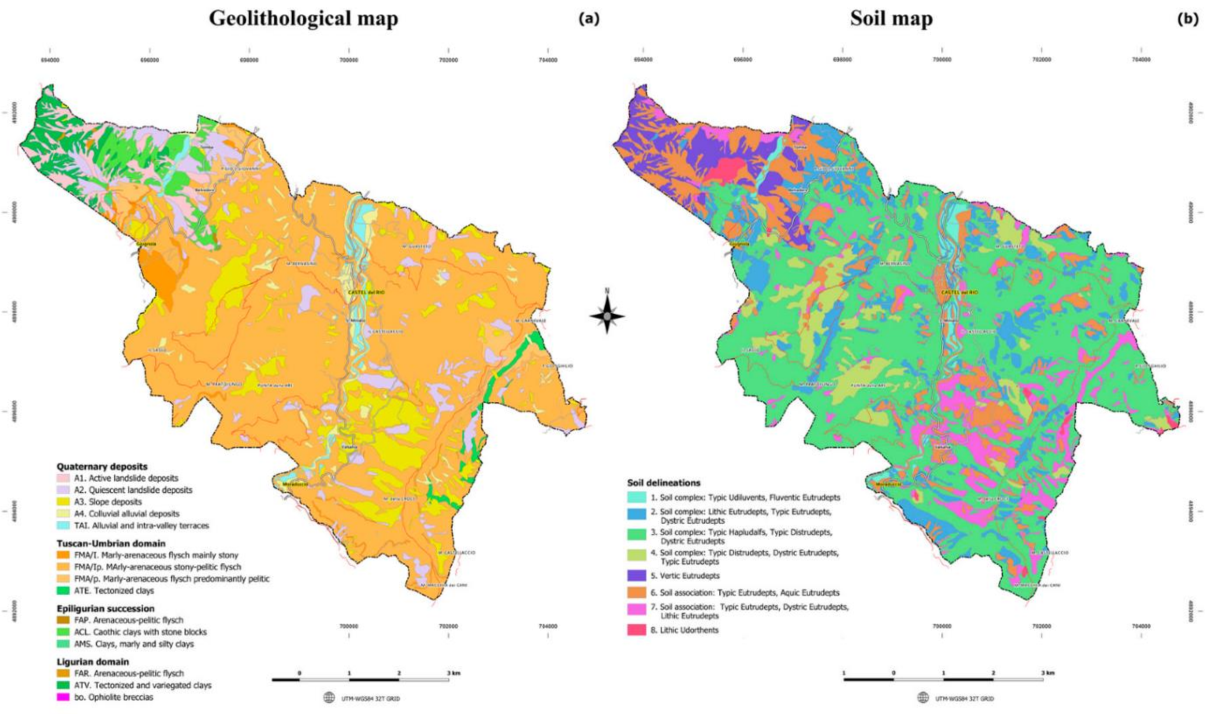

Figure 2. Geolithological (a) and soil (b) maps of Castel del Rio, Emilia-Romagna Region, Italy.

A land unit map (Figure 2b) was built by crossing different soil-forming factors (i.e., altitude, slope, geology, and land use). Each land unit included specific soil types according to these soil-forming factors (Table 1).

Table 1. Soil types, according to Soil Survey Staff (2014), of the land units identified within Castel del Rio, Emilia-Romagna Region, Italy.

Land Units	Area (ha)	Soil Types
1. Recent sandy–gravelly alluvial deposits of river terraces. Land use characterised by arable land and orchards in flat areas and bushes, or with riparian woods in steep areas.	84	Typic Udiluvents with A–C horizons and moderately deep Fluventic Eutrudepts with A–Bw–C horizon sequence
2. Sandstone–pelitic formation affected by sheet erosion. Land use characterised by arable land or uncultivated bushland.	699	Thin or moderately deep Lithic Eutrudepts and Typic Eutrudepts with A–Bw–C horizons, Dystric Eutrudepts with A–B–C horizon sequence
3. Sandstone–pelitic formation with the prevalence of the sandstone component. Land use characterised by forest cover.	2618	Typic Hapludalfs with A–Bt–C horizons, Typic Dystrudepts and Dystric Eutrudepts with A–Bw–C horizon sequence
4. Sandstone formations and sometimes on-slope debris. Land use characterised by chestnut cover.	364	Typic Dystrudepts with A–Bw–C horizon sequence, Dystric Dystrudepts, and rarely Typic Eutrudepts
5. Clayey formations affected by erosion and cracks during the summer. Land use characterised by meadow–pasture or arable land.	245	Shallow to moderately deep Vertic Eutrudepts with A–Bw–C horizon sequence
6. Areas affected by existing or dormant instability with sheet and channelled erosion phenomena. Land use characterised by grass or bush cover.	725	Moderately deep Typic Eutrudepts with A–Bw–C horizons sometimes affected by waterlogging (Aquic Eutrudepts)
7. Areas affected by hydrogeological instability. Land use characterised by forest cover.	470	Typic Eutrudepts and Dystric Eutrudepts with A–Bw–C horizons, moderately deep, or more rarely shallow Lithic Udorthents with A–C horizon sequence
8. Areas characterised mostly by outcrops of clayey rocks, affected by strong erosion with the formation of gullies morphologies. Land use characterised by uncultivated lands or shrublands.	45	Shallow Lithic Udothents with A–C horizon sequence

To build the suitability map for CSFP, the areas were considered suitable if located within the Castanetum phytoclimatic zone (De Philippis, 1951), namely at an altitude ranging between 300 and 1000 m above sea level (Del Favero, 2002; Arcidiaco et al., 2006; Lolli & Musolesi, 2006;

Bounous, 2004) with north-facing exposition, from northwest to northeast (Lolli & Musolesi, 2006; Bounous, 2004) (Table 2). In this context, it is important to mention that the considered thresholds for altitude and exposure can be used for the northern part of the Apennine Mountain Range in Italy because of having the best climatic (air temperature and rainfalls) conditions for chestnut plants (Bounous, 2004). Regarding the slope gradient, it was considered suitable if it was less than 20°, allowing for the easy management of groves, including chestnut nut harvesting (Comel, 1975) and preventing intense soil erosion processes (Diaz et al., 2018). In terms of lithology, carbonate-free rocks as soil parent material (i.e., rhyolite, trachyte, pyroclastic deposits, siliceous rocks, sandstones, and greenschists) were considered. Such lithologies were selected on the basis of the most frequent lithological types found under chestnut grove cultivation in Italy (Mariotti et al., 2019) (Table A1 of Appendix A).

Table 2. Restriction rates for *Castanea sativa* Mill. cultivation for fruit production related to altitude, exposure, slope gradient, and lithology.

Characters		Absent	Slight	Moderate	Severe
Altitude (a)		300–1000 m asl	150–300 m asl	1000–1200 m asl or 50–150 m asl	>1200 m asl or <50 m asl
Exposure (b)		NE-NW	E-W	SW-SE	S
Slope gradient (c)		<20°	20–30°	30–35°	>35°
Lithology (d)	Igneous rocks	Rhyolite Trachyte	Diorite Volcanic tuffs	Gabbro Andesite	Granite Basalt
	Sedimentary rocks	Pyroclastic deposits Siliceous sandstones	Conglomerates Arenites Sandstones	Dolomitic limestones Calcarenites	Marls Marly clays Clays
	Metamorphic rocks	Greenschists	Schists	Marbles	Quartzite

asl = above sea level; (a) Del Favero, 2002; Arcidiaco et al., 2006; Lolli & Musolesi, 2006; Bounous, 2004 (b) Lolli & Musolesi, 2006; Bounous, 2004; (c) Comel, 1975; (d) Table A1.

From a pedological point of view, because of the preference for well-drained soils and soils with acidic conditions and a limited number of fine soil particles (Rodrigues et al., 2021; Nicoletti et al., 2021), the soil types considered suitable for CSFP were those included within the land units 2, 3, and 4, which developed on dystric facies carbonate-free (Figure 2b). In this sense, to check the reliability of the land units, within each suitable land unit, one soil profile was dug under CSFP and described according to Schoeneberger et al. (Schoeneberger et al., 2012). The soil samples collected from the identified soil horizons were analysed in terms of pH, which was potentiometrically determined in a 1:2.5 solution ratio in deionised water. The particle size distribution was estimated using the pipette method (Klute, 1986). The concentration of carbonate was estimated through the volumetric analysis of the CO_2 released by the contact of soil with a 6 M HCl solution (Loeppert & Suarex, 1996). Soil organic C (SOC) and soil nitrogen (SN) were determined using a CHN elemental analyser (Flash 2000, Thermo Fisher Scientific, Waltham, MA, USA). The cation exchange capacity (CEC) and the exchangeable cation contents were determined according to the method proposed by Orsini and Rémy (Orsini & Remy, 1976) and modified by Ciesielski and Sterckeman (Ciesielski & Sterckeman, 1997). Specifically, soil samples were suspended in 0.017 M hexamminecobalt (III) chloride solution. The amounts of the extracted Co and exchangeable cations were measured using an inductively coupled plasma optical emission spectrometer (Ametek, Spectro Arcos, Kleve, Germany). Afterwards, the soils were classified according to the keys of soil taxonomy of the Soil Survey Staff (2014).

Once we defined the suitable topographic, altitudinal, lithological, and pedological conditions for CSFP, the suitability map was built by overlapping such suitable areas using the QGIS 3.26.3 software (Figure 3). The reliability of this procedure is supported by previous studies (De Feudis et al., 2021; Tercan & Dereli, 2020; Chen et al., 2022; Zheng et al., 2021), which used several environmental data to evaluate the land suitability for certain crops in both agricultural and natural ecosystems. Within this process, a land-use map (Regione Emilia-Romagna, 2020) was also included to exclude waterbodies and urban areas. The use of the open-source QGIS software was based on the fact that it allows users to analyse and edit spatial information, in addition to composing and exporting georeferenced maps (De Feudis et al., 2021). QGIS supports both raster and vector layers; vector data are stored as point, line, or polygon features, and in addition, multiple formats of raster images are supported (De Feudis et al., 2021).

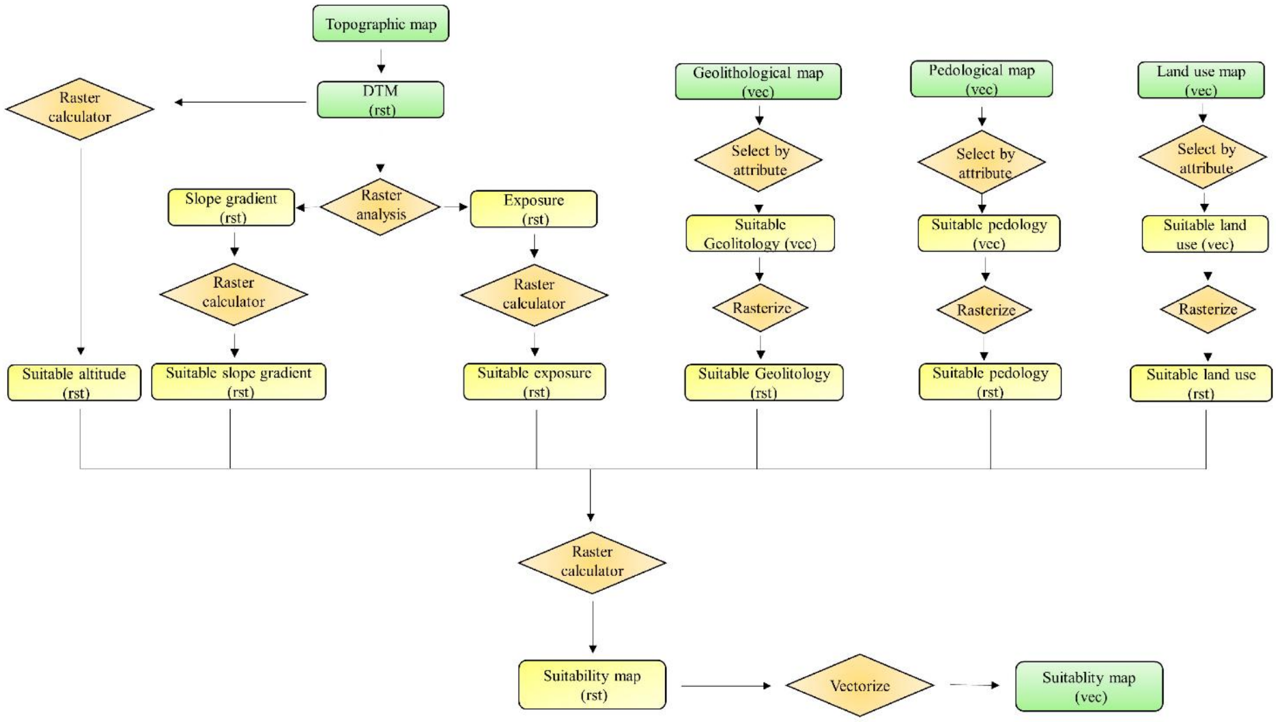

Figure 3. Flowchart of GIS-based processing for suitability map building. Between brackets, rst and vec indicate raster and vector file types, respectively.

6.2.3 GIS-Based Approach for the Identification of Areas Currently under Chestnut Grove Cultivation for Fruit Production

To identify the chestnut stands within the study site, Google Earth Pro remote-sensing images from April 2020 were collected. We used remote-sensing images in early spring because of the late vegetation restart growth of chestnut plants compared with the other forest plants that generally harbour within the areas where the chestnut plants grow. Conversely, images from the summer, autumn, and winter seasons cannot allow the identification of chestnut groves because of the similar vegetation stage among forest plants. Therefore, within the acquired remote-sensing images from Google Earth Pro, CSFP were easily identified because of both the late vegetation regrowth and the quincunx plantation pattern. The identified areas were delimited, and their extension was measured.

To evaluate the reliability of this approach, the obtained data from remote-sensing images were compared with the data from the 2017 land-use map of the Emilia-Romagna Region (Regione Emilia-Romagna, 2020). Further, the chestnut grove areas identified using remote-sensing images were compared with the suitability map. Both comparisons were performed using QGIS software.

6.3 RESULTS

The analysis of the altitude showed that most of the study site (87.3%) can be considered suitable for the growth of CSFP, while unsuitable parts include the areas mainly located close to the Santerno river (Figure 4a). Regarding the exposure, the suitable area was 1968.8 ha, which amounted to 37.7% of the study site (Figure 4b). The mean slope was 22.6°, ranging from 0.05° to 58.4°, and the area showing the most suitable slope for CSFP represented 43.9% of the whole study area (Figure 4c).

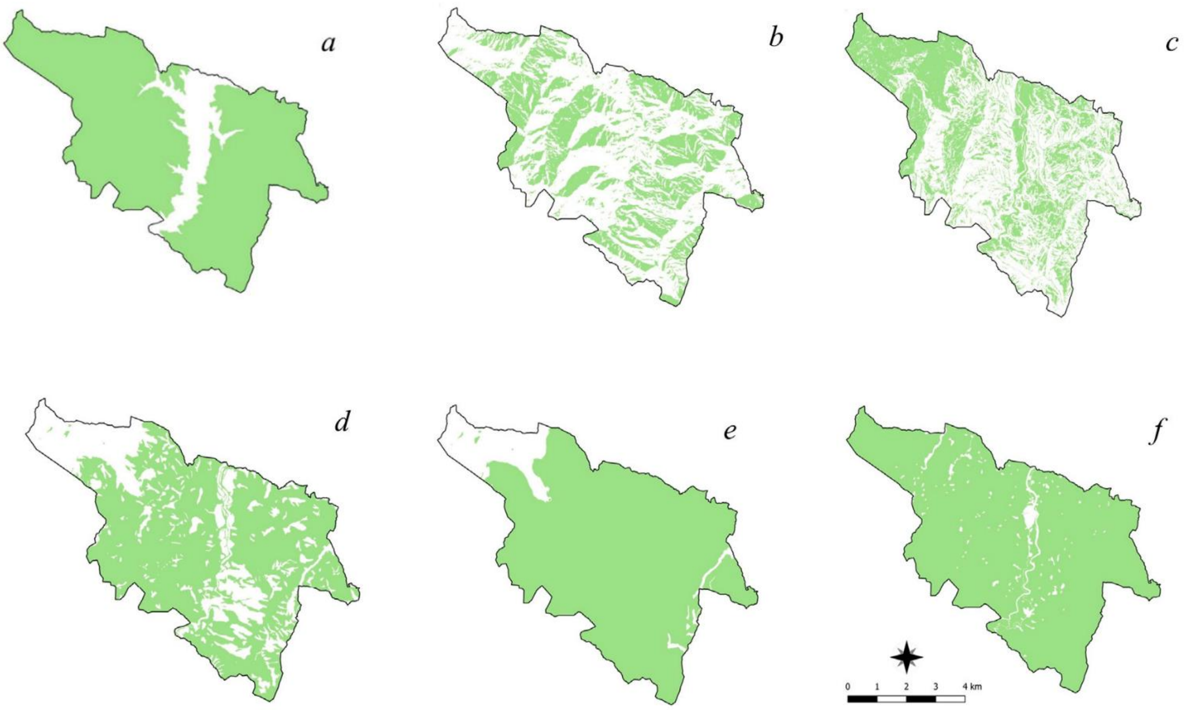

Figure 4. Suitable areas (green colour) in terms of altitude (a), exposure (b), slope gradient (c), soil type (d), geolithology (e), and land use (f) for the cultivation of chestnut stands for fruit production in Castel del Rio, Emilia-Romagna Region, Italy.

Through the analysis of the geolithology, it was revealed that the study site was mainly characterised by silicious sandstone formations (88.5%) and, to a lesser extent, clay formations (11.5%). The geolithological type defined as “silicious sandstone” formation, considered suitable for chestnut groves, was 4644 ha (Figure 4e).

The pedological map showed that the suitable area for CSFP accounted for 3681 ha, corresponding to 70.1% of the study site (Figure 4d). Generally, soils of such areas have pH values < 7 because of the absence of carbonates; however, subalkaline conditions can be also found due to the high base concentrations with positive effects on base saturation values.

The soil profiles dug within the land units confirmed the soil types reported within the pedological map (Table 3). Indeed, Alfic Dystrudepts, Typic Dystrudepts, and Dystric Eutrudepts were found. The described soils had a coarse texture with consequent low values of SOC content and CEC. The soils showed pH values of less than 7 with the exception of the soils in land unit 2, where some calcic horizons were observed, and the amount of exchangeable Ca was higher than the other land units. Most of the soils had a BS larger than 50%, and lower values were found in soils with lower pH values.

Table 3. Main morphological, physical, and chemical features of soil profiles dug within the land units 2, 3, and 4 of Castel del Rio, Emilia-Romagna Region, Italy.

Land Unit and Soil Type	Horizon	Depth (cm)	pH	$CaCO_3$	Sand	Silt	Clay	CEC	Ca_{ex}	Mg_{ex}	K_{ex}	Na_{ex}	BS	SOC	SN
				g kg⁻¹	g kg⁻¹			cmol(+) kg⁻¹					%	%	%
Land unit 2	A1	0–5	7.6	29.3	330	535	135	22.6	11.6	0.1	1.5	0.2	59.0	4.9	0.3
Typic	A2	5–16	7.5	70.0	346	517	137	20.0	9.2	0.1	1.0	0.2	52.5	2.2	0.2
Eutrudepts	Bw	16–28	7.5	100.1	256	483	261	15.0	7.8	0.1	0.8	0.1	58.5	1.3	0.1
	2Bw	28–41	7.6	0	168	530	302	27.3	12.4	0.1	1.3	0.1	51.0	0.7	0.1
	2BC	41–60+	7.5	0	89	527	384	32.6	14.3	0.1	1.8	0.1	49.7	0.5	0.1
Land unit 3	Oe	0–0.5	4.9		----	----	----	21.1	7.1	3.4	0.7	0.2	53.6	22.7	1.1
Alfic	A1	0.5–4	4.8	0	387	403	210	7.3	0.8	0.7	0.2	0.1	24.5	4.5	0.2
Dystrudepts	A2	4–7/9	4.5	0	363	427	210	9.5	1.0	0.7	0.2	0.1	20.4	5.6	0.2
	AB	7/9–14	5.0	0	366	403	231	8.4	0.9	0.2	0.0	0.0	22.4	1.6	0.1

Land Unit and Soil Type	Horizon	Depth (cm)	pH	$CaCO_3$ g kg⁻¹	Sand	Silt	Clay	CEC	Ca_{ex}	Mg_{ex}	K_{ex}	Na_{ex}	BS %	SOC %	SN %
					g kg⁻¹			cmol(+) kg⁻¹							
	Bt	14–20	4.9	0	336	398	266	7.4	0.3	0.3	0.0	0.1	8.3	1.1	0.1
	BC1	20–35	5.4	0	355	461	184	8.5	0.4	0.6	0.0	0.1	12.0	0.8	0.1
	BC2	35–46	4.9	0	362	432	206	8.9	0.4	0.8	0.0	0.1	14.7	1.1	0.1
	C	46–60+	5.6	0	450	392	158	6.5	0.5	0.9	0.0	0.1	22.9	0.2	0.0
Land unit 4	A1	0–3	6.9	0	350	454	196	20.3	8.3	1.4	0.3	0.1	49.8	5.3	0.3
Dystric	A2	3–10	7.2	0	328	490	182	14.7	6.4	1.0	0.1	0.1	52.1	2.4	0.2
Eutrudepts	AB	10–23	6.9	0	327	487	186	9.3	5.1	0.9	0.1	0.1	67.0	1.2	0.1
	Bw1	23–38	6.9	0	266	495	239	9.7	4.6	1.0	0.0	0.1	58.4	0.6	0.0
	Bw2	38–50	6.9	0	264	441	295	9.3	4.1	1.0	0.0	0.1	57.0	0.6	0.0
	BC	50–60+	6.8	0	306	439	255	8.9	3.5	1.1	0.0	0.1	52.4	0.4	0.0

CEC = cation exchange capacity; Ca_{ex}, Mg_{ex}, K_{ex}, and Na_{ex} = exchangeable Ca, Mg, K, and Na, respectively; BS = base saturation; SOC = soil organic carbon; SN = soil total nitrogen.

Through the overlapping of the land use with the areas suitable from topographical, geolithological, and pedological points of view, the suitable area for CSFP within the study site was 525.5 ha, accounting for 10% of the whole study site area (Figure 5). Most of the suitable area was observed in the northeastern part of the study site and at the northwestern exposition of the mountainous area located between the Sillaro and Santerno rivers.

The analysis of land use and georeferenced remote-sensing images showed that the CSFP currently cultivated within the study site spread for 379 and 414 ha, respectively, mainly located in the mountainous area between the Sillaro and Santerno rivers. Considering the CSFP area identified using remote-sensing images, it was mostly (98%) within the CSFP area defined by land use, while the additional areas were mainly observed in the western and eastern parts of the study site (Figure 6).

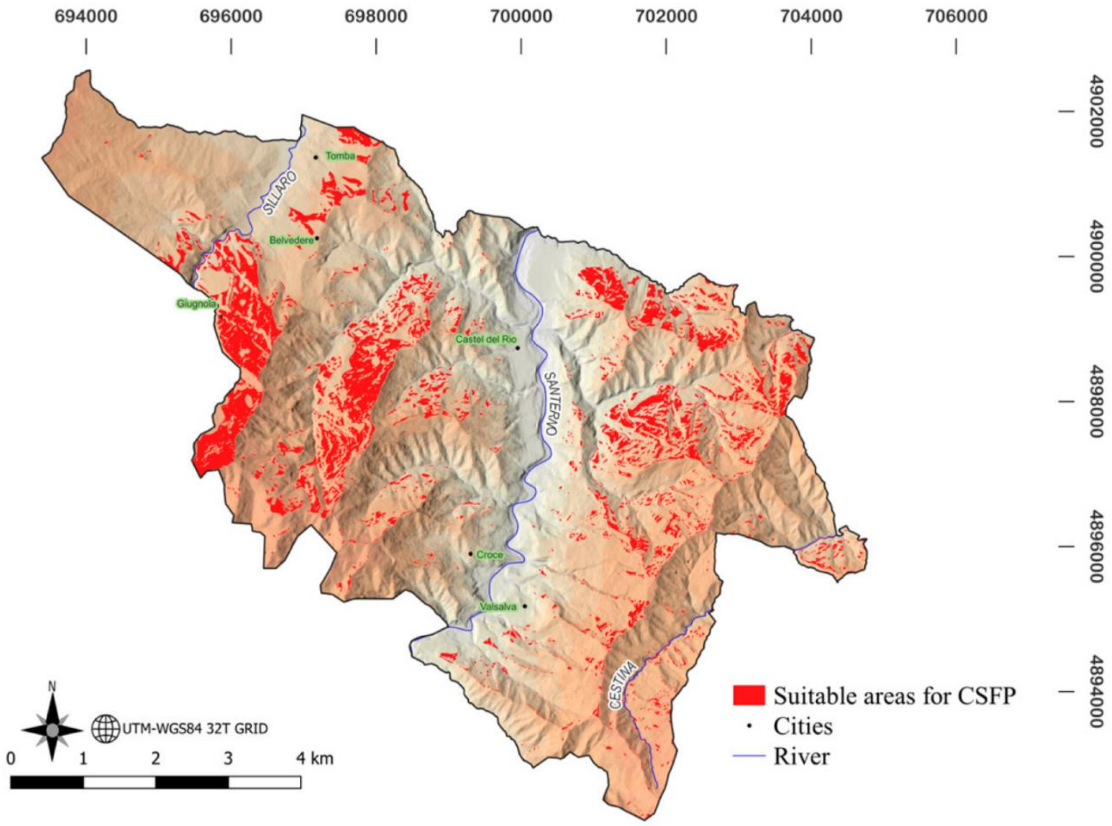

Figure 5. Suitability map for chestnut stands for fruit production (CSFP) for Castel del Rio,

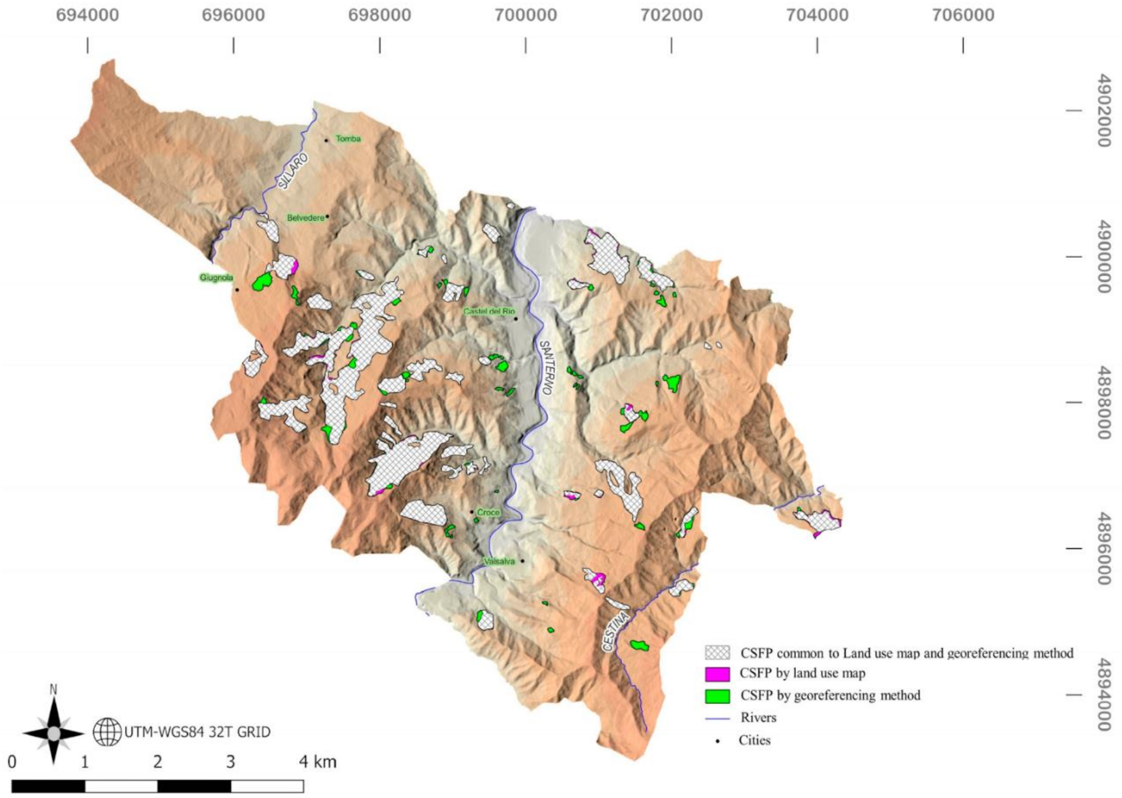

Emilia-Romagna Region, Italy.

Figure 6. Map of Castel del Rio, Emilia-Romagna Region (Italy), showing the areas for chestnut stands for fruit production (CSFP) identified only with the land-use map (purple area), only with the georeferencing approach (green area), and with both methodologies (squared area).

It is important to note that the CSFP area acquired through remote-sensing images highly matched that acquired through the land-use map, which suggests the high accuracy of such methodology (Figure 6). In addition, with the remote-sensing imaging methodology, it was found that the mean area of the CSFP was about 5.8 ha.

The overlapping between the currently CSFP cultivated areas identified with remote sensing and the CSFP suitable map revealed that 59% of currently cultivated chestnut groves are not within the suitability area (Figure 7). In addition, most of such CSFP located outside of suitable areas had a non-suitable slope gradient (>20°).

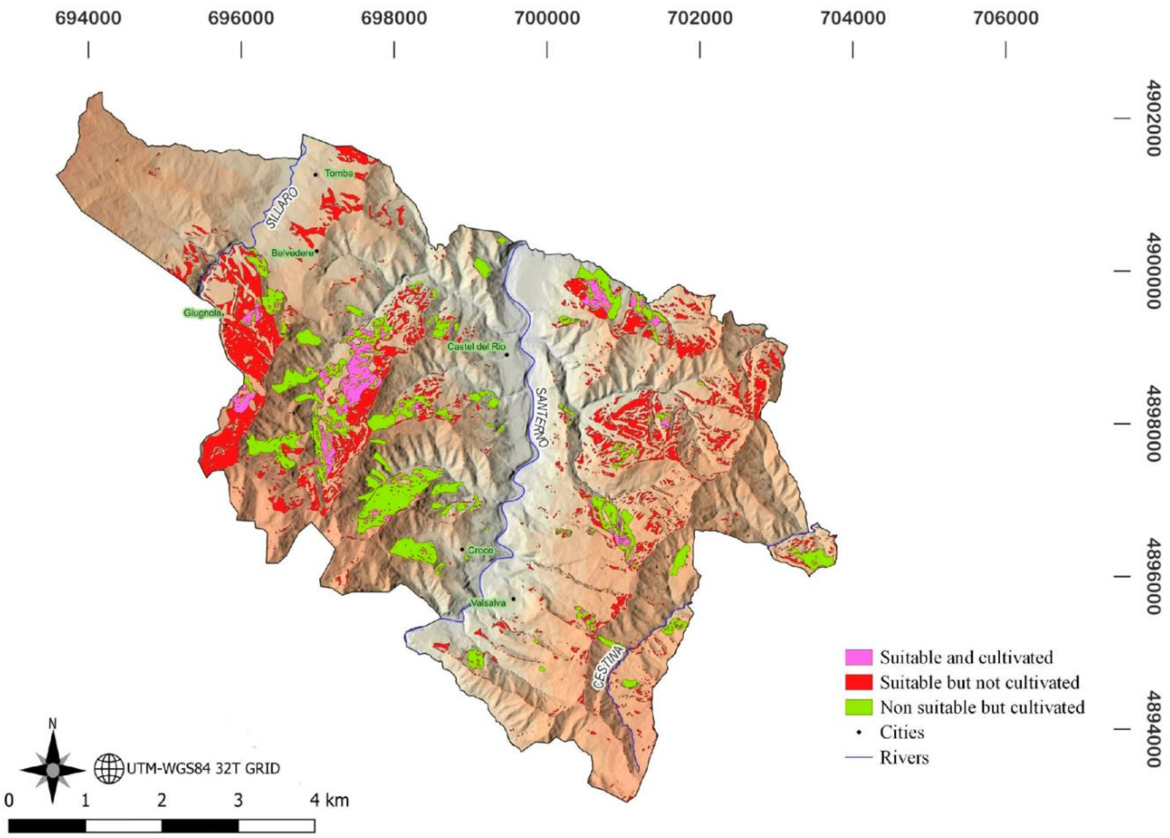

Figure 7. Map of Castel del Rio, Emilia-Romagna Region (Italy), showing the suitable areas for the cultivation of chestnut stands for fruit production (CSFP) and currently used for CSFP, the suitable areas for the cultivation of the CSFP but currently not used for CSFP, and the overlapping of suitable and cultivated CSFP areas.

6.4 DISCUSSION

The GIS-based approach was successfully used in the current study to evaluate land suitability for chestnut cultivation. Six parameters, namely land use and topographic features (altitude, slope gradient, and exposure), as well as lithological and pedological features, were taken into consideration.

The altitudinal suitability map showed that most of the study site can be potentially suitable for CSFP. The unsuitable areas in terms of altitude were located close to the Santerno river. In these areas, the altitude was lower than 300 m asl where the mean air temperatures were greater than 15 °C and annual rainfall below 600–700 mm, and therefore they were commonly excessively warm and dry for the optimal growth and development of chestnut groves (Pérez-Girón et al., 2020; Freitas et al., 2021). In fact, Pérez-Girón et al. (2020) and Freitas et al. (2021) stated that high temperatures do not allow budburst, flowering, fruit set, and maturation other than to maintenance costs. Further, the authors reported that low precipitation reduces plant development, leading to the production of smaller organs hampering flower production and grain filling, and limiting the size and number of individual leaves. The unsuitable climatic condition of this area was confirmed by the absence of chestnut stands (Regione Emilia-Romagna, 2020).

Unlike the altitudinal map, the exposure map defined most of the study site as unsuitable for CSFP because of the southern exposition. Exposure plays a key role in terms of chestnut plant growth and nut production (Lolli & Musolesi, 2006; Bounous, 2004). Specifically, the plants with southern exposure receive more direct heat than the ones with northern exposure, resulting from the sun drying both the soil and the vegetation, which may cause water stress Lolli & Musolesi, 2006; Bounous, 2004; Orsini & Remy, 1976; Ciesielsky & Sterckeman, 1997). This is particularly important during the flowering stage, which occurs in the summer months at Italian latitudes, resulting in thermal stress and finally less or no fruit development (Soil Survey Staff, 2014; De Philippis, 1951; Scott, 1986; Sidari et al., 2008; McVicar et al., 2007).

Although the study site was characterised by a hilly mountain landscape, the areas with a slope of less than 20° accounted for 43.9% of the entire Castel del Rio area. A low degree of slope prevents the occurrence of intense soil erosion processes (Garcia-Ruiz et al., 2015), which promote soil deepening (Carter & Ciolkosz, 1991; Fazlollahi Mohammadi, 2016), with possible positive consequences on root development and plant production (Di Iorio et al., 2005; Akıncı et al., 2013). In addition, the limited soil erosion occurring within the areas with a slope gradient < 20° could promote soil organic matter accumulation (Tang et al., 2010) known to improve soil ecosystem services including plant growth and yield (Akıncı et al., 2013; Tang et al., 2010). Besides the negative effects of high slope gradients on soil quality, although there is no basic and common guideline for a favourable slope for chestnut production, steep slopes cause difficulties during harvest with a consequent increase in harvesting costs. However, it is important to point out that although slope gradients > 20° cannot be considered suitable for CSFP, such areas could be addressed for the establishment of chestnut groves for wood production due to the recent development of machines and technologies that can also be used in steep areas (Ezzati et al., 2021; Cavalli & Amishev, 2019). Slope gradients > 20° prevent agricultural mechanisation with a consequent increase in management costs. Conversely, low slope gradients allow for the cost-effective management of farms, thus facilitating agricultural practices (Liu et al., 2018). In addition, low slope gradients limit soil erosion processes, which, in turn, positively affect crop yield (Sheng, 1989).

In terms of the lithological and pedological features, most of the study site can be considered suitable for CSFP. These results are in accordance with those reported by Sanesi (1977) and Antoniazzi (1977), which, through a study conducted within the Santerno river valley, showed the presence of chestnut stands on sandstone formations. In this context, it is important to highlight that the suitable soils had generally "dystric" features, namely an effective base saturation of less than 60% (Soil Survey Staff, 2014), which matched with the silicious sandstone formation from which they developed. In addition, such matching would indicate the greater role of parent material on soil properties than the other soil-forming factors in the present study site.

Although CSFP was historically present within the considered study site, the overlapping of the areas suitable in terms of altitude, exposure, slope gradient, lithology, and soil types showed that the suitable area for CSFP accounted only for 10% of the study site. This area included just 24.6% of the CSFP that are currently cultivated, suggesting the need for incentives from institutions to farmers to use such suitable areas for the creation of CSFP. Although most of the suitable area was observed in the northeastern part of the study site and the mountainous area located between the Sillaro and Santerno rivers, several suitable areas spread all over the study site. However, they showed a limited area (≤50 m^2), which does not allow economically sustainable chestnut production. Further, the limited suitable area would indicate the distribution of chestnut groves also in non-suitable areas. Indeed, through a comparison of the areas currently used for CSFP and the suitability map, most of them were in non-suitable areas, where the most limiting factor was the slope gradient. To reduce the soil erosion processes occurring in areas with high slope gradients, mulching and the conservation of grass cover are suggested (Ahmad et al., 2020). However, to reduce soil erosion and facilitate cultivation operations, terracing is the most recommended intervention (Ahmad et al., 2020; Tarolli & Straffelini, 2020; Moreno-de-las-Heras et al., 2019). In this regard, despite non-suitable areas having slope gradients of >20°, they still had CSFP because of terracing, which was the major morphological transformation implemented by farmers in these mountainous areas to obtain cultivable land in steep areas (Dossche et al., 2016; Cevasco et al., 2015; Tarolli et al., 2014). Terraces increase soil organic carbon accumulation, slow down the erosive power of the surface water flow, and improve soil water storage (Tarolli et al., 2014; Antle et al., 2007; Arnaez et al., 2011). However, terracing needs high investment and maintenance (Emerton & Snyder, 2008; Gassman et al., 2006), and the presence of farmers who would maintain the terraces in these mountainous areas. Therefore, land abandonment in terms of rural depopulation and/or the lack of management of CSFP could cause soil degradation in such areas (Tarolli et al., 2014; De

Feudis et al., 2020). Besides this, the obtained suitability map highlighted the potential loss of 59% of the currently cultivated CSFP in the next years. Such loss will be observed if the price of chestnuts does not also cover the costs related to CSFP management practices coping with degradation processes due to unsuitable conditions. Although most of the currently cultivated CSFP can be potentially lost, the suitability map showed that a wide area of the study site can be converted to CSFP (423 ha) in light of the demand increase for chestnuts due to their health benefits (Corona et al., 2021; Vasconcelos et al., 2010). In this sense, we do not know if such areas were CSFP in the past and, therefore, need to be restored; regardless, the establishment of CSFP might promote the improvement of soil quality (De Feudis et al., 2020).

Although the suitability map can be a helpful tool for land use planning, the knowledge of the current use of territory results is necessary to foresee the management practices that should be carried out for land conservation and or conversion (De la Rosa et al., 2004). In this context, the present study shows the reliability of remote-sensing images to identify the currently cultivated CSFP. However, the main drawback of such a procedure is that it is highly time-consuming because the CSFP areas should be manually identified. To cope with this issue, since CSFP are characterised by a distance of 10 m between chestnut plants and a later vegetation regrowth than other plant species, CSFP areas can be identified using a semi-automatic classification plugin in QGIS (Tempa & Aryal, 2022; Wassie et al., 2018), which is cost-effective. As a whole, the remote-sensing images approach showed a high fragmentation of CHEF, which is a generally negative feature for agriculture (Ntihinyurwa & De Vries, 2021). Within the investigated area, our findings suggest the promotion of land conversion to CSFP in suitable areas. Conversely, the CSFP located within unsuitable areas might be abandoned, especially those of small dimensions, to reduce the fragmentation.

6.5 CONCLUSIONS

The present work aimed to identify the areas that can potentially allow for CSFP cultivation by taking into consideration the geomorphological and pedological features, to provide maps that are easy to read by land planners and show the areas suitable for CSFP, and to propose a remote-sensing-based methodology able to identify the lands currently used for CSFP. Although the considered study site was recognised as an important area for chestnut production, the built suitability map demonstrated that only 10% of this area can be considered suitable for chestnut cultivation. Further, the remote-sensing images showed that most of the currently cultivated CSFPs were not within such suitable areas (59%) and, therefore, can undergo degradation processes mainly due to the high slope gradients. In this regard, it is important to highlight that, in some of these stands, farmers transform the land morphology by building terraces to obtain cultivable land on steep slopes. The limited suitable area for CSFP detected in the present study indicates that policymakers should consider careful planning in mountainous areas to promote chestnut cultivation within the identified suitable areas. Further, since most CSFP are currently cultivated within non-suitable areas, policymakers should help farmers in the implementation of ameliorative interventions to undertake both chestnut production and land conservation. The high matching observed between the CSFP areas acquired through remote-sensing images with those acquired through the institutional land-use map suggests the high accuracy of remote sensing to identify CSFP. This fact implicates the helpfulness of remote sensing for land planners in acquiring detailed information about land use.

Due to its easy execution, the methodology used for building land suitability maps coupled with land-use monitoring using remote-sensing images can be applied to CSFP at a wider geographical scale and to other forest and agricultural plants. Regardless of such potential, the present study highlights the need to have detailed lithological and pedological data to obtain reliable land suitability maps.

AUTHOR CONTRIBUTIONS

Conceptualisation, G.V. and L.V.A.; methodology, M.R., M.G., G.V., W.T. and L.V.A.; validation, L.V.A.; investigation, M.R. and M.G.; resources, L.V.A.; data curation, M.R.; writing—original draft preparation, M.D.F. and M.R.; writing—review and editing, M.D.F., G.V., W.T. and L.V.A.; visualisation, M.R. and M.D.F.; supervision, L.V.A.; project administration, L.V.A.; funding acquisition, L.V.A. All authors have read and agreed to the published version of the manuscript.

FUNDING

This research was co-funded by Fondazione Cassa di Risparmio di Imola, 8345.01 22-2022.0111-METODOLOGIA PER LA VALUTAZIONE QUALI-QUANTITATIVA DELLA CONSISTENZA CASTANICOLA.

DATA AVAILABILITY STATEMENT

Not applicable.

APPENDIX A

Table A1. Geolithological formation types and morphological features of Italian areas currently under chestnut stand cultivation for fruit production cultivation.

Region	Geolithology	Municipality/Locality	Altitude m asl	Slope %	Sources
Piedmont	Mycascists, gneisses, gneiss glanders	Low Alpine slopes (Turin and Cuneo)	400–900	30–60	IPLA-Regione Piemonte, 2007
	Detrital conoids referred to as gneisses	Low Alpine slopes (Turin and Cuneo)	300–900	30–80	IPLA-Regione Piemonte, 2007
	Siliceous matrix colluvium with gneiss predominance	Low mountain slopes (Verbano)	200–700	30–60	IPLA-Regione Piemonte, 2007
	Porphyries with mica-schists and quartzites included	Gentle mountain slopes (Vercellese, Novarese)	400–700	15–40	IPLA-Regione Piemonte, 2007
	Porphyries covered by ancient alluvial deposits	Transition between plain and pre-alpine reliefs	200–400	10–20	IPLA-Regione Piemonte, 2007
	Gneiss	Biella and Turin Pre-Alps	400–700	15–40	IPLA-Regione Piemonte, 2007
Lombardy	Schistous and micaceous gneisses	Bacino torrente Bitto di Gerola (SO)	820–850	50–60	ERSAL-Regione Lombardia, 1994
	Slope debris gneisses and mica-schists	Val Grosina (SO)	670–700	35–40	Assi et al., 1993
	Marly limestones, dolomitic limestones, and dolomites	Bergamasque Hinterland	270–670	35–40	ERSAL-Regione Lombardia,1992
	Ferretised pebbles and sands in an advanced state of alteration	Pinewood of Appiano Gentile-Tradate	320–375	5–40	ERSAL-Regione Lombardia, 1988

Region	Geolithology	Municipality/Locality	Altitude m asl	Slope %	Sources
Trentino	Hard limestones, porphyries, siliceous sandstones, and glacial siliceous deposits	Valle delle Chiese (Darzo, Lodrone, Daone)	400–700	35–50	Sartori & Mancabelli, 2009
	Rhyolites, rhyodacites, phyllites, and mica-schists with widespread glacial overburden	Valsugana (RoncegnoT., Strigno, Castagnè, Caldonazzo)	500–900	25–45	Sartori & Mancabelli, 2009
	Limestones and marly limestones with possible glacial cover with mixed lithology	Brentonico Plateau (Castione)	200–800	30–40	Sartori & Mancabelli, 2009
	Hard limestones, marly limestones with glacial cover with mixed lithology	Upper Garda Trentino (Nago, Drena, Tenna)	200–600	35–45	Sartori & Mancabelli, 2009
	Rhyolites, rhyodacites, and dacites with glacial overburdens	Cembra Valley (Albiano)	500–800	30–60	Sartori & Mancabelli, 2009
Friuli V.G.	Flysch with alternating arenites with calcareous-siliceous marls	Pre-Alpine reliefs Col Budoia	100–150	20–30	ERSA Agenzia Regionale per lo Sviluppo Rurale, 2006
	Conglomerate of predominantly calcareous nature with arenaceous and itic interlayers	Pre-Alpine reliefs Sequals Col Pallotta	300–350	25–35	ERSA Agenzia Regionale per lo Sviluppo Rurale, 2006
Veneto	White mica phyllites, corite, and albite	Venetian Pre-Alps	450–650	10–30	Marcolin et al., 2020
	Calcareous conglomerates in karst morphologies	Montello and Berici Hills	100–200	5–10	ARPAV Regione Veneto, 2006
	Acid volcanic rocks (rhyolites and trachytes)	Euganean Hills	300–600	15–30	ARPAV Regione Veneto, 2006
Emilia-Romagna	Sandstones and pelitic sandstones	Upper Frignano (MO) Upper Reno Valley	900–1000	50–70	De Feudis et al., 2020
	Pelitic limestone flysch	High Apennines Reggiano-Parmense	800–1000	40–60	Vittori Antisari et al., 2008
	Pelitic sandstones and marly limestones	Upper Santerno and Savena Valleys	850–1000	30–50	Vittori Antisari et al., 2005
	Conglomeratic-pelitic sandstone deposits	Sillaro and Lavino Valleys	450–600	10–38	Guidi et al., 2007
	Sandstones with arenaceous-pelitic intercalations	Upper Idice Valley	250–500	30–45	Dell'Abate et al., 2006

Region	Geolithology	Municipality/Locality	Altitude m asl	Slope %	Sources
Tuscany	Quartz-latitic volcanites and pyroclastic deposits	Monte Amiata (Arcidosso, Castel del Piano, Seggiano (GR))	950–1250	10–35	Regione Toscana, 2020
	Silty schists, marls, and sandstones	Londa (FI), Vernio (PO)	500–700	35–60	Regione Toscana, 2020
	Turbiditic flysch, marls, and marly clays	Camporgiano (LU)	50-160	35-40	Regione Toscana, 2020
	Quartzose-felspathic sandstones	Arezzo, Poppi (AR), Firenzuola (FI), Molazzano (LU)	400-900	14-40	[75]
	Pebbly sediments and polygenic conglomerates interbedded with clayey sands	Aulla, Nardi (MS)	150–270	10–25	Regione Toscana, 2020
	Calcareous polygenic conglomerates	Aulla (MS)	100–400	15–30	Regione Toscana, 2020
Latium	Earthy tuffs with black and white pumice	Sabatini Mountains	300–700	10–20	Mattioli et al., 2016
	Earthy tuffs	Montesanti	980–1000	25–30	Blom et al., 2009
Abruzzo	Pelitic-arenaceous alternation with debris-colluvial belts at the base of slopes	Rocca S. Maria, Montorio del Vomano (TE) Montereale (AQ)	800–1200	20–35	Chiuchiarelli et al., 2006
	Ancient terraces with fluvio lacustrine and clastic volcanic sediments	Oricola, Carsoli (AQ)	500–800	0–13	Chiuchiarelli et al., 2006
	Linear slopes on marly limestone substrates	Monreale, Monte Genzano, Pettorato sul Gizio (AQ)	800–1200	20–35	Chiuchiarelli et al., 2006
Molise	Dolomitic limestone affected by pyroclastic cover	S. Massimo	850–900	10–20	Colombo, 2010
Campania	Mesozoic carbonate rocks with pyroclastic overburden	Lattari and Picentini Mountains (Campania Region, 2004)	300–1100	35–60	Regione Campania, 2020
	Carbonate rocks with pyroclastic overburden	Upper Telesina Valley	600–750	20–30	Regione Campania, 2020
	Mesozoic dolomite and limestone with pyroclastite cover	Caruso and Cuculo Mountains mountain system	100–600	15–35	Regione Campania, 2020
	Sandstones, marly sandstones, and conglomerates	Pre-Apennine hills of basso Ufita and Conca Avellinese	300–400	15–30	Regione Campania, 2020

Region	Geolithology	Municipality/Locality	Altitude m asl	Slope %	Sources
	Conglomerates and sands	Pre-Apennine hills of Benevento	300–400	25–40	Regione Campania, 2020
	Clay formations with pyroclastic coverings	Irpinia and Sannio hills	250–450	20–30	Regione Campania, 2020
	Fluvio-lacustrine deposits	Upper Sele Valley	300–500	15–25	Regione Campania, 2020
	Fluvio-lacustrine deposits	Lauro-Baianese Valley	150–300	10–20	Regione Campania, 2020
Basilicata	Vulture volcanic reliefs with pyroclastic coverings	Santa Maria	700–800	10–15	Cassi & Viviano, 2006
Calabria	Phylladic schists and granites	Coastal chain and Presila of Cosenza	300–900	10–30	Arcidiaco et al., 2006
	Alteration sand of granites	Sila Greca, Upper Ionian Cosenza	500–1000	20–30	Arcidiaco et al., 2006
	Alteration granites	Presila of Crotone and Catanzaro	800–100	15–25	Arcidiaco et al., 2006
	Phyllites, leucoscists, biotic schists	Serre of Catanzaro and M.te Reventino	600–900	10–25	Arcidiaco et al., 2006
	Alteration sand of granites	Serre Vibonesi	600–900	10–20	Arcidiaco et al., 2006
	Heavily altered granite rocks and tertiary conglomerates	Western and Eastern Aspromonte	300–1200	15–40	Arcidiaco et al., 2006
Sardinia	Palaeozoic granites and schists	Mandrolisai. Municipalities of Desulo, Tonara, Balvi, Aritzo	600–700	20–30	Regione Autonoma della Sardegna, 2014
	Metavolcanites and ignimbrites	Goceano, Monte Pisani	700–900	20–25	Regione Autonoma della Sardegna, 2014
Sicily	Heavily weathered sandstones	Erei Mountains, Rossomanno (EN)	550–890	15–25	Fierotti et al., 1988
	Inert quartz-arenites to micaceous pelite	Forest of Ficuzza. Rocca Busambra (PA)	600–1000	10–15	Costantini & Dazzi, 2013
	Altered calcarenites and limestones	Mount Peloritani, Musolino, Novara (ME)	380–1050	10–15	Fierotti et al., 1988
	Basic volcanic rocks	Mount Etna, Randazzo, Pirao (CT)	600–1210	10–20	Fierotti et al., 1988

CONFLICTS OF INTEREST

The authors declare no conflicts of interest.

REFERENCES

AbdelRahman, M. A., Natarajan, A., & Hegde, R. (2016). Assessment of land suitability and capability by integrating remote sensing and GIS for agriculture in Chamarajanagar district, Karnataka, India. *The Egyptian Journal of Remote Sensing and Space Science*, *19*(1), 125-141.

Ahmad, N. S. B. N., Mustafa, F. B., & Didams, G. (2020). A systematic review of soil erosion control practices on the agricultural land in Asia. *International Soil and Water Conservation Research*, *8*(2), 103-115.

Akıncı, H., Özalp, A. Y., & Turgut, B. (2013). Agricultural land use suitability analysis using GIS and AHP technique. *Computers and electronics in agriculture*, *97*, 71-82.

Alewell, C., Meusburger, K., Brodbeck, M., & Bänninger, D. (2008). Methods to describe and predict soil erosion in mountain regions. *Landscape and Urban Planning*, *88*(2-4), 46-53.

Antle, J. M., Stoorvogel, J. J., & Valdivia, R. O. (2007). Assessing the economic impacts of agricultural carbon sequestration: Terraces and agroforestry in the Peruvian Andes. *Agriculture, Ecosystems & Environment*, *122*(4), 435-445.

Antolini, G., Auteri, L., Pavan, V., Tomei, F., Tomozeiu, R., & Marletto, V. (2015). A daily high-resolution gridded climatic data set for Emilia-Romagna, Italy, during 1961-2010. *International Journal of Climatology*, *36*(4), 1970-1986.

Antoniazzi, A., & Camera di commercio industria artigianato e agricoltura (Forlì). (1978). *La carta dei suoli della Media Valle del Santerno:(Appennino romagnolo)*. Consiglio nazionale delle ricerche, Centro di studio della genesi, classificazione e cartografia del suolo.

Arcidiaco, L.; Ciancio, O.; Garfì, V.; Iovino, F.; Menguzzato, G.; & Nicolaci, A. (2006) Area di vegetazione e campo di idoneità ecologica del castagno in Calabria. L'Italia For. E Mont., 6, 489–506. Available online: https://hdl.handle.net/11695/319 (accessed on 2 November 2022).

Arnaez, J., Lasanta, T., Errea, M. P., & Ortigosa, L. (2011). Land abandonment, landscape evolution, and soil erosion in a Spanish Mediterranean mountain region: The case of Camero Viejo. *Land degradation & development*, *22*(6), 537-550.

Arnous, M. O., & Hassan, M. A. A. (2006, November). Image processing and land information system for soil assessment of El-Maghara Area, North Sinai, Egypt. In *International Conf. on Water Resources and Arid Environment*.

ARPAV Regione Veneto (2005). *Carta Dei Suoli del Veneto*; Note Illustrative; APRAV: Padova, Italy; ISBN 88-7504-097-4.

Assi, I., Comolli, R., & Previtali, F. (1993). Prime osservazioni sui suoli della Val Grosina. *Natura Bresciana. Nat. Brescia Ann. Mus. Civ. Sc*, *29*, 97-122.

Atay Kaya, İ., & Kut Görgün, E. (2020). Land use and land cover change monitoring in Bandırma (Turkey) using remote sensing and geographic information systems. *Environmental Monitoring and Assessment*, *192*(7), 430.

Aymen, A. T., Al-husban, Y., & Farhan, I. (2021). Land suitability evaluation for agricultural use using GIS and remote sensing techniques: The case study of Ma'an Governorate, Jordan. *The Egyptian Journal of Remote Sensing and Space Science*, *24*(1), 109-117.

Blom, J. M., Vannini, A., Vettraino, A. M., Hale, M. D., & Godbold, D. L. (2009). Ectomycorrhizal community structure in a healthy and a Phytophthora-infected chestnut (Castanea sativa Mill.) stand in central Italy. *Mycorrhiza*, *20*(1), 25-38.

Bounous, G. (2002). *Il castagno. Coltura, ambiente ed utilizzazioni in Italia e nel mondo* (pp. 1-312). IL SOLE 24 ORE/EDAGRICOLE.

Brinkman, S., & Young, A. (1976). A framework for land evaluation. *Food and Agriculture Organization of the United Nations, Wageningen, Netherlands*.

Bruzzese, S., Blanc, S., & Brun, F. (2020). Strategies for the valorisation of chestnut resources in Italian mountainous areas from a sustainable development perspective. *Resources*, *9*(5), 60.

Carter, B. J., & Ciolkosz, E. J. (1991). Slope gradient and aspect effects on soils developed from sandstone in Pennsylvania. *Geoderma*, *49*(3-4), 199-213.

Cassi, F., & Viviano, L. (2006). Suoli della Basilicata—Carta pedologica della Regione Basilicata in scala 1: 250.000. *Regione Basilicata—Dip. Agricoltura e Sviluppo Rurale. Direzione Generale; Reg. Basilicata-Dip. Agric. Svilup. Rurale. Dir. Gen.: Potenza, Italy*.

Cavalli, R., & Amishev, D. (2019). Steep terrain forest operations–challenges, technology development, current implementation, and future opportunities. *International Journal of Forest Engineering*, *30*(3), 175-181.

Cevasco, R., Moreno, D., & Balzaretti, R. (2015). Historical chestnut cultures, climate, and rural landscapes in the Apennines. In *The Future of Heritage as Climates Change* (pp. 150-168). Routledge.

Chen, Z., Huang, M., Xiao, C., Qi, S., Du, W., Zhu, D., & Altan, O. (2022). Integrating remote sensing and spatiotemporal analysis to characterize artificial vegetation restoration suitability in desert areas: A Case Study of Mu Us Sandy Land. *Remote Sensing*, *14*(19), 4736.

Chiuchiarelli, I., Santucci, S., Paolanti, M., & Rivieccio, R. (2006). *Ambienti e territorio: carta dei suoli della regione Abruzzo: scala 1: 250.000*. ARSSA. Regione Abruzzo: Scerni, Italy.

Cienciała, A., Sobolewska-Mikulska, K., & Sobura, S. (2021). Credibility of the cadastral data on land use and the methodology for their verification and update. *Land Use Policy*, *102*, 105204.

Ciesielski, H., Sterckeman, T., Santerne, M., & Willery, J. P. (1997). Determination of cation exchange capacity and exchangeable cations in soils by means of cobalt hexamine trichloride. Effects of experimental conditions. *Agronomie*, *17*(1), 1-7.

Colombo, C. (2010) Itinerari Pedologici Italiani/1. In *Guida Pedologica ai Suoli Forestali del Matese Molisano*; ARACNE: Rome, Italy; ISBN 978-88-548-3343-2.

Comel, A. (1975). Le basi pedologiche per la valutazione dei terreni. Edagricole: Milano, Italy; pp. 1–138

Conedera, M., & Krebs, P. (2007). History, present situation and perspective of chestnut cultivation in Europe. In *II Iberian Congress on Chestnut 784* (pp. 23-28).

Conedera, M., Krebs, P., Gehring, E., Wunder, J., Hülsmann, L., Abegg, M., & Maringer, J. (2021). How future-proof is Sweet chestnut (Castanea sativa) in a global change context?. *Forest Ecology and Management*, *494*, 119320.

Conedera, M., Krebs, P., Tinner, W., Pradella, M., & Torriani, D. (2004a). The cultivation of Castanea sativa (Mill.) in Europe, from its origin to its diffusion on a continental scale. *Vegetation history and archaeobotany*, *13*(3), 161-179.

Conedera, M., Manetti, M. C., Giudici, F., & Amorini, E. (2004b). Distribution and economic potential of the Sweet chestnut (Castanea sativa Mill.) in Europe. *Ecologia mediterranea*, *30*(2), 179-193.

Conedera, M.; Tinner, W.; Krebs, P.; de Rigo, D. & Caudullo, G. (2016) Castanea sativa in Europe: Distribution, habitat, usage and threats. In *European Atlas of Forest Tree Species*; San-Miguel-Ayanz, J., de Rigo, D., Caudullo, G., Houston Durrant, T., Mauri, A., Eds.; European Commision: Luxembourg,; p. e0125e0. Available online: **https://w3id.org/mtv/FISE-Comm/v01/e0125e0** (accessed on 20 November 2022)

Corona, P., Frangipane, M. T., Moscetti, R., Lo Feudo, G., Castellotti, T., & Massantini, R. (2021). Chestnut cultivar identification through the data fusion of sensory quality and FT-NIR spectral data. *Foods*, *10*(11), 2575.

Costantini, E. A., & Dazzi, C. (Eds.). (2013). *The soils of Italy* (pp. 19-38). Dordrecht, Netherlands: Springer.

De Feudis, M., Falsone, G., Gherardi, M., Speranza, M., Vianello, G., & Antisari, L. V. (2021). GIS-based soil maps as tools to evaluate land capability and suitability in a coastal reclaimed area (Ravenna, northern Italy). *International Soil and Water Conservation Research*, *9*(2), 167-179.

De Feudis, M., Falsone, G., Vianello, G., & Antisari, L. V. (2020). Stable organic carbon pool rises in soil under chestnut (Castanea sativa Mill.) forest for timber production after 15 years since grafting onto satin-cut stumps. *EQA-International Journal of Environmental Quality*, *40*, 1-10.

De Feudis, M., Falsone, G., Vianello, G., & Vittori Antisari, L. (2020). The conversion of abandoned chestnut forests to managed ones does not affect the soil chemical properties and improves the soil microbial biomass activity. *Forests*, *11*(8), 786.

De la Rosa, D., Mayol, F., Díaz-Pereira, E., Fernandez, M., & de la Rosa Jr, D. (2004). A land evaluation decision support system (MicroLEIS DSS) for agricultural soil protection: With special reference to the Mediterranean region. *Environmental Modelling & Software*, *19*(10), 929-942.

De Philippis, A. (1951) Forest ecology and phytoclimatology. *Unasylva*, *5*, 1.

Del Favero, R. (2002). I Tipi Forestali della Lombardia. Regione Lombardia. *Progetto Strategico*, *9*(6).

Dell'Abate, M. T., Giovannini, C., Pontalti, F., Vianello, G., & Vittori Antisari, L. (2006). Caratterizzazione Quali-Quantitativa Della Sostanza Organica Degli Epipedon Di Suoli Bruni Acidi Dell'appennino Emiliano Sotto Bosco Di Latifoglie E Di Conifere. In *Atti Convegno Nazionale Società Italiana di Scienze del Suolo "Suolo Ambiente Paesaggio",* (Vol. 1, pp. 332-342). Società Italiana di Scienza del Suolo: Imola, Italy, 2006; pp. 332–342. ISBN 978.88.90283116

Di Iorio, A., Lasserre, B., Scippa, G. S., & Chiatante, D. (2005). Root system architecture of Quercus pubescens trees growing on different sloping conditions. *Annals of Botany*, *95*(2), 351-361.

Diaz, J. V. R., Varela, E. R. D., Anta, M. B., & Álvarez, P. Á. (2018). Sweet chestnut agroforestry systems in North-western Spain: Classification, spatial distribution and an ecosystem services assessment. *Forest systems*, *27*(1), 10.

Dossche, R., Rogge, E., & Van Eetvelde, V. (2016). Detecting people's and landscape's identity in a changing mountain landscape. An example from the northern Apennines. *Landscape Research*, *41*(8), 934-949.

Elsheikh, R., Shariff, A. R. B. M., Amiri, F., Ahmad, N. B., Balasundram, S. K., & Soom, M. A. M. (2013). Agriculture Land Suitability Evaluator (ALSE): A decision and planning support tool for tropical and subtropical crops. *Computers and electronics in agriculture*, *93*, 98-110.

Emerton, L., & Snyder, K. A. (2018). Rethinking sustainable land management planning: Understanding the social and economic drivers of farmer decision-making in Africa. *Land Use Policy*, *79*, 684-694.

ERSA Agenzia Regionale per lo Sviluppo Rurale (2006). *Suoli e Paesaggi del Friuli Venezia Giulia*; Pianura: Gorizia, Italy; Volume 1

ERSAL Regione Lombardia (1988). Progetto Carta Pedologica. In *I suoli del Parco Pineta di Appiano Gentile—Tradate e Aree Limitrofe*; Grafiche Boniardi: Milano, Italy.

ERSAL Regione Lombardia (1992). Progetto Carta Pedologica. In *I Suoli Dell'Hinterland Bergamasco*; Arti Grafiche Chiribella: Bozzolo, Italy.

ERSAL Regione Lombardia (1994). *Progetto Ricerca Integrata Sulla Degradazione dei Versanti in Territori Montani. I Suoli del Bacino del Torrente Bitto di Gerola*; Arti Grafiche Vertemati: Vimercate, Italy.

Ezzati, S., Tavankar, F., Ghaffariyan, M. R., Venanzi, R., Latterini, F., & Picchio, R. (2021). The impact of weather and slope conditions on the productivity, cost, and GHG emissions of a ground-based harvesting operation in mountain hardwoods. *Forests*, *12*(12), 1612.

FAO. (2015). Understanding Mountain Soils: a contribution from mountain areas to the International Year of Soils 2015, by Romeo, R., Vita, A., Manuelli, S., Zanini, E., Freppaz, M. & Stanchi, S. Rome, Italy.

FAOSTAT (2022). Statistics Division of Food and Agriculture Organization of the United Nations, Roma. Available online: https://www.fao.org/faostat/en/#home (accessed on 25 November 2022).

Fazlollahi Mohammadi, M., Jalali, S. G. H., Kooch, Y., & Said-Pullicino, D. (2016). Slope gradient and shape effects on soil profiles in the northern mountainous forests of Iran. *Eurasian soil science*, *49*(12), 1366-1374.

Fierotti, G., Dazzi, C., & Raimondi, S. (1988) *Carta dei Suoli della Sicilia-Soil Map of Sicily, Alla Scala 1:250.000 con Commenti*; Regione Siciliana: Palermo, Italy.

Freitas, T. R., Santos, J. A., Silva, A. P., & Fraga, H. (2021). Influence of climate change on chestnut trees: A review. *Plants*, *10*(7), 1463.

García-Ruiz, J. M., Beguería, S., Nadal-Romero, E., González-Hidalgo, J. C., Lana-Renault, N., & Sanjuán, Y. (2015). A meta-analysis of soil erosion rates across the world. *Geomorphology*, *239*, 160-173.

Gassman, P. W., Osei, E., Saleh, A., Rodecap, J., Norvell, S., & Williams, J. (2006). Alternative practices for sediment and nutrient loss control on livestock farms in northeast Iowa. *Agriculture, Ecosystems & Environment*, *117*(2-3), 135-144.

Guidi, S., Gulminelli, A., & Battaglia, D. P. (2007). I Patriarchi da frutto dell'Emilia-Romagna, Regione Emilia-Romagna: Bologna, Italy; Volume 1, pp. 1–155

Habibie, M. I., Noguchi, R., Shusuke, M., & Ahamed, T. (2021). Land suitability analysis for maize production in Indonesia using satellite remote sensing and GIS-based multicriteria decision support system. *GeoJournal*, *86*(2), 777-807.

IPLA—Regione Piemonte. (2007). Carta dei Suoli del Piemonte 1: 250.000. *Note Illustrative.* SELCA: Firenze, Italy

Isard, S. A. (1986). Factors influencing soil moisture and plant community distribution on Niwot Ridge, Front Range, Colorado, USA. *Arctic and Alpine Research*, *18*(1), 83-96.

ISTAT. Coltivazioni: Coltivazioni Legnose Fruttifere. Available online: **www.istat.it** (accessed on 22 November 2022)

Joss, B. N., Hall, R. J., Sidders, D. M., & Keddy, T. J. (2008). Fuzzy-logic modeling of land suitability for hybrid poplar across the Prairie Provinces of Canada. *Environmental monitoring and assessment*, *141*(1), 79-96.

Klute, A. (Ed.). (1986). *Methods of soil analysis. Part 1. Physical and mineralogical methods* (No. Ed. 2, pp. 1188-pp).

Kurowska, K., Marks-Bielska, R., Bielski, S., Aleknavičius, A., & Kowalczyk, C. (2020). Geographic information systems and the sustainable development of rural areas. *Land*, *10*(1), 6.

Lauteri, M., Monteverdi, M. C., & Scarascia-Mugnozza, G. (2009, October). Preservation of chestnut (Castanea sativa Mill.) genetic resources and Adaptive potential in relation to environmental changes. In *I European Congress on Chestnut-Castanea 2009 866* (pp. 677-682).

Liu, Q., Liu, Y., Peng, J., Zhang, T., Li, Y., & Hu, Y. N. (2018). Linking GRNN and neighborhood selection algorithm to assess land suitability in low-slope hilly areas. *Ecological indicators*, *93*, 581-590.

Loeppert, R. H., & Suarez, D. L. (1996). Carbonate and gypsum. *Methods of soil analysis: Part 3 chemical methods*, *5*, 437-474.

Lolli, G., & Musolesi, M. (2006). Il castagneto da frutto: manuale pratico di innesto, potatura e conduzione: tecniche di recupero dei castagneti abbandonati, conversione dei cedui in castagneti da frutto: indagini svolte nell'Appennino bolognese.

Marcolin, E., Manetti, M. C., Pelleri, F., Conedera, M., Pezzatti, G. B., Lingua, E., & Pividori, M. (2020). Seed regeneration of sweet chestnut (Castanea sativa Miller) under different coppicing approaches. *Forest Ecology and Management*, *472*, 118273.

Mariotti, B., Tani, A., & Maltoni, A. (2019). Linee guida per la gestione selvicolturale dei castagneti da frutto. CREA: Rome, Italy; ISBN 978-88-3385-017-7.

Massantini, R., Moscetti, R., & Frangipane, M. T. (2021). Evaluating progress of chestnut quality: A review of recent developments. *Trends in Food Science & Technology*, *113*, 245-254.

Mattioli, W., Mancini, L. D., Portoghesi, L., & Corona, P. (2016). Biodiversity conservation and forest management: The case of the sweet chestnut coppice stands in Central Italy. *Plant*

Biosystems-An International Journal Dealing with all Aspects of Plant Biology, *150*(3), 592-600.

McVicar, T. R., Van Niel, T. G., Li, L., Hutchinson, M. F., Mu, X., & Liu, Z. (2007). Spatially distributing monthly reference evapotranspiration and pan evaporation considering topographic influences. *Journal of hydrology*, *338*(3-4), 196-220.

Mikoláš, M., Ujházy, K., Jasík, M., Wiezik, M., Gallay, I., Polák, P., ... & Keeton, W. S. (2019). Primary forest distribution and representation in a Central European landscape: Results of a large-scale field-based census. *Forest Ecology and Management*, *449*, 117466.

Moreno-de-las-Heras, M., Lindenberger, F., Latron, J., Lana-Renault, N., Llorens, P., Arnáez, J., ... & Gallart, F. (2019). Hydro-geomorphological consequences of the abandonment of agricultural terraces in the Mediterranean region: Key controlling factors and landscape stability patterns. *Geomorphology*, *333*, 73-91.

Nicoletti, R., Beccaro, G. L., Sekara, A., Cirillo, C., & Di Vaio, C. (2021). Endophytic fungi and ecological fitness of chestnuts. *Plants*, *10*(3), 542.

Nocetti, M., Brunetti, M., & Bacher, M. (2016). Efficiency of the machine grading of chestnut structural timber: prediction of strength classes by dry and wet measurements. *Materials and structures*, *49*(11), 4439-4450.

Ntihinyurwa, P. D., & de Vries, W. T. (2021). Farmland fragmentation, farmland consolidation and food security: Relationships, research lapses and future perspectives. *Land*, *10*(2), 129.

Orsini, L., & Remy, J. C. (1976). The simultaneous determination of cation-exchange capacity and total exchangeable bases (BE) using cobaltihexammine chloride. *Sci. du Sol*, *4*, 269-275.

Ozsahin, E., & Ozdes, M. (2022). Agricultural land suitability assessment for agricultural productivity based on GIS modeling and multi-criteria decision analysis: the case of Tekirdağ province. *Environmental Monitoring and Assessment*, *194*(1), 41.

Pérez-Girón, J. C., Alvarez-Alvarez, P., Díaz-Varela, E. R., & Lopes, D. M. M. (2020). Influence of climate variations on primary production indicators and on the resilience of forest ecosystems in a future scenario of climate change: Application to sweet chestnut agroforestry systems in the Iberian Peninsula. *Ecological Indicators*, *113*, 106199.

Pezzi, G., Maresi, G., Conedera, M., & Ferrari, C. (2011). Woody species composition of chestnut stands in the Northern Apennines: the result of 200 years of changes in land use. *Landscape ecology*, *26*(10), 1463-1476.

Ray, P., Chattaraj, S., Bandyopadhyay, S., Jena, R. K., Singh, S. K., & Ray, S. K. (2021). Shifting cultivation, soil degradation, and agricultural land-use planning in the northeastern hill region of India using geo-spatial techniques. *Land Degradation & Development*, *32*(14), 3870-3892.

Regione Autonoma della Sardegna (2014). *Piano Forestale Particolareggiato del Complesso Forestale "Goceano, UGB Fiorentini, Monte Pisanu, Anela". Analisi Multidisciplinari*; DREAM: Pratovecchio, Italy.

Regione Campania (2020). Progetto carta dei suoli della Campania. Assessorato all'Agricoltura, Settore SIRCA, Geoportale Regione Campania, Sistema Informativo Territoriale della Regione Campania, Naples, Italy; Available online: https://sit2.regione.campania.it/node (accessed on 26 October 2022).

Regione Emilia-Romagna. Carta Geologica 1:10000—Banca Dati Geologica, 1:10.000—Unità Geologiche—10k. (2006). Available online: https://geoportale.regione.emilia-romagna.it/catalogo/dati-cartografici/informazioni-geoscientifiche/geologia/banca-dati-geologica-1-10.000/layer-11 (accessed on 27 October 2022).

Regione Emilia-Romagna. DTM 5×5—Geoportale Regione. (2009). Available online: https://geoportale.regione.emilia-romagna.it/catalogo/dati-cartografici/altimetria/layer-2 (accessed on 27 October 2022).

Regione Emilia-Romagna. Uso del suolo di dettaglio dell'anno 2017—Coperture vettoriali uso del suolo di dettaglio—Edizione 2020—Geoportale Regione. (2020). Available online: https://geoportale.regione.emilia-romagna.it/download/dati-e-prodotti-cartografici-preconfezionati/pianificazione-e-catasto/uso-del-suolo/2017-coperture-vettoriali-uso-del-suolo-di-dettaglio-edizione-2020 (accessed on 27 October 2022).

Regione Toscana (2020). Catalogo dei suoli della Carta dei suoli della Toscana in scala 1:250.000. Programma interregionale "Agricoltura e qualità", misura5, Florence, Italy. Available online: **https://www.regione.toscana.it/-/pedologia** (accessed on 26 October 2022)

Rodrigues, A., Gonçalves, A. B., Costa, R. L., & Gomes, A. A. (2021). GIS-based assessment of the chestnut expansion potential: A case-study on the Marvão productive area, Portugal. *Agriculture*, *11*(12), 1260.

Saleh, A. M., Belal, A. B., & Mohamed, E. S. (2015). Land resources assessment of El-Galaba basin, South Egypt for the potentiality of agriculture expansion using remote sensing and GIS techniques. *The Egyptian Journal of Remote Sensing and Space Science*, *18*(1), S19-S30.

Sanesi, G., & Consiglio nazionale delle ricerche. Progetto finalizzato conservazione del suolo. (1977). *I suoli del bacino dei torrenti Diaterna e lineamenti pedologici del Mugello e dell'alta valle del Santerno (Firenze)*. G. Capponi.

Sartori, G., & Mancabelli, A. (Eds.). (2009). *Carta dei suoli del Trentino: scala 1: 250.000*. Museo tridentino di scienze naturali: Trento, Italy; Consiglio per la Ricerca e la Sperimentazione in Agricoltura: Roma, Italy

Schoeneberger, P. J., Wysocki, D. A., & Benham, E. C. (Eds.). (2012). *Field book for describing and sampling soils*. Government Printing Office.

Sheng, T. C. (1989). *Soil conservation for small farmers in the humid tropics* (Vol. 60). Food & Agriculture Org..

Sidari, M., Ronzello, G., Vecchio, G., & Muscolo, A. (2008). Influence of slope aspects on soil chemical and biochemical properties in a Pinus laricio forest ecosystem of Aspromonte (Southern Italy). *European Journal of Soil Biology*, *44*(4), 364-372.

Siqueira, D. S., Marques Jr, J., & Pereira, G. T. (2010). Corrigendum to" The use of landforms to predict the variability of soil and orange attributes"[Geoderma 155 (1–2)(2010) 55–66]. *Geoderma*, *156*(3-4), 410.

Soil Survey Staff. (2014). Keys to Soil Taxonomy (12th ed.). USDA Natural Resources Conservation Service.

Sonneveld, M. P. W., Hack-ten Broeke, M. J. D., Van Diepen, C. A., & Boogaard, H. L. (2010). Thirty years of systematic land evaluation in the Netherlands. *Geoderma*, *156*(3-4), 84-92.

Tamantini, S., Bergamasco, S., Portoghesi, L., Vettraino, A. M., Zikeli, F., Mugnozza, G. S., & Romagnoli, M. (2022). Detection, description, and technological properties of colour aberration in wood of standards and shoots from a chestnut (Castanea sativa Mill.) coppice stand. *European Journal of Forest Research*, *141*(4), 683-698.

Tang, X., Liu, S., Liu, J., & Zhou, G. (2010). Effects of vegetation restoration and slope positions on soil aggregation and soil carbon accumulation on heavily eroded tropical land of Southern China. *Journal of Soils and Sediments*, *10*(3), 505-513.

Tarolli, P., & Straffelini, E. (2020). Agriculture in hilly and mountainous landscapes: threats, monitoring and sustainable management. *Geography and sustainability*, *1*(1), 70-76.

Tarolli, P., Preti, F., & Romano, N. (2014). Terraced landscapes: From an old best practice to a potential hazard for soil degradation due to land abandonment. *Anthropocene*, *6*, 10-25.

Tempa, K., & Aryal, K. R. (2022). Semi-automatic classification for rapid delineation of the geohazard-prone areas using Sentinel-2 satellite imagery. *SN Applied Sciences*, *4*(5), 141.

Tercan, E., & Dereli, M. A. (2020). Development of a land suitability model for citrus cultivation using GIS and multi-criteria assessment techniques in Antalya province of Turkey. *Ecological Indicators*, *117*, 106549.7

Triantafilis, J., Ward, W. T., & McBratney, A. B. (2001). Land suitability assessment in the Namoi Valley of Australia, using a continuous model. *Soil Research*, *39*(2), 273-289.

Vasconcelos, M. D. C. D., Bennett, R. N., Quideau, S., Jacquet, R., Rosa, E. A., & Ferreira-Cardoso, J. V. (2010). Evaluating the potential of chestnut (Castanea sativa Mill.) fruit pericarp and integument as a source of tocopherols, pigments and polyphenols.

Vasu, D., Srivastava, R., Patil, N. G., Tiwary, P., Chandran, P., & Singh, S. K. (2018). A comparative assessment of land suitability evaluation methods for agricultural land use planning at village level. *Land use policy*, *79*, 146-163.

Vittori Antisari, L., Vianello, G., Pontalti, F., Lorito, S., & Gherardi, M. (2008). Land use effects on organic matter in brown soils of the emilian apennines. *Adv. GeoEcol.*, *39*, 311–328

Vittori Antisari, L., Vianello, G., Simoni, A., & Giovannini, C. (2005). Influenza dei fattori clima e tempo sull'evoluzione di suoli bruni acidi delle formazioni arenacee silicoclastiche alloctone dell'Appennino bolognese. *Bollettino Della Societa'italiana Della Scienza Del Suolo*, *54*, 279-286.

Wassie, Y. A., Koeva, M. N., Bennett, R. M., & Lemmen, C. H. J. (2018). A procedure for semi-automated cadastral boundary feature extraction from high-resolution satellite imagery. *Journal of spatial science*, *63*(1), 75-92.

Yalew, S. G., Van Griensven, A., Mul, M. L., & van der Zaag, P. (2016). Land suitability analysis for agriculture in the Abbay basin using remote sensing, GIS and AHP techniques. *Modeling Earth Systems and Environment*, *2*(2), 101.

Zheng, C., Wen, Z., Liu, Y., Guo, Q., Jiang, Y., Ren, H., ... & Yang, Y. (2021). Integrating habitat suitability and the near-nature restoration priorities into revegetation plans based on potential vegetation distribution. *Forests*, *12*(2), 218.

Zlatanov, T., Schleppi, P., Velichkov, I., Hinkov, G., Georgieva, M., Eggertsson, O., ... & Vacik, H. (2013). Structural diversity of abandoned chestnut (Castanea sativa Mill.) dominated forests: Implications for forest management. *Forest Ecology and Management*, *291*, 326-335.

7. HILLSLOPE MORPHOLOGICAL FEATURES MODULATE SOIL MICROBIAL COMMUNITIES AND CHESTNUT INK DISEASE VIA CLAY AND WATER REDISTRIBUTION

Submitted to *Applied Sciences* on September 27, 2025

William Trenti[1], Mauro De Feudis[1],*, Sara Marinari[2], Sergio Murolo[3], Giulia Tabanelli[1], Federico Puliga[1], Rosita Marabottini[2], Alessandra Zambonelli[1], Fausto Gardini[1], Livia Vittori Antisari[1]

[1] Department of Agricultural and Food Sciences, Alma Mater Studiorum-University of Bologna, Viale Fanin 40, Bologna, Italy
[2] Department for Innovation in Biological, Agro-food and Forest systems, University of Tuscia, Viterbo, Italy
[3] Department of Agricultural, Food and Environmental Sciences, Polytechnic University of Marche, Ancona, Italy
*correspondence: mauro.defeudis2@unibo.it

ABSTRACT

Ink disease, caused by the soil-borne pathogens *Phytophthora cambivora* and *Phytophthora cinnamomi*, is threatening sweet chestnut (*Castanea sativa*) groves across Europe. This study investigates whether the morphology of soil and related properties influence the development of ink disease throughout the entire soil profile. In a *C. sativa* stand in Northern Italy, soil pits were excavated near symptomatic (INK1, 978 m a.s.l.) and healthy trees (INK2, 988 m a.s.l.; INK3, 998 m a.s.l.) along an altitudinal transect. The slope gradients at these sites were 3%, 9%, and 30%, respectively. Soils were classified as Luvisols. Results suggest that the lower slope position and gentler gradient of INK1 may have facilitated the downslope transport of clay and water from INK2 and INK3, leading to increased clay accumulation throughout the INK1 soil profiles. This, in turn, enhanced saturated hydraulic conductivity (Ks) and the wilting point (WP), favoring water retention in deeper horizons, where *Phytophthora* DNA was detected. Indeed, INK1 had a higher WP (14.9%) compared to INK2 (11.7%) and INK3 (8.2%), and

exhibited the highest Ks (25.1%), significantly exceeding values in INK2 (4.6%) and INK3 (6.5%). The presence of the pathogen in INK1 appeared to affect microbial functionality, as indicated by the dominance of contact (~20 %) and medium-distance ectomycorrhizal (~60 %) exploration types over long-distance ones. Overall, our findings highlighted the key role of soil processes, particularly clay and water redistribution, in shaping microbial communities and soil-borne pathogen dynamics through their influence on edaphic properties.

7.1 INTRODUCTION

Since the end of World War II, forested areas in Italy have steadily increased, driven by reforestation efforts and the abandonment of agricultural and pasture lands (Corona et al., 2008). Today, forests cover more than 37% of the national territory. Chestnut trees (Castanea sativa Mill.), which thrive in hilly and mountainous regions between 250 and 1000 meters above sea level, are an important component of these ecosystems. In the 1950s, the Statistical National Institute (ISTAT) inventory recorded 447,000 hectares of fruit chestnut groves and 275,186 hectares of coppice chestnut stands (Venanzi et al., 2016). At present, fruit chestnut groves have declined to 147,000 hectares, while coppice forests now cover approximately 600,000 hectares. However, many of these forests are aging and abandoned due to socioeconomic changes, policy shifts, and phytosanitary challenges (Venanzi et al., 2016; Fernandes et al., 2022). At the European level, chestnut forests are recognized as habitats of Community interest (Natura 2000 habitat code: 9260 Castanea sativa forest) (European Commission, 20017).

Despite the support of European and local rural development programs aimed at restoring chestnut groves (Buckley, 2020; Gullino et al., 2020), their success has been limited. Restoration efforts are often hindered by fragmented landownership and the lack of generational turnover among landowners.

Unmanaged chestnut forests are increasingly vulnerable to phytosanitary threats such as chestnut blight (Cryphonectria parasitica), ink disease (Phytophthora cambivora, P.

cinnamomi), brown rot (Gnomoniopsis castanea), and the Asian chestnut gall wasp (Dryocosmus kuriphilus) (Maresi et al., 2013; Murolo et al., 2022; Prospero et al., 2023). Among these, ink disease is one of the most serious threats, causing crown dieback, leaf yellowing, branch mortality, and in severe cases, rapid tree decline. Symptoms can take years to fully develop (Prospero et al., 2023). The primary causal agents in Europe are Phytophthora cambivora (Petri) Buisman and Phytophthora cinnamomi Rands, although other species may also be involved Prospero et al., 2023; Jung et al., 2018).

Most of the studies have examined the influence of land management, landscape features, and climate on ink disease development. For instance, heavy rainfall, heatwaves, and drought have been linked to its spread (Brasier et al., 1993; Davison, 1988; Jung et al., 1996; Jung et al., 2013). Disease incidence is also higher near natural drainage lines where inoculum moves with surface runoff (Peterson et al., 2014; Vannini et al., 2021), and roads through chestnut stands can serve as dispersal routes (Anselmi et al., 1999). Furthermore, intensive management and tillage have been associated with disease outbreaks in Portugal (Martins et al., 2007).

Conversely, the role of soil has received less attention, despite its fundamental role in modulating plant resilience and pathogen severity (Jung et al., 2018). Prior studies have mainly investigated soil porosity (Fonseca et al., 2004; Martins et al., 1999), while the influence of soil-forming factors linked to landscape morphology (e.g., slope position and gradient) remains understudied. We hypothesize that ink disease risk is higher in chestnut trees growing on soil at lower slope gradients, especially at the base of slopes. Such positions tend to favor water infiltration, increasing soil moisture (Liang et al., 2017; Ribolzi et al., 2011), and may create optimal conditions for infection by P. cinnamomi, which spreads via motile zoospores in water-saturated soils (Davison, 2011; Corcobado et al., 2013). Risk is further amplified in foot slope positions, where both surface and subsurface flow accumulate (Lin et al., 2006; Tromp-van Meerveld & McDonnell, 2006).

The consequences of ink disease are severe, affecting not only tree vitality but also the landscape, ecosystem services, and local economies that depend on chestnut production. In many cases, the disease symptoms may remain latent for decades following infection (Rubeuro, 1979; Tsao, 1990). However, recent studies in the northern Apennines suggest that some chestnut stands may be coexisting with Phytophthora spp., indicating a potential equilibrium between the pathogen, the host, environmental conditions, and the soil microbiota (Marzocchi et al., 2024).

While most soil microbiology studies focus on surface layers (up to 30 cm deep), where microbial activity is the highest, much less is known about the microbiome of the subsoil, despite its ecological relevance (Jiao et al., 2018). Soil microorganisms are key players in organic matter decomposition, nutrient cycling, and the maintenance of soil structure (Mendes et al., 2011; Piotrowska-Długosz et al., 2022). They are also widely recognized as indicators of soil health (Banerjee & van der Heijden, 2023). Furthermore, microorganisms are primary producers of extracellular enzymes that regulate organic matter turnover and nutrient dynamics (Burns et al., 2013; Zuccarini et al., 2020). These enzymes are sensitive to changes in soil properties and climatic conditions (Fanin et al., 2022), making them useful indicators for soil degradation and recovery processes (Bhaduri et al., 2022; Vázquez et al., 2020). The activity of soil enzymes is generally governed by factors such as soil organic matter, pH, and porosity (Moscatelli et al., 2018; Wang et al., 2022).

Soil morphological properties are key factors influencing soil formation and play a critical role in organic carbon storage and cycling. Slope position and aspect regulate hydrological processes and solar radiation exposure, thus shaping the microclimate (Huang et al., 2015; Li et al., 2021). These microclimatic variations influence microbial biomass and diversity, as well as microbial activity related to respiration and enzymatic functions involved in nutrient cycling and SOM decomposition (Wang et al., 2022; Xu et al., 2015).

This study aims to investigate how soil morphological properties affects: (1) the development of chestnut ink disease, and (2) the structure of Oomycota, fungal, and bacterial communities across both topsoil and subsoil horizons. To achieve this, we adopted an integrated approach combining pedological investigation on the field, soil physicochemical characterization, microbial DNA metabarcoding, and extracellular enzyme activity assays to provide a holistic understanding the soil–plant–microbial interactions, considering all genetic horizons of investigated soils.

7.2 MATERIALS AND METHODS

7.2.1 Study area and experimental design

The study was conducted in the municipality of Alto Reno Terme, in the Apennine Mountains of Bologna Province (northern Italy), near the border between the Emilia-Romagna and Tuscany regions (Figure 1). The area (WGS 84 UTM 32N: 4887250 mN, 656900 mE) is predominantly covered by fruit chestnut groves, including many centuries-old trees, which represent the dominant land use. Chestnut cultivation has historically shaped this landscape, as documented by initiatives under the National Rural Network Program (2014–2020) (Rete Rurale Nazionale, 2023).

Geologically, the area is characterized by dormant landslide deposits overlying the turbiditic arenaceous–pelitic member of the Castiglione dei Pepoli Formation (Vittori Antisari et al., 2023). The climate features warm summers and moderately cold winters, with a mean annual temperature of 10.9 °C. Monthly averages range from 20.7 °C in August to 2.5 °C in January (Figure S1 of the Supplementary Materials). Mean annual precipitation is 1,647 mm, unevenly distributed across the year, with peaks in winter, spring, and autumn, particularly in November. No marked dry season is observed.

An abandoned chestnut grove located on the south-facing slope of Mount Granaglione was selected as the study site. The grove extends from 970 to 1,050 m a.s.l. and has been unmanaged since 2008. It contains mature chestnut trees (>60 years old) spaced approximately 10 m apart. The understory is overgrown with ferns and brambles, with average ground cover of 40%.

Three sampling sites were selected along a 60 m altitudinal transect (10 m elevation difference per site): INK1 (978 m a.s.l.; 3% slope), INK2 (988 m a.s.l.; 9% slope), and INK3 (998 m a.s.l.; 30% slope) (Figures 1 and 2).

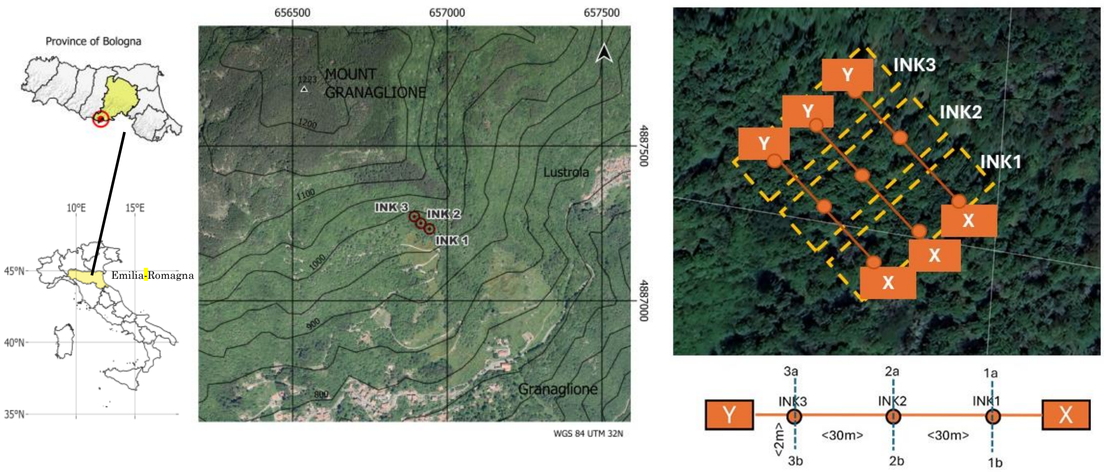

Figure 1. Location of the study area (left) and soil sampling design along the hillslope transect (right). The areas outlined by a dashed line are the study sites INK1, INK2, and INK3. The X–Y line represents the transect across which soil profiles (orange circles) and samples were collected. While 1a, 1b, 2a, 2b, 3a, and 3b denote additional sampling points associated with each profile.

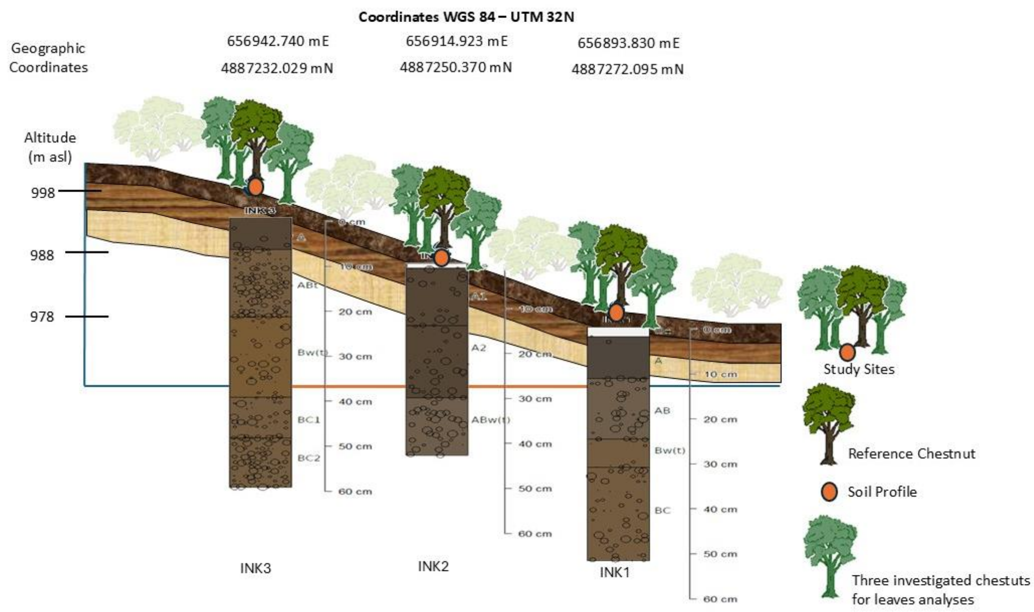

Figure 2. Diagram of the soil profiles and their relative positions along the hillslope.

In July 2023, at each site, three reference trees were selected and a soil profile was excavated 1 m downslope from each of them. Two additional auger samples (designated "a" and "b") were taken 2 m from each profile to assess horizon variability (Figure 1). Soil profiles and horizons were described following Schoeneberger et al. (Schoeneberger et al., 2012) (see Figure 2).

We acknowledge that investigating a single chestnut grove may limit the generalizability of our results. However, soil heterogeneity can be high even at small spatial scales (Cambardella et al., 1994; Pätzold et al., 2008), as slight differences in soil-forming factors can strongly affect pedogenetic processes (Türkeş et al., 2023). Vertical and horizontal water movement often varies along hillslopes, even at the microtopographic scale (Liu et al., 2022; Thompson et al., 2010). Moreover, mountain landscapes are characterized by pronounced topographic variability, which enhances soil diversity (Vittori Antisari et al., 2023; Oueslati et al., 2013; Seibert et al., 2007).

Approximately 500 g of soil were collected from each genetic horizon for physicochemical and biochemical analyses. For DNA metabarcoding, each horizon was sampled using a sterile 5 cm-diameter soil corer. Samples were stored in a refrigerated container and transported to the laboratory.

Chestnut trees at INK1 showed clear symptoms of decline—reduced canopy density, chlorotic leaves, dead branches, and dark flame-shaped lesions at the root collar—indicative of *Phytophthora* infection. Trees at INK2 and INK3 appeared healthy (Figure S2 of the Supplementary Materials).

The three reference trees per site were also sampled for leaf nutrient analysis using the protocol described by Vittori Antisari et al. (2018). Leaves from symptomatic trees (site INK1) had lower concentrations of N, K, Ca, and B, while healthy trees had lower Mn content (Table 1) than leaves from healthy plants (sites INK2 and INK3).

Table 1. Mean (n = 3) nutrient content in leaves of the reference chestnut trees located at INK1, INK2 and INK3 sites. Different letters indicate significant differences among the three sites ($p \leq 0.05$) according to Kruskal-Wallis's test.

Nutrient	Unit	INK1	INK2	INK3
N	%	2.1a	2.5b	2.7c
Al	g kg^{-1}	0.12a	0.21b	0.12a
Fe	g kg^{-1}	0.15a	0.27b	0.16a
Mn	g kg^{-1}	0.41a	0.27b	0.27b
K	g kg^{-1}	7.1a	7.8b	10.7c
Ca	g kg^{-1}	6.8a	7.6b	10.1c
Mg	g kg^{-1}	2.2	2.0	2.0
P	g kg^{-1}	1.8c	1.6a	1.7b
B	mg kg^{-1}	2.7a	20.2b	20.2b

7.2.2 Soil physicochemical analyses

Soil pH was determined in a 1:2.5 (w:v) soil-to-water suspension after two hours of shaking, using a Crison pH meter. Total organic carbon (OC) and total nitrogen (TN) were measured by Dumas combustion using a CHN elemental analyzer (Flash 2000, Thermo Fisher Scientific, USA). Particle-size distribution was determined using the pipette method (Gee & Bauder, 1986). Additional analytical details are provided in Appendix A.

7.2.3 Soil biochemical and enzyme analyses

Microbial biomass carbon (Cmic), microbial biomass nitrogen (Nmic), and basal respiration (BR) were measured following the protocol described by De Feudis et al. (2020), with full details in the Appendix A.

The activities of ß-cellobiohydrolase (EC 3.2.1.91), α-glucosidase (EC 3.2.1.21), ß-glucosidase (EC 3.2.1.20), and xylosidase (EC 3.2.2.27) were assessed using 4-MUF sub-strates (4-MUF-ß-D-cellobioside, 4-MUF-α-D-glucoside, 4-MUF-ß-D-glucoside, and 4-MUF-ß-D-xyloside, respectively), following Marx et al. (2001) and Vepsäläinen et al. (2001). Moist soil samples (equivalent to 1 g oven-dried) were homogenized in 50 mL of Na-acetate buffer (pH 5.5) using an UltraTurrax at 9,600 rpm for 3 minutes. Aliquots (100 µL) of the suspension were dispensed into 96-well microplates in triplicate for each substrate, and then mixed with 100 µL of a 1 mM substrate solution (final concentration: 500 µM). Fluorescence was measured at excitation/emission wavelengths of 360/450 nm using a Fluoroskan Ascent plate reader (Thermo Fisher Scientific) at 0, 30, 60, 120, and 180 minutes, with incubation at 30 °C.

Enzyme activity values were normalized to microbial biomass (Cmic) and total organic carbon (OC), resulting in microbial biomass-specific and organic carbon-specific enzyme activity indices, allowing comparisons across profiles. Specifically, the microbial biomass-specific and organic carbon-specific enzyme activity indices were calculated dividing each enzyme activity by the Cmic and OC contents, respectively.

7.2.4 DNA extraction and taxonomic assignment

Total DNA was extracted using the DNeasy PowerSoil Kit (Qiagen, Hilden, Germany), following the manufacturer's instructions. Each sample was analyzed in triplicate. For microbial and fungal communities, the V3–V4 region of the 16S rRNA gene and the ITS region were amplified using primers 341F/805R (García-López et al., 2023) and ITS1F/ITS4R (Gardes & Bruns, 1993; White et al., 1990), respectively. PCR products included Illumina adapters and unique indices for sequencing.

Libraries were sequenced using 300-bp paired-end reads on an Illumina MiSeq platform (Illumina, San Diego, CA). Base calling, demultiplexing, and adapter trimming were performed with BCL Convert v3.9.3. Reads were trimmed and filtered with Trimmomatic v0.39 and assessed with FastQC. Processed FASTQ files were analyzed with Kraken2 using the SILVA rRNA database (release 138.1) (Wood et al., 2019), and taxonomic abundances were estimated with Bracken (Lu et al., 2017).

Microbial communities were analyzed at the phylum level. Fungal communities were further resolved to the genus level to assign ecological guilds, including ectomycorrhizal groups, using the FungalTraits database (Põlme et al., 2020).

All horizons were also tested for Phytophthora spp. using the nested PCR protocol of Burgess et al. (Burgess et al., 2022) with P4 primers, previously validated on positive control DNA of Phytophthora cambivora. DNA from each sample was normalized to 2 ng/µL prior to amplification.

It is worth noting that relic DNA may constitute 20–80% of total soil DNA (Carini et al., 2017), with persistence times ranging from weeks to years depending on soil characteristics (Levy-Booth et al., 2007). In this study, relic DNA was not removed, allowing us to capture both active and inactive microbial signatures potentially involved in disease dynamics.

7.2.5 Indices calculation and statistical analyses

Soil hydraulic properties, including saturation (THS), field capacity (FC, at –330 cm matric potential), wilting point (WP, at –15,000 cm), and saturated hydraulic conductivity (KS), were estimated for each genetic horizon using the EU pedotransfer function interface (https://ptfinterface.rissac.hu/app_direct/ptf/, (Szabó et al., 2021). Input variables included depth, OC, bulk density, and particle-size distribution. Available water capacity (AWC) was calculated subtracting WP to FC. THS, FC, WP, and AWC were corrected for coarse fragments using the formula: adjusted value = value × (100 – Sk)/100, where Sk is the percentage of skeletal content. KS was corrected following Naseri et al. (Naseri et al., 2020), using an m value of 1.8 (intermediate between spherical and oblate fragment shapes).

The Synthetic Enzymatic Index (SEI), which integrates overall microbial functional capacity, was calculated as the sum of enzyme activities and expressed per unit of OC (SEI/OC) and microbial biomass C (SEI/Cmic), following Vittori Antisari et al. (2018).

Statistical differences in physicochemical and biological variables among soil profiles were assessed using the Kruskal–Wallis test, following evaluation of heteroscedasticity. All analyses were performed in RStudio (R v4.4.1), using the ‘agricolae’ package.

7.3 RESULTS

7.3.1 Soil classification, physicochemical and hydraulic properties

The investigated soil profiles were classified as Luvisols according to the World Reference Base for Soil Resources (IUSS, 2022). Specifically, INK1 was identified as a Skeletic Luvisol (loamic, epidystric), INK2 as a Leptic Skeletic Luvisol (loamic), and INK3 as a Skeletic Luvisol (loamic). These classifications reflect the high content of coarse fragments throughout the profiles—20%, 22%, and 44% for INK1, INK2, and INK3, respectively.

Using the USDA Soil Taxonomy (Soil Survey Staff, 2022), the presence of clay illuviation features in INK2 and INK3 sites supported their classification as Lithic Hapludalfs (loamy-skeletal, mesic) and Lithic Hapludalfs (loamy-skeletal, mesic, truncated), respectively. In contrast, soil profiles in INK1, which exhibited cambic horizons with only weak argillic development, were classified as a Ruptic-Alfic Dystrudept. Their dystric nature was supported by the low pH (5.6) and base saturation (34.0%).

The physicochemical and hydraulic properties of the soils are presented in Tables S1 and S2 of the Supplementary materials. Overall, the soil texture was silty loam across all horizons, except for the Bw(t) horizon in INK1, which exhibited a loamy texture. Results from the Kruskal–Wallis test (Figure 3) showed significantly lower pH and base saturation values in INK1 (5.6 and 33.9%, respectively) compared to INK2 (6.5 and 47.3%) and INK3 (6.6 and 51.4%). No significant differences in clay content were observed, likely due to high within-profile variability (Figure 3).

Due to the high within-profile variability in water-related properties, few statistically significant differences emerged. However, notable differences were observed in the permanent wilting point (WP) and saturated hydraulic conductivity (Ks). INK1 had a higher WP (14.9%) compared to INK2 (11.7%) and INK3 (8.2%), and exhibited the highest Ks (25.1%), significantly exceeding values in INK2 (4.6%) and INK3 (6.5%) (Figure 4).

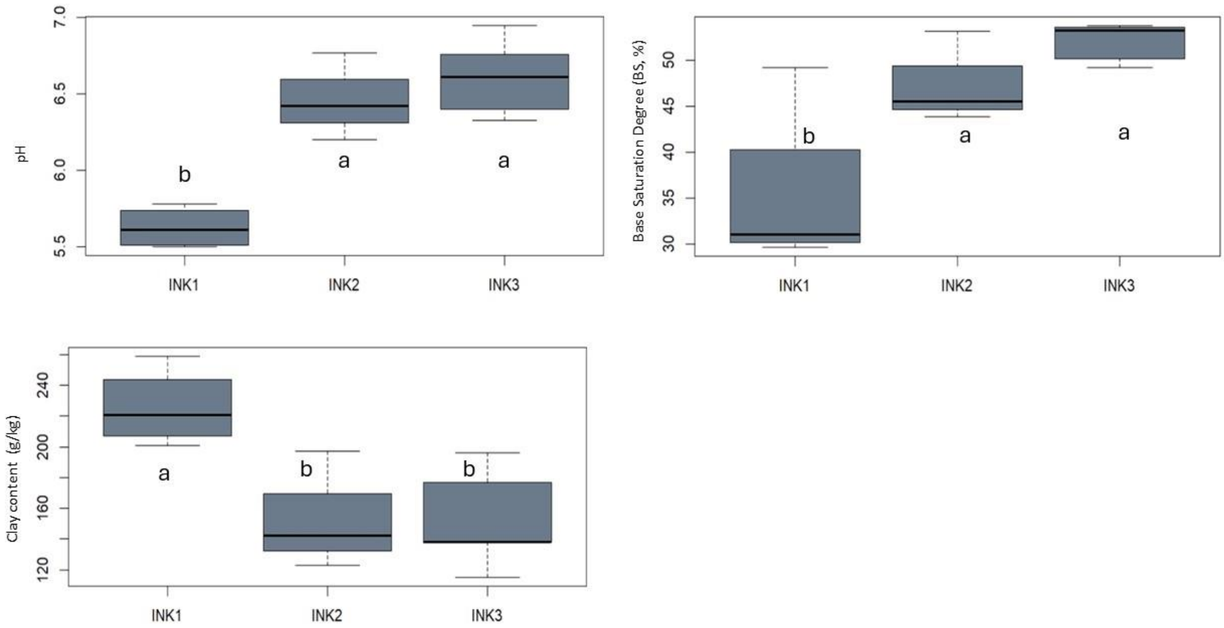

Figure 3. Boxplots showing pH, base saturation, and clay content in soils under diseased chestnut trees (INK1) and healthy chestnut trees (INK2 and INK3). Different letters indicate significant differences (p ≤ 0.05) according to Kruskal-Wallis test.

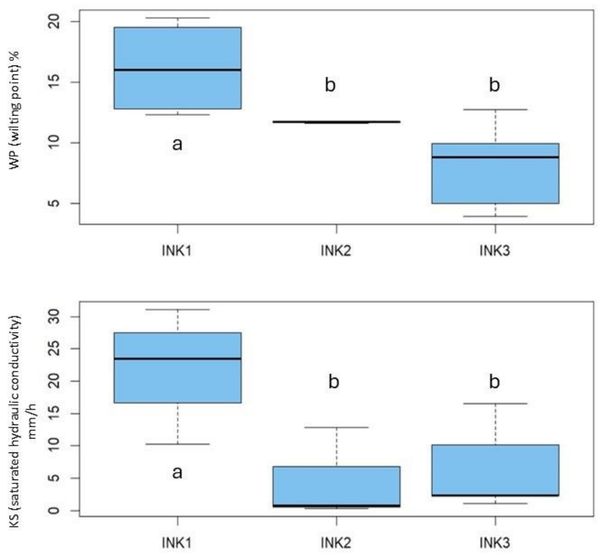

Figure 4. Boxplots showing the permanent wilting point (WP) and saturated hydraulic conductivity (Ks) in soils under diseased (INK1) and healthy (INK2, INK3) chestnut trees. Different letters indicate significant differences (p ≤ 0.05) based on Kruskal-Wallis test.

7.3.2 Soil organic matter, related properties and enzyme activities

As expected, most parameters related to soil organic matter content (Table S3 of the Supplementary materials) showed the highest values in the A horizon and decreased with depth. Among the carbon and nitrogen cycle indicators, no significant differences were observed across sites, except for water-extractable organic carbon (WEOC) and the WEOC:water-extractable nitrogen (WEN) ratio. These two parameters were significantly higher in INK1 compared to INK2 and INK3 (Figure 5).

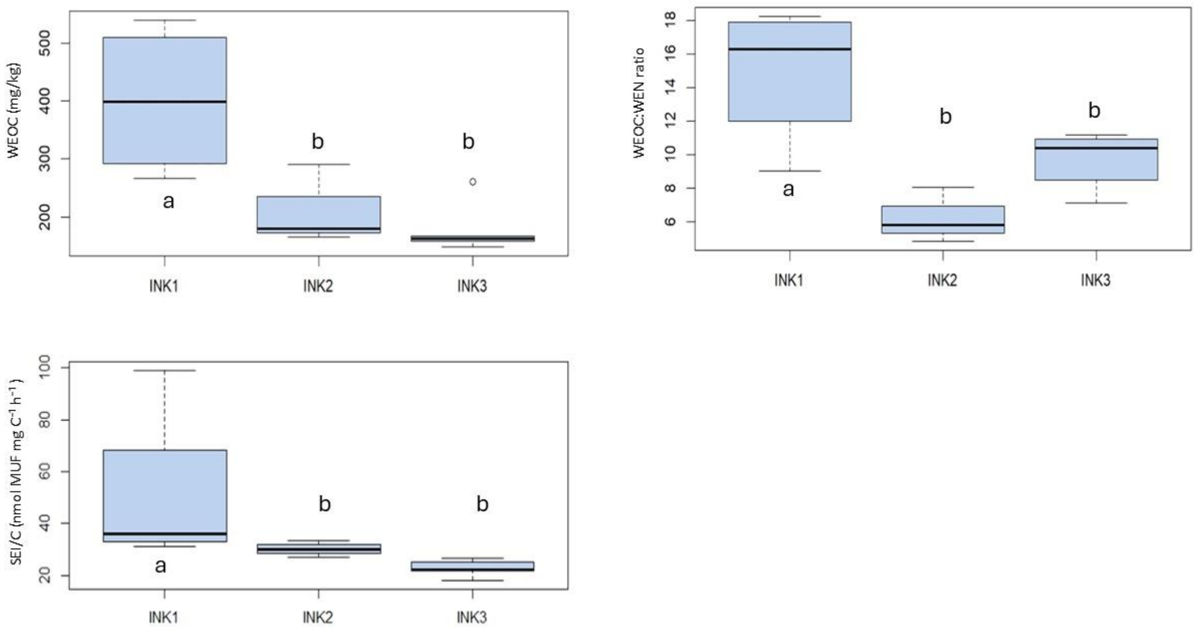

Figure 5. Boxplots showing WEOC content, the WEOC:WEN ratio, and the synthetic enzymatic index (SEI/OC) in soils under diseased (INK1) and healthy (INK2 and INK3) chestnut trees. Different letters indicate significant differences ($p \leq 0.05$) according to Kruskal-Wallis test. WEOC: water-extractable organic carbon; WEN: water-extractable nitrogen; SEI/OC: synthetic enzymatic index per unit of soil organic carbon.

Across entire soil profiles, enzyme activities and derived indices did not exhibit statistically significant differences among the sites (Table S4 of the Supplementary materials), likely due to high within-profile variability. However, when considering specific diagnostic horizons, both organic carbon-specific and microbial biomass-specific enzyme activities reached maximum values in the Bw(t) horizon of INK1 (Figure S3 of the Supplementary materials). Notably, elevated specific enzymatic activities were also detected in the AB and Bw(t) horizons of INK1.

Overall, the Synthetic Enzymatic Index normalized to organic carbon (SEI/OC) was significantly higher in INK1 (average: 50.5 nmol MUF mg^{-1} C h^{-1}) than in INK2 (30.1 nmol MUF mg^{-1} C h^{-1}) and INK3 (22.7 nmol MUF mg^{-1} C h^{-1}), with a Kruskal–Wallis test result of $\alpha = 0.05$, $p = 0.01$ (Figure 5).

7.3.3 Biodiversity of the fungal and bacterial communities

Figure 6 presents the results of the metagenomic analysis of bacterial communities, showing the relative abundance of the major phyla across different soil horizons. Acidobacteriota and Proteobacteria were the predominant phyla identified. While the relative abundance of Proteobacteria remained relatively stable across all samples, Acidobacteriota showed notable variation. Acidobacteriota abundance was similar in INK2 and INK3 but markedly increased in INK1, especially in the AB horizon. An inverse trend was observed for minor phyla, which decreased in proportion as Acidobacteriota increased. Additionally, Nitrospirota, a group of nitrifying bacteria, were found in appreciable amounts (up to 7%) in deeper horizons of INK2 and INK3—specifically in INK2 Bw(t) and INK3 BC2—whereas they were scarcely represented in INK1.

Phytophthora was detected exclusively in INK1 soils, with a faint amplification band observed in samples from the BC horizon.

Fungal community composition at the phylum level exhibited greater variability across the profiles compared to bacterial communities. As illustrated in Figure 7, the surface horizons of all profiles harbored fungal assemblages distinct from those in subsoil horizons. In the topsoil, a relatively balanced distribution was observed among Basidiomycota, Ascomycota, and Mortierellomycota. In contrast, Basidiomycota dominated the deeper horizons.

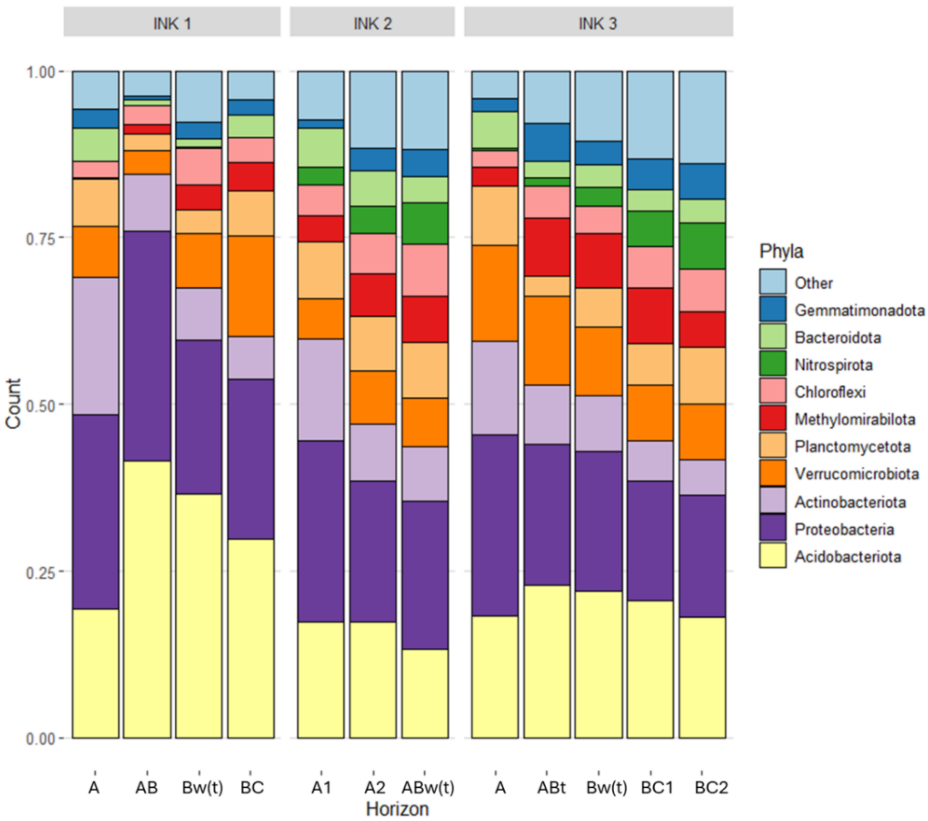

Figure 6. Distribution of bacterial phyla across soil horizons in profiles under diseased (INK1) and healthy (INK2 and INK3) chestnut trees. Phyla with relative abundance <5% are grouped as "Other".

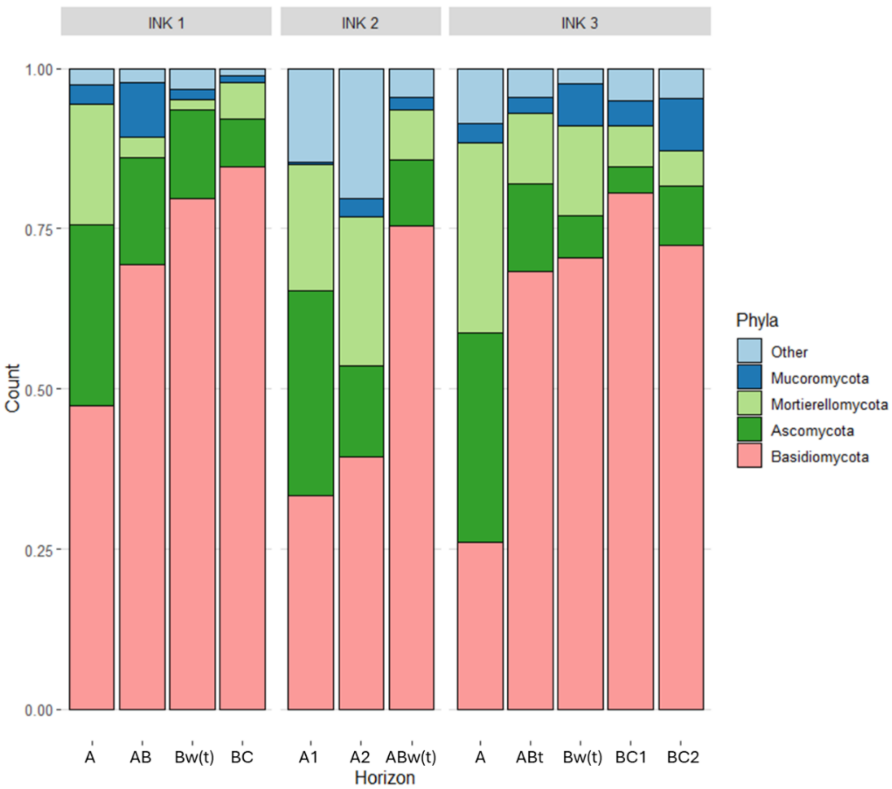

Figure 7. Distribution of fungal phyla across soil horizons in profiles under diseased (INK1) and healthy (INK2 and INK3) chestnut trees. Phyla with relative abundance <5% are grouped as "Other".

Fungal communities were further analyzed at the genus level to assess trophic strategies (Figure 8). In the mineral horizons of INK1, ectomycorrhizal fungi were dominant, accounting for 36% to 82% of the total fungal community. Notable genera included *Russula*, *Lactarius*, and *Lactifluus* (Figure S4 of the Supplementary Materials). In contrast, INK3 was dominated by soil saprotrophs, which represented 39% to 82% of the fungal assemblage, including genera such as *Geminibasidium* and *Saitozyma*. INK2 showed an intermediate pattern: its topsoil was dominated by ectomycorrhizal fungi (48%), while the subsoil exhibited a higher abundance of soil saprotrophs (ranging from 40% to 64%).

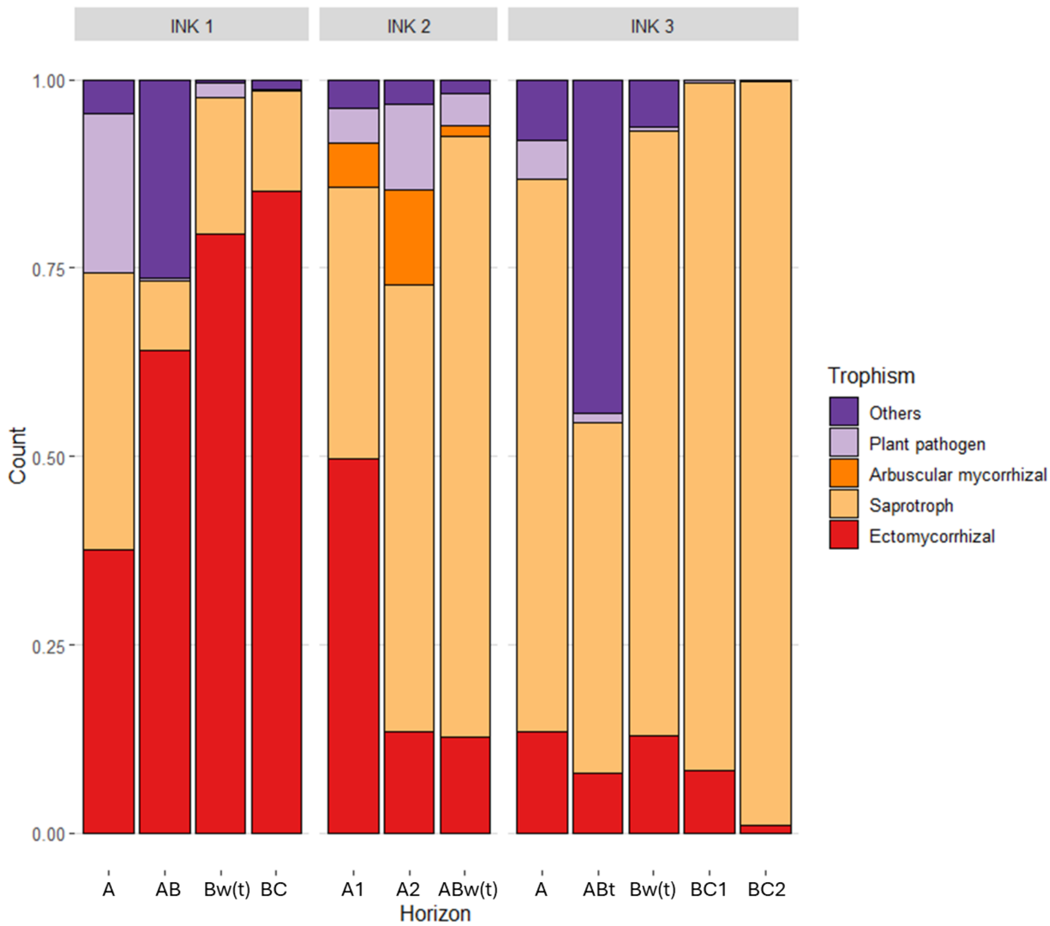

Figure 8. Relative abundance of fungal trophic groups at genus level in the horizons of soil profiles under ill chestnut plants (INK1) and healthy chestnut plants (INK2 and INK3).

An interesting finding was the presence of plant pathogenic fungi in the topsoil of INK1, accounting for up to 20% of the fungal community, predominantly from the genus *Rhizoctonia*.

Similarly, plant pathogens were also found in the A2 horizons of INK2, primarily represented by the genus *Bipolaris*.

The distribution of mycorrhizal exploration types varied among profiles (Figure 9). In INK1, the mycorrhizal community was primarily composed of contact and medium-distance types, while short-distance types were scarce, and long-distance types were absent. In contrast, both INK2 and INK3 were characterized by a high abundance of short-distance mycorrhizae.

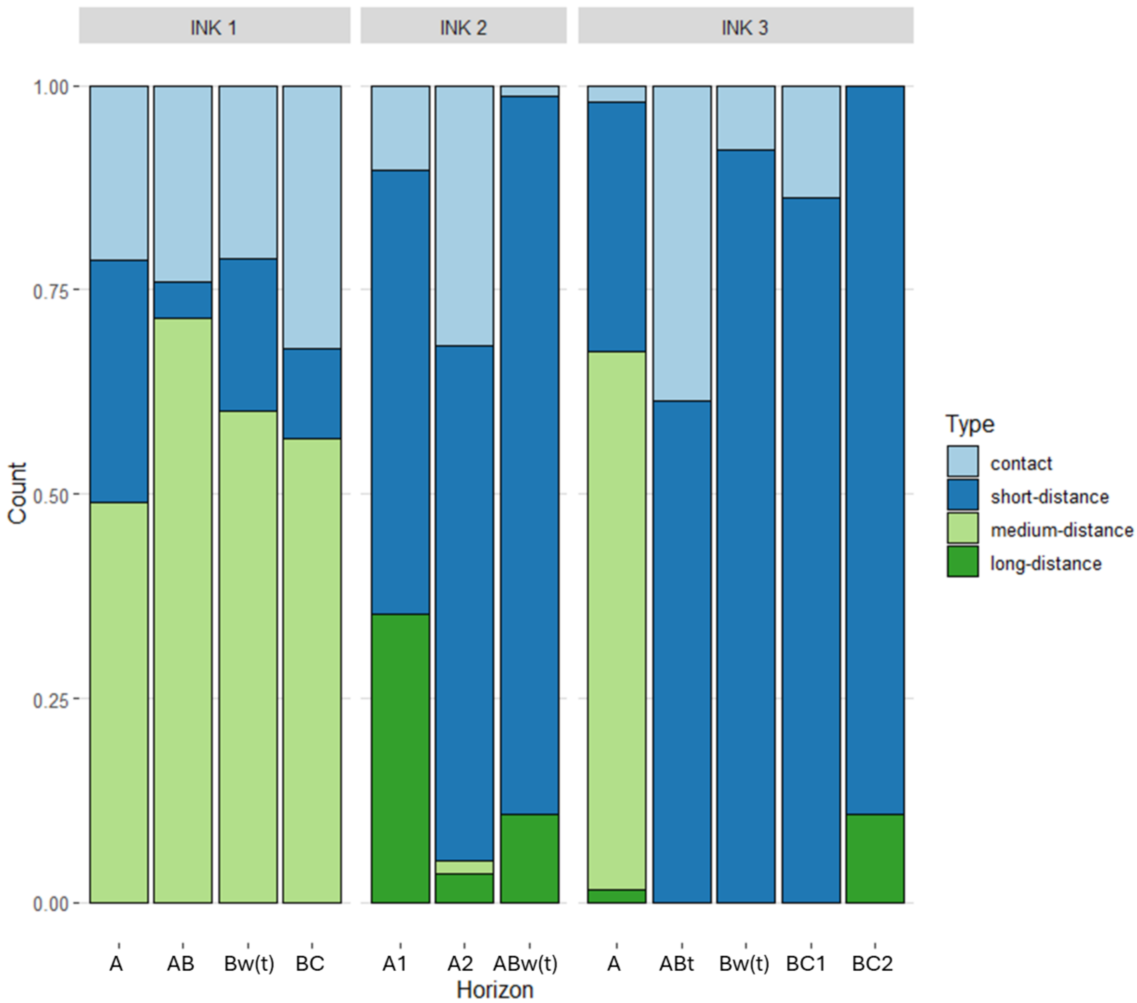

Figure 9. Distribution of fungal mycorrhiza at genus level in the horizons of soil profiles under ill chestnut plants (INK1) and healthy chestnut plants (INK2 and INK3).

7.4 DISCUSSION

The investigated soils were classified as Luvisols (IUSS, 2022), characterized by the mobilization and translocation of clay particles, leading to the formation of argic horizons. This process, known as lessivage, is driven by vertical water flux and facilitated by features such as cracks, pores, sandy-loam textures, organic matter content, and the presence of rock fragments (Quénard et al., 2011). Additionally, the position on the hillslope influences both vertical and lateral clay redistribution by water flow (Krevh et al., 2023). At our study site, we hypothesize that clay particles are not only vertically translocated but also move laterally, both on the surface and within the subsurface, from upslope to downslope areas during rainfall events, resulting in a general clay accumulation throughout the soil profiles of INK1 (Figure 10).

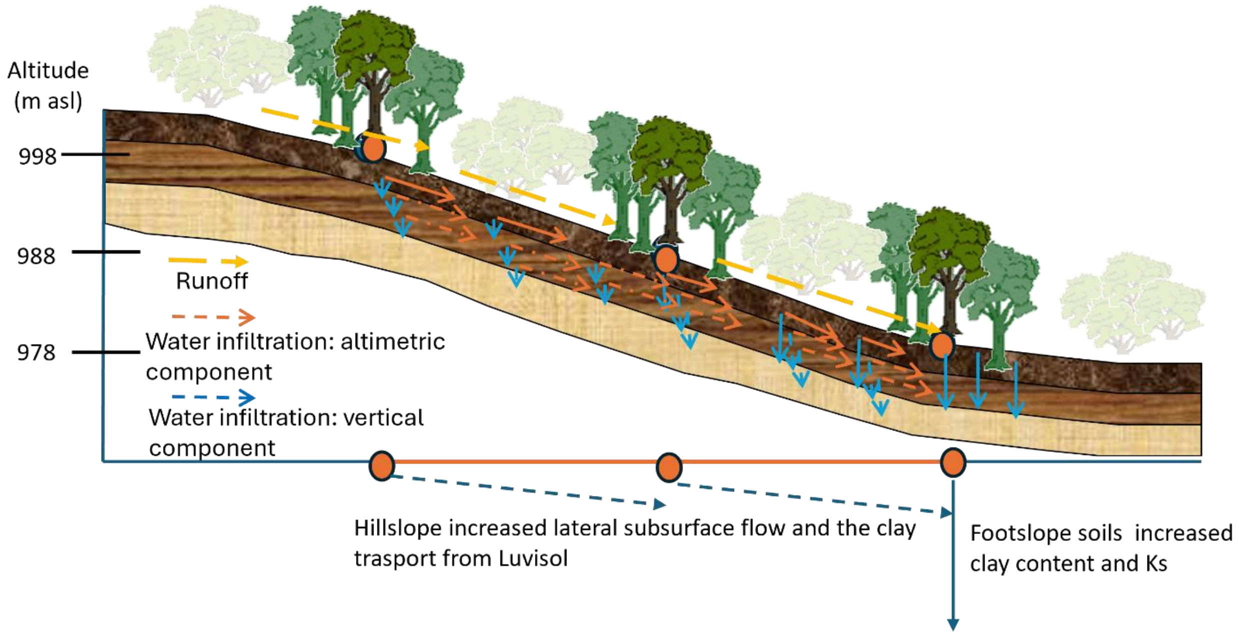

Figure 10. Conceptual figure illustrating water infiltration, surface runoff, and lateral subsurface flow across the study site's slope positions. KS: saturated hydraulic conductivity.

The presence of downslope water movement toward INK1 is supported by the higher saturated hydraulic conductivity (KS) observed in these soil profiles compared to the upslope profiles (INK2 and INK3), which exhibit lower KS values (Zambon et al., 2021). The steeper slope of INK3 further promotes runoff and reduces water infiltration, potentially contributing to the observed differences in horizon development. The absence of an organic horizon in INK3 and its shallow development in INK2, compared to the thicker organic horizon in INK1, supports the hypothesis of more intense runoff in the upper positions (Berg & McClaugherty, 2020).

INK1 showed dystric properties in the subsoil, and its location at the footslope likely promotes clay accumulation due to both surface and subsurface lateral water movement. This accumulation may be associated with the higher KS observed in INK1 (>23 mm h^{-1}), which enhances infiltration and leaching, resulting in lower soil pH values (Jobbágy & Jackson, 2003; Slessarev et al., 2016). Additionally, it is plausible that the elevated KS in INK1 is partly influenced by the higher content of soil organic matter (SOM), which is known to improve soil structure, enhance macroporosity, and thus facilitate water infiltration (Minasny & McBratney, 2018). The presence of organic matter promotes the formation of stable aggregates and biopores, particularly via root and microbial activity, which contributes to increased saturated hydraulic conductivity (de Jonge et al., 2009). Therefore, the increase of specific enzymatic activity may reflect the microbial response to different environmental conditions and soil properties (e.g. SOM and clay content, water retention, pH) established according to the slope aspect and position (Wang et al., 2022).

The development of *Phytophthora*-related symptoms appears influenced by topographic position, as suggested by previous studies (Vannini et al., 2010). The clay content and water infiltration in INK1, evidenced by the presence of redoximorphic features in the AB horizon, indicate sustained moist conditions (Doro et al., 2017; Mohanty & Mousli, 2000). Such conditions support the survival and activity of *Phytophthora*, consistent with other findings (Gyeltshen et al., 2021; Rhoades et al., 2003). *Phytophthora* DNA was detected in the BC horizon of INK1, despite its known short persistence in soil (Kunadiya et al., 2021).

The elevated WEOC content in INK1 could be related to root exudation stimulated by pathogen infection (Lanoue et al., 2010; Meier et al., 2013; Preece et al., 2024). Pathogen-induced changes in plant metabolism may alter the carbon-to-nitrogen ratio of the soluble organic matter, as reflected in the increased WEOC:WEN ratio observed. This suggests lower nitrogen availability, potentially affecting both plant and microbial communities. Pathogens may also induce the rhizodeposition of carbon-rich metabolites, such as phenolics (Dinis et al., 2011; Lovat & Donnelly, 2019), further increasing WEOC levels. Alternatively, the elevated WEOC could result from greater soil moisture (Christ & David, 1996; Fröberg et al., 2006; Kaiser et al., 2001).

Soil microbial activity generally increases in response to available carbon (Jansson & Persson, 2023), but limited nitrogen availability may lead to microbial nitrogen immobilization. In this study, nitrogen deficiency in chestnut trees may be partially explained by this process. The microbial community composition in INK1, characterized by a reduced presence of nitrifying taxa such as Nitrospirota, reflects changes in nitrogen cycling. Nitrospirota, sensitive to pH and nutrient availability, are involved in nitrite and complete ammonia oxidation (D'Angelo et al., 2023). The decline in pH and altered edaphic conditions may also explain the increased abundance of Acidobacteriota in the deeper horizons of INK1, as these bacteria are adapted to acidic, nutrient-poor environments (Kalam et al., 2020). This highlights the need to evaluate microbial vertical distribution to better understand soil functioning (Maitra et al., 2024; Naylor et al., 2022; Carteron et al., 2021)

Consistent with other studies (Dukunde et al., 2019; López-Mondéjar et al., 2015), the dominant bacterial phyla included Acidobacteria, Proteobacteria, Verrucomicrobiota, and Actinobacteria. Significant shifts were observed in INK1, where Acidobacteriota dominated the deeper horizons. These microbial shifts, along with the detection of *Phytophthora* in INK1, correlate with increased specific enzyme activities, indicating a physiological adaptation rather than a biomass increase (Marinari et al., 2022). Hydrolytic enzyme activity is influenced by substrate availability and microbial composition (Coonan et al., 2020; Qu et al., 2020). The specific enzymatic activity, calculated per unit of organic carbon, allows comparison among horizons and profiles (Trasar-Cepeda et al., 2008).

The elevated hydrolytic activity observed in deeper INK1 horizons, where *Phytophthora* was present and soil properties altered, suggests that microbial communities maintain nutrient cycling functions despite stress conditions. The higher SEI/OC values in INK1, especially in the AB and Bw(t) horizons, suggest increased metabolic activity in response to the presence of *Phytophthora* and altered soil characteristics. This may indicate a shift in microbial functional strategies and ecosystem equilibrium (Nannipieri et al., 2012). Given the central role of fungi in soil organic matter decomposition (Frey et al., 2014), shifts in fungal communities likely influenced enzyme dynamics.

We observed changes in fungal trophic strategies and mycorrhizal exploration types in INK1. Our findings align with previous studies indicating a positive correlation between soil moisture and ectomycorrhizal growth (Castaño et al., 2017; Kilpeläinen et al., 2017).

Increased water infiltration appears to enhance both pathogen proliferation (e.g., Rhizoctonia spp. In the A horizon) and ectomycorrhizal activity. Ectomycorrhizal fungi, known to offer protection against *Phytophthora* (Branzanti et al., 1999; Corcobado et al., 2014; Scattolin et al., 2012), were more abundant in INK1 subsoil. Their increased presence may reflect a compensatory mechanism in response to infection.

Variation in mycorrhizal exploration types across INK1 horizons may be driven by soil moisture and nutrient status. The dominance of contact and medium-distance types in INK1 aligns with wetter conditions, as contact exploration strategies prevail in high-moisture soils (Agerer, 2001). Additionally, root pathogen presence may select for these mycorrhizal types, which are more efficient at nutrient acquisition under stress. The reduced nitrogen availability in INK1 may further promote medium-distance exploration forms, better suited to acquiring labile nitrogen (Defrenne et al., 2019; Hobbie & Agerer, 2010), compared to the short-distance forms dominating INK2 and INK3.

Although the study relied on three fully characterized soil profiles per site, two supporting auger borings were conducted nearby to verify soil morphological properties and kind of genetic horizons. These auxiliary observations confirmed the occurrence of comparable pedogenetic horizons at each site, reinforcing the representativeness of the selected profiles. Nevertheless, as the horizons within a profile are not statistically independent replicates, and site conditions may still vary locally, we acknowledge that the limited number of profiles restricts the statistical inference and generalization of our results (Garten, 1993; Conant et al., 2003). However, the sampling by pedogenic horizon, together with the integration of physicochemical, microbiological, and molecular data, provides a robust exploratory framework. This study may therefore serve as a conceptual and methodological basis for future research involving replicated designs.

7.5 CONCLUSIONS

This study explored the relationships between soil morphological properties, microbial communities, and the incidence of ink disease in a chestnut grove located in a mountainous area of the northern Apennines. By combining soil field morphological and physicochemical characterization with microbial community profiling and extracellular enzyme assays, we identified clear differences among three soil profiles situated along a hillslope gradient. The soil profiles located in the footslope position (INK1) was characterized by higher both clay and organic C content, greater moisture retention, and reduced ectomycorrhizal diversity, coinciding with the presence of *Phytophthora* DNA and foliar nutrient deficiencies in overlying trees.

Our findings suggest that soil-forming factors related to slope morphology can influence both the persistence of pathogenic microorganisms and the functional structure of the soil microbiota. These interactions, in turn, affect host plant health. The study highlights the importance of integrating pedological variables into investigations of forest pathology and soil microbiology, particularly in complex topographic settings.

This work provides a replicable methodological framework for linking soil properties to plant health in forest ecosystems. Applying this approach across replicated designs in other mountainous areas may help inform targeted management strategies aimed at mitigating ink disease risk under changing climate and land-use conditions

SUPPLEMENTARY MATERIAL

The following supporting information can be downloaded at: https://www.mdpi.com/article/doi/s1, Figure S1: Walter & Lieth climatic diagram of the municipality of Alto Reno Terme for the period 1991-2020. Numbers at the top indicate mean annual temperature and annual precipitation; numbers on the left indicate daily maximum average temperature of the hottest month and daily minimum average temperature of the coldest month. Plotted with R package "climatol"; Figure S2: Pictures showing symptomatic chestnut plant in INK1 study site (a), and asymptomatic chestnut plants in INK2 (b) and INK3 (c) study sites; Figure S3: Specific enzymatic activities along the horizons of soil profiles per unit of OC (a) and Cmic (b). CELL (cellulase), NAG (chitinase), BG (β-glucosidase), AG (α-glucosidase), PHOS (phosphatase), SU (sulpha tase), XY (xylase), BUT (butyrase), LAP (leucine aminopeptidase); Figure S4: Sankey diagram of the 10 most representative genera for each soil horizon and site: a) INK1 profile, b) INK2 profile and c) INK3 profile; Table S1: Physicochemical characteristics of the soil under ill chestnut plants (INK1) and healthy chestnut plants (INK2 and INK3). CEC: cation exchange capacity; Caexch: exchangeable Ca; BS: base saturation; BD: bulk density; Table S2: Hydraulic properties of the soil under ill chestnut plants (INK1) and healthy chestnut plants (INK2 and INK3). THS: water content at saturation; FC: water content at field capacity = -33 kPa; WP: water content at permanent wilting point = -1,500 kPa; AWC: available water capacity; KS: saturated hydraulic conductivity; Table S3: Values of properties related to organic matter in the soil under ill chestnut plants (INK1) and healthy chestnut plants (INK2 and INK3). OC: soil organic carbon; TN: total nitrogen; Cmic: microbial bimass-C; SBR: soil basal respiration; WEOC: water-extractable organic carbon; WEN: water-extractable nitrogen; Table S4: Enzimatic activities in the soil under ill chestnut plants (INK1) and healthy chestnut plants (INK2 and INK3). CELL (cellulase), NAG (chitinase), BG (β-glucosidase), AG (α-glucosidase), PHOS (phosphatase), SU (sulpha tase), XY (xylase), BUT (butyrase), LAP (leucine aminopeptidase), SEI (Synthetic Enzymes Index); OC (organic C); Cmic (microbial biomass-C).

AUTHOR CONTRIBUTIONS

Conceptualization, L.V.A.; formal analysis, W.T., F.P. and L.V.A.; investigation, W.T., M.D.F., F.P. and R.M.; data curation, W.T. and L.V.A.; writing—original draft preparation, M.D.F. and F.P..; writing—review and editing, M.D.F., F.G., S.M., S.M. and L.V.A.; supervision, A.Z., F.G. and L.V.A.; funding acquisition, L.V.A. All authors have read and agreed to the published version of the manuscript.

FUNDING

This research was funded under the National Recovery and Resilience Plan (NRRP), Mission 4 Component 2 Investment 1.4 - Call for tender No. 3138 of 16 December 2021, rectified by Decree n.3175 of 18 December 2021 of Italian Ministry of University and Research funded by the European Union – NextGenerationEU; Project code CN_00000033, Concession Decree No. 1034 of 17 June 2022 adopted by the Italian Ministry of University and Research, CUPJ33C22001190001, Project title "National Biodiversity Future Center - NBFC

DATA AVAILABILITY STATEMENT

The datasets used and/or analyzed during the current study are available from the corresponding author on reasonable request.

ACKNOWLEDGMENTS

We would like to thank Hugo Ludlam for his thorough English editing of the entire manuscript.

CONFLICTS OF INTEREST

The authors declare no conflicts of interest.

APPENDIX A

Soil physicochemical analyses

The cation exchange capacity (CEC) and the exchangeable cations contents were determined according to the method proposed by Orsini and Rèmy (1976) and modified by Ciesielski and Sterckeman (1997) using 0.017 M hexamine cobalt(III) chloride as extracting solution and the amounts of Co and exchangeable cations were measured by inductively coupled plasma optical emission spectrometer (ICP–OES, Ametek, Spectro Arcos, Germany).

Microbial biomass C and N were estimated by the fumigation–extraction method using 0.5 M K_2SO_4 as extracting solution. Specifically, for each sample 10 g of 2–mm air dried soil was adjusted to 50% of field capacity and pre–incubated for 5 days. The soil samples were fumigated with $CHCl_3$ for 24 h at 25 °C. After, the fumigated and non−fumigated samples were mixed with 40 mL 0.5 M K_2SO_4 for 30 min on a horizontal shaker. The suspensions were filtered through 0.45μm membrane filter and C and N contents in the filtered solution were determined by a TOC–V CPN total organic carbon analyzer (Shimadzu, Japan). The microbial biomass C was calculated as EC/k_{EC}, where EC = (organic C extracted from fumigated soils) − (organic C extracted from non-fumigated soils) and k_{EC} = 0.45. Microbial biomass N was calculated as EN/k_{EN}, where EN = (total N extracted from fumigated soils) − (total N extracted from non-fumigated soils) and k_{EN} = 0.54.

C and N inside the filtered solution obtained from non–fumigated soil samples were considered as water–extractable organic C (WEOC) and water– extractable N (WEN).

Basal respiration was determined by quantifying the CO_2 released in the process of microbial respiration during 28 days of incubation at 25°C after conditioning of the samples at 50% of their field capacity and a pre–incubation of 5 days. In particular, 10 g of 2–mm air dried soil sample was placed in 0.5 L jars with hermetic lids and after 1–3–7–10–14–21–28 days the beginning of incubation, the amount of CO_2 emitted from incubated soils was measured by alkali (1 M NaOH solution) absorption of the evolved CO_2 and titration of the residual OH– with a standardized HCl solution. The soil basal respiration (BR) of each soil sample was calculated as the average of the values measured during the incubation period.

Orsini, L., & Remy, J. C. (1976). Utilisation du chlorure de cobaltihexammine pour la determination simultanee de la capacite d'echange et des bases echangeables des sols. Bulletin de l'Association Francaise pour l'Etude du Sol. Science du Sol.

Ciesielski, H., Sterckeman, T., Santerne, M., & Willery, J. P. (1997). Determination of cation exchange capacity and exchangeable cations in soils by means of cobalt hexamine trichloride. Effects of experimental conditions. Agronomie, 17(1), 1-7.

REFERENCES

Agerer, R. (2001). Exploration types of ectomycorrhizae: a proposal to classify ectomycorrhizal mycelial systems according to their patterns of differentiation and putative ecological importance. *Mycorrhiza*, *11*(2), 107-114.

Anselmi, N., Vettraino, A. M., Franco, S., & Vannini, A. (1999). Recrudescenza del mal dell'inchiostro del castagno in Italia: nuove acquisizioni e suggerimenti di lotta. *Linea Ecologica*, XXXI, 53–58. (Italian)

Banerjee, S., & Van Der Heijden, M. G. (2023). Soil microbiomes and one health. *Nature Reviews Microbiology*, *21*(1), 6-20.

Berg, B., & McClaugherty, C. (2020). What Factors May Influence the Accumulation of Humus Layers?. In *Plant Litter: Decomposition, Humus Formation, Carbon Sequestration* (pp. 247-272). Cham: Springer International Publishing.

Bhaduri, D., Sihi, D., Bhowmik, A., Verma, B. C., Munda, S., & Dari, B. (2022). A review on effective soil health bio-indicators for ecosystem restoration and sustainability. *Frontiers in Microbiology*, *13*, 938481.

Branzanti, M. B., Rocca, E., & Pisi, A. (1999). Effect of ectomycorrhizal fungi on chestnut ink disease. *Mycorrhiza*, *9*(2), 103-109.

Brasier, C. M., Robredo, F., & Ferraz, J. F. P. (1993). Evidence for Phytophthora cinnamomi involvement in Iberian oak decline. *Plant pathology*, *42*(1), 140-145.

Buckley, P. (2020). Coppice restoration and conservation: a European perspective. *Journal of Forest Research*, *25*(3), 125-133.

Burgess, T. I., White, D., & Sapsford, S. J. (2022). Comparison of primers for the detection of Phytophthora (and other oomycetes) from environmental samples. *Journal of Fungi*, *8*(9), 980.

Burns, R. G., DeForest, J. L., Marxsen, J., Sinsabaugh, R. L., Stromberger, M. E., Wallenstein, M. D., ... & Zoppini, A. (2013). Soil enzymes in a changing environment: current knowledge and future directions. *Soil Biology and Biochemistry*, *58*, 216-234.

Cambardella, C. A., Moorman, T. B., Novak, J. M., Parkin, T. B., Karlen, D. L., Turco, R. F., & Konopka, A. E. (1994). Field-scale variability of soil properties in central Iowa soils. *Soil science society of America journal*, *58*(5), 1501-1511.

Carini, P., Marsden, P. J., Leff, J. W., Morgan, E. E., Strickland, M. S., & Fierer, N. (2016). Relic DNA is abundant in soil and obscures estimates of soil microbial diversity. *Nature microbiology*, *2*(3), 1-6.

Carteron, A., Beigas, M., Joly, S., Turner, B. L., & Laliberté, E. (2021). Temperate forests dominated by arbuscular or ectomycorrhizal fungi are characterized by strong shifts from saprotrophic to mycorrhizal fungi with increasing soil depth. *Microbial Ecology*, *82*(2), 377-390.

Castaño, C., Alday, J. G., Parladé, J., Pera, J., de Aragón, J. M., & Bonet, J. A. (2017). Seasonal dynamics of the ectomycorrhizal fungus Lactarius vinosus are altered by changes in soil moisture and temperature. *Soil Biology and Biochemistry*, *115*, 253-260.

Christ, M. J., & David, M. B. (1996). Temperature and moisture effects on the production of dissolved organic carbon in a Spodosol. *Soil Biology and Biochemistry*, *28*(9), 1191-1199.

Conant, R.T.; Paustian, K.; Elliott, E.T. (2003) Quantifying and reporting uncertainty in estimates of soil organic carbon stocks and changes. *Soil Biol. Biochem.*, 35, 19–30.

Coonan, E. C., Kirkby, C. A., Kirkegaard, J. A., Amidy, M. R., Strong, C. L., & Richardson, A. E. (2020). Microorganisms and nutrient stoichiometry as mediators of soil organic matter dynamics. *Nutrient Cycling in Agroecosystems*, *117*(3), 273-298.

Corcobado, T., Solla, A., Madeira, M. A., & Moreno, G. (2013). Combined effects of soil properties and Phytophthora cinnamomi infections on Quercus ilex decline. *Plant and soil*, *373*(1), 403-413.

Corcobado, T., Vivas, M., Moreno, G., & Solla, A. (2014). Ectomycorrhizal symbiosis in declining and non-declining Quercus ilex trees infected with or free of Phytophthora cinnamomi. *Forest Ecology and Management*, *324*, 72-80.

Corona, P., Calvani, P., Mugnozza, G. S., & Pompei, E. (2008). Modelling natural forest expansion on a landscape level by multinomial logistic regression. *Plant Biosystems-An International Journal Dealing with all Aspects of Plant Biology*, *142*(3), 509-517.

D'Angelo, T., Goordial, J., Lindsay, M. R., McGonigle, J., Booker, A., Moser, D., ... & Orcutt, B. N. (2023). Replicated life-history patterns and subsurface origins of the bacterial sister phyla Nitrospirota and Nitrospinota. *The ISME Journal*, *17*(6), 891-902.

Davison, E. M. (1988). The role of waterlogging and Phytophthora cinnamomi in the decline and death of Eucalyptus marginata in Western Australia. *GeoJournal*, *17*(2), 239-244.

Davison, E. M. (2011). How do Phytophthora spp. de Bary kill trees?. *New Zealand Journal of Forestry Science*, *41*.

De Feudis, M., Falsone, G., Vianello, G., & Vittori Antisari, L. (2020). The conversion of abandoned chestnut forests to managed ones does not affect the soil chemical properties and improves the soil microbial biomass activity. *Forests*, *11*(8), 786.

de Jonge, L. W., Moldrup, P., & Schjønning, P. (2009). Soil Infrastructure, Interfaces & Translocation Processes in Inner Space (" Soil-it-is"): towards a road map for the constraints and crossroads of soil architecture and biophysical processes. *Hydrology and Earth System Sciences*, *13*(8), 1485-1502.

Defrenne, C. E., Philpott, T. J., Guichon, S. H., Roach, W. J., Pickles, B. J., & Simard, S. W. (2019). Shifts in ectomycorrhizal fungal communities and exploration types relate to the environment and fine-root traits across interior Douglas-fir forests of western Canada. *Frontiers in Plant Science*, *10*, 643.

Dinis, L. T., Peixoto, F., Zhang, C., Martins, L., Costa, R., & Gomes-Laranjo, J. (2011). Physiological and biochemical changes in resistant and sensitive chestnut (Castanea) plantlets after inoculation with Phytophthora cinnamomi. *Physiological and molecular plant pathology*, *75*(4), 146-156.

Doro, L., Jones, C., Williams, J. R., Norfleet, M. L., Izaurralde, R. C., Wang, X., & Jeong, J. (2017). The variable saturation hydraulic conductivity method for improving soil water content simulation in EPIC and APEX models. *Vadose Zone Journal*, *16*(13), 1-14.

Dukunde, A., Schneider, D., Schmidt, M., Veldkamp, E., & Daniel, R. (2019). Tree species shape soil bacterial community structure and function in temperate deciduous forests. *Frontiers in microbiology*, *10*, 1519.

European Commission (2007). Interpretation Manual of European Union Habitats. October 14 2007

Fanin, N., Mooshammer, M., Sauvadet, M., Meng, C., Alvarez, G., Bernard, L., ... & Nottingham, A. T. (2022). Soil enzymes in response to climate warming: Mechanisms and feedbacks. *Functional Ecology*, *36*(6), 1378-1395.

Fernandes, P., Colavolpe, M. B., Serrazina, S., & Costa, R. L. (2022). European and American chestnuts: An overview of the main threats and control efforts. *Frontiers in Plant Science*, *13*, 951844.

Fonseca, T. F., Abreu, C. G., & Parresol, B. R. (2004). Soil compaction and chestnut ink disease. *Forest Pathology*, *34*(4), 273-283.

Frey, S. D., Ollinger, S., Nadelhoffer, K. E., Bowden, R., Brzostek, E., Burton, A., ... & Wickings, K. (2014). Chronic nitrogen additions suppress decomposition and sequester soil carbon in temperate forests. *Biogeochemistry*, *121*(2), 305-316.

Fröberg, M., Berggren, D., Bergkvist, B., Bryant, C., & Mulder, J. (2006). Concentration and fluxes of dissolved organic carbon (DOC) in three Norway spruce stands along a climatic gradient in Sweden. *Biogeochemistry*, *77*(1), 1-23.

García-López, J. D., Barbieri, F., Banos, A., Madero, J. M. G., Gardini, F., Montanari, C., & Tabanelli, G. (2023). Use of two autochthonous bacteriocinogenic strains as starter cultures in the production of salchichónes, a type of Spanish fermented sausages. *Current Research in Food Science*, *7*, 100615.

Gardes, M., & Bruns, T. D. (1993). ITS primers with enhanced specificity for basidiomycetes-application to the identification of mycorrhizae and rusts. *Molecular ecology*, *2*(2), 113-118.

Garten, C.T. Jr. (1993) Variability in soil properties at a landscape scale. *Soil Sci. Soc. Am. J.*, 57(6), 1693–1700.

Gee, G. W., & Bauder, J. W. (1986). Particle-size analysis. *Methods of soil analysis: Part 1 Physical and mineralogical methods*, *5*, 383-411.

Gullino, P., Mellano, M. G., Beccaro, G. L., Devecchi, M., & Larcher, F. (2020). Strategies for the management of traditional chestnut landscapes in Pesio Valley, Italy: a participatory approach. *Land*, *9*(12), 536.

Gyeltshen, J., Dunstan, W. A., Grigg, A. H., Burgess, T. I., & St. J. Hardy, G. E. (2021). The influence of time, soil moisture and exogenous factors on the survival potential of oospores and chlamydospores of Phytophthora cinnamomi. *Forest Pathology*, *51*(1), e12637.

Hobbie, E. A., & Agerer, R. (2010). Nitrogen isotopes in ectomycorrhizal sporocarps correspond to belowground exploration types. *Plant and Soil*, *327*(1), 71-83.

Huang, Y. M., Liu, D., & An, S. S. (2015). Effects of slope aspect on soil nitrogen and microbial properties in the Chinese Loess region. *Catena*, *125*, 135-145.

Hudson, B. D. (1994). Soil organic matter and available water capacity. *Journal of soil and water conservation*, *49*(2), 189-194.

IUSS Working Group. (2014). World reference base for soil resources 2014. International soil classification system for naming soils and creating legends for soil maps. *(No Title).*

Jansson, S. L., & Persson, J. (1982). Mineralization and immobilization of soil nitrogen. *Nitrogen in agricultural soils*, *22*, 229-252.

Jiao, S., Chen, W., Wang, J., Du, N., Li, Q., & Wei, G. (2018). Soil microbiomes with distinct assemblies through vertical soil profiles drive the cycling of multiple nutrients in reforested ecosystems. *Microbiome*, *6*(1), 146.

Jobbágy, E. G., & Jackson, R. B. (2003). Patterns and mechanisms of soil acidification in the conversion of grasslands to forests. *Biogeochemistry*, *64*(2), 205-229.

Jung, T., & Blaschke, H. (1996). Phytophthora root rot in declining forest trees. *PHYTON-HORN-*, *36*, 95-102.

Jung, T., Pérez-Sierra, A., Durán, A., Jung, M. H., Balci, Y., & Scanu, B. (2018). Canker and decline diseases caused by soil-and airborne Phytophthora species in forests and woodlands. *Persoonia-Molecular Phylogeny and Evolution of Fungi*, *40*(1), 182-220.

Jung, T., Vettraino, A. M., Cech, T., & Vannini, A. (2013). The impact of invasive Phytophthora species on European forests. In *Phytophthora: A global perspective* (pp. 146-158). Wallingford UK: CABI.

Kaiser, K., Kaupenjohann, M., & Zech, W. (2001). Sorption of dissolved organic carbon in soils: effects of soil sample storage, soil-to-solution ratio, and temperature. *Geoderma*, *99*(3-4), 317-328.

Kalam, S., Basu, A., Ahmad, I., Sayyed, R. Z., El-Enshasy, H. A., Dailin, D. J., & Suriani, N. L. (2020). Recent understanding of soil acidobacteria and their ecological significance: a critical review. *Frontiers in Microbiology*, *11*, 580024.

Kilpeläinen, J., Barbero-López, A., Vestberg, M., Heiskanen, J., & Lehto, T. (2017). Does severe soil drought have after-effects on arbuscular and ectomycorrhizal root colonisation and plant nutrition?. *Plant and Soil*, *418*(1), 377-386.

Kirk, J. L., Beaudette, L. A., Hart, M., Moutoglis, P., Klironomos, J. N., Lee, H., & Trevors, J. T. (2004). Methods of studying soil microbial diversity. *Journal of microbiological methods*, *58*(2), 169-188.

Krevh, V., Groh, J., Weihermüller, L., Filipović, L., Defterdarović, J., Kovač, Z., ... & Filipović, V. (2023). Investigation of hillslope vineyard soil water dynamics using field measurements and numerical modeling. *Water*, *15*(4), 820.

Kunadiya, M. B., Burgess, T. I., A Dunstan, W., White, D., & StJ. Hardy, G. E. (2021). Persistence and degradation of Phytophthora cinnamomi DNA and RNA in different soil types. *Environmental DNA*, *3*(1), 92-104.

Lanoue, A., Burlat, V., Henkes, G. J., Koch, I., Schurr, U., & Röse, U. S. (2010). De novo biosynthesis of defense root exudates in response to Fusarium attack in barley. *New Phytologist*, *185*(2), 577-588.

Levy-Booth, D. J., Campbell, R. G., Gulden, R. H., Hart, M. M., Powell, J. R., Klironomos, J. N., ... & Dunfield, K. E. (2007). Cycling of extracellular DNA in the soil environment. *Soil Biology and Biochemistry*, *39*(12), 2977-2991.

Li, T., Liang, J., Chen, X., Wang, H., Zhang, S., Pu, Y., ... & Liu, X. (2021). The interacting roles and relative importance of climate, topography, soil properties and mineralogical composition on soil potassium variations at a national scale in China. *Catena*, *196*, 104875.

Liang, W. L., Li, S. L., & Hung, F. X. (2017). Analysis of the contributions of topographic, soil, and vegetation features on the spatial distributions of surface soil moisture in a steep natural forested headwater catchment. *Hydrological Processes*, *31*(22), 3796-3809.

Lin, H. S., Kogelmann, W., Walker, C., & Bruns, M. A. (2006). Soil moisture patterns in a forested catchment: A hydropedological perspective. *Geoderma*, *131*(3-4), 345-368.

Liu, H., Zhang, J., Liao, A., Liu, C., Du, M., Huang, A., ... & Guo, J. (2022). Estimation of variability in soil water content in a forested critical-zone experimental catchment in Eastern China. *Journal of Contaminant Hydrology*, *248*, 104022.

López-Mondéjar, R., Voříšková, J., Větrovský, T., & Baldrian, P. (2015). The bacterial community inhabiting temperate deciduous forests is vertically stratified and undergoes seasonal dynamics. *Soil Biology and Biochemistry*, *87*, 43-50.

Lovat, C. A., & Donnelly, D. J. (2019). Mechanisms and metabolomics of the host–pathogen interactions between chestnut (Castanea species) and chestnut blight (Cryphonectria parasitica). *Forest Pathology*, *49*(6), e12562.

Lu, J., Breitwieser, F. P., Thielen, P., & Salzberg, S. L. (2017). Bracken: estimating species abundance in metagenomics data. *PeerJ Computer Science*, *3*, e104.

Maitra, P., Hrynkiewicz, K., Szuba, A., Jagodziński, A. M., Al-Rashid, J., Mandal, D., & Mucha, J. (2024). Metabolic niches in the rhizosphere microbiome: dependence on soil horizons, root traits and climate variables in forest ecosystems. *Frontiers in Plant Science*, *15*, 1344205.

Maresi, G., Longa, O., & Turchetti, T. (2013). Brown rot on nuts of Castanea sativa Mill: an emerging disease and its causal agent. *IForest-Biogeosciences and Forestry*, *6*(5), 294.

Marinari, S., Radicetti, E., Petroselli, V., Allam, M., & Mancinelli, R. (2022). Microbial indices to assess soil health under different tillage and fertilization in potato (Solanum tuberosum L.) crop. *Agriculture*, *12*(3), 415.

Martins, L. M., Oliveira, M. T., & Abreu, C. G. (1998). Soils and climatic characteristic of chestnut stands that differ on the presence of the ink disease. In *II International Symposium on Chestnut 494* (pp. 447-450).

Martins, L., Castro, J., Macedo, W., Marques, C., & Abreu, C. (2007). Assessment of the spread of chestnut ink disease using remote sensing and geostatistical methods. *European Journal of Plant Pathology*, *119*(2), 159-164.

Marx, M. C., Wood, M., & Jarvis, S. C. (2001). A microplate fluorimetric assay for the study of enzyme diversity in soils. *Soil biology and biochemistry*, *33*(12-13), 1633-1640.

Marzocchi, G., Maresi, G., Luchi, N., Pecori, F., Gionni, A., Longa, C. M. O., ... & Ferretti, F. (2024). 85 years counteracting an invasion: chestnut ecosystems and landscapes survival against ink disease. *Biological Invasions*, *26*(7), 2049-2062.

Meier, I. C., Avis, P. G., & Phillips, R. P. (2013). Fungal communities influence root exudation rates in pine seedlings. *FEMS microbiology ecology*, *83*(3), 585-595.

Mendes, R., Kruijt, M., De Bruijn, I., Dekkers, E., Van Der Voort, M., Schneider, J. H., ... & Raaijmakers, J. M. (2011). Deciphering the rhizosphere microbiome for disease-suppressive bacteria. *Science*, *332*(6033), 1097-1100.

Minasny, B., & McBratney, A. B. (2018). Limited effect of organic matter on soil available water capacity. *European journal of soil science*, *69*(1), 39-47.

Mohanty, B. P., & Mousli, Z. (2000). Saturated hydraulic conductivity and soil water retention properties across a soil-slope transition. *Water Resources Research*, *36*(11), 3311-3324.

Moscatelli, M. C., Secondi, L., Marabottini, R., Papp, R., Stazi, S. R., Mania, E., & Marinari, S. (2018). Assessment of soil microbial functional diversity: land use and soil properties affect CLPP-MicroResp and enzymes responses. *Pedobiologia*, *66*, 36-42.

Murolo, S., Bertoldi, D., Pedrazzoli, F., Mancini, M., Romanazzi, G., & Maresi, G. (2022). New Symptoms in Castanea sativa Stands in Italy: chestnut mosaic virus and nutrient deficiency. *Forests*, *13*(11), 1894.

Nannipieri, P., Giagnoni, L., Renella, G., Puglisi, E., Ceccanti, B., Masciandaro, G., ... & Marinari, S. A. R. A. (2012). Soil enzymology: classical and molecular approaches. *Biology and fertility of soils*, *48*(7), 743-762.

Naseri, M., Peters, A., Durner, W., & Iden, S. C. (2020). Effective hydraulic conductivity of stony soils: General effective medium theory. *Advances in Water Resources*, *146*, 103765.

Naylor, D., McClure, R., & Jansson, J. (2022). Trends in microbial community composition and function by soil depth. *Microorganisms*, *10*(3), 540.

Oueslati, I., Allamano, P., Bonifacio, E., & Claps, P. (2013). Vegetation and topographic control on spatial variability of soil organic carbon. *Pedosphere*, *23*(1), 48-58.

Patzold, S., Mertens, F. M., Bornemann, L., Koleczek, B., Franke, J., Feilhauer, H., & Welp, G. (2008). Soil heterogeneity at the field scale: a challenge for precision crop protection. *Precision Agriculture*, *9*(6), 367-390.

Peterson, E., Hansen, E., & Hulbert, J. (2014). Source or sink? The role of soil and water borne inoculum in the dispersal of Phytophthora ramorum in Oregon tanoak forests. *Forest Ecology and Management*, *322*, 48-57.

Piotrowska-Długosz, A., Długosz, J., Frąc, M., Gryta, A., & Breza-Boruta, B. (2022). Enzymatic activity and functional diversity of soil microorganisms along the soil profile–A matter of soil depth and soil-forming processes. *Geoderma*, *416*, 115779.

Põlme, S., Abarenkov, K., Henrik Nilsson, R., Lindahl, B. D., Clemmensen, K. E., Kauserud, H., ... & Tedersoo, L. (2020). FungalTraits: a user-friendly traits database of fungi and fungus-like stramenopiles. *Fungal diversity*, *105*(1), 1-16.

Preece, C., Yang, K., Llusià, J., Winkler, J. B., Schnitzler, J. P., & Peñuelas, J. (2024). Combined effects of drought and simulated pathogen attack on root exudation rates of tomatoes. *Plant and Soil*, *497*(1), 629-645.

Prospero, S., Heinz, M., Augustiny, E., Chen, Y. Y., Engelbrecht, J., Fonti, M., ... & Fonti, P. (2023). Distribution, causal agents, and infection dynamic of emerging ink disease of sweet chestnut in Southern Switzerland. *Environmental Microbiology*, *25*(11), 2250-2265.

Qu, Y., Tang, J., Li, Z., Zhou, Z., Wang, J., Wang, S., & Cao, Y. (2020). Soil enzyme activity and microbial metabolic function diversity in soda saline–alkali rice paddy fields of northeast China. *Sustainability*, *12*(23), 10095.

Quénard, L., Samouëlian, A., Laroche, B., & Cornu, S. (2011). Lessivage as a major process of soil formation: a revisitation of existing data. *Geoderma*, *167*, 135-147.

Rete Rurale Nazionale (2023). La Corona di Matilde. Alto Reno. Terra di Castagni, https://www.reterurale.it/flex/cm/pages/ServeBLOB.php/L/IT/IDPagina/23098.

Rhoades, C. C., Brosi, S. L., Dattilo, A. J., & Vincelli, P. (2003). Effect of soil compaction and moisture on incidence of phytophthora root rot on American chestnut (Castanea dentata) seedlings. *Forest Ecology and Management*, *184*(1-3), 47-54.

Ribeiro, O. K. (1978). *A source book of the genus Phytophthora. Mycologia*, 71, 460.

Ribolzi, O., Patin, J., Bresson, L. M., Latsachack, K. O., Mouche, E., Sengtaheuanghoung, O., ... & Valentin, C. (2011). Impact of slope gradient on soil surface features and infiltration on steep slopes in northern Laos. *Geomorphology*, *127*(1-2), 53-63.

Scattolin, L., Dal Maso, E., Mutto Accordi, S., Sella, L., & Montecchio, L. (2012). Detecting asymptomatic ink-diseased chestnut trees by the composition of the ectomycorrhizal community. *Forest Pathology*, *42*(6), 501-509.

Schoeneberger, P. J., Wysocki, D. A., & Benham, E. C. (Eds.). (2012). *Field book for describing and sampling soils*. Government Printing Office.

Seibert, J., Stendahl, J., & Sørensen, R. (2007). Topographical influences on soil properties in boreal forests. *Geoderma*, *141*(1-2), 139-148.

Slessarev, E. W., Lin, Y., Bingham, N. L., Johnson, J. E., Dai, Y., Schimel, J. P., & Chadwick, O. A. (2016). Water balance creates a threshold in soil pH at the global scale. *Nature*, *540*(7634), 567-569.

Soil Survey Staff (2022). Keys to Soil Taxonomy, 13th ed. USDA-Natural Resources Conservation Service.

Szabó, B., Weynants, M., & Weber, T. K. (2021). Updated European hydraulic pedotransfer functions with communicated uncertainties in the predicted variables (euptfv2). *Geoscientific Model Development*, *14*(1), 151-175.

Thompson, S. E., Katul, G. G., & Porporato, A. (2010). Role of microtopography in rainfall-runoff partitioning: An analysis using idealized geometry. *Water Resources Research*, *46*(7).

Trasar-Cepeda, C., Leirós, M. C., & Gil-Sotres, F. (2008). Hydrolytic enzyme activities in agricultural and forest soils. Some implications for their use as indicators of soil quality. *Soil Biology and Biochemistry*, *40*(9), 2146-2155.

Tromp-van Meerveld, H. J., & McDonnell, J. J. (2006). On the interrelations between topography, soil depth, soil moisture, transpiration rates and species distribution at the hillslope scale. *Advances in water resources*, *29*(2), 293-310.

Tsao, P. H. (1990). Why many Phytophthora root rots and crown rots of tree and horticultural crops remain undetected 1. *EPPO bulletin*, *20*(1), 11-17.

Türkeş, M., Dede, V., Dengiz, O., Şenol, H., & Serin, S. (2023). Periglacial landforms and soil formation on summit of the Mount lda (Kaz Dağı), Biga Peninsula-Turkey. *Physical Geography*, *44*(5), 531-580.

Vannini, A., Natili, G., Anselmi, N., Montaghi, A., & Vettraino, A. M. (2010). Distribution and gradient analysis of Ink disease in chestnut forests. *Forest Pathology*, *40*(2), 73-86.

Vannini, A., Natili, G., Thomidis, T., Belli, C., & Morales-Rodriguez, C. (2021). Anthropogenic and landscape features are associated with ink disease impact in Central Italy. *Forest Pathology*, *51*(6), e12722.

Vázquez, E., Benito, M., Espejo, R., & Teutscherova, N. (2020). Response of soil properties and microbial indicators to land use change in an acid soil under Mediterranean conditions. *Catena*, *189*, 104486.

Venanzi, R., Picchio, R., & Piovesan, G. (2016). Silvicultural and logging impact on soil characteristics in Chestnut (Castanea sativa Mill.) Mediterranean coppice. *Ecological Engineering*, *92*, 82-89.

Vepsäläinen, M., Kukkonen, S., Vestberg, M., Sirviö, H., & Niemi, R. M. (2001). Application of soil enzyme activity test kit in a field experiment. *Soil Biology and Biochemistry*, *33*(12-13), 1665-1672.

Vittori Antisari, L., Papp, R., Vianello, G., & Marinari, S. (2018). Effects of Douglas fir stand age on soil chemical properties, nutrient dynamics, and enzyme activity: a case study in Northern Apennines, Italy. *Forests*, *9*(10), 641.

Vittori Antisari, L., Trenti, W., Buscaroli, A., Falsone, G., Vianello, G., & De Feudis, M. (2022). Pedodiversity and organic matter stock of soils developed on sandstone formations in the Northern Apennines (Italy). *Land*, *12*(1), 79.

Wang, M., Ji, L., Shen, F., Meng, J., Wang, J., Shan, C., & Yang, L. (2022). Differential responses of soil extracellular enzyme activity and stoichiometric ratios under different slope aspects and slope positions in Larix olgensis plantations. *Forests*, *13*(6), 845.

White, T. J., Bruns, T., Lee, S. J. W. T., & Taylor, J. (1990). Amplification and direct sequencing of fungal ribosomal RNA genes for phylogenetics. *PCR protocols: a guide to methods and applications*, *18*(1), 315-322.

Wood, D. E., Lu, J., & Langmead, B. (2019). Improved metagenomic analysis with Kraken 2. *Genome biology*, *20*(1), 257.

Xu, Z., Yu, G., Zhang, X., Ge, J., He, N., Wang, Q., & Wang, D. (2015). The variations in soil microbial communities, enzyme activities and their relationships with soil organic matter decomposition along the northern slope of Changbai Mountain. *Applied Soil Ecology*, *86*, 19-29.

Zambon, N., Johannsen, L. L., Strauss, P., Dostal, T., Zumr, D., Cochrane, T. A., & Klik, A. (2021). Splash erosion affected by initial soil moisture and surface conditions under simulated rainfall. *Catena*, *196*, 104827.

Zuccarini, P., Asensio, D., Ogaya, R., Sardans, J., & Peñuelas, J. (2020). Effects of seasonal and decadal warming on soil enzymatic activity in a P-deficient Mediterranean shrubland. *Global Change Biology*, *26*(6), 3698-3714.

8. GENERAL CONCLUSIONS AND FUTURE RESEARCH

This doctoral research path focused on the use of GIS techniques in several steps of the soil mapping process, in order to produce maps capable of informing land managers and promote the monitoring and conservation of terrestrial biodiversity, in accordance with the goals of the NBFC. The study area, consisting of two Regional Parks in the Northern Apennine mountains, served as an ideal laboratory for this research thanks to its high complexity and relative abundance in cartographic data. First, existing pedological knowledge was applied to direct the completion of the soil survey of the area: relevant environmental covariates, chosen based on expert knowledge, were used to stratify the area into land units, i.e. sectors which share the same soil forming factors. The informative layers were elevation, slope, lithology, and land use. Those same land units then served as a base for the first soil map, obtained via conventional methods. Then, DSM techniques were used to produce another soil map of the same area, this time using Random Forests with recursive feature elimination to extract the most decisive covariates out of a larger set which included DEM derivatives and remotely sensed data. The model selected five covariates: DEM, slope, winter diffuse insolation, summer NDVI, and distance from lakes. The map obtained though this method displayed high accuracy as well as consistency with the soil-landscape relationships that are known to operate in this area, thus making it a viable tool for land management. The recursive feature elimination process offered insights into the main drivers of soil differentiation in the area, and applying the model to different areas, e.g. the Casentino Forests National Park, could simplify and speed up the soil survey step of the mapping procedure. Furthermore, using only DEM derivatives and remotely sensed data allows to overcome the discontinuities that affect many cartographic products in Italy.

As a follow-up to these studies, I am currently exploring a similar approach to map soil properties and ecosystem services. I am applying different methods of covariate selection to extract optimal subsets of covariates from an array of over 50 DEM derivatives and remotely sensed data layers to map organic carbon stock at 30 cm and the pH of the first mineral horizon (Figure 1 a and b respectively). I calculated Shannon diversity index on the soil map to verify if soil diversity hotspots are present, and where they are located in the Parks (Figure 2).

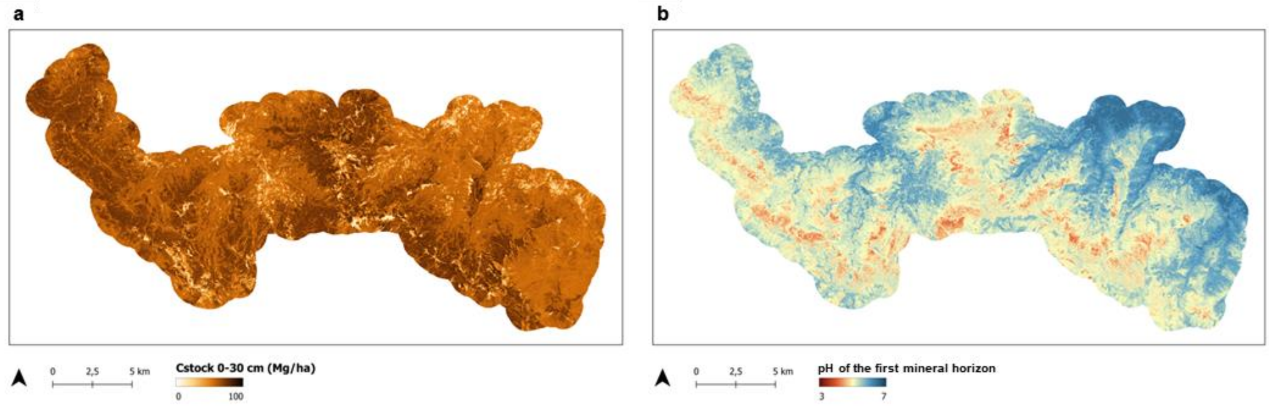

Figure 1. Examples of maps of the Frignano and Corno alle Scale Regional Parks made using random forests and covariate selection methods. a: organic carbon stock in the first 30 cm of soil; b: pH of the first mineral horizon.

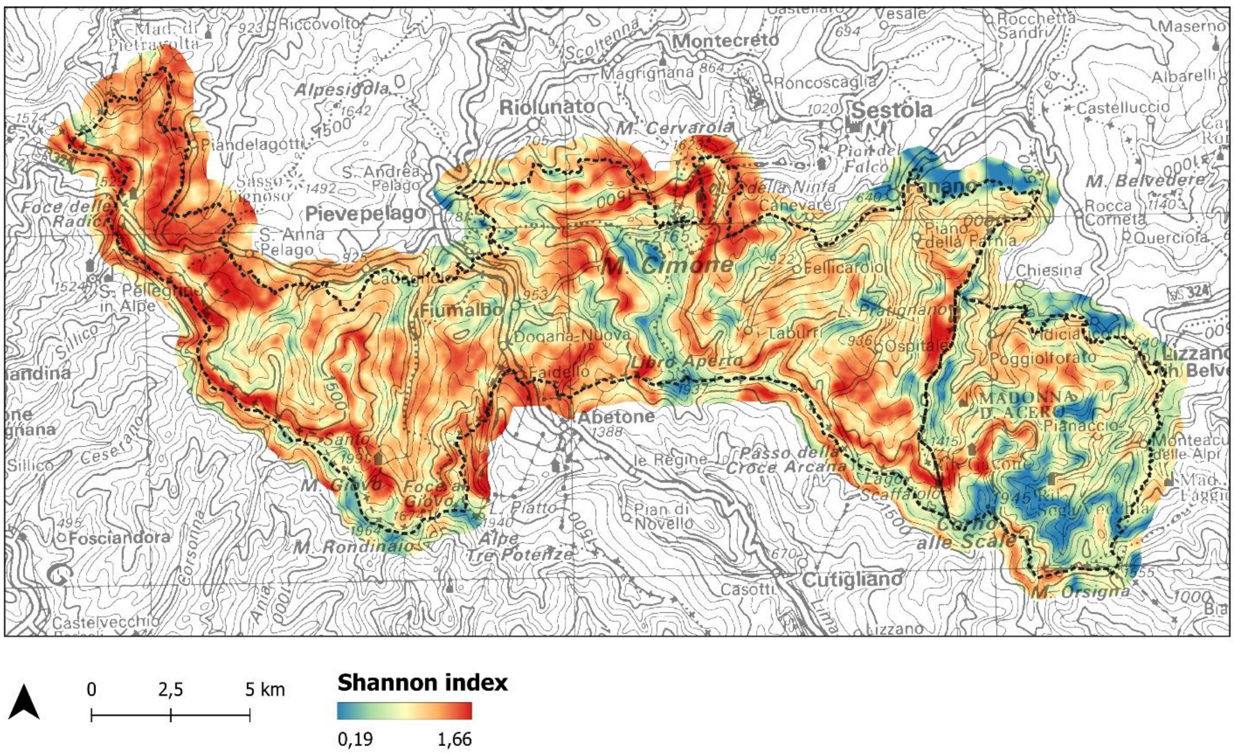

Figure 2. Map of the Shannon index of the soil classes previously mapped in the Frignano and Corno alle Scale area. Soil diversity appears to be higher in correspondence with the treeline and where hydromorphic conditions are present. This suggests that soil diversity could be impacted by changing temperatures and precipitation patterns.

Other studies carried out in the course of the PhD program on this study area investigated the role of pedodiversity on organic matter dynamics and microbial activity, as well as the factors which most influence soil evolution and differentiation. It was found that climate is a stronger driver than vegetation in shaping soil evolution, and that considering soil diversity can add insight to studies that investigate soil organic matter dynamics.

The second focus of my doctoral path was on the reestablishment of chestnut cultivation in the Northern Apennines. A map of land suitability was produced for the municipality of Castel Del Rio (BO), renowned for the quantity and quality of their chestnut production. The method used is widely applicable, and the map highlighted the presence of considerable areas of land which are suitable for chestnut fruit production but are not cultivated. On the other hand, the map also highlighted large areas which present limitations but are cultivated nonetheless. Sadly, the extreme weather events of May 2023 remarked the importance of considering land suitability: of the more than 500 ha which were affected by landslides in the municipality of Castel Del Rio (RER, 2024), 57 ha were within chestnut groves. Of these 57 ha, 51 belonged to areas which our study identified as presenting limitations to chestnut cultivation (Figure 3), mostly consisting in excessive steepness.

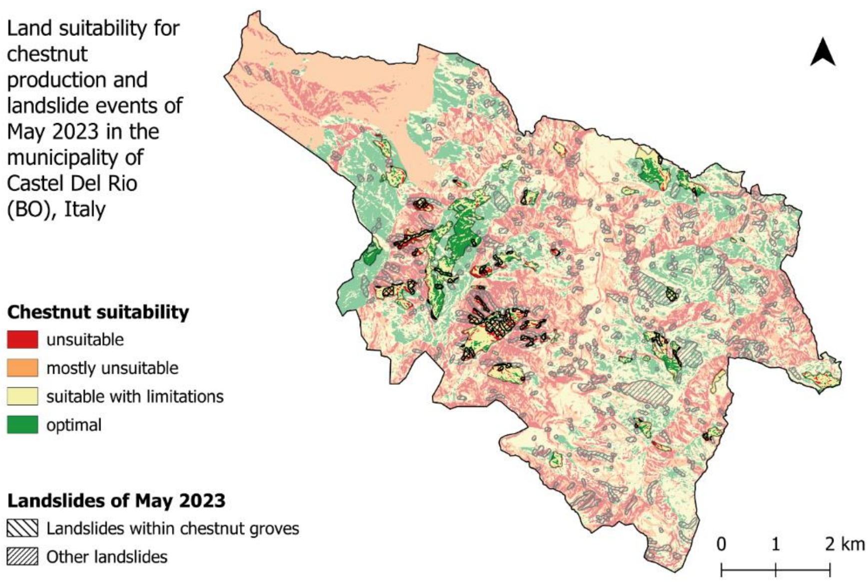

Figure 3. Map of the land suitability of chestnut fruit production in the municipality of Castel Del Rio (BO), Italy, and areas affected by landslides in the events of May 2023. The vivid areas of the map represent active chestnut groves.

As found in our most recent study, land morphology may also have a role in the spread of ink disease. Footslope areas where water naturally converges, paired with a finer soil texture such as that found in argillic horizons, could promote the proliferation of this soil-borne fungus that threatens chestnut groves.

Overall, this doctoral research demonstrates how the integration of GIS-based soil mapping, digital modeling, and ecological interpretation can not only enhance our understanding of soil–landscape relationships but also provide practical tools to support sustainable land management, biodiversity conservation, and the resilience of traditional agroecosystems such as chestnut cultivation in the Northern Apennines.

REFERENCES

RER (2024). Banca dati eventi franosi post eventi meteorologici maggio 2023 - Aree interessate da indirizzi normativi e misure temporanee di salvaguardia a seguito delle frane del maggio 2023 nelle Province di Reggio Emilia, Modena, Ravenna, Forlì-Cesena, Rimini e nella Città Metropolitana di Bologna - agg. agosto 2024. Available on https://geoportale.regione.emilia-romagna.it/catalogo/dati-cartografici/informazioni-geoscientifiche/zone-a-rischio-naturale/layer-90